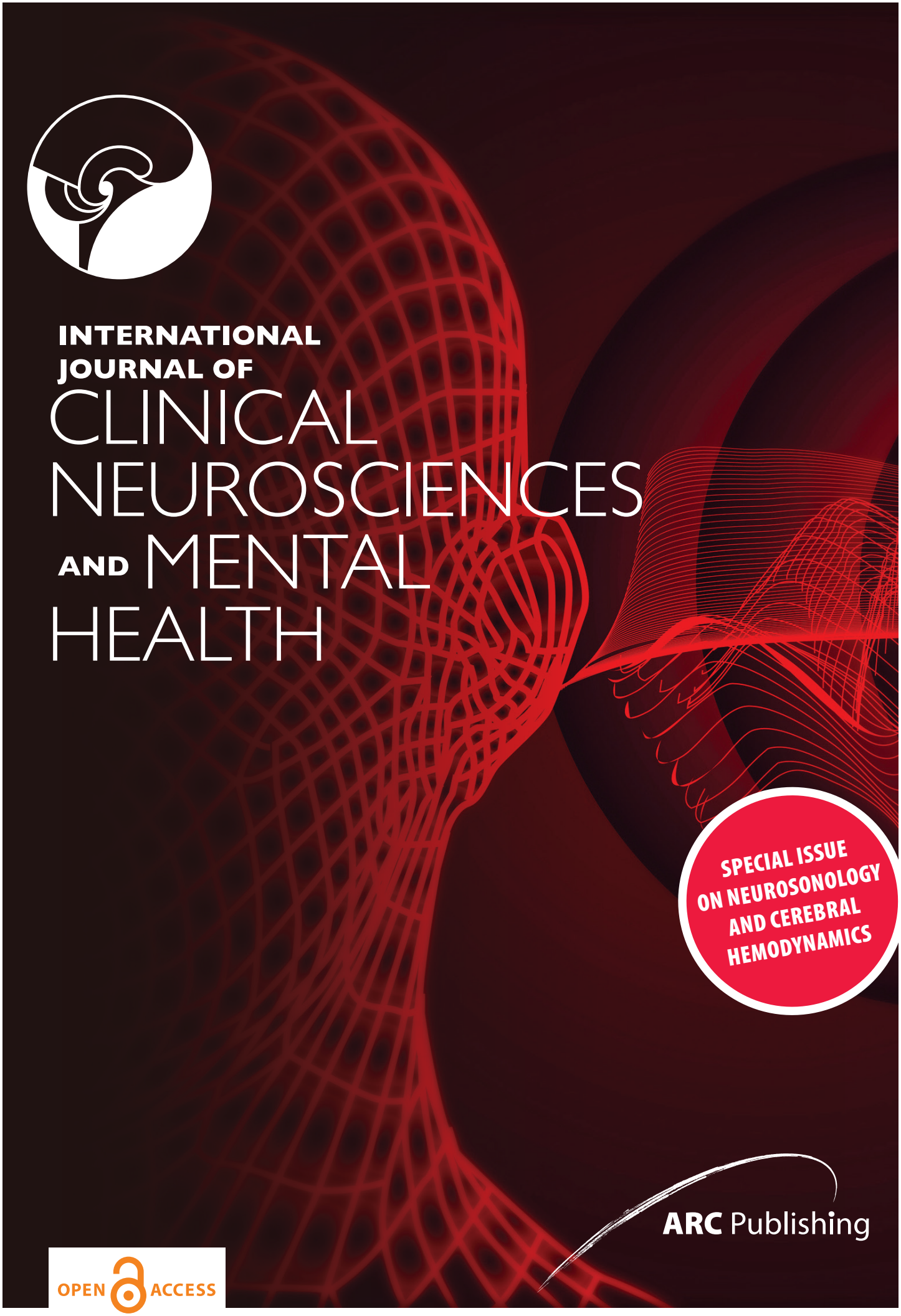
INTERNATIONAL
JOURNAL OF
CLINICAL
NEUROSCIENCES
AND MENTAL
HEALTH
SPECIAL ISSUE
ON NEUROSONOLOGY
AND CEREBRAL
HEMODYNAMICS
ARC Publishing
OPEN ACCESS

ARC Publishing

*Outstanding services in medical writing, statistics and publishing.*

Providing superior medical writing, statistics and training services, allowing you to comply with the highest clinical research quality standards and to get the most of your data.

Promoting the sharing of scientific knowledge through any form of publication.

# Medical Writing

We at ARC Publishing provide a wide range of services aiming at satisfying different medical writing needs.

**Scientific writing for publication purposes**

*You are a busy clinician with great data but your everyday tasks deprive you from the time necessary for their analysis and reporting.*

For those who have data but do not have enough time to prepare their publication, we provide a wide range of solutions.

Our staff will be pleased to write your:

- Manuscripts for peer-reviewed journals
- Abstracts for congresses or proceedings books
- Poster presentations
- Oral communications

In addition, we can also review your academic thesis, book chapter or any other scientific material.

**Medical writing and translation for organisations**

*You are an organisation interested in preparing scientific materials.*

For those organisations (e.g. a company, an institute, a medical association or society, etc.) aiming to disseminate scientific knowledge, we have the solution!

Our staff will be pleased to help you:

- Translate any study document from Portuguese to English or from English to Portuguese
- Write manuscripts, posters, oral communications or any other form of communicating your results
- Write online scientific content
- Edit and publish conference proceedings
- Edit and publish scientific journals or newsletters

To know more details about our medical writing services, please contact us: **info@arc-publishing.org**

INTERNATIONAL JOURNAL OF
# CLINICAL NEUROSCIENCES AND MENTAL HEALTH



http://ijcnmh.arc-publishing.org

# INSTRUCTIONS FOR AUTHORS

## 1. AIMS AND SCOPE

The International Journal of Clinical Neurosciences and Mental Health is an open-access peer-reviewed journal published trimonthly by ARC Publishing. Our goal is to provide high-quality publications in the areas of Psychiatry and Mental Health, Neurology, Neurosurgery and Medical Psychology. Expert leaders in these medical areas constitute the international editorial board. The journal publishes original research articles, review articles, drug reviews, case reports, case snippets, viewpoints, letters to the editor, editorials and guest editorials. The International Journal of Clinical Neurosciences and Mental Health follows the highest scientific standards, such as the CONSORT / STROBE guidelines and the Uniform Requirements for Manuscripts Submitted to Biomedical Journals (ICJME). The journal offers: • Trusted peer review process • Fast submission-to-publication time • Open-access publication without author fees • Multidisciplinary audience and global exposure

## 2. TYPES OF PAPERS

The International Journal of Clinical Neuroscience and Mental Health publishes scientific articles in the following categories: Original research articles; Reviews; Drug reviews; Case reports; Case snippets; Viewpoints; Letters to the editor; Editorials and guest editorials.

### 2.1. Original research articles

The International Journal of Clinical Neurosciences and Mental Health welcomes original clinical research related with psychiatry, mental health, medical psychology, neurosurgery and neurology. Reports of randomized clinical trials should follow the CONSORT Guidelines and reports of observational studies should comply with STROBE Guidelines. Body text of an Original Research Article should have no more than 4000 words (word count excludes title page, abstract, acknowledgments, references and tables). A maximum of 6 illustrations (figures or tables) are allowed. Supplementary online material may be submitted at the editor discretion.

### 2.2. Review articles and Drug Reviews

Review articles on CNS-related drugs, psychiatry, mental health, medical psychology, neurosurgery and neurology topics are welcome. Both invited and unsolicited submissions are accepted. Manuscripts should be limited to a maximum of 4,500 words, excluding title page, abstract, acknowledgments, references and tables.

### 2.3. Case reports and case snippets

Case Reports and Case Snippets should have no more than 750 and 500 words, respectively (word count excludes references); one figure or table can be included. Only highly meaningful Case Reports are accepted, including major educational content or major clinical findings. Case Snippets should describe a diagnosis or therapeutic challenge.

### 2.4. Viewpoints

Viewpoints should provide an expert opinion on important topics for medical research or practice, with possibility for covering social and policy aspects. This section encourages dialogue and debate on relevant issues with expert views based on evidence. Viewpoints are limited to 1500 words (word count excludes references) and can include one figure or table.

### 2.5. Letters to the Editor

Letters to the Editor should share views on published articles, any findings insufficient for a research article or present ideas of any subject in the scope of the journal.Letters to the Editor have a maximum of 600 words (including references) and can include one figure or table.

### 2.6. Editorials and Guest Editorials

Authors are invited by the Editor-in-Chief to comment on specific topics and express their opinions. Editorials and Guest Editorials have a maximum of 1,000 words and can include one figure or table.

## 3. MANUSCRIPT SUBMISSION

These instructions advise on how the manuscript should be prepared and submitted. Manuscripts that do not comply with the guidelines will not be considered for review. All manuscripts should be prepared in A4-size or US-letter size, in UK or US English. Manuscripts should be submitted in *.doc and *.pdf formats, in the appropriate section of the journal website: https://ijcnmh.manuscripts.arc-publishing.org

### 3.1. Cover Letter

A cover letter should be submitted together with the manuscript, in *.doc or *.pdf format, addressed to the Editor-in-Chief. A template for the cover letter is available for download in the journal website. The cover letter should contain statements about originality of your publication, Ethics Committee approval and informed consent (if applicable), conflicts of interest and why in your opinion your manuscript should be published.

### 3.2. Manuscript Preparation

The manuscript must be divided in 2 files: the Title page (submitted in *.doc format and *.pdf formats) and the Manuscript body (submitted in *.doc and *.pdf formats).

TITLE PAGE > This should be submitted as a separate file from your manuscript (to assure anonymity in the peer review process) and should include: Article title; Authors' names, titles (e.g. MD, PhD, MSc, etc.) and institutional affiliations; Corresponding author: name, mailing address, telephone and fax numbers; Keywords (maximum of 10); A running head (up to 50 characters); Abstract word count (up to 250 words); Body text word count; The number of figures and tables.

MANUSCRIPT BODY > The Manuscript body must be anonymous, not containing the names or affiliations of the authors. Manuscript body must be structured in the following order: title, abstract, body text, acknowledgements, references, tables, and figures captions/legends. The text must be formatted as follow: • Arial fonts, size: 11 points • Single line spacing (see paragraph menu) • Aligned to the left (not justified) • Showing continuous line numbers on the left border of the page *(For MS Word you can add line numbers by going to: Page Layout -> Line Numbers -> select "Continuous"; for OpenOffice: Tools -> Line Numbering -> tick "Show numbering")*

***Title:*** A descriptive and scientifically accurate article title should be provided.

***Abstract (250 words maximum):*** An abstract should be prepared for Original Research Articles, Review Articles and Drug Reviews. Should be structured and include: background/objective, material and methods, results, and conclusions. These sections should be separated by the respective headings. If the publication is associated with a registered clinical trial, the trial registration number should be referred at the end of the abstract.

***Body text:*** Original research articles: Original research articles should be structured as follows: Introduction: Should present the background for the investigation and justify its relevancy. Claims should be supported by appropriate references. Introduction should end by stating the objectives of the study. Methods: Should allow the reproduction of results and therefore must provide enough detail. Appropriate subheadings can be included, if needed. Results: Should include detailed descriptions of generated data. This section can be separated into subsections with concise self-explanatory subheadings. Discussion and Conclusions: Should be brief but comprehensive and well argued, summarise and discuss the main findings, their clinical relevance, the strengths and limitations of the study, future perspectives with suggestion of experiments to be addressed in the future. Review articles and Drug Reviews: These types of articles should be organized in sections and subsections.

***Acknowledgements:*** This section should name everyone who has contributed to the work but does not qualify as an author. People mentioned in this section must be informed and only upon consent should their names be included along with their contributions. Financial support (with grant number, if applicable) should also be stated here. Any conflict of interests should be declared. If authors have no declaration it should be written: "The authors declare no conflict of interests".

***References:*** References citation in the text should be numbered sequentially along the text, within brackets.

The use of a reference management tool (such as Endnote or Reference Manager) is recommended. References must be formatted in Vancouver style. Only published or accepted for publication material can be referenced. Personal communications can be included in the text but not in the references list.

***Tables:*** Tables should be smaller than a page, without picture elements or text boxes. Tables should have a concise but descriptive title and should be numbered in Arabic numerals. Table footnotes should explain any abbreviations or symbols that should be indicated by superscript lowercase letters on the body table.

***Figures:*** Figures should have a concise but descriptive title and should be numbered in Arabic numerals. If the article is accepted for publication, the authors may be asked to submit higher resolution figures. Copyright pictures shall not be published unless you submit a written consent from the copyright holder to allow publishing. Each figure file shall not be larger than 30MB. Figures should be tested and printed on a personal printer prior submission. The printed image, resized to the intended dimensions, is almost a replication of how the picture will look online. It shall be clearly perceived, non-pixelated nor grainy. Only flattened versions of layered images are allowed. Each figure can only have a 2-point white space border, thus cropping is strongly advised. For text within figures, Arial fonts between 8 to 11 points should be used and must be readable. When symbols are used, the font information should be embedded. Photographs should be submitted as *.tif or *.eps at high-resolution (300 dpi or more). Graphics should be submitted in *.eps format. MS Office graphics are also acceptable. All figures, tables and graphics should have white background and not transparent. Lines, rules and strokes should be between 0.5-1.5 points for reproducibility purposes.

### 3.3. Supporting Information

***Code of Experimental Practice and Ethics:*** The minimal ethics requirements are those recommended by the Code of Ethics of the World Medical Association (Declaration of Helsinki). Authors should provide information regarding ethics on research participants, patient informed consent, data privacy as well as competing interests. If the authors have submitted a related manuscript elsewhere should disclose this information prior submission.

***Nomenclature:*** All units should be in International System (SI). Drugs should be designated by their International Non-Proprietary Name (INN).

### 3.4. Submission Checklist

Please ensure you have addressed the following issues prior submission: Details for competing interests; Details for financial disclosure; Details for authors contribution; Participants informed consent statement; Contributor copyright authorization of figures included in the manuscript, not produced by the authors and subjected to copyright; Authorship, affiliations and email addresses are correct; Cover letter addressed to the Editor-in-Chief; Identification of potential reviewers and their email addresses (to be introduced at the online submission platform); Manuscript, figure and tables comply with the author guidelines, including the correct format, SI units and standard nomenclature; Separated files for Title page (*.doc and *.pdf) and Manuscript body (*.doc and *.pdf) – 4 in total; Manuscript body does not contain the names or affiliations of the authors. If you have any questions, please contact ijcnmh@arc-publishing.org

## 4. OVERVIEW OF THE EDITORIAL PROCESS

The International Journal of Clinical Neurosciences and Mental Health aims to provide an efficient and constructive view of the manuscripts submitted to achieve a high quality level of publications. The editorial board is constituted by expert leaders in several areas of medicine particularly in Clinical Neuroscience and Mental Health. Once submitted, the manuscript is assigned to an editor which evaluates and decides whether the manuscript is accepted for peer-review. At this initial phase, the editor evaluates if the manuscript fulfils the scope of the journal according to the content and minimum quality standards. For peer-review, one or two additional expert field editors will comment on the manuscript and decide on whether it is accepted for publishing with minor corrections or not accepted for publishing. The editor may ask authors to resubmit after major revision. Decision is based on technical and scientific merits of the work. Reviewers can be asked to be disclosed or stay anonymous. Authors can exclude specific editors or reviewers from the process, upon submission, a rational should be provided. Upon evaluation, an email is sent to the corresponding author with the decision. If accepted, the manuscript enters the production process. It takes approximately 6-7 weeks for the manuscript to be published.

### 4.1. Appeal Process

The editors will respond to appeals from authors which manuscripts were rejected. Their interests should be sent to the Editor. Two directions can be followed: If the Editor does not accept the appeal, further right to appeal is denied; If the Editor accepts the appeal, a further review will be asked. After the new review, the editor can reject or accept the appeal. If rejected, nothing else can be done, if accepted the author is able to resubmit the manuscript.

The reasons for not accepting a manuscript for consideration can be: The manuscript does not follow the scope of the journal; The manuscript has potential interest but there are methodological concerns after peer-review or editorial examination.

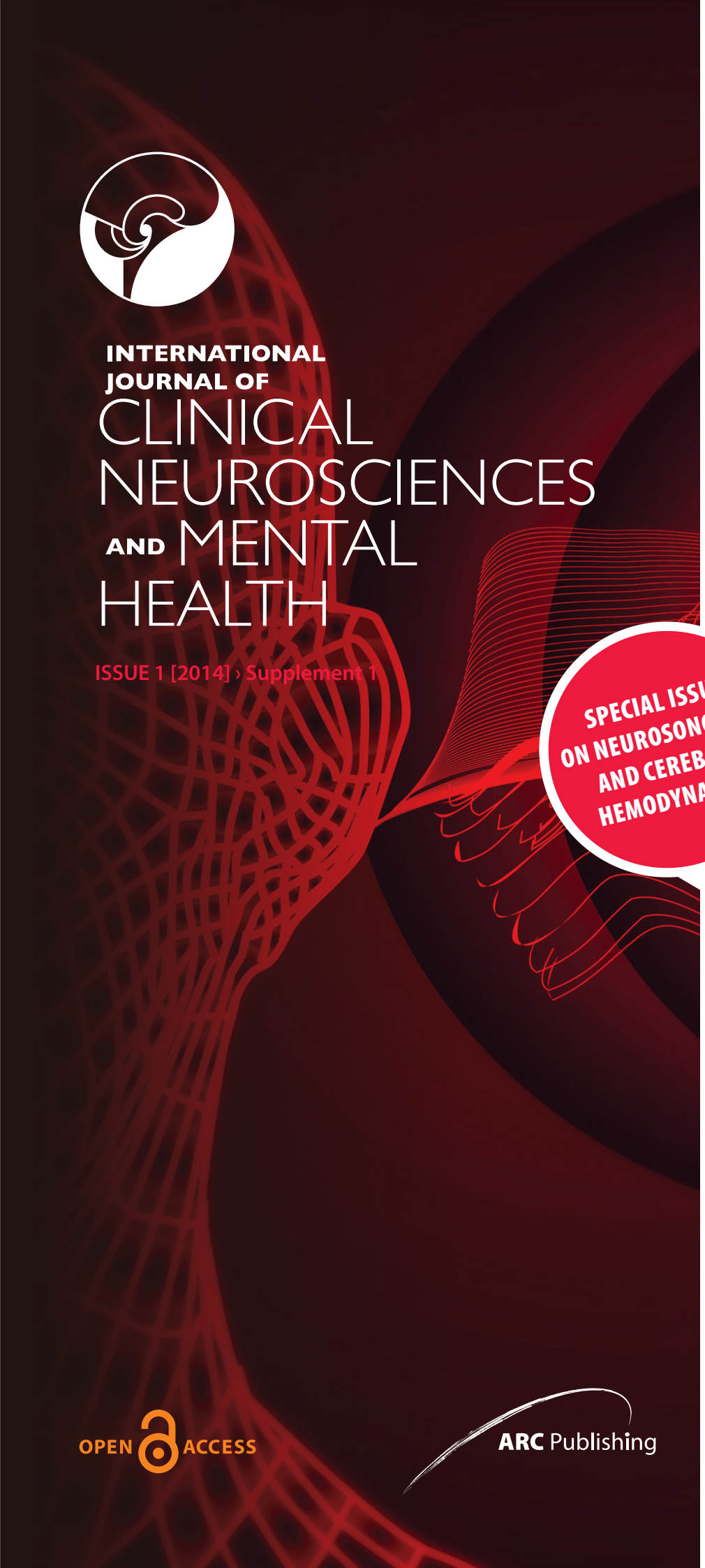

INTERNATIONAL JOURNAL OF
CLINICAL NEUROSCIENCES AND MENTAL HEALTH

ISSUE 1 [2014] › Supplement 1

SPECIAL ISSUE ON NEUROSONOLOGY AND CEREBRAL HEMODYNAMICS

18th Meeting of the
**European Society of Neurosonology and Cerebral Hemodynamics**

3rd Meeting of the
**Cerebral Autoregulation Network**

Porto, Portugal, May 24–27, 2013

**Guest Editors:**
E. Azevedo *(Porto)*
V. Oliveira *(Lisbon)*
J. Sargento-Freitas *(Coimbra)*
D. Russell *(Oslo)*
L. Csiba *(Debrecen)*

OPEN ACCESS

ARC Publishing

# Table of Contents

# Table of Contents (*cont.*)

01

# Guest Editorials

INTERNATIONAL JOURNAL OF
CLINICAL NEUROSCIENCES
AND MENTAL HEALTH

GUEST EDITORIAL

# Carving the foremost developments in neurosonology and cerebral hemodynamics from an inspiring meeting

Elsa Azevedo

President of the Portuguese Society of Neurosonology
Chair of the 18th Meeting of ESNCH and 3rd Meeting of CARNet

Special Issue on Neurosonology and Cerebral Hemodynamics

In May 2013 the international experts on neurosonology and cerebral hemodynamics pooled their knowledge and expertise to produce an historical and fertile scientific meeting. It took the form of a joint meeting between the European Society of Neurosonology and Cerebral Hemodynamics (ESNCH) and the Cerebral Autoregulation Network (CARNet).

The meeting hosted over 400 participants from 47 countries of the five continents in over 30 hours of active discussion and major updates in these fields.

Following on the success of the reunion, the organizing and scientific committees felt compelled to assemble the major breakthroughs of the event in a publication meant to carve these developments for future reference.

The present issue of the International Journal of Clinical Neurosciences and Mental Health began to take shape compiling the various lectures presented throughout the meeting and tutorials, articles with original contributions of innovative findings and exciting case reports.

Authors of selected abstracts of the meeting were invited to participate in this issue, presenting their work as articles. All submissions were reviewed by two members of the scientific committee until final version approval to ensure maintenance of the high methodological standards present all over the conference.

We believe that this issue translates the foremost developments in neurosonology, cerebral hemodynamics and autoregulation during the recent years into a rigorous, comprehensive and extensive publication designed to engrave the memory of a stimulating meeting.

Correspondence: Elsa Azevedo
Department of Neurology, Hospital São João, Faculty of Medicine, University of Porto, Porto, Portugal
Alameda Prof. Hernani Monteiro, 4200-319 Porto, Portugal
Email: elsaazevedo1@gmail.com

Citation: Azevedo, E. Carving the foremost developments in neurosonology and cerebral hemodynamics from an inspiring meeting. IJCNMH 2014; 1(Suppl. 1):S01

Open Access Publication Available at http://ijcnmh.arc-publishing.org



ARC Publishing

INTERNATIONAL JOURNAL OF
CLINICAL NEUROSCIENCES
AND MENTAL HEALTH

GUEST EDITORIAL

# State-of-the-art and new perspectives in Neurosonology

László Csiba

Past-President of ESNCH

Special Issue on Neurosonology and Cerebral Hemodynamics

The neurosonological techniques play an important role in the vascular and non-vascular (degenerative, peripheral nervous system diseases) neurological diseases.

The neurosonological methods proved their strength, not only in the prevention and diagnosis of vascular diseases, but also at intensive care unit monitoring and in therapeutic intervention (e.g. sonothrombolysis and gene therapy) in central nervous system diseases.

The neurosonological methods detect and follow the early impairment of endothelium function and changes of cerebral hemodynamics before and after pharmacological interventions.

This edition summarizes the recent advances of neurosonology, based on the most outstanding presentations of the European Society of Neurosonology and Cerebral Hemodynamics conference organised in Porto, 2013.

Updated results of arterial wall imaging, endothelial dysfunction testing, cerebral blood flow measurement, ultrasound in thrombolysis and new trends will be presented with detailed illustrations.

This book gives an overview about diagnostic and therapeutic advances of extra- and transcranial ultrasound, possible clinical and research applications and, besides "the state of art", the future perspectives will be also presented.

The growing utilization and fast improvement of ultrasonic methods in the diagnosis and therapy of vascular and other diseases justifies an update survey on major breakthroughs.

I hope that this special edition will be useful in the daily work and stimulate the sonologists to use more intensively the neurosonological methods for the benefit of our patients and for clinical research.

Correspondence: László Csiba
Department of Neurology, Debrecen University
4032 Debrecen, Móricz krt.22, Hungary
Email: csiba@med.unideb.hu

Citation: Csiba, L. State-of-the-art and new perspectives in Neurosonology. IJCNMH 2014; 1(Suppl. 1):S02

# 02
# Reviews

INTERNATIONAL JOURNAL OF
CLINICAL NEUROSCIENCES
AND MENTAL HEALTH

REVIEW

# Physics of ultrasounds

Victor Oliveira[1]

Special Issue on Neurosonology and Cerebral Hemodynamics

## Abstract

Neurosonology relies on the use of ultrasounds adapted to the characteristics of the human body, mainly the density of biological structures in order to obtain imaging of vessels, brain parenchyma and muscles as well as the Doppler Effect to study velocities of the blood flow.

Aside from the expertise to perform examinations, a sonographer must be aware of the physics behind the machine in order to better understand the capabilities and limitations of these exams.

We summarize the most important principles used in neurosonology.

**Keywords:** Transcranial Doppler, Doppler effect, Blood flow velocity, Fast fourier transform, Pulse repetition frequency.

[1]Department of Neurology, Hospital Santa Maria, Lisboa, Portugal

Correspondence: Victor Oliveira
Department of Neurology, Hospital Santa Maria
Avenida Professor Egas Moniz, 1649-035 Lisboa, Portugal
Email adress: voliveira98@hotmail.com

Citation: Oliveira et al. Physics of ultrasounds. IJCNMH 2014; 1(Suppl. 1):S03

Received: 08 Sep 2013; Accepted: 20 Nov 2013; Published: 09 May 2014

Ultrasound (US) imaging and Doppler Effect (**Figure 1**) are major achievements in physics and their application to medicine has provided a number of advantages in the investigation the vascular system.

One should remember Christian Andreas Doppler (1803–1853), an Austrian mathematician from Salzburg concerned with color variation of the stars who stated that the color changes in time were due to the relationship between the speed of light and the speed of the moving stars [1].

Medical applications in vascular medicine had another milestone in the 1950's when the Japanese scientists Shigeo Satomura and Ziro Kaneko produced the first ultrasound device able to register Doppler shift in blood vessels; the so called "Doppler Rheograph" [2, 3].

Since then, fast developments in technology have allowed a wide diffusion of a number of reliable devices joining the capability to depict vascular structures and at the same time, measuring blood flow velocities.

In 1982, another milestone happened when Rune Aaslid introduced a device able to register Doppler signals through the intact skull [4].

The use of ultrasounds in vascular medicine and in cerebral circulation in particular seems to have an endless way to pursue.

Continuous Doppler, pulsatile Doppler, transcranial color coded Doppler (TCCD) and Doppler monitoring for diagnosis as well as to assist thrombolysis [5] are some of the various modalities instigate for cerebrovascular medicine.

Knowledge of the physics of ultrasound is fundamental for the sonographer to understand the technologies that one is using.

To produce ultrasounds applied to vascular medicine it is necessary to use a device where the main component are crystals or ceramic which when stimulated by an electric current, vibrate at high frequency (piezoelectric effect), producing ultrasonic waves. The frequency of these ultrasonic waves depends on the composition of the piezoelectric component and on the electric current that activates it.

These piezoelectric elements in the probe have also the capability to act reversibly, that is: to receive back the pressure of ultrasonic energy and transform it into electrical energy.

That energy is processed by the equipment to allow depiction imaging and also to display measurements.

For medical diagnosis the frequency ranges from 7.5–10 MHz for vascular and other superficial structures to 2–5 MHz for deeper structures like abdominal organs. Higher frequencies give a better resolution but are weaker in penetration than lower frequencies [6].

Different densities absorb different amounts of US energy (acoustic impedance). High density structures, like the bones, capture the large majority of ultrasound of energy so there is no refection. This is why there is major limitation for imaging bones by ultrasounds.

While crossing different structures with different densities, ultrasounds are subject to several phenomena that weakens their energy (attenuation): A part of it is retained within the structures and is turned into heat (absorption). Some amount diverges erroneously when hitting irregular surfaces (scattering). Others diverge when crossing interfaces and will not be re-captured by the probe (divergence) [7].

Attenuation, coefficient of body structures, is lower for water, blood and fat but is higher for bones [8].

The heart of the US equipment is the probe allowing, emitting and receiving US signals.

Piezoelectric elements can be arranged in the probe in different ways.

## Types of probes

Linear array - elements are placed one after another emitting parallel beams. The surface of the probe is flat, producing square images. It is used for superficial vascular imaging.

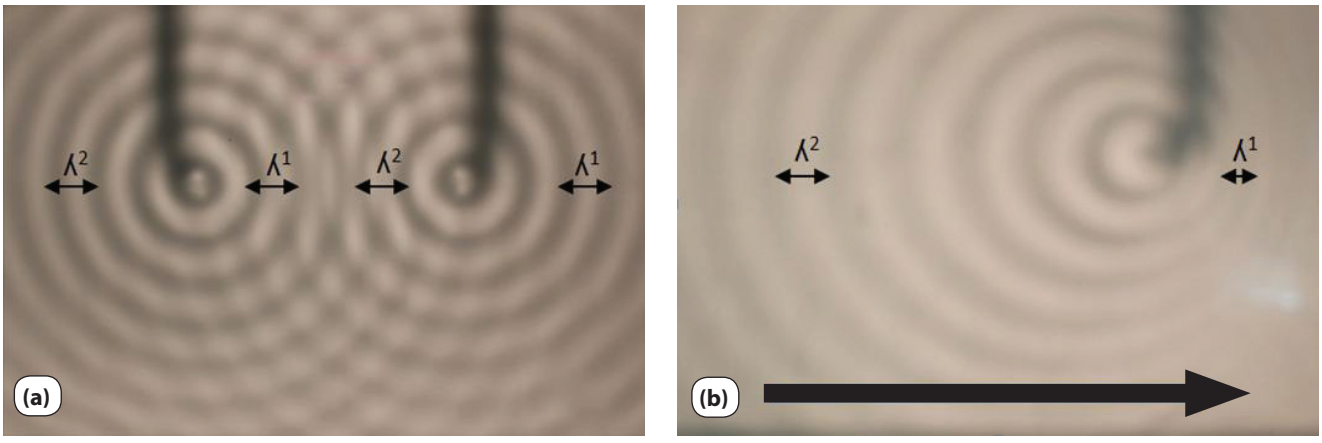


**Figure 1. The Doppler Effect:** Wavelength: spatial period of a wave (λ): **(a)** Two stationary sources of acoustic waves: sound pitch (frequency) perceived equal both on the left and on the right sides ($\lambda^1 = \lambda^2$): no Doppler effect; **(b)** A source of acustic waves moving from the left ($\lambda^2$) to the right ($\lambda^1$): Sound pitch (frequency) perceived higher on the right than on the left sides ($\lambda 1 > \lambda 2$).

Sector array - elements are placed concentrically emitting a divergent beam depicting a sector image. The surface of the probe is convex. It is used for deep structures such as abdominal viscera, echocardiography and also for TCCD.

Phased array - is an electronic sector scanner formed by a group of elements that fires sequentially with a defined time delay from the previous one. The total ultrasound information received may scan tissues at a pre-defined angle. A major advantage is to use merely a small coupling area. This is particularly useful in echocardiography and transcranial Doppler.

## Main physical principles of ultrasound

US are emitted intermittently, pulsing with a determined frequency this is an important characteristic called pulse repetition frequency (PRF).

PRF can be defined as the number of pulses emitted by unit of time. It must be issued in a way allowing US pulse to make its way to the target and return back to the probe. For medical purposes PRF ranges from 1 to 10 KHz [9].

PRF must be at least twice the Doppler shift in order to be registered. This is defined by the Nyquist sample theorem that states that image must be sampled at twice the higher frequency of signal [10].

Waveforms are depicted according to the Fourier Transform calculation in the common version of Fast Fourier Transform (FFT) converts time into frequency and vice versa. In short this allows extracting amplitude and frequency from the Doppler signal depicting the distribution of flow velocities/speeds.

When the values are lower than this, an artifact occurs (aliasing). This a common experience when, as in motion pictures, the spokes of the wheels of a car or the fans an airplane seem to run in the opposite direction to reality.

In US imaging, the waveform is depicted with the upper part of the wave in the bottom of the image.

## Doppler effect

This is a major application of US in medicine, mainly for the study of blood flow velocities.

Doppler Effect consists in the emission of an US beam that hits a moving object, in our case, elements of blood.

The velocity of the reflected beam is modified according to the direction and velocity of the moving blood elements, the piezoelectric element that switches US into electric energy. This allows quantification of the velocities and the identification of the direction in relation to the probe: toward or away to the blood flow direction.

Ultrasound beams are emitted intermittently in a pulsatile manner with a predefined frequency per second (pulse repetition frequency—PRF) in order to reach the target and be backscattered in a defined period of time.

The PRF must be set, in order to allow the transducer to receive the signal back before a new one can be emitted. For diagnostic purposes the US signal is formed by a range of frequencies (frequency spectra).

The most accurate measurements are obtained when the ultrasound beam and blood flow are in the same direction forming an angle of 0º. This corresponds to a value of cos θ = 1. The value of θ varies between 0 and 1. Since this is rarely the case in circulation, it is necessary to consider the angle formed by the incidence of the US beam with the blood flow in order to obtain the real velocity. At the limit, an angle of incidence of 90º (cos θ = 0) of the detect-

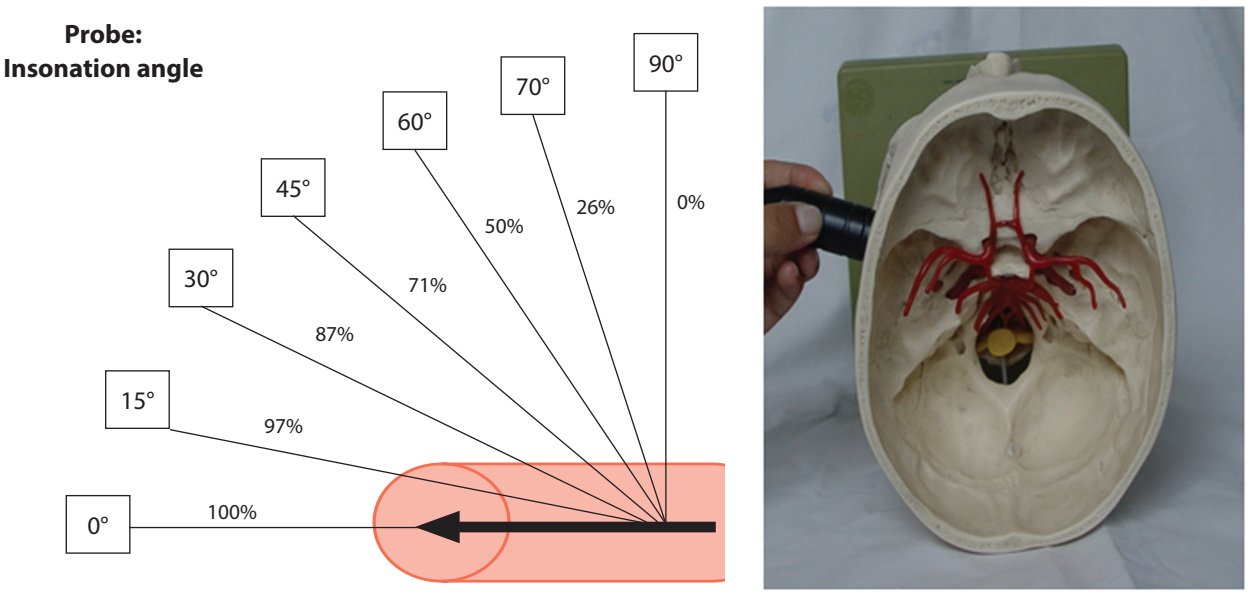


**Figure 2.** Transcranial Doppler: Insonation of Middle Cerebral Artery. The probe is in same direction of the blood flow, (Angle 0°).

able Doppler shift occurs and so, no measurement will be possible (**Figure 2**).

Color codification of the Doppler Effect allows easy identification of blood flow in small and deep structures. Since a moving flow will be depicted in color and so easily identified.

Color coded imaging is also useful to identify flow direction (to or away from the probe). Stenotic and irregular beds of vessels will cause acceleration or turbulent flows which will be depicted in color with characteristic patterns.

Blood flow velocities evaluated by means of Doppler Effect together with the B-Mode depiction of the vessel walls provide an important tool in vascular medicine since it allows us to measure flow velocities in a defined point of a vessel by placing a cursor in a specific point of the B-Mode image of the vessel (**Figure 3**).

To enhance color Doppler imaging it may be useful to use Doppler Power. This has the capability to depict in one single color the Doppler Effect. The advantage is enhanced since all the Doppler Effect is depicted in one single color. The major drawbacks are absence of information in direction and changes in velocity of flow (**Figure 4**). Transcranial Doppler sonography uses pulsed wave Doppler at mainly 4 MHz which can cross the skull into some regions of the lower density bone windows (**Figure 5**). This is remarkable because ultrasound waves must cross the bone window twice, once each way. Despite a large amount of lost energy, the remainder is still enough to be interpreted.

Since the B-Mode only scarcely crosses the bone, limited information can be obtained by this method, blood flow velocities being the most important tool.

Transcranial Color Code Doppler (TCCD) is obtained by current Duplex Doppler machines with specific software and using 4MHz probes.

Again, B-Mode imaging is very limited but depiction of the Doppler Effect of moving blood in vessels, allows for an indirect representation of the vessels.

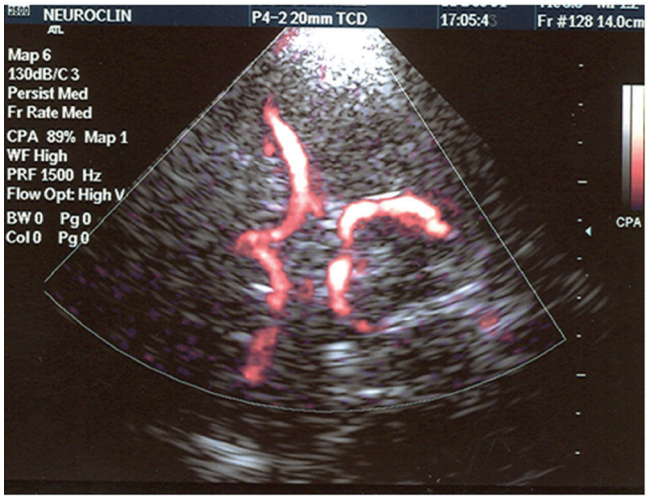


**Figure 4**. Transcranial color coded Doppler (TCCD): Circle of Willis. Color coded blood flow velocities in "Power Doppler" mode indirectly depicts the vessels.

## Conclusions

In spite of their limitations US gained a definitive role in the investigation of all vascular patients.

Digital subtraction angiography and more recent modalities with computerized tomography (Angio-CT) and magnetic resonance (Angio-MR) have their role but also their limitations, but measurements of blood flow velocities are generally more accurate and easily obtained with Doppler technology.

For current investigations such as screening, diagnostics, monitoring purposes or even to decide upon a surgical option such as endarterectomy [11], vascular ultrasonography is an important tool.

Some of the main advantages include; non-invasiveness, no discomfort for the patient, no preparation needed,

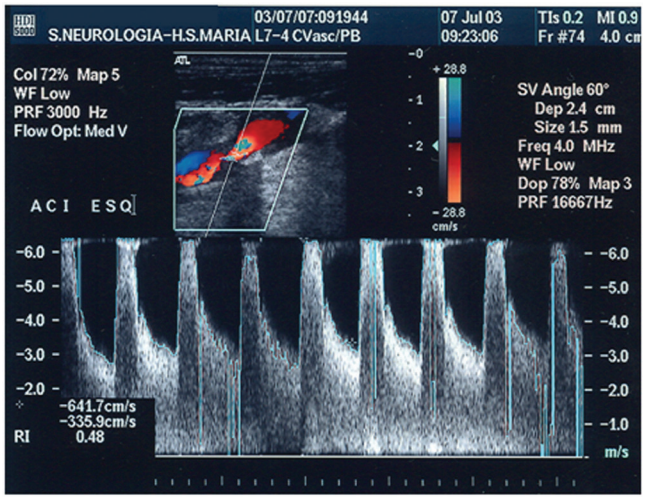


**Figure 3**. Color Duplex Scan: Internal carotid plaque causing high grade stenosis. Calcified plaque produces ultrasonic shadow. Mixed colors, meaning a turbulent flow. Blood flow velocities are depicted in waveforms.

**Figure 5.** Trans-illuminated skull: The temporal bone windows.

easily available, relatively non-expensive, repeatable without limitations and interpreted in real time.

Recent technologies produce small and portable equipments allowing bed-side examinations on wards in hospitals, emergency departments and even operating rooms, but on the other hand, one must be aware that this method is "operator dependent" meaning that expertise and anatomical, as well as clinical knowledge, is necessary to correctly perform and interpret these examinations.

## Abbreviations

FFT: Fast fourier transform; PRF: Pulse repetition frequency; TCCD: Transcranial color coded Doppler; US: Ultrasound

## Competing interests

The author declares no conflict of interest.

## References


1. Eden A. Christian Doppler: Leben und Werk. Salzburg: Landespressebureau. 1988.
2. Kaneko Z, Kotani H, Komuta K, Satomura S. Studies on peripheral circulation by Ultrasonic Blood Rheograph. Jpn Circ J 1961; 25:203-13.
3. Kato K, Kido Y, Motomiya M, Kaneko Z, Kotani H. On the mechanism of generation of detected sound in ultrasonic flowmeter. Memoires. Inst. Scient. Indust. Res. Osaka Univ. 1962; 19: 51-7.
4. Aaslid R, Markwalder T-M, Nornes H: Noninvasive Transcranial Doppler ultrasound recording of flow velocity in basal cerebral arteries. J Neurosurg 1982; 57:769-74.
5. Alexandrov A, Molina C, Grotta, J, Garami Z, Ford S, J. Alvares-Sabin et al. Ultrasound-enhanced systemic thrombolysis for acute ischemic stroke. NEJM 2004; 351: 2170–2178.
6. Chan VWS. Ultrasound Imaging for Regional Anesthesia. Toronto Printing Company. 2009.
7. Thrush A, Hartshorne T. Peripheral Ultrasound: How, Why and When. Elsevier Churchill Livingstone. 2005.
8. White P, Clement G, Hynynen K: Longitudinal and shear mode ultrasound propagation in human skull bone. Ultrasound in Medicine and Biology 2006; 32:1085-96.
9. Bogdahan U, Becker G, Schlachetzki (ed). Echoenhancers and transcanial color duplex sonography. Blackwell Wissenschafts – Verlag, Berlin – Wien. 1998.
10. Bartels E. Color-coded duplex ultrasonography of cerebral vessels. F K Schattauer Verlagsgesellschaft mbH, Stuttgard. 1999.
11. McDowell H, Gross G, Halsey J. Carotid endarterectomy monitored with transcranial Doppler. Ann Surg 1992; 21: 514–19.

INTERNATIONAL JOURNAL OF
CLINICAL NEUROSCIENCES
AND MENTAL HEALTH

REVIEW

# Ultrasonography of carotid stenosis

Jürgen Klingelhöfer[1]

Special Issue on Neurosonology and Cerebral Hemodynamics

## Abstract

The classification of internal carotid artery stenosis is of great impact. The degree of stenosis is the main criterion for the decision between an invasive or non-invasive treatment of extracranial internal carotid artery (ICA) stenoses. By now the North American Symptomatic Carotid Endarterectomy Trial (NASCET) criteria have been internationally approved for radiological grading. According to NASCET the stenosed lumen is compared with the lumen of the distal internal carotid artery. All ultrasound criteria do have limitations and can therefore cause pitfalls in determining the degree of stenosis using one criterion exclusively. Therefore a multi-parametric grading of stenoses should be favored. The multi-parametric "DEGUM" ultrasound criteria have been revised and a novel differentiation between main (primary) and additional (secondary) criteria has been proposed. Recently a similar consensus was reached by the Neurosonology Research Group (NSRG) of the World Federation of Neurology (WFN). Main criteria include the following: imaging of the stenosis in B-mode sonography; visualization of the stenosis by color-coded imaging of flow; measurement of the maximum systolic flow velocity in the area of greatest narrowing of the lumen; systolic flow velocity measurement in the poststenotic segment; assessment of the collateral supply. Additional criteria include the following: indirect findings of an internal carotid artery stenosis in the common carotid artery; evidence of flow disturbances; end-diastolic flow velocity in the area of greatest narrowing of the lumen; the so-called confetti-sign; the carotid ratio. The main advantage of a multi-parametric grading of ICA stenoses is the synergetic effect of the different single criterion. Combining these ultrasound criteria, neurosonography allows reliable grading of carotid stenoses as a basis for decision making.

**Keywords:** Carotid stenosis, ICA stenosis, Degree of stenosis, Duplex ultrasonography, Peak systolic velocity, NASCET, ECST.

[1]Department of Neurology, Medical Center Chemnitz, Chemnitz, Germany

Correspondence: Jürgen Klingelhöfer
Department of Neurology, Medical Center Chemnitz
Dresdner Straße 178, 09131 Chemnitz, Germany
Email adress: juergen_klingelhoefer@gmx.de

Citation: Klingelhöfer, J. Ultrasonography of carotid stenosis. IJCNMH 2014; 1(Suppl. 1):S04

Received: 12 Sep 2013; Accepted: 23 Dec 2013; Published: 09 May 2014

Open Access Publication Available at http://ijcnmh.arc-publishing.org



ARC Publishing

## Introduction

Ultrasonography of the carotid arteries is the modality of choice for triage, diagnosis, therapy and monitoring of patients suffering from atherosclerotic disease. The degree of stenosis is the main criterion for the decision between an invasive (thromboendarterectomy (TEA) or dilatation and stent) or non-invasive treatment of extracranial ICA stenoses. In asymptomatic stenosis the rapid increase in the degree of stenosis is the most important indicator of an increased risk of stroke [1].

## NASCET versus ECST

In Germany, as in other European countries, the local diameter narrowing (European Carotid Surgery Trial (ECST) method) was popular [2, 3] whereas in North America the distal diameter of the ICA was taken as denominator (distal diameter narrowing, North American Symptomatic Carotid Endarterectomy Trial (NASCET) method) [4]. According to NASCET the stenosed lumen is compared with the lumen of the distal ICA (**Figure 1**). By now the NASCET criteria have been internationally approved for radiological grading.

In **Table 1** degrees of stenoses measured by NASCET method are compared to the ones of the same stenoses measured by ECST method. The ECST method results in higher degrees of stenosis especially in the range of up to 70% stenosis. That is why the same stenosis can be classified as 50% (NASCET) by a radiologist and 70% (ECST) by an ultrasound investigator.

This is why measuring following the ECST method and recommending carotid surgery following the NASCET criterion of 70% can be a possibility of a malpractice.

Therefore it is essential that the different methods used for the classification (either NASCET or ECST) are mentioned in the findings.

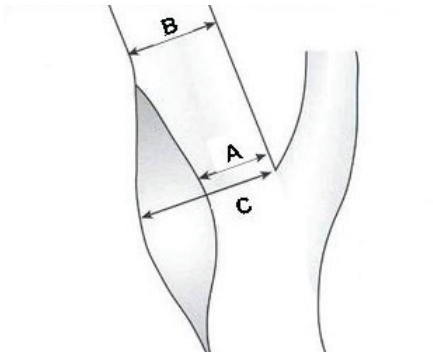


**Figure 1.** Different methods for grading carotid stenosis. Differentiation between the European Carotid Surgery Trial (ECST) and the North American Symptomatic Carotid Endarterectomy Trial (NASCET).

ECST: Percentage of local diameter reduction: the degree of stenosis **(A)** is determined in relation to the original lumen **(C)** of the ICA **(A vs. C)**.

NASCET: Percentage of distal diameter reduction: the degree of stenosis **(A)** is determined in relation to the distal lumen **(B)** of the ICA **(A vs. B)**.

**Table 1.** Classification of the same stenosis measured by NASCET and by ECST.

| Degree of stenosis | |
|---|---|
| **NASCET method** | **ECST method** |
| 30% | 50-60% |
| 50% | 70% |
| 60% | 75% |
| 70% | 80% |
| 80% | 90% |

### Conversion from ECST to NASCET and vice versa

It is possible to perform a conversion [5] from ECST to NASCET using this formula:

$$\text{NASCET\%} = (\text{ECST} - 40)\% / 0.6$$

A conversion from NASCET to ECST is possible by using this formula:

$$\text{ECST\%} = 40 + 0.6 \times \text{NASCET\%}$$

## Peak systolic velocity as exclusive hemodynamic parameter for the classification of stenosis

Between Europe and North America there was another basic different methodological approach in classification of ICA stenosis. North America classifies stenoses using only one hemodynamic parameter as the primary and only criterion defined in a consensus of the Radiological Society of North America (RSNA)[6].

This only hemodynamic parameter represents the lower limit value of peak systolic velocity (PSV) (**Figure 2**), which includes any possible findings of stenoses ≥70%. The intention of this methodological approach of the RSNA was not to quantify stenoses in steps of 10% but to dichotomize them in ≥70% or <70%, to dichotomize in invasive such as TEA or non-invasive, conservative therapy. Here the RSNA demands a threshold-PSV that includes all stenoses that are classified ≥70%. For this threshold-PSV different values are published in literature. Moneta et al. analyzed this at a bigger sample [7]. If for stenoses classified 60-99% (NASCET) a threshold-PSV of 200 cm/s was assumed, then the sensitivity was high (93%) and the specificity low (76%) with an accuracy of 84% at which the accuracy was defined as the maximum sum of sensitivity and specificity. If for stenoses 60-99% (NASCET) a threshold-PSV of 300 cm/s was assumed, then the sensitivity was as well high (95%) and the specificity low (78%) with an accuracy of 87%. Assuming a threshold-PSV of 260 cm/s for stenoses of 60-99 % (NASCET) the accuracy of 88% has been the highest; meanwhile the sensitivity was 86% and the specificity 91%.

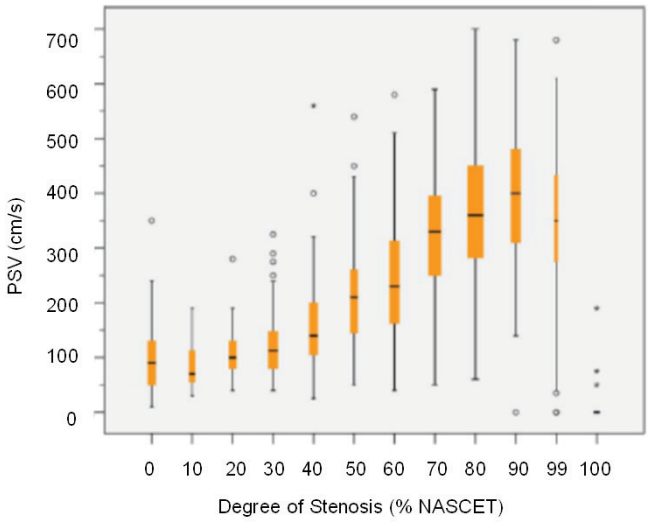


**Figure 2.** Box plot chart of peak systolic velocity (PSV; cm/s) vs NASCET degree of stenosis (%) for 977 stenoses from 5 studies [7-11]. The plot shows median PSV, 25% to 75% (boxes), and 0% to 100% interquartile range (T-bars), except outliers (circles) and extreme values (stars) [12].

## Does the approach of peak systolic velocity alone provide a sufficient reliable and reproducible grading of carotid stenoses and valid results?

A consensus for threshold values based on a meta-analysis was published [6]. There are also several publications of correlations between PSV and the degree of stenosis measured by X-ray angiography which have shown substantial scattering of results in all published studies [7-12]. That was the reason for the NASCET group [13] and recently the American Heart Association to not recommend carotid surgery in symptomatic patients if diagnosed only on duplex sonography [14]. A stenosis can be graded following its morphologic effects using the more morphologically orientated angiography or by its hemodynamic effects using the more hemodynamically orientated ultrasonography. Both techniques do have their limitations. This is the reason why there is no perfect correlation between these different approaches. The PSV—for many reasons and no matter what threshold-PSV chosen—is only of limited value if taken alone as well as this criterion is very often in disagreement with the angiographic result.

It is well-known that there are many factors that might influence the PSV, which are briefly described here.

### Technical parameters

Technical parameters that can affect the accuracy of carotid ultrasonography results include the Doppler angle, sample volume box, color Doppler sampling window, color velocity scale, and color gain [15].

### Doppler angle

At the one hand the angle of insonation can influence the PSV to a critical point (**Figure 3**), on the other hand errors and different conventions especially occur while positioning the Doppler angle. The measuring of the angle of insonation is needed for converting recorded Doppler frequencies into velocities [16]. The recordings of the highest frequencies in systole reveal from the streamlines with the highest velocities and with the smallest Doppler angle (**Figure 3**). Due to the cosine function (Doppler equation) the possible error converting Doppler shift to velocity increases with increasing Doppler angle. This is the reason why the variability of velocity estimation is higher if compared to the recorded frequency. In disturbed flow conditions with stream lines that differ from the vessel course it is more difficult to estimate the Doppler angle. This can be done at least fairly well in laminar conditions.

### Spectrum analysis

The technical problems of spectrum analysis can also significantly affect the PSV. Due to vortices and flow separation there are low-frequency components as well as high-frequency (velocity) components representing the jet within the typical Doppler spectrum generated by a short stenosis. Underestimation of the PSV can happen due to the too low relative weight of the high-frequency components. Without special filtering this effect would have an even stronger impact [17].

### Morphology of the stenosis

An important component of carotid ultrasonography is to adequately document the location, internal characteristics, and surface detail of plaque. Plaque can be simply characterized as homogeneous or heterogeneous. The pathogenetic substrate is a plaque that causes hemodynamic effects due to an area reduction and surface eventually creating emboli or an occlusion. The anatomic correlate for the

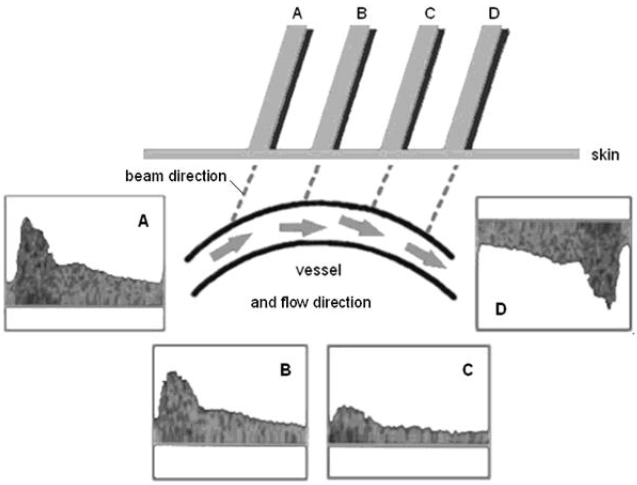


**Figure 3.** Effect of the Doppler angle to the Doppler signal. A higher-frequency Doppler signal (**A**) is obtained if the beam is aligned more to the direction of flow. In the recordings, beam **A** is more aligned than beam **B** and therefore produces higher-frequency Doppler signals. The beam/flow angle at **C** is almost 90° and there is a very poor Doppler signal. The flow at **D** is away from the beam and there is a negative signal.

hemodynamic effect and the measured flow velocities is area reduction by a stenosis not diameter reduction. The type of stenosis—whether it is a concentric or eccentric—is essential for the relationship between area and diameter reduction [18].

### Collaterals

The influence of collateral flow to the PSV is of fundamental importance.

The collateral flow toward the territory supplied by the stenozed artery determines the velocities in a stenosis. The higher the capacity of this collateral network, the less the poststenotic pressure decrease and, consequently, the intrastenotic PSV [19]. Next to the area restriction the resulting pressure drop indicates the PSV. In case of good collateral supply to the irrigated territory this pressure drop is smaller. The result is a reduced flow volume and flow velocity in the severely stenosed artery. In contrast, when there is no collateral supply available very high velocities can be recorded from the same degree of stenosis [19, 20].

### Velocity in a nearly occluded artery

There is the possibility of the same PSV in a moderate stenosis and a nearly occluded artery [18, 21]. The PSV in a stenosis increases with increasing degree of stenosis but decreases in vessels with near occlusion. In 80%-90% stenoses the highest PSV will be seen. The PSV is lower and variable in cases of stenoses near occlusion [19, 22-24]. That is why this criterion of the intrastenotic PSV alone is no good indicator for the differentiation between a moderately stenosed and a nearly occluded artery.

Looking at all these influencing factors it seems obvious that the approach of PSV in terms of being used as a single simplified diagnostic parameter is not reliable. PSV measurements in a stenosis alone are not sufficient to differentiate a moderate from a severe (≥70% NASCET) stenosis with sufficient clinical reliability. The possibility to combine PSV with further criteria makes it possible to decide whether the measured PSV is the result of a less or more severe stenosis within the scatter range. The advantage of a multiparametric approach is that the diagnostic ultrasound offers the possibility of using both morphological and hemodynamic criteria.

Consequently the NASCET method as the morphologic correlate and the colour coded imaging of flow for the detection of low degree diseases and occlusion have been included into the new intersociety guidelines that were published in Germany [22, 25]. Therefore, these multi-parametric "DEGUM" ultrasound criteria have been revised and a novel differentiation between main (primary) and additional (secondary) criteria has been proposed. The "Neurosonology Research Group (NSRG) of the WFN" has reached a similar consensus recently [12]. Both guidelines point out the importance of a multiparametric approach with main and additional criteria. The differentiation between main and additional criteria is caused by the different reliability of the single criterion.

This multiparametric approach allows a grading of severe stenosis in steps of 10%, so it is possible to differentiate between a stenosis of 70%, 80%, 90% or an occlusion.

## The multiparametric approach - Main (primary) criteria

### Criterion 1 - B-Mode

*Non-stenosing plaques (up to 10% according to NASCET)*

Imaging of the plaques is the domain of B-mode sonography in non-stenosing plaques (**Figure 4**).

B-mode sonography provides important information regarding the presence of plaques and their size, morphology, and classification (**Figure 5**). In order to determine their size and location it is helpful to scan several longitudinal and transverse planes. In addition to the size and location of a plaque its surface, structure and echogenicity have to be assessed. For follow-ups a documentation of the maximum thickness and length of a plaque should be made. A percentage grading according to NASCET does not make sense.

### Criterion 2 - Color coded imaging of flow

*Moderate stenoses (20–40% according to NASCET)*

This remains the specific field of B-mode imaging in the longitudinal and cross-sectional planes. The reduction of diameter, the thickness and length of the plaque as well as the residual lumen should be measured. In this case color coded imaging of flow is essential to identify the area of greatest narrowing of the ICA lumen.

The color velocity scale is the most important parameter of the carotid ultrasonography color Doppler setup. The color velocity scale is an operator-defined range of velocities that requires adjustment, analogous to the window width and level of a gray-scale image. It is not synonymous with the pulse repetition frequency (PRF), but the PRF is related to the velocity scale setting, so that increasing the velocity scale increases the PRF and vice versa [26-29]. The image frame rate may appear slow if a very low color velocity scale is applied, since the PRF decreases and the time between transmit pulses in a pulse packet increases [26].

If the velocity of blood flow exceeds ½ the PRF (Nyquist limit), then the direction and velocity are inaccurately displayed and flow appears to change direction (aliasing).

#### Aliasing

The maximum clearly measurable Doppler frequency shift (Fmax) referred to as the Nyquist frequency corresponds to half the PRF:

$$\mathbf{Fmax = PRF/2} \qquad \mathbf{PRF = 2 \times Fmax}$$

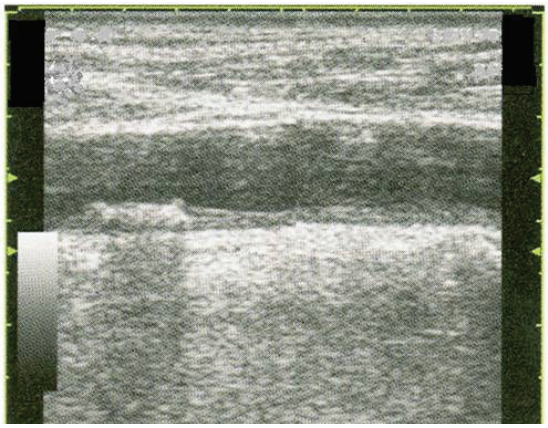

**Figure 4.** Wall thickening over an extended vessel segment. Additionally circumscribed plaques with echogenic spots and distinct acoustic shadowing.

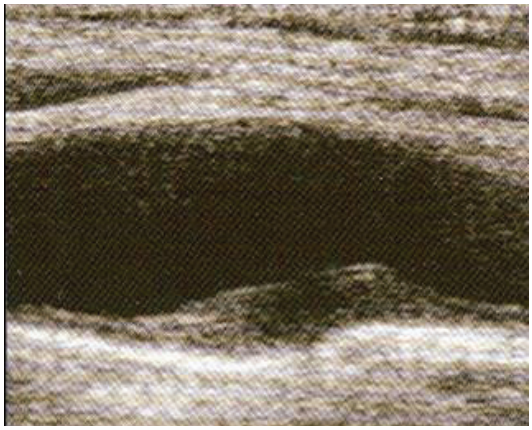

**Figure 5.** Isolated, long hypoechoic plaque.

If the Doppler frequency is greater than half the PRF, it can not be precisely identified.

Consequently the peaks of the spectral curves are cut off and displayed again below the zero line with apparently reversed flow direction (**Figure 6**). This "incorrect" registration, the so-called aliasing phenomenon is also familiar from the cinema: the spoke of a wheel of an accelerating carriage initially turn in the direction of movement, then appear to stop moving (Nyquist limit), then to turn in the opposite direction, and finally with increased acceleration they again turn in the direction of movement. These changes depend on whether the number of revolutions of the wheel is greater or less the frame rate (which in this case represents the Nyquist limit).

In color-coded duplex sonography the frequencies which exceed the aliasing threshold are color coded with the colors of the opposing half of the color scale (**Figure 7** and **Figure 8**). The aliasing phenomenon can be avoided, up to a certain limit, by raising PRF.

Aliasing can be advantageously used to identify the area of greatest narrowing of the ICA lumen

The local flow velocity acceleration is visible by the local aliasing occurring in the area of greatest narrowing of the lumen (at appropriate device setting). Aliasing can be advantageously used to demonstrate high or low flow and turbulence. If the color velocity scale is set below the mean velocity of blood flow, aliasing throughout the entire vessel lumen makes it impossible to identify the high-velocity turbulent color jet associated with a right stenosis. Conversely, if the color velocity scale is set significantly higher than the mean velocity of blood flow, aliasing may disappear, resulting in a missed stenosis (**Figure 9**).

Therefore the adjustment of the appropriate color scale in a carotid artery stenosis is very important. Color Doppler image obtained with the color scale set too low (e.g. 4 cm/s) shows aliasing in the entire segment of the ICA. On the other hand, a color Doppler image obtained with the color scale set too high (e.g. 115 cm/s) shows no

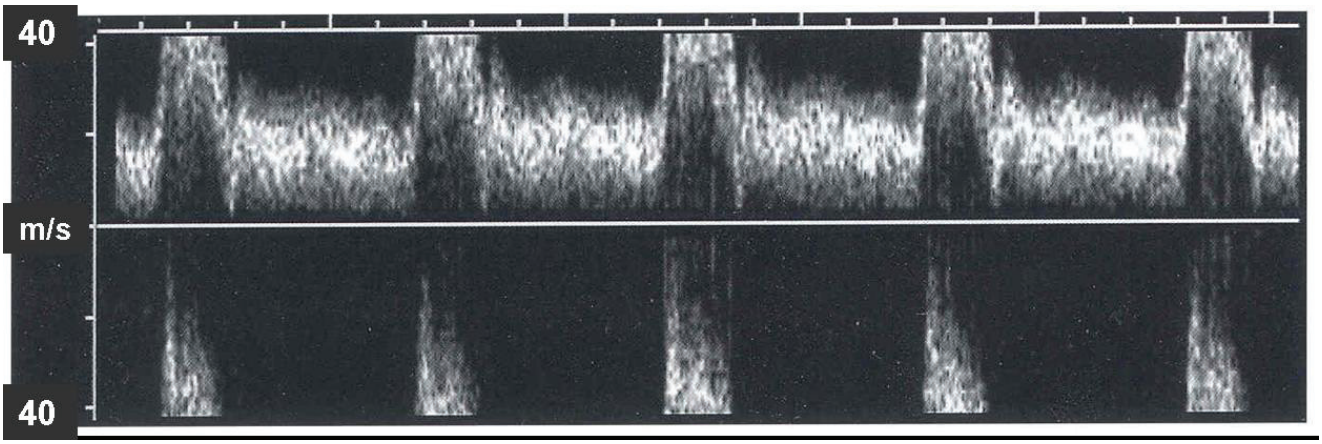


**Figure 6.** Color coding with the aliasing effect.

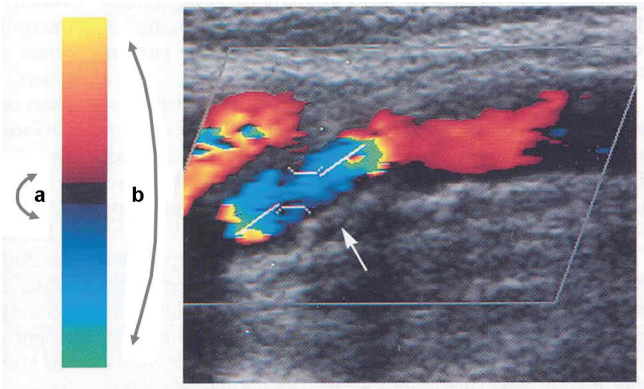


**Figure 7.** Color coding with the aliasing effect. The aliasing effect (shown here in the case of a high-grade stenosis) is characterized by a transition of the orange and yellow shades at one end of the color scale to light blue and green shades at the other end of the scale **(b)** [30].

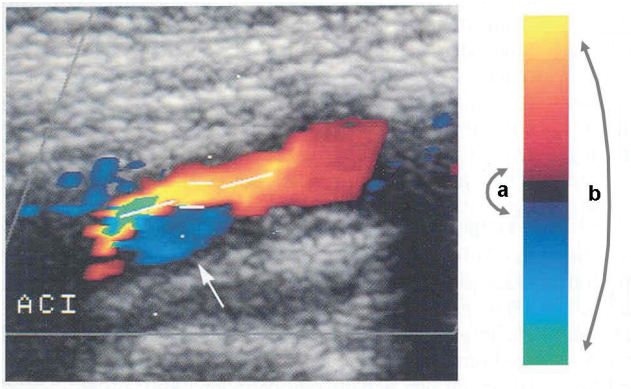


**Figure 8.** Color coding in the case of a true change in flow direction and comparison of true change in flow direction versus aliasing. Folding over or wrapping around of the color as a result of a change in flow direction (distal to a medium-sized plaque). The transition of red to dark blue **(a)** proceeds through a black line which represents a velocity of 0 cm/s [30].

aliasing. Therefore—at a too low color scale—we gradually increase the aliasing threshold (PRF) to a remaining aliasing phenomenon only at a circumscribed segment. Using this procedure we can identify the area of the greatest narrowing of the ICA lumen. Color Doppler image obtained with the optimal color scale setting shows the region of highest velocity, which corresponds to the narrowest segment of the ICA. Velocity sampling should be performed at this region.

### Criterion 2 - Color coded imaging of flow

*Moderate stenoses (50–60% according to NASCET)*

In these stenoses a combination of B-mode imaging, color flow, local velocity increase should be performed for grading. In general, threshold-PSV is below 230 cm/s. In moderate stenoses collateral flow cannot be found.

Grading of carotid stenosis by diagnostic ultrasound should be primarily based on morphological information

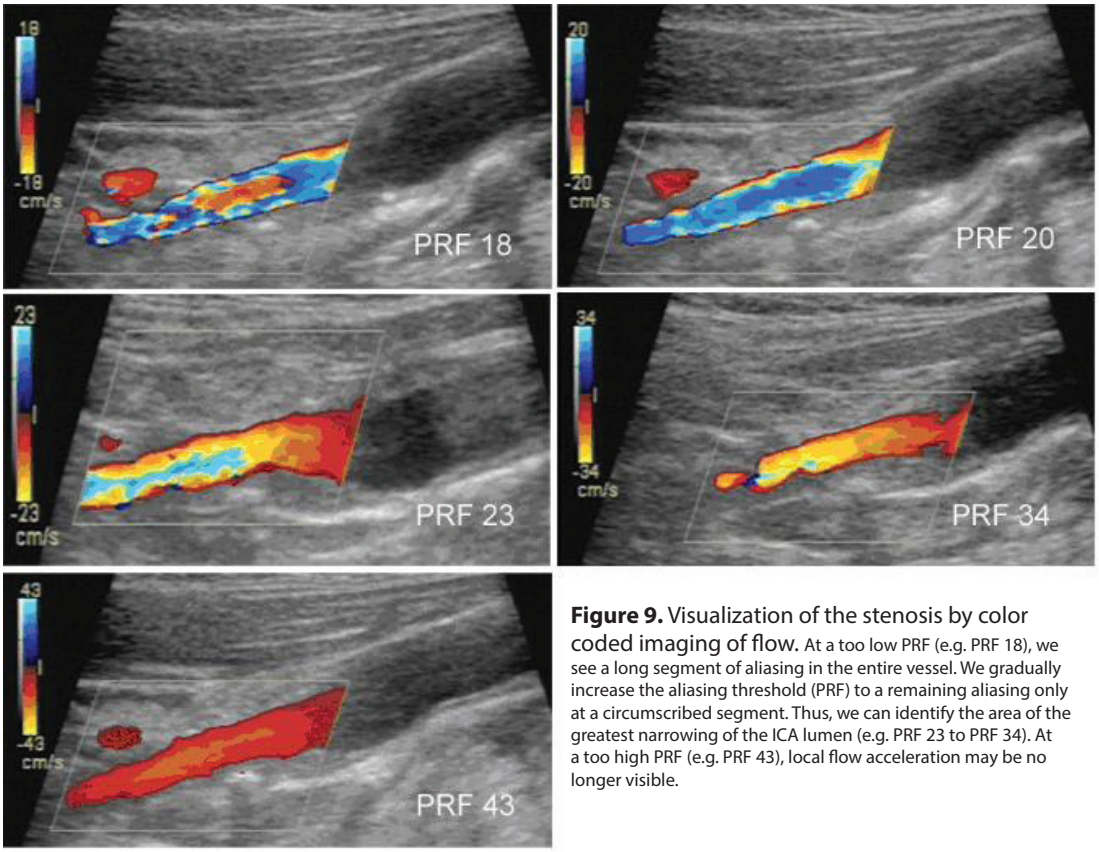


**Figure 9.** Visualization of the stenosis by color coded imaging of flow. At a too low PRF (e.g. PRF 18), we see a long segment of aliasing in the entire vessel. We gradually increase the aliasing threshold (PRF) to a remaining aliasing only at a circumscribed segment. Thus, we can identify the area of the greatest narrowing of the ICA lumen (e.g. PRF 23 to PRF 34). At a too high PRF (e.g. PRF 43), local flow acceleration may be no longer visible.

(B-mode, color coded imaging of flow) in low to moderate degrees of stenosis. In addition the degree of narrowing, plaque thickness, plaque length, and residual lumen should be reported.

### Criterion 2 - Color coded imaging of flow

*High grade, hemodynamically relevant stenosis (>70% according to NASCET)*

In high grade stenoses, the combined hemodynamic criteria, such as increased PSV, end-diastolic velocity and the "carotid ratio" (ratio of internal to common carotid artery PSV) are typically the method of choice (**Figure 10**).

### Criterion 2 - Color coded imaging of flow

*Occlusion of ICA*

Color coded imaging of flow is important as a guide for velocity measurement and is essential for differentiating occlusion from stenosis (**Figure 11**).

### Criterion 3 - Stenotic PSV

The PSV should be measured in the area of greatest narrowing. This area of greatest narrowing should be determined using color coded imaging of flow with adjustment of the PRF (aliasing).The insonation angle should be below 60° (**Figure 3**).

The angle correction has to be set to the direction of jet flow. If the stenosis can not be shown directly due to an acoustic shadow, the Doppler recording occurs in the jet flow immediately poststenotic (**Figure 12**).

In a degree of stenosis below 40% according to NASCET the intrastenotic average-PSV is ≤ 160 cm/s, in case of classification of 50% (NASCET) the average-PSV is 210 cm/s. In case of 60% (NASCET) the average-PSV is 240 cm/s, in case of a stenosis of 70% (NASCET) the threshold-PSV is 230 cm/s and the average-PSV 330 cm/s. In a stenosis of 80% (NASCET) the average-PSV is 370 cm/s. In 80-90% stenoses the highest intrastenotic PSV will be seen. In near occlusion PSV is lower and variable [19, 22-24, 31].

### Criterion 4 - Poststenotic PSV

A further main criterion represents the poststenotic PSV in the vessel section distal to the disturbed flow field. It is recommended that the poststenotic flow velocity distal to the flow disturbances is examined, in which a reduction of velocities (comparison with the unaffected contralateral side) allows additional grading within the category of severe stenosis. Irrespective of the intrastenotic PSV we can assume that in a considerable reduction of poststenotic velocity (e.g. poststenotic PSV <30 cm/s) and signal pulsatility the reduction of ICA diameter is about 90% and the residual lumen is less than 1mm. The extent of the reduction of poststenotic PSV correlates with the reduction of flow volume. The differentiation between 70% and 80% to 90% stenosis (NASCET) is supported by the degree of reduction of poststenotic PSV. Using PSV values alone, this differentiation is not possible.

In a degree of stenosis up to 70% (NASCET) the maximum poststenotic velocity is more than 50 cm/s.

In a degree of stenosis at 80% (NASCET) the maximum poststenotic velocity is below 50 cm/s.

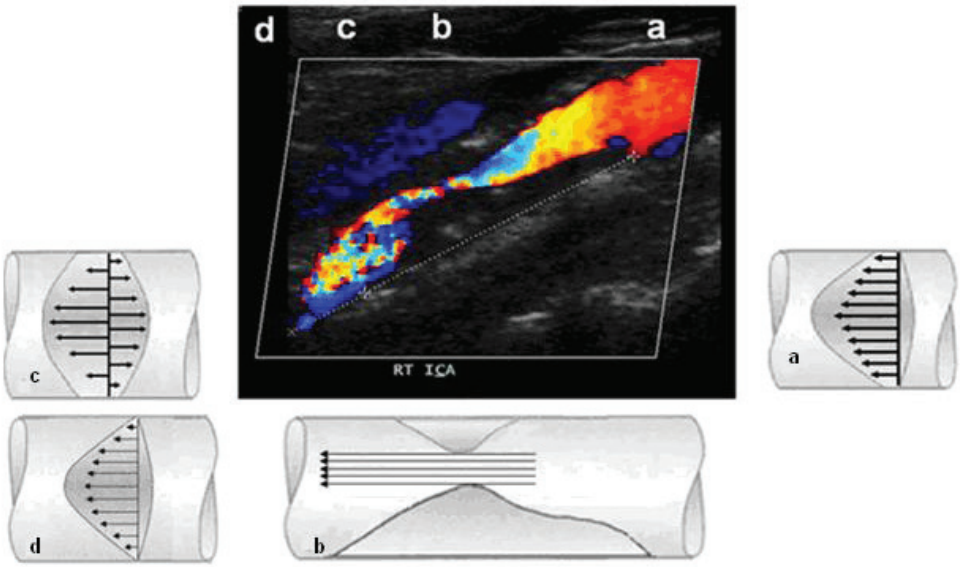


**Figure 10.** High grade stenosis. Prestenotic in the CCA **(a)**: reduced systolic and end-diastolic flow velocity; increased pulsatility (reduced end-diastolic flow velocity due to the increase of the flow resistance). In the stenosed region **(b)** significantly increased PSV (aliasing). Distal to the stenosis **(c)** considerable amount of inverse frequency components. With color coding red and blue shades (separated by a black line, indicate disturbed flow). In the poststenotic region **(d)** reduced flow velocity.

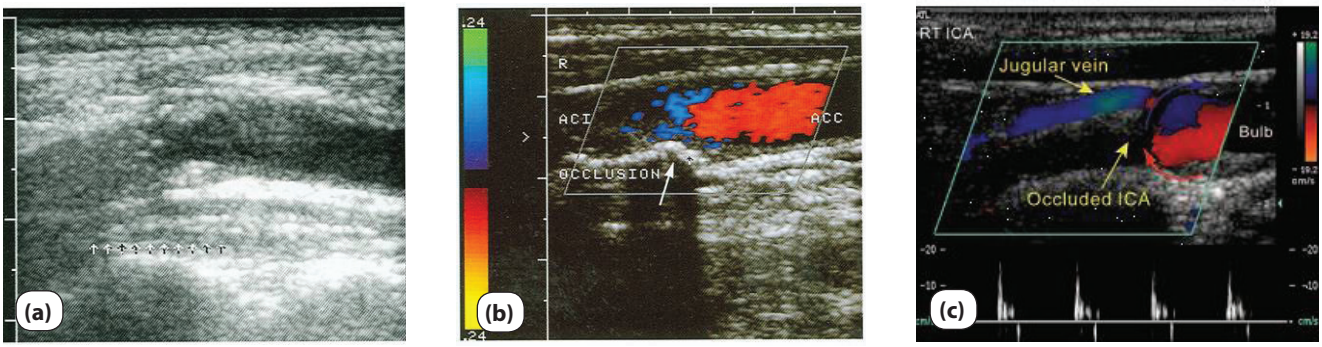


**Figure 11.** Occlusion of ICA. **(a)** In the case of an old occlusion, the occluded lumen can be well visualized in B-mode on account of the increased echogenicity. **(b)** In the case of a recently formed occlusion, the nonperfused lumen appears as a hypoechoic region in B-mode. The occlusion can only be detected by flow reversal using the color coding mode (arrow). **(c)** A biphasic Doppler signal can be recorded usually in the region of the reversed flow, just before the occluded segment (arrow).

In a degree of stenosis at 90% (NASCET) the maximum poststenotic velocity is below 30 cm/s.

### Criterion 5 - Collaterals

In order to maintain blood circulation in the brain in cases of high-grade stenoses or occlusions of cerebral arteries, numerous collateral connections between the arteries are available. These are supported by a compensatory hyperperfusion in their feeding arteries.

Typical collateral systems are:

- Collaterals of ophthalmic artery.
- Collaterals of the anterior communicating artery.
- Collaterals of the posterior communicating artery.
- Collaterals of the cerebral convexity (leptomeningeal anastomoses).

The most important collateral artery between the external and internal carotid arteries is the ophthalmic artery. In this system, collateral circulations are formed between the terminal branches of the external carotid artery and the fronto-orbital terminal branches of the ophthalmic artery (supratrochlear artery). Furthermore, in cases of high-grade stenoses or occlusions, it is particularly important to investigate the flow direction and velocity in the precommunicating segment of the anterior cerebral artery (A1 segment), proving cross flow, and the flow velocities in the P1 segment of the posterior cerebral artery, indicating collateral flow through the posterior communicating artery.

The assessment of the collateral systems requires transcranial Doppler (TCD). The inclusion of the collaterals in the classification of stenosis has the advantage of a clear identification of hemodynamically relevant and thus high-grade stenoses (≥70% NASCET). Established collateral flow is the most powerful criterion, excluding a less than severe stenosis irrespective of the intrastenotic PSV. There is a clear sonographic evidence of collaterals in severe stenosis or occlusion [29].

## The multiparametric approach – Additional (secondary) criteria

### Criterion 6 - Prestenotic diastolic flow deceleration of the CCA

Typically in severe ICA stenoses (≥70% NASCET) there is a distinct prestenotic diastolic flow deceleration of the

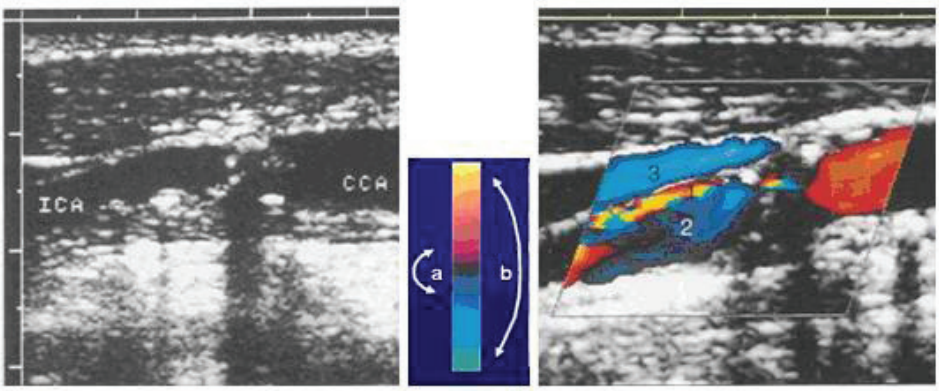


**Figure 12.** Left: Plaque with a high-grade lumen narrowing. Right: By color coding it is easy to differentiate between the jet flow in the stenosis (aliasing, **1**) and the reversed flow in the poststenotic region (deep blue, **2**). The jugular vein is coded light blue **(3)** [30].

common carotid artery (CCA) due to the increased flow resistance (**Figure 13**). This increased flow resistance is the consequence of the following distinct obstructive vessel disease in the ICA.

### Criterion 7 - Poststenotic flow disturbances

Typically in severe stenoses (≥70% NASCET) there are pronounced poststenotic separation effects due to transition from laminar to turbulent flow ("steps in the gravel").

If measurement of PSV is not possible in the area of greatest narrowing of the lumen, thus, criterion 7 is important.

Evidence of a severe stenosis: behind the extended acoustic shadow (**Figure 14**) aliasing and flow disturbances are visible in color coded imaging. For a high reliability aliasing and flow disturbances prove a high grade stenosis in the vessel segment not visible due to the extent acoustic shadow.

### Criterion 8 - End-diastolic flow velocity in the area of greatest narrowing of the lumen

In severe stenosis (≥70% NASCET) end-diastolic flow velocities more than 100 cm/s are to be expected. Criterion 8 is important if intrastenotic PSV can not be measured sufficiently.

### Criterion 9 - Confetti sign

The so-called confetti sign is the consequence of perivascular tissue vibrations. The confetti sign is generated by vibration of perivascular soft tissue due to an impingement of a highly accelerated jet flow.

The finding is distal to severe stenoses (≥70% NASCET) with a typical delta-shaped configuration (**Figure 15**).

### Criterion 10 - Index of stenosis / carotid velocity ratio ICA/CCA – "carotid ratio" (ratio of PSV of the ICA and CCA)

$$Index = \frac{PSV_{ICA}}{PSV_{CCA}}$$

The carotid ratio is important for example for the identification of a tandem stenosis or an ICA hyperperfusion.

**Table 2** provides a summary of all main/primary criteria and additional/secondary criteria for stenoses graded 10% to occlusion according to NACEST.

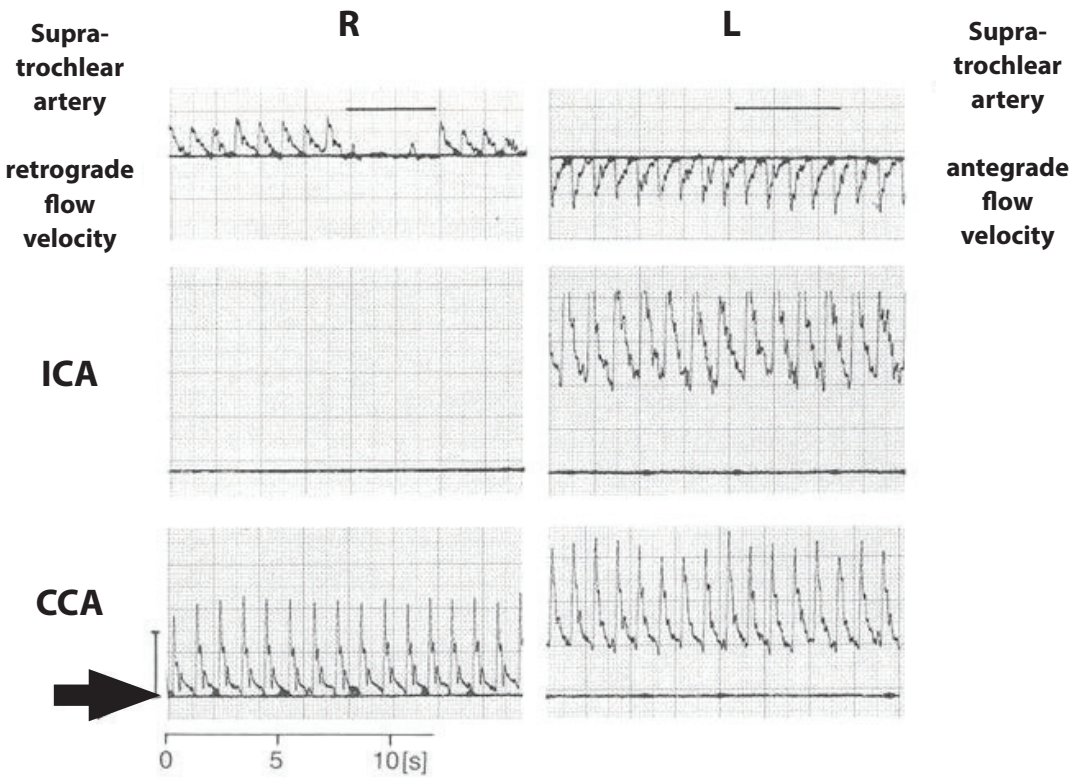


**Figure 13.** Bilateral comparative recordings of the CCA, ICA and supratrochlear artery in a patient with an occlusion of the right ICA. No flow signal in the right ICA, high-grade reduced end-diastolic flow velocity in the right CCA (arrow). The reduction in diastolic flow velocity between the right and left CCA is the result of the increased flow resistance that involves an increase in the pulsatility. Systolic flow velocity remains nearly comparable between right and left CCA.

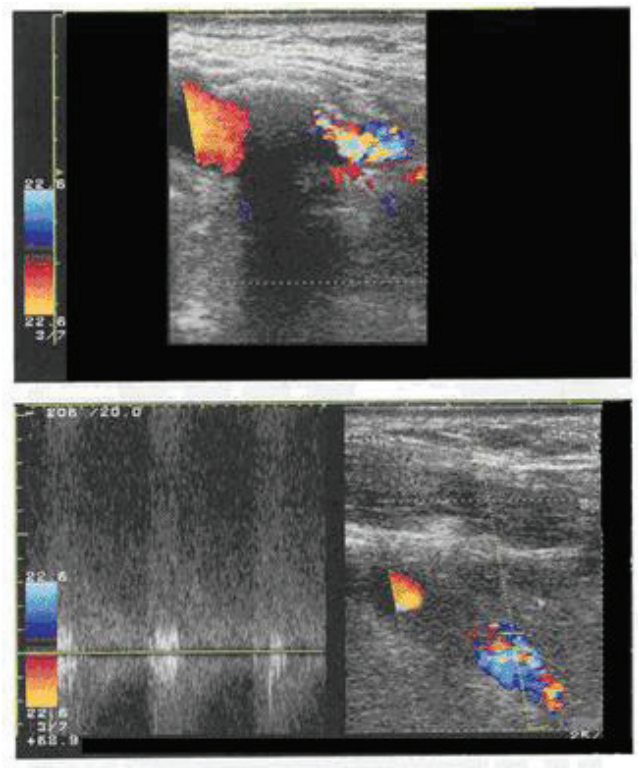

**Figure 14.** Measurement of PSV is not possible in the area of greatest narrowing due to an extended acoustic shadow (upper part). Behind this extent acoustic shadow aliasing and flow disturbances are visible in color coded imaging (lower part).

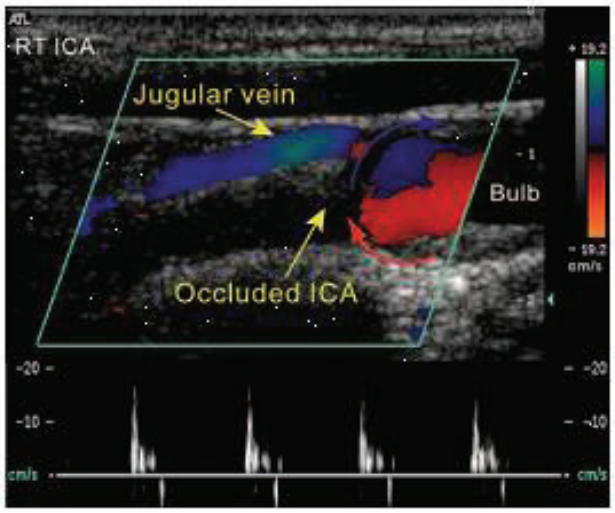


**Figure 15.** Confetti sign distal to a severe ICA stenosis with the typical delta-shaped configuration [32].

## Conclusion

Combining these ultrasound criteria, neurosonology is an excellent method for reliable and reproducible grading of carotid stenoses.

Valid results are to be expected through a qualified use of neurosonology by a well-trained and experienced ultrasound investigator.

**Table 2.** Summary of all main/primary (Crit. No. 1-5) and additional/secondary (Crit. No. 6-10) criteria for stenoses graded 10% to occlusion according to NACEST. Grading of the stenoses occur in steps of 10%. The PSV values of criterion 3 are taken from Figure 2.

| Criteria | | Grading of ICA stenosis | | | | | | |
|---|---|---|---|---|---|---|---|---|
| | | 10-40% | 50% | 60% | 70% | 80% | 90% | Occlusion |
| 1 | B-mode: verification of stenosis | +++ | + | + | + | + | + | +++ |
| 2 | Color coded imaging of flow: local flow acceleration (aliasing) | + | + | + | ++ | +++ | +++ | no flow |
| 3 | Stenotic PSV (cm/s): | | | | | | | |
| | PSV average (cm/s) | ≤160 | 210 | 240 | 330 | 370 | variable | negative |
| | PSV lower limit / treshold-PSV (cm/s) | 100 | 125 | 150 | 230 | 280 | | |
| 4 | Poststenotic PSV (cm/s) | >50 normal | >50 normal | >50 normal | ≥50 normal | <50 reduced | <30 strongly reduced | negative |
| 5 | Collaterals | negative | negative | negative | (+) | ++ | +++ | +++ |
| 6 | Prestenotic CCA flow velocity deceleration | negative | negative | negative | + | ++ | +++ Increased pulsatility | +++ |
| 7 | Poststenotic flow disturbances | negative | + | + | ++ | +++ | variable | negative |
| 8 | Stenotic end-diastolic flow velocity (EDV) (cm/s) | <100 | <100 | <100 | >100 | >100 | variable | negative |
| 9 | Confetti sign | negative | negative | (+) | ++ | ++ | variable | negative |
| 10 | Index/carotid ratio ICA/CCA | <2 | ≥2 | ≥2 | >4 | >4 | variable | negative |

(+) can exist + exist ++ regulary present +++ very pronounced present

Diagnostic ultrasound has the potential to classify and grade carotid disease with high reliability, taking into account morphological and complex hemodynamic parameters.

## Abbreviations

CCA: Common carotid artery; ECST: European Carotid Surgery Trial; ICA: Internal carotid artery; NASCET: North American Symptomatic Carotid Endarterectomy Trial; NSRG: Neurosonology Research Group; PRF: Pulse repetition frequency; PSV: Peak systolic velocity; RSNA: Radiological Society of North America; TCD: Transcranial Doppler; TEA: Thromboendarterectomy

## Competing interests

The authors declare no conflict of interest.

## References


1. Hennerici M, Hülsbömer HB, Hefter H et al. Natural history of asymptomatic extracranial arterial disease. Results of a long-term prospective study. Brain 1987; 110:777-791.
2. European Carotid Surgery Trialists'Collaborative Group. MRC European Carotid Surgery Trial: interim results for symptomatic patients with severe (70-99%) or with mild (0-29%) carotid stenosis. Lancet 1991; 337:1235-1243.
3. ECST Collaborative Group. Randomised trial of endarterectomy for recently symptomatic carotid stenosis: final results of the MRC European Carotid Surgery Trial (ECST). Lancet 1998; 351:1379-1387.
4. North American Symptomatic Carotid Endarterectomy Trail (NASCET) Collaborators. Beneficial effect of carotid endarterectomy in symptomatic patients with high-grade carotid stenosis. N Engl J Med 1991; 325:445-453.
5. Rothwell PM, Gibson RJ, Slattery J, Sellar RJ, Warlow CP. Equivalence of measurements of carotid stenosis. A comparison of three methods on 1001 angiograms. European Carotid Surgery Trialists' Collaborative Group. Stroke 1994; 25:2435-2439.
6. Grant EG, Benson CB, Moneta GL et al. Carotid artery stenosis: gray-scale and Doppler US diagnosis – Society of Radiologists in Ultrasound Consensus Conference. Radiology 2003; 229:340-346.
7. Moneta GL, Edwards JM, Papanicolaou G, Hatsukami T, Taylor LM Jr, Strandness DE Jr, et al. Screening for asymptomatic internal carotid artery stenosis: duplex criteria for discriminating 60% to 99% stenosis. J Vasc Surg 1995; 21:989-994.
8. Fillinger MF, Baker RJ Jr, Zwolak RM, Musson A, Lenz JE, Mott J, et al. Carotid duplex criteria for a 60% or greater angiographic stenosis: variation according to equipment. J Vasc Surg 1996; 24:856-864.
9. Hunink MG, Polak JF, Barlan MM, O'leary DH. Detection and quantification of carotid artery stenosis: efficacy of various Doppler velocity parameters. AJR Am J Roentgenol 1993; 160:619-625.
10. Koga M, Kimura K, Minematsu K, Yamaguchi T. Diagnosis of internal carotid artery stenosis greater than 70% with power Doppler duplex sonography. AJNR Am J Neuroradiol 2001; 22:413-417.
11. Neschis DG, Lexta FJ, Davis JT, Carpenter JP. Duplex criteria for determination of 50% or greater carotid stenosis. J Ultrasound Med 2001; 20:207-215.
12. Von Reutern GM, Goertler MW, Bornstein NM, Del Sette M, Evans DH, Hetzel A, et al. Recommendations for grading carotid stenosis by means of ultrasonic methods. Stroke 2012; 43:916-921.
13. Eliasziw M, Rankin RN, Fox AJ, Haynes RB, Barnett HJ. Accuracy and prognostic consequences of ultrasonography in identifying severe carotid artery stenosis. NASCET Group. Stroke 1995; 26:1747-1752.
14. Latchaw RE, Alberts MJ, Lev MH, Connors JJ, Harbaugh RE, Higashida RT, et al. Recommendations for imaging of acute ischemic stroke: a scientific statement from the American Heart Association. Stroke 2009; 40:3646-3678.
15. Tahmasebpour HR, Buckley AR, Cooperberg PL, Fix CH. Sonographic examination of the carotid arteries. RadioGraphics 2005; 25:1561-1575.
16. Phillips DJ, Beach KW, Primozich J, Strandness DE Jr. Should results of ultrasound Doppler studies be reported in units of frequency or velocity? Ultrasound Med Biol 1989; 15:205-212.
17. Von Reutern, GM. Von Büdingen, HJ, eds. Ultrasound diagnosis of cerebrovascular disease. Stuttgart, New York: Thieme. 1993.
18. Spencer MP, Reid JM.Quantitation of carotid stenosis with continuous wave (C-W) Doppler Ultrasound. Stroke 1979; 10: 326-330.
19. Spencer MP. Hemodynamics of arterial stenosis. In: Spencer MP ed. Ultrasonic diagnosis of cerebrovascular disease. Dordrechts: Martinus Nijhoff Publishers. 1987.
20. Von Reutern, GM. Measuring the degree of internal carotid artery stenosis. In: Bartels E, Poppert H eds. New Trends in Neurosonology and Cerebral Hemodynamics – an Update. Perspectives in Medicine 2012; 1:104-107.
21. Kaps M, von Reutern GM, Stolz E, von Büdingen HJ, eds. Ultraschall in der Neurologie, Stuttgart, New York: Thieme. 2005.
22. Arning C, Widder B, von Reutern GM, Stiegler H, Gortler M. [Revision of DEGUM ultrasound criteria for grading internal carotid artery stenosis and transfer to NASCET measurement]. Ultraschall Med 2010; 31:251-257.
23. Widder B, von Reutern GM, Neuerburg-Heusler D. Morphologic and Doppler sonographic criteria for determining the degree of stenosis of the internal carotid artery. Ultraschall Med 1986; 7:70-75.
24. Görtler M, Widder B, Schütz U. Assessing carotid artery stenosis by Doppler- and colour-coded duplex sonography. In Klingelhöfer J, Bartels E, Ringelstein EB, (eds). New trends in cerebral hemodynamics and neurosonology. Amsterdam: Elsevier. 1997. p 67-72.
25. Arning C, von Reutern GM, Widder B, Stiegler H, Görtler M. Graduierung von Karotisstenosen. Der Nervenarzt 2011; 8:1036-1037.
26. Zagzebski JA. Doppler instrumentation. In: Rowland J, Potts L, eds. Essentials of ultrasound physics. St Louis: Mosby. 1996.
27. Bluth EI, Stavros AT, Marich KW, et al. Carotid duplex sonography: a mulricenter recommendation for standardized imaging and Doppler criteria. RadioGraphics 1988; 8:487-506.
28. Nelson TR, Pretorius DH. The Doppler signal: where does it come from and what does it mean? AJR Am J Roentgenol 1988; 151:439-447.
29. Beckett WW, Davis PC, Hoffmann JC. Pitfalls in duplex carotid evaluation contralateral to significant stenosis/occlusion. AJNR Am J Neuroradiol 1990;11:1049-1053.
30. Bartels E, Color-coded Duplex Ultrasonography of the Cerebral Vessels. Stuttgart: F.K. Schattauer. 1999.
31. Beach KW, Leotta DF, Zierler RE. Carotid Doppler velocity measurements and anatomic stenosis: Correlation is futile. Vascular and Endovascular Surgery 2012; 46(6):466-474.
32 Widder B, Görtler M. Doppler- und Duplexsonographie der hirnversorgenden Arterien. Berlin, Heidelberg: Springer. 2004.

INTERNATIONAL JOURNAL OF
CLINICAL NEUROSCIENCES
AND MENTAL HEALTH

REVIEW

# Clinical impact of Intima-Media Thickness measurement

Miguel Rodrigues[1]

Special Issue on Neurosonology and Cerebral Hemodynamics

## Abstract

The Intima-Media Thickness (IMT) as measured by ultrasonography of carotid arteries is an acknowledged non-invasive method for assessing the impact of vascular risk factors and the progression of cardiovascular disease. The average of the far wall IMT of the common carotid artery (CIMT) from right and left sides is most frequently used. It correlates well with histology and it is a precursor phenotype of early atherosclerosis.

Its increase is associated with vascular risk factors. Systematic reviews have quantified this risk, showing that an increase of 0.1 mm in the CIMT is associated with an increased relative risk of 8% of myocardial infarction and 12% of stroke.

The evaluation of this parameter is simple, fast, and inexpensive, when integrated into a routine cervical artery ultrasound examination. However, CIMT also has applications in clinical research as an important study outcome, and then a standard measurement protocol should be applied to avoid information and measurement biases. The main consensus statements, both from Europe and North America, outline the technical conditions for IMT assessment and favor the use of automated edge detection software.

The relation between CIMT and vascular risk factors or vascular events has been extensively reported. Nevertheless, the implications of CIMT change observed in repeated measurements are not so thoroughly established in the available follow-up studies.

The CIMT is an attractive method of measuring target organ damage. However, it will remain a structural evaluation only, a static photograph that does not capture the complex interplay between vessel inflammation and thrombogenic processes.

**Keywords:** Carotid atherosclerosis, Intima-media thickness, IMT, CIMT, cardiovascular risk assessment

[1]Neurology Department, Hospital Garcia de Orta, Almada, Portugal

Correspondence: Miguel Rodrigues
Neurology Department, Hospital Garcia de Orta
Av Torrado da Silva, Pragal, 2801-951 Almada, Portugal
Email: mig.rodrigues69@gmail.com

Citation: Rodrigues, M. Clinical impact of Intima-Media Thickness measurement. IJCNMH 2014; 1(Suppl. 1):S05

Received: 27 Aug 2013; Accepted: 17 Nov 2013; Published: 09 May 2014

Open Access Publication Available at http://ijcnmh.arc-publishing.org



ARC Publishing

## Introduction

Atherosclerosis associated diseases are one of the most important contributors for the global burden of disease worldwide. Atherosclerotic vessel changes start very early in life, but its progression rate varies between subjects, according to intrinsic non-modifiable and modifiable or environmental factors [1, 2]. Risk scores, combining risk factors present at the individual level, can predict the probability of cardiovascular events, but methods that are able to directly measure the impact of atherosclerotic processes on vessels are interesting alternatives. Several methods access subclinical atherosclerosis, and carotid Intima-Media Thickness (IMT) measurement is one of the most attractive methods, allowing direct visualization of the vessel wall [2]. Although the IMT can be easily measured in other vessels like the femoral or radial arteries, most literature supports carotid artery IMT as the most reliable and better correlated with vascular risk factors.

## Carotid Intima-Media Thickness measurement

After the seminal work by Pignolli et al. [3] that showed the good correlation between ultrasound image and histology of the common carotid artery wall, sonographic image of the vessel wall became increasingly popular. The IMT is a double layer structure defined by the distance between the interface of the anechoic lumen and echogenic intima, and another interface between the hypoechoic media and echogenic adventitia [4]. As this structure is typically thinner than 1.0 millimeters in the common carotid artery of normal subjects, strict protocols and standards of measurement apply when evaluating this complex.

### European and North-American consensus on Intima-Media Thickness measurement

Pursuing comparable and consistent methodology on IMT measurement, expert consensus were produced in Europe and North America [4, 5]. These consensus define precise parameters concerning recommended equipment and imaging protocol (**Table 1**).

The European Consensus also establishes clear definitions for both carotid IMT and atherosclerotic plaques [4]. IMT is defined as a double-line pattern visualized by ultrasound on both walls of the common carotid artery in a longitudinal image of the vessel. Two parallel lines form it: the lumen-intima interface, and the media-adventitia interface. Plaque is a focal structure encroaching into the arterial lumen, at least 0.5 mm or 50% thicker than the surrounding IMT value, or which thickness is exceeding 1.5 mm, measured from the intima-lumen interface to the media-adventitia interface.

### Which Carotid Intima-Media Thickness to use?

Several studies showed that far wall IMT measurement is more reliable, contrasting with near wall IMT which is more dependent on technical issues [4]. Common carotid artery IMT (CIMT) is easier to access and more influenced by vascular risk factors than bulb or internal carotid IMT. The later are more difficult to display, depending on technical issues and operator experience. Twenty seven percent of the IMT variability at the common carotid level is explained by classical vascular risk factors, whereas bulb and internal carotid IMT variability is less influenced by those factors (11% and 8%, respectively) [6]. When considering just CIMT, the maximal point value reflects more advanced stages of atherosclerosis. Mean IMT is less susceptible to outlier measurements and therefore more reliable. One sided values can be used to report the highest mean IMT found or one can choose to display values separately for the left and right side, but it is correct to calculate an average mean IMT from both sides to produce only one IMT for each individual [4].

### Manual versus semi-automated edge detection measurement

Information available from several follow-up and population-based studies used manual IMT measurement, but semi-automated software is becoming more popular as some ultrasound equipments already have built-in software solutions. Manual measurement implies that the operator draws the limits of the IMT based on his visual assessment of the interface lumen-intima and media-adventicia, possibly aided by enhancing the quality or increasing the size of the image. In semi-automated measurement the software defines the limits of the IMT on a pre-specified segment chosen by the operator. In this method further adjustments can be made by the operator [7].

Manual IMT has the advantage of being universally available and is inexpensive, but requires rigorous quality control and can be time consuming. Semi-automated edge detection software has the great advantage of providing in a quick single assessment the mean and maximal value of more than a hundred point evaluations. Nevertheless, the quality of the data depends on the accuracy of the built-in or offline software used, and if the operator has to override the software frequently, it can also be time consuming and unreliable. The financial cost of the software can also limit the availability of this method, but newer ultrasound equipments should already have the necessary software packages by default [4, 7].

### Reference values for Carotid Intima-Media Thickness

There is no consensual established cut-off to define increased carotid IMT, so two approaches can be used. A conservative approach is to considerer all CIMT above 0.9 mm as an indicator of increased future cardiovascular risk, which is not consensual among all follow-up studies[8]. Other approach is to produce age- and gender-specific reference values like those established for the French population [9] and make use of the 75th percentile as a cut-off value [5]. The first approach, being immediately available,

**Table 1**. Standard equipment and imaging parameters.

| Instrumentation and display | Imaging of the vessel wall |
|---|---|
| State-of-the-art ultrasound system<br>Digital image acquisition and storage, preferably DICOM<br>Phantom scans every 6 months and after any system changes<br>Semiannual routine preventive maintenance | Longitudinal view with parallel vessel walls, with good visualization of both walls |
| Transducer<br>Linear array<br>Minimal compression (<10:1)<br>Fundamental frequency ≥7 MHz<br>Footprint ≥3 cm | Optimal diameter should be obtained during diastole |
| Display<br>Depth 4 cm<br>Single focal zone<br>Frame rate ≥25 Hz<br>High dynamic range<br>Clear 3-lead electrocardiographic signal<br>Annotate images to describe segments, angles, and other findings | IMT measured in the far wall, in a 10 mm segment at least 5 mm from bifurcation |
| Carefully adhere to predefined scanning protocol | Plaques should not be included in the IMT segment |
| | Lateral probe position |
| | Acquisition in the center of the screen |
| | Automated edge detection methods are preferable, as are less operator dependent |

IMT= Intima-Media Thickness

is the most attractive, but as reference values differ among countries and ethnic groups [10], a fixed predetermined cut-off is probably inadequate for several populations.

## Relation between increased Carotid Intima-Media Thickness and established risk factors and vascular disease

It is clearly demonstrated in single- and multi-country studies that when any number of traditional cardiovascular risk factors increase, so does the CIMT [9, 10].

CIMT has been extensively correlated with traditional cardiovascular risk factors, like aging, male gender, hypertension, body mass index (BMI), LDL and HDL cholesterol, diabetes, smoking, and also with emerging risk factors like inflammation and atherosclerotic changes in other organs: brain, heart, kidneys, lower limb arteries, and brachial artery [11].

## Clinical significance of Carotid Intima-Media Thickness

CIMT can be used in several clinical settings: as a population cardiovascular risk marker, as a surrogate endpoint in clinical trials, and as a clinical decision and risk stratification tool for individual patients.

Regarding the use as a population risk marker, a first meta-analysis combining cross-sectional data from studies available until 2006 showed that for each 0.1 mm increase in IMT, the risk of stroke rises 15% (Hazard Ratio - HR 1.15; 95% CI 1.12-1.17) and the risk of myocardial infarction increases 18% (HR 1.18; 95% CI 1.16-1.21) [12]. In 2012 the same authors revised these numbers using additional studies, decreasing the risk estimate of stroke for each 0.1 mm to 12% (HR 1.12; 95% CI 1.10-1.15) and for myocardial infarction to 8% (HR 1.08; 95% CI 1.05-1.10) [13]. Moreover, it is stated in the same publication that when using the Framingham Risk Score with the CIMT more than 90% of the subjects, with or without previous vascular events, did not change Framingham Risk Score classification. For those classified as being at an intermediate risk score, the added information of the CIMT measurements presented a slightly higher score value, reclassifying more than 20% of the subjects in the higher risk category, while 4.6% lowered risk category [13]. Meanwhile, CIMT progression in repeated measurements from follow-up studies available so far did not predict future cardiovascular events in the general population [14]. As a population risk marker, the evidence is that CIMT measurement in the general population does not significantly modify the risk profile, so it should not be done routinely [13]. Still, this CIMT increase over time is documented in several subpopulations, like tobacco users, hypertensive, diabetic, hiperlipidemic, obese, and metabolic syndrome populations [15], subjects with rheumatic disease [16], HIV-infected patients [17], or people with periodontal disease [18]. Other areas like inflammatory bowel disease [19] or assessment of the Ideal Cardiovascular Health (American Heart Association) in adolescents [20] are promising but require further research.

As a surrogate endpoint in clinical trials, the interventions were evaluated for its ability to modify CIMT rate progression and the agreement between this modification and the mortality and morbidity trials. Several statins (simvastatin, atorvastatin, fluvastatin, lovastatin, rosuvasta-

tin), using high dosages for periods ranging from 12 to 48 months, proved to modify CIMT rate progression, which was also in agreement with mortality and morbidity trials [21, 22]. Non-statin lipid lowering drugs (torcetrapib, ezetimibe, niacin, fibrates, and acyl–coenzyme A: cholesterol acyltransferase inhibitors) failed to produce results both in CIMT progression and mortality and morbidity trials [22]. In respect to antihypertensive therapy, numerous drugs (verapamil, amlodipine, nifedipine, lacidipine, doxazosine, metoprolol, enalapril, lisinopril, fosinopril, quinapril, ramipril, trandolapril, losartan, telmisartan, candesartan, irbesartan) were able to achieve convincing effects on CIMT progression and mortality and morbidity trials in primary prevention of cardiovascular effects [22, 23], while ramipril versus placebo and losartan versus atenolol did not shown agreement between ultrasound results and mortality and morbidity trials [22]. In diabetic patients, quite a few drugs, like glucose-lowering drugs, antiplatelet drugs (aspirin, ticlopidine, cilostazol), completed trials showing change on CIMT progression rate [24-26].

Regarding the use of CIMT in clinical decision and risk stratification at the individual level, in 2006 the Screening for Heart Attack Prevention and Education (SHAPE) algorithm included IMT measurement above the 50th percentile or the presence of carotid plaques as an useful test for atherosclerosis in apparently healthy individuals (men above 45 years-old or women above 55 years-old) to set lower LDL targets for intervention [2]. Some years later the Society of Atherosclerosis Imaging and Prevention did an expert panel evaluation of 33 scenarios where CIMT could be used, and found a single measurement to be appropriate to determine coronary heart disease (CHD) risk in the following settings: intermediate risk subjects, metabolic syndrome patients, diabetics without known CHD, people with a family history of premature CHD with calculated intermediate risk, and those with a known coronary artery calcium score of zero and calculated risk between 11 and 20% [27]. Serial IMT imaging was not considered appropriate, with the so far available studies, for monitoring of CHD risk status, due to lack of evidence on technical success of serial IMT in clinical settings and insufficient reliable data on anticipated progression rates.

## Conclusion

IMT of the common carotid artery is widely used, even if the strict technical requirements for its measurement are not always met. A few recent reviews on the subject cast some shadows on CIMT usefulness, especially in the setting of repeated assessment in follow-up studies, which was not yet soundly associated with cardiovascular disease risk progression. Regardless, the papers published on CIMT measurement in Pubmed on various clinical settings are now over 2,400, and increasing, with 80% having been issued on the last 10 years, as this review is being written.

Leaving the discussion of risk prediction aside, CIMT is a proven method to evaluate subclinical atherosclerosis. However, it is only the reflection of a moment in time, a static image that cannot tell the interplay of present structural wall changes and complex dynamic processes like vessel inflammation or thrombosis, which in the end will determine the occurrence of cardiovascular events.

### Abbreviations

BMI: Body mass index; CHD: Coronary heart disease; CIMT: Common carotid artery Intima-Media Thickness; IMT: Intima-Media Thickness

### Competing interests

The authors declare no conflict of interest.

### References


1. Goldstein LB, Bushnell CD, Adams RJ, Appel LJ, Braun LT, Chaturvedi S, et al. Guidelines for the primary prevention of stroke: a guideline for healthcare professionals from the American Heart Association/American Stroke Association. Stroke 2011; 42(2):517-84.
2. Naghavi M, Falk E, Hecht HS, Jamieson MJ, Kaul S, Berman D, et al. From vulnerable plaque to vulnerable patient--Part III: Executive summary of the Screening for Heart Attack Prevention and Education (SHAPE) Task Force report. Am J Cardiol 2006; 98(2A):2H-15H.
3. Pignoli P, Tremoli E, Poli A, Oreste P, Paoletti R. Intimal plus medial thickness of the arterial wall: a direct measurement with ultrasound imaging. Circulation 1986; 74(6):1399-406.
4. Touboul PJ, Hennerici MG, Meairs S, Adams H, Amarenco P, Bornstein N, et al. Mannheim carotid intima-media thickness and plaque consensus (2004-2006-2011). An update on behalf of the advisory board of the 3rd, 4th and 5th watching the risk symposia, at the 13th, 15th and 20th European Stroke Conferences, Mannheim, Germany, 2004, Brussels, Belgium, 2006, and Hamburg, Germany, 2011. Cerebrovasc Dis 2012; 34(4):290-6.
5. Stein JH, Korcarz CE, Hurst RT, Lonn E, Kendall CB, Mohler ER, et al. Use of carotid ultrasound to identify subclinical vascular disease and evaluate cardiovascular disease risk: a consensus statement from the American Society of Echocardiography Carotid Intima-Media Thickness Task Force. Endorsed by the Society for Vascular Medicine. J Am Soc Echocardiogr 2008; 21(2):93-111.
6. Polak JF, Person SD, Wei GS, Godreau A, Jacobs DR, Jr., Harrington A, et al. Segment-specific associations of carotid intima-media thickness with cardiovascular risk factors: the Coronary Artery Risk Development in Young Adults (CARDIA) study. Stroke 2010; 41(1):9-15.
7. Bots ML, Sutton-Tyrrell K. Lessons from the past and promises for the future for carotid intima-media thickness. J Am Coll Cardiol 2012; 60(17):1599-604.
8. Mancia G, Fagard R, Narkiewicz K, Redon J, Zanchetti A, Bohm M, et al. 2013 ESH/ESC Guidelines for the management of arterial hypertension: The Task Force for the management of arterial hypertension of the European Society of Hypertension (ESH) and of the European Society of Cardiology (ESC). J Hypertens 2013; 31(7):1281-357.
9. Touboul PJ, Labreuche J, Vicaut E, Belliard JP, Cohen S, Kownator S, et al. Country-based reference values and impact of cardiovascular risk factors on carotid intima-media thickness in a French population: the 'Paroi Arterielle et Risque Cardio-Vasculaire' (PARC) Study. Cerebrovasc Dis 2009; 27(4):361-7.
10. Touboul PJ, Vicaut E, Labreuche J, Acevedo M, Torres V, Ramirez-Martinez J, et al. Common carotid artery intima-media thickness: the Cardiovascular Risk Factor Multiple Evaluation in Latin America (CARMELA) study results. Cerebrovasc Dis 2011; 31(1):43-50.

11. Peters SA, Grobbee DE, Bots ML. Carotid intima-media thickness: a suitable alternative for cardiovascular risk as outcome? Eur J Cardiovasc Prev Rehabil 2011; 18(2):167-74.
12. Lorenz MW, Markus HS, Bots ML, Rosvall M, Sitzer M. Prediction of clinical cardiovascular events with carotid intima-media thickness: a systematic review and meta-analysis. Circulation 2007; 115(4):459-67.
13. Den Ruijter HM, Peters SA, Anderson TJ, Britton AR, Dekker JM, Eijkemans MJ, et al. Common carotid intima-media thickness measurements in cardiovascular risk prediction: a meta-analysis. JAMA 2012; 308(8):796-803.
14. Lorenz MW, Polak JF, Kavousi M, Mathiesen EB, Volzke H, Tuomainen TP, et al. Carotid intima-media thickness progression to predict cardiovascular events in the general population (the PROG-IMT collaborative project): a meta-analysis of individual participant data. Lancet 2012; 379(9831):2053-62.
15. Hurst RT, Ng DW, Kendall C, Khandheria B. Clinical use of carotid intima-media thickness: review of the literature. J Am Soc Echocardiogr 2007; 20(7):907-14.
16. Tyrrell PN, Beyene J, Feldman BM, McCrindle BW, Silverman ED, Bradley TJ. Rheumatic disease and carotid intima-media thickness: a systematic review and meta-analysis. Arterioscler Thromb Vasc Biol 2010; 30(5):1014-26.
17. Longenecker CT, Hoit BD. Imaging atherosclerosis in HIV: carotid intima-media thickness and beyond. Transl Res 2012; 159(3):127-39.
18. Beck JD, Elter JR, Heiss G, Couper D, Mauriello SM, Offenbacher S. Relationship of periodontal disease to carotid artery intima-media wall thickness: the atherosclerosis risk in communities (ARIC) study. Arterioscler Thromb Vasc Biol 2001; 21(11):1816-22.
19. Theocharidou E, Gossios TD, Giouleme O, Athyros VG, Karagiannis A. Carotid Intima-Media Thickness in Patients With Inflammatory Bowel Disease: A Systematic Review. Angiology 2013.
20. Pahkala K, Hietalampi H, Laitinen TT, Viikari JS, Ronnemaa T, Niinikoski H, et al. Ideal cardiovascular health in adolescence: effect of lifestyle intervention and association with vascular intima-media thickness and elasticity (the Special Turku Coronary Risk Factor Intervention Project for Children [STRIP] study). Circulation 2013; 127(21):2088-96.
21. Riccioni G. Statins and carotid intima-media thickness reduction: an up-to-date review. Curr Med Chem 2009; 16(14):1799-805.
22. Peters SA, den Ruijter HM, Grobbee DE, Bots ML. Results from a carotid intima-media thickness trial as a decision tool for launching a large-scale morbidity and mortality trial. Circ Cardiovasc Imaging 2013; 6(1):20-5.
23. Riccioni G. The effect of antihypertensive drugs on carotid intima media thickness: an up-to-date review. Curr Med Chem 2009; 16(8):988-96.
24. Yokoyama H, Katakami N, Yamasaki Y. Recent advances of intervention to inhibit progression of carotid intima-media thickness in patients with type 2 diabetes mellitus. Stroke 2006; 37(9):2420-7.
25. Mita T, Watada H, Shimizu T, Tamura Y, Sato F, Watanabe T, et al. Nateglinide reduces carotid intima-media thickening in type 2 diabetic patients under good glycemic control. Arterioscler Thromb Vasc Biol 2007; 27(11):2456-62.
26. Stocker DJ, Taylor AJ, Langley RW, Jezior MR, Vigersky RA. A randomized trial of the effects of rosiglitazone and metformin on inflammation and subclinical atherosclerosis in patients with type 2 diabetes. Am Heart J 2007; 153(3):445 e1-6.
27. Appropriate use criteria for carotid intima media thickness testing. Atherosclerosis 2011; 214(1):43-6.

INTERNATIONAL JOURNAL OF
CLINICAL NEUROSCIENCES
AND MENTAL HEALTH

REVIEW

# Carotid arteries ultrasound for predicting coronary artery disease

Hrvoje Budincevic[1], Marina Milosevic[1], Natasa L. Andrijic[2], Saira A. Musemic[2], and Natan M. Bornstein[3]

Special Issue on Neurosonology and Cerebral Hemodynamics

## Abstract

Ischemic heart disease and stroke are the leading causes of death in the world. Myocardial infarction or even death might be the initial presentation of ischemic heart disease. Myocardial infarction is the leading cause of long-term mortality in stroke surviving patients.

The aim of this paper is to present the possibilities of predicting coronary artery disease in stroke patients. Evaluating carotid arteries intima-media thickness (IMT), plaque morphology, and degree of stenosis can give us valuable additional information for predicting cardiovascular risk and silent coronary artery disease in otherwise asymptomatic patients. Measuring IMT and assessing carotid atherosclerotic plaque is justified in subjects with high vascular risk profile.

**Keywords:** Coronary artery disease, Carotid artery ultrasound, Intima-media thickness, Carotid stenosis.

[1]Department of Neurology, Stroke and Intensive Care Unit, University Hospital "Sveti Duh" Zagreb, Croatia

[2]Department of Neurology, Clinical Center of University of Sarajevo, Bosnia and Herzegovina

[3]Stroke Unit, Department of Neurology, Sackler Faculty of Medicine, Tel-Aviv Medical Center, Tel-Aviv University, Tel Aviv, Israel

Correspondence: Natan M. Bornstein

Head of Stroke Unit, Department of Neurology, Sackler Faculty of Medicine, Tel-Aviv Medical Center, Tel-Aviv University,

6 Weizman st. Tel Aviv 6423906, Israel

Email adress: natanb@tlvmc.gov.il

Citation: Budincevic et al. Carotid arteries ultrasound for predicting coronary artery disease. IJCNMH 2014; 1(Suppl. 1):S06

Received: 08 Sep 2013; Accepted: 14 Nov 2013; Published: 09 May 2014

## Introduction

Approximately 13 million deaths per year are caused by vascular diseases, ischemic heart disease and stroke account for 22.3% of the total yearly deaths in the world, of which 12.2% and 9.7% are due to ischemic heart disease and stroke, respectively [1]. Myocardial infarction is the leading cause of long-term mortality in stroke surviving patients [2], although stroke is the leading cause of disability in the world [3]. Atherosclerotic carotid artery disease is the cause of ischemic stroke in about 20% of cases [4]. The aim of this paper is to present the possibilities of predicting coronary artery disease in stroke patients.

The diagnosis of coronary artery disease (CAD) is often too late, because myocardial infarction or even death might be the first sign of CAD [5]. In contrary to carotid artery disease where severity of the stenosis is the main player, rupture-prone plaques in coronary artery disease cause acute myocardial infarctions and sudden cardiac deaths [6, 7]. About 68% of patients with acute myocardial infarction have a mild degree (<50%) of coronary artery stenosis [6]. Approximately 76% of sudden cardiac deaths are caused by the rupture-prone plaque and only 24% by severe stenosis [7].

Asymptomatic carotid bruit increases the risk of myocardial infarction and cerebrovascular death [8]. The non-invasive and reliable diagnostic tool for evaluating carotid artery atherosclerosis plaque or stenosis (CAS) is an ultrasound including measurement of intima-media thickness (IMT), which represents mainly medial layer hypertrophy [9-12]. IMT is usually measured in the common carotid artery and the internal carotid artery [13, 14]. In recent years, automated and semi-automated measurements of IMT were developed [15]. According to Mannheim consensus conference, measurement of IMT should be done on the far wall of the common carotid artery, with quality index greater than 0.5 [13, 14]. IMT, plaque, and stenosis should be regarded as distinct phenotypes, with distinct biological aspects and determinants [16].

## Intima-media thickness and carotid plaque for predicting cardiovascular risk

Relationship between IMT and cerebral or cardiac vascular risk has been shown in several studies. The Carotid Atherosclerosis Progression Study (CAPS) included 5056 people with mean follow–up of 4.2 years [17]. The baseline measurements of IMT were taken at three sites and cerebrovascular risk factor and clinical events were monitored. The primary endpoints were myocardial infarction, stroke, and combined myocardial infarction, stroke, or death. The study showed that the incidence of myocardial infarction was 1.07% per year and the incidence of stroke 0.5% per year. Common carotid artery IMT (CCA-IMT) and bifurcation IMT were associated with risk of myocardial infarction and the combined endpoints, hazard rate ratio (HRR) per 1 SD CCA-IMT increase were 1.43 (95% CI, 1.35 to 1.51) for myocardial infarction, 1.47 (95% CI, 1.35 to 1.60) for stroke, and 1.45 (1.38 to 1.52) for myocardial infarction, stroke or death; all p<0.0001. This study showed that carotid IMT can independently predict future vascular events.

The Atherosclerosis Risk in Communities study (ARIC) has shown that the risk of CAD gradually increases with higher values of IMT [18]. Each increase of carotid IMT by 0.19mm raises the risk of CAD by 92% (95% CI, 50-90%) for women and 32% (95% CI, 23-51%) for men. The Rotterdam study included 7893 patients with mean follow-up 2.7 years [19]. The measurement of IMT was done bilaterally on near and far walls of the common carotid arteries. The odds ratio (OR) for stroke per SD increase (0.163mm) was 1.41 (95% CI, 1.25-1.82). After the adjustment of risk factors the OR was 1.34 (95% CI, 1.08-1.67) for stroke and 1.2 (95% CI, 0.98-1.58) for myocardial infarction.

French epidemiological Paroi Artérielle et Risque Cardiovasculaire (PARC) study evaluated the correlation between CCA-IMT and absolute cardiovascular risk measured by Framingham and PROCAM scores in 6416 patients [20]. This study has shown that The Framingham score and CCA-IMT values were significantly but non-linearly correlated [20]. In further sub-analysis of 5400 patients of the PARC study it was shown that subjects without risk factors had mean CCA-IMT 0.712 ± 0.122 mm in men and 0.682 ± 0.105 mm in women (p<0.0001) [21]. Each 10-year increment in age was associated with a sex-adjusted increase in mean CCA-IMT of 0.049 mm. In subjects with one risk factor, mean CCA-IMT was 0.765 ± 0.121 vs. subjects without risk factors (p<0.0001). Mean CCA-IMT increased continuously with increasing number of risk factors, irrespective of age groups. In multivariable analysis age, sex, and number of cardiovascular risk factors appeared independently associated with mean CCA-IMT [21]. These results suggest that CCA-IMT may help to identify the population with an intermediate cardiovascular risk [21] .

A recent analysis of the ARIC study showed that coronary heart disease (CHD) risk prediction could be improved by adding all carotid artery segments IMT (A-C IMT) or common carotid artery IMT (CCA-IMT) with plaque information to traditional risk factors. The evaluation of carotid artery for plaque presence and CCA-IMT measurement provides a good alternative to measuring A-C IMT for CHD risk prediction [22]. Also, increased CCA-IMT is associated with brain infarction, and this may help in selecting patients with a high risk for brain infarction [23].

In spite of the above mentioned studies, several studies have shown that the carotid plaque is more closely related to CAD than measuring of the IMT [24-28]. Recently published meta-analysis of 11 population-based studies has shown that the ultrasound assessment of carotid plaque has a significantly higher accuracy for predicting

future myocardial infarction or CAD events compared with carotid IMT assessment [28]. The analysis of 27 diagnostic cohort studies in detecting CAD has shown that the ultrasound assessment of carotid plaque has a higher accuracy for predicting CAD, but the results weren't statistically significant. This meta-analysis is also important because it pointed out two types of IMT, with and without plaque thickness [28]. IMT without plaque is not atherosclerotic and it might have a different phenotype, representing mainly hypertensive medial hypertrophy [11]. The authors suggest that IMT with plaque can be called plaque thickness [11].

Although, the plaque measurement might be superior to IMT in predicting risk for CAD, it can be used for treatment evaluation [29]. The plaque measurement is more sensitive to the effects of therapy [29].

## Stroke and coronary artery disease

Autopsy study on 341 patients with fatal stroke has shown that coronary plaques, coronary stenosis, and myocardial infarction were present in 72.4%, 37.5%, and 40.8% respectively, which was statistically significant compared to autopsies of 462 patients with other neurological diseases [2]. Two-thirds of myocardial infarction cases were clinically silent and found only on autopsy. The prevalence of coronary plaques, coronary stenosis, and myocardial infarction was 79.0%, 42.9%, and 46%, respectively, when plaque was present in any segment of the extracranial or intracranial brain arteries, which was significantly more prevalent in comparison with patients without extracranial or intracranial plaques. The frequency of coronary atherosclerosis and myocardial infarction was similar between stroke subtypes and the presence of carotid plaque was as closely associated to coronary atherosclerosis or myocardial infarction as the presence of carotid stenosis or occlusion. It is to note that stroke patients even without atherosclerotic plaque in any segment of the cerebral arteries had a high prevalence of coronary plaques and stenosis, 51% and 18% respectively.

The Asymptomatic Myocardial Ischemia in Stroke and Atherosclerotic Disease (AMISTAD) study [30] that analyzed 315 acute ischemic stroke without known CAD who underwent coronary angiography has shown that coronary plaques were present in 61.9% and the coronary stenosis (>50%) was present in 25.4% of patients. The presence of plaques in carotid or femoral arteries was associated with higher prevalence of CAD. Marked increase in the prevalence of coronary plaque, especially in those with arterial lumen reduction of 50%, was associated with the increasing severity of carotid atherosclerosis. Silent coronary stenosis (>50%) was more frequent in patients with carotid occlusion or high degree of carotid artery stenosis.

The Tel Aviv Prospective Angio Survey (TAPAS) study [31] that evaluated 1405 consecutive patients who were undergoing coronary angiography for the presence of asymptomatic carotid artery CAS has shown that the degree of internal carotid artery (ICA) stenosis was related to the extent of CAD. Independent predictors of severe CAS defined by Peak Systolic Velocity (PSV) on Doppler were the presence of left-main or three-vessel CAD, older age, a history of stroke, smoking status, and diabetes mellitus. The prevalence of significant ICA stenosis is lower in specific CAD subsets than previously reported, most probably because different methods for classification of carotid stenosis were used, and because recently there is better adherence to optimal medical treatment and statins use in contrast to the studies of 1999 and 2005 [32, 33].

## Conclusion

Atherosclerosis is the common pathophysiological cause for development of coronary and carotid artery disease. The degree of carotid stenosis plays a more important role in pathophysiology of embolic stroke. Evaluating carotid arteries for IMT, plaque morphology, and degree of stenosis can give us valuable additional information for predicting cardiovascular risk and silent CAD in otherwise asymptomatic patients. Therefore measuring IMT and assessing carotid atherosclerotic plaque is justified in subjects with high vascular risk profile.

### Abbreviations

CAD: Coronary artery disease; CAS: Carotid artery stenosis; CCA-IMT: Common carotid artery intima-media thickness; CHD: Coronary heart disease; ICA: Internal carotid artery; IMT: Intima-media thickness; OR: Odds ratio; PSV: Peak systolic velocity

### Competing interests

The authors declare no conflict of interest.

### References

1. World Health Organization. The Global Burden of Disease: 2004 Update. 1 ed. Switzerland. : WHO Press; 2008.
2. Gongora-Rivera F, Labreuche J, Jaramillo A, Steg PG, Hauw JJ, Amarenco P. Autopsy prevalence of coronary atherosclerosis in patients with fatal stroke. Stroke 2007; 38(4):1203-10.
3. Lloyd-Jones D, Adams R, Carnethon M, De Simone G, Ferguson TB, Flegal K, et al. Heart disease and stroke statistics--2009 update: a report from the American Heart Association Statistics Committee and Stroke Statistics Subcommittee. Circulation 2009; 119(3):e21-181.
4. Sacco RL, Ellenberg JH, Mohr JP, Tatemichi TK, Hier DB, Price TR, et al. Infarcts of undetermined cause: the NINCDS Stroke Data Bank. Ann Neurol 1989; 25(4):382-90.
5. Thygesen K, Alpert JS, White HD. Universal definition of myocardial infarction. Eur Heart J 2007; 28(20):2525-38.
6. Falk E, Shah PK, Fuster V. Coronary plaque disruption. Circulation 1995; 92(3):657-71.
7. Kolodgie FD, Burke AP, Skorija KS, Ladich E, Kutys R, Makuria AT, et al. Lipoprotein-associated phospholipase A2 protein expression in the natural progression of human coronary atherosclerosis. Arterioscler Thromb Vasc Biol 2006; 26(11):2523-9.
8. Pickett CA, Jackson JL, Hemann BA, Atwood JE. Carotid bruits as a prognostic indicator of cardiovascular death and myocardial infarction: a meta-analysis. Lancet 2008; 371(9624):1587-94.

9. von Reutern GM, Goertler MW, Bornstein NM, Del Sette M, Evans DH, Hetzel A, et al. Grading carotid stenosis using ultrasonic methods. Stroke 2012; 43(3):916-21.
10. Spence JD, Hackam DG. Treating arteries instead of risk factors: a paradigm change in management of atherosclerosis. Stroke 2010; 41(6):1193-9.
11. Finn AV, Kolodgie FD, Virmani R. Correlation between carotid intimal/medial thickness and atherosclerosis: a point of view from pathology. Arterioscler Thromb Vasc Biol 2010; 30(2):177-81.
12. Grant EG, Benson CB, Moneta GL, Alexandrov AV, Baker JD, Bluth EI, et al. Carotid artery stenosis: gray-scale and Doppler US diagnosis--Society of Radiologists in Ultrasound Consensus Conference. Radiology 2003; 229(2):340-6.
13. Touboul PJ, Hennerici MG, Meairs S, Adams H, Amarenco P, Bornstein N, et al. Mannheim carotid intima-media thickness consensus (2004-2006). An update on behalf of the Advisory Board of the 3rd and 4th Watching the Risk Symposium, 13th and 15th European Stroke Conferences, Mannheim, Germany, 2004, and Brussels, Belgium, 2006. Cerebrovasc Dis 2007; 23(1):75-80.
14. Touboul PJ, Hennerici MG, Meairs S, Adams H, Amarenco P, Bornstein N, et al. Mannheim carotid intima-media thickness and plaque consensus (2004-2006-2011). An update on behalf of the advisory board of the 3rd, 4th and 5th watching the risk symposia, at the 13th, 15th and 20th European Stroke Conferences, Mannheim, Germany, 2004, Brussels, Belgium, 2006, and Hamburg, Germany, 2011. Cerebrovasc Dis 2012; 34(4):290-6.
15. Molinari F, Zeng G, Suri JS. A state of the art review on intima-media thickness (IMT) measurement and wall segmentation techniques for carotid ultrasound. Comput Methods Programs Biomed 2010; 100(3):201-21.
16. Spence JD, Hegele RA. Noninvasive phenotypes of atherosclerosis: similar windows but different views. Stroke 2004; 35(3):649-53.
17. Lorenz MW, von Kegler S, Steinmetz H, Markus HS, Sitzer M. Carotid intima-media thickening indicates a higher vascular risk across a wide age range: prospective data from the Carotid Atherosclerosis Progression Study (CAPS). Stroke 2006; 37(1):87-92.
18. Chambless LE, Heiss G, Folsom AR, Rosamond W, Szklo M, Sharrett AR, et al. Association of coronary heart disease incidence with carotid arterial wall thickness and major risk factors: the Atherosclerosis Risk in Communities (ARIC) Study, 1987-1993. Am J Epidemiol 1997; 146(6):483-94.
19. Bots ML, Hoes AW, Koudstaal PJ, Hofman A, Grobbee DE. Common carotid intima-media thickness and risk of stroke and myocardial infarction: the Rotterdam Study. Circulation 1997; 96(5):1432-7.
20. Touboul PJ, Vicaut E, Labreuche J, Belliard JP, Cohen S, Kownator S, et al. Correlation between the Framingham risk score and intima media thickness: the Paroi Arterielle et Risque Cardio-vasculaire (PARC) study. Atherosclerosis 2007; 192(2):363-9.
21. Touboul PJ, Labreuche J, Vicaut E, Belliard JP, Cohen S, Kownator S, et al. Country-based reference values and impact of cardiovascular risk factors on carotid intima-media thickness in a French population: the 'Paroi Arterielle et Risque Cardio-Vasculaire' (PARC) Study. Cerebrovasc Dis 2009; 27(4):361-7.
22. Nambi V, Chambless L, He M, Folsom AR, Mosley T, Boerwinkle E, et al. Common carotid artery intima-media thickness is as good as carotid intima-media thickness of all carotid artery segments in improving prediction of coronary heart disease risk in the Atherosclerosis Risk in Communities (ARIC) study. Eur Heart J 2012; 33(2):183-90.
23. Touboul PJ, Elbaz A, Koller C, Lucas C, Adrai V, Chedru F, et al. Common carotid artery intima-media thickness and brain infarction : the Etude du Profil Genetique de l'Infarctus Cerebral (GENIC) case-control study. The GENIC Investigators. Circulation 2000; 102(3):313-8.
24. Ebrahim S, Papacosta O, Whincup P, Wannamethee G, Walker M, Nicolaides AN, et al. Carotid plaque, intima media thickness, cardiovascular risk factors, and prevalent cardiovascular disease in men and women: the British Regional Heart Study. Stroke 1999; 30(4):841-50.
25. Chan SY, Mancini GB, Kuramoto L, Schulzer M, Frohlich J, Ignaszewski A. The prognostic importance of endothelial dysfunction and carotid atheroma burden in patients with coronary artery disease. J Am Coll Cardiol 2003; 42(6):1037-43.
26. Brook RD, Bard RL, Patel S, Rubenfire M, Clarke NS, Kazerooni EA, et al. A negative carotid plaque area test is superior to other noninvasive atherosclerosis studies for reducing the likelihood of having underlying significant coronary artery disease. Arterioscler Thromb Vasc Biol 2006; 26(3):656-62.
27. Johnsen SH, Mathiesen EB, Joakimsen O, Stensland E, Wilsgaard T, Lochen ML, et al. Carotid atherosclerosis is a stronger predictor of myocardial infarction in women than in men: a 6-year follow-up study of 6226 persons: the Tromso Study. Stroke 2007; 38(11):2873-80.
28. Inaba Y, Chen JA, Bergmann SR. Carotid plaque, compared with carotid intima-media thickness, more accurately predicts coronary artery disease events: a meta-analysis. Atherosclerosis 2012; 220(1):128-33.
29. Spence JD. Carotid plaque measurement is superior to IMT Invited editorial comment on: carotid plaque, compared with carotid intima-media thickness, more accurately predicts coronary artery disease events: a meta-analysis-Yoichi Inaba, M.D., Jennifer A. Chen M.D., Steven R. Bergmann M.D., Ph.D. Atherosclerosis 2012; 220(1):34-5.
30. Amarenco P, Lavallee PC, Labreuche J, Ducrocq G, Juliard JM, Feldman L, et al. Prevalence of coronary atherosclerosis in patients with cerebral infarction. Stroke 2011; 42(1):22-9.
31. Steinvil A, Sadeh B, Arbel Y, Justo D, Belei A, Borenstein N, et al. Prevalence and predictors of concomitant carotid and coronary artery atherosclerotic disease. J Am Coll Cardiol 2011; 57(7):779-83.
32. Tanimoto S, Ikari Y, Tanabe K, Yachi S, Nakajima H, Nakayama T, et al. Prevalence of carotid artery stenosis in patients with coronary artery disease in Japanese population. Stroke 2005; 36(10):2094-8.
33. Kallikazaros I, Tsioufis C, Sideris S, Stefanadis C, Toutouzas P. Carotid artery disease as a marker for the presence of severe coronary artery disease in patients evaluated for chest pain. Stroke 1999; 30(5):1002-7.

INTERNATIONAL JOURNAL OF
CLINICAL NEUROSCIENCES
AND MENTAL HEALTH

REVIEW

# Cerebral hemodynamics and the aging brain

Sushmita Purkayastha[1, 2, 3] and Farzaneh A. Sorond[1, 2, 3]

Special Issue on Neurosonology and Cerebral Hemodynamics

## Abstract

Aging is associated with a number of degenerative changes in the structure and function of blood vessels. Recent studies have examined the impact of age on cerebral hemodynamics and brain structure and function. These studies have shown age related changes in resting cerebral blood flow, cerebral vasoreactivity, cerebral autoregulation, and neurovascular coupling. Studies have also shown that aging is associated with cortical atrophy and cerebral white matter injury. More recent studies have also examined the relationship between age related cerebral hemodynamics and brain structure and function. Cross-sectional studies have shown that both cerebral vasoreactivity and pulsatility index are associated with cerebral white matter injury. Similarly, cerebral vasoreactivity has also been associated with impaired mobility which is known to be a clinical consequence of cerebral white matter injury in the elderly people. Neurovascular coupling has also been associated with slow gait and impaired executive function.

Despite the advances in this field, our understanding of the relationship between cerebral hemodynamics and structural changes in the aging brain is limited. We also know very little about the relationship between cerebral hemodynamics and clinical outcomes of structural brain disease. A better understanding of these relationships is an essential step towards identifying therapeutic targets and preventive strategies for age related cerebrovascular disease. This review summarizes the available data from recent studies examining cerebral hemodynamics and the aging brain.

**Keywords:** Cerebral hemodynamics, Aging brain, Cerebrovascular disease, Cerebral vasoreactivity, Cerebral autoregulation, Neurovascular coupling, White matter lesions, Cognitive impairment, Cerebral blood flow.

[1]Institute for Aging Research, Hebrew SeniorLife, Boston, MA, USA

[2]Department of Neurology, Stroke Division, Brigham and Women's Hospital, Boston, MA, USA

[3]Harvard Medical School, Boston, MA, USA

Correspondence: Farzaneh A. Sorond

Department of Neurology, Stroke Division, Brigham and Women's Hospital,

45 Francis Street, Boston, MA, 02115, USA

Email: fsorond@partners.org

Citation: Purkayastha et al. Cerebral hemodynamics and the aging brain. IJCNMH 2014; 1(Suppl. 1):S07

Received: 12 Sep 2013; Accepted: 07 Dec 2013; Published: 09 May 2014

## Introduction

Aging is a leading risk factor for vascular disease. Even in the absence of traditional vascular risk factors such as hypertension, diabetes, or hyperlipidemia, vascular dysfunction is a nearly universal complement to advancing age [1]. Age related alterations in cellular homeostasis contribute to vascular remodeling, oxidative stress, and pro-atherogenic changes in the blood vessels.

Cerebrovascular aging is particularly relevant to functional disability in old age. Aging is associated with changes in regulation of cerebral blood flow (CBF), which may threaten cerebral perfusion and ultimately affect activities of daily living as a result of ischemia, syncope, falls, and cognitive impairments. The cerebrovascular system undergoes multiple changes throughout the human lifespan, probably beginning as early as the fourth decade in life [2].

This review summarizes the overall systemic structural and physiological changes related to vascular aging, with a special emphasis on the cerebrovascular system and ensuing age related declines in motor and cognitive function.

## Structural changes associated with systemic vascular aging

Aging is associated with several structural changes in the vascular tree; the large conduit arteries become elongated and tortuous, the arterial lumen size increases and the arterial walls thicken. In addition, there is increased calcium deposition and collagen content in the intimal and medial layers with increased elastin fragmentation and thinning [3]. Accumulation of advanced glycation end (AGE) products from nonenzymation reaction of glucose with proteins, lipids, and nucleic acids leads to loss of vascular elasticity. Accumulation of the stiffer AGE-linked dysfunctional collagen results in increased collagen to elastin ratio and the mechanical stress on the vessel wall is borne by the collagen instead of the elastin. The age-related upregulation of tissue renin-angiotensin system is also linked to increased migration capacity of vascular smooth muscle cells and thickening of the vascular wall [4]. Overall, these age-related changes lead to stiffening of the arterial tree.

Aging is also associated with microvascular damage and rarefaction. Reduced vascular response to ischemic insults results in increased apoptotic endothelial cell death and impaired angiogenesis. Failure of normal activation of hypoxia-inducible factor-1α (HIF-1α) with aging leads to reduced trafficking of endothelial progenitor cells (EPC) to sites of ischemia as well as reduced expression of vascular endothelial growth factor (VEGF) and insulin like growth factor (IGF-1). Attenuation of IGF-1 further diminishes EPC survival and cell growth.

Irreversible changes at cellular level also play a role in vascular aging. Gradual age-related telomere attrition is associated with arrested cell proliferation [5]. Age related decline in stem cell number and function is also thought to lead to impaired vascular homeostasis and loss of repair capacity of the vascular system culminating in age-related atherosclerosis and progression of vascular disease [5]. Another factor known to decline with age is Sirtuin-1 (SIRT-1), which regulates the anti-aging signaling network. SIRT-1 exerts beneficial effects on the vasculature by promoting endothelium-dependent vascular relaxation, endothelial proliferation, and neovascularization. These age related process synergize, overlap, interact, and accumulate to alter the structure and function of the vascular system [5].

## Physiological changes associated with systemic vascular aging

Aging is associated with endothelial dysfunction as a result of increased oxidative stress and reduced bioavailability of nitric oxide (NO) [6]. Therefore, blood flow in response to increased metabolic demand of the tissue is compromised. Flow-mediated vasodilatation (FMD) of the brachial artery following vascular occlusion is indicative of endothelium dependent vasodilatation. A reduction in FMD accompanied by elevated oxidative stress was observed in elderly individuals [7]. Oxidative stress is also implicated in cellular signaling pathways causing platelet aggregation, cell adhesion and inflammation in the vasculature. Normal aging is also associated with upregulation of pro-inflammatory vascular gene expression profile and increased plasma concentrations of inflammatory markers, which contribute to vascular dysfunction, endothelial apoptosis, and development of atherosclerosis [8].

Stiffening of the conduit arteries with age increases the aortic pulse wave velocity (PWV). As a result, systolic blood pressure is augmented and diastolic pressure is decreased, which leads to a widened pulse pressure. Augmentation of PWV and increases in pulse pressure is linked to increased collagen deposition, fibrosis, and intimal and medial thickening. These vascular changes result in ventricular hypertrophy due to increased workload of the heart and transmit higher pressure and higher flow pulsatility to the end organs, eventually causing adverse cardio- and cerebrovascular events [3].

## Structural changes in the cerebral vessels

Several alterations across the entire cerebrovascular tree occur with age. Arterioles in the deep white matter regions become tortuous and with increasing vascular tortuosity, CBF becomes perfusion-dependent, leaving these deep white matter regions vulnerable to chronic hypoperfusion [9]. Periventricular venous collagenosis is also evident with aging. These changes result in narrowing or even occlusion of the lumen resulting in chronic ischemia and/or edema in the deep brain white matter regions. Similar to the systemic vessels, reduced activation of HIF-1α and VEGF expression also result in age related decline in ce-

rebral angiogenesis and hypoxic-ischemic response. Capillaries also undergo degeneration, loss of endothelium and thickening of the basement membrane with age. Animal studies have reported decreases in capillary number and density and increased inter-capillary distance with age [9]. The pericytes in the capillaries also undergo degeneration which mediates ischemic damage to the brain vessels by reducing CBF response during brain activation. Accumulations of neurotoxins occur following breakdown of the blood brain barrier [10]. Vessels in the cerebral gray matter also undergo similar structural changes with substantial rarefaction of the cerebral arterioles, decline in capillary density, thickening and fibrosis in and around the basement membrane of these vessels.

## Physiological changes in the cerebral vessels

### Cerebral blood flow

Advancing age is associated with a decline in resting CBF. Several studies utilizing transcranial Doppler (TCD) ultrasonography and functional imaging techniques have consistently reported a decrease in blood flow velocity through major cerebral arteries and a decline in regional cerebral perfusion with aging [2, 11]. CBF in the cerebral cortex and the basal forebrain has been found to be consistently lower with age. However, the underlying mechanism for this decrease is unknown. Age related atrophy in cerebral volume and microvascular rarefaction may contribute to the decline in CBF. Alternatively, the decrease in CBF in the aged brain could be a secondary effect of attenuation in neural activation and a shift towards lower cerebral metabolic activity rather than a primary factor contributing to the decline in neural activation [12].

### Cerebral vasoreactivity

Cerebral vasoreactivity (VR) to various stimuli such as changes in end-tidal carbon dioxide ($CO_2$) or drugs is used to assess cerebral perfusion reserve. Cerebral VR, which is a NO-dependent process, is also considered a measure of endothelial function in the cerebral arteries [13-15]. The impact of age on cerebral VR is controversial. Some studies have reported a decline in VR with age [11]. In the Rotterdam study, VR declined at a rate of 0.6%/kPa per year with increasing age up to 90 years, though data was scarce for the advanced age population. Sex-related differences in VR have also been reported with aging. Age related reduction in VR was seen in postmenopausal women, but not in men, suggesting possible hormonal influences affecting VR [16]. Age related differences in regional cerebral vascular response to changes in end-tidal $CO_2$ have also been reported using positron emission tomography [14]. Vasodilatation in the cerebellum and insular cortex during hypercapnia and vasoconstriction in the frontal cortex during hypocapnia was greater in the younger subjects compared to the older subjects, suggesting less effective vascular response in cerebral perforating arteries, possibly as a result of arteriosclerosis with normal aging. Utilizing blood oxygenation level-dependent (BOLD) functional MRI during a dual task of global hypercapnic breath-holding and finger tapping task in young and old subjects, mean BOLD signal amplitudes were significantly smaller in the older subjects, again suggesting age related decline in VR to vasodilatory stimulus despite similar neuronal activation [17].

### Dynamic cerebral autoregulation

Dynamic cerebral autoregulation (dCA) is the intrinsic property of the cerebral vessels to maintain flow despite rapid changes in systemic pressure. Many studies have been conducted to assess dCA in normal aging [18]. While different measurement conditions, protocols, and assessment techniques were used, the conclusions were similar. In one study dCA assessed with frequency domain transfer function analysis during steady state sitting and standing was shown to be preserved in the elderly subjects [19]. Another study, utilizing the time domain correlation index between spontaneous changes in blood pressure and CBF velocity, also reported no differences in dCA between young and old subjects [20]. Carey et al. estimated autoregulatory index from dynamic pressure stimulus using lower body negative pressure and Valsalva maneuver and depressor stimulus using bilateral thigh cuff inflation and also showed that dCA was unaffected by aging [21]. While all these studies conclude that aging is not associated with a decline in dCA, it is important to note that the age range of the subjects in these studies varied between 50-75 years. Therefore, the impact of advanced age (>75 years) on dCA is unknown.

### Pulsatility index

Pulsatility index (PI), which measures cerebrovascular compliance, is calculated from the CBF velocity as the difference between systolic and diastolic flow velocities divided by the mean flow velocity [18]. Higher PI is reflective of lower cerebrovascular compliance. The percent change in PI measured during a dynamic exercise study was similar between the young and older subjects with a delay in response to PI in the older group suggesting less influence of exercise-induced sympathetic activity in cerebral vasculature of the older subjects [22]. Another study measuring PI during lower body negative pressure induced orthostasis in physically unfit and fit young and old subjects reported that PI was not influenced by either age or fitness level [23]. However, in both these studies blood pressure was monitored once every minute which might have confounded the results.

### Neurovascular coupling

Neurovascular coupling (NVC) or functional hyperemia is measure of close spatial and functional relationship between neural activation and CBF. NVC ensures that blood flow is increased to meet the increased metabolic demands of the activated neurons [15]. A mismatch between the de-

mand and supply would result in relative hypoperfusion and brain dysfunction. A study using functional TCD measurements during a visual stimulation in subjects ranging from 10–60 years did not find any age-related difference in visual activation-induced CBF velocity changes, suggesting that NVC is unaffected by aging [24]. In another study involving young and old subjects, functional TCD was used to assess NVC in the anterior and posterior cerebral arteries during visual and executive function tasks to activate the occipital and frontal lobes, respectively [25]. While the younger group showed task specific flow activation in either territory, the older group showed a generalized increase in blood flow in both the territories in response to both tasks, suggesting generalization of cerebral activity to compensate for age-related loss of region specific function. Similar generalization of cerebral activity was also reported with functional MRI during cognitive tasks in elderly people [26]. Overall NVC seems to be altered with aging.

## Clinical manifestations of hemodynamic changes with aging

Cerebral small vessel disease, manifested by white matter hyperintensities (WMH) on brain magnetic resonance imaging (MRI), is a common finding in elderly individuals. These MRI findings, which consist of areas of increased brightness and appear as punctate or confluent patches in deep subcortical white matter tracts, particularly those close to the ventricles, have been associated with impairments in cognition and physical function in the elderly people [15]. With normal aging, WMH progress by about 44% in the deep and 30% in the periventricular white matter over a 3 year period with greatest progression seen in the frontal region [27]. The suggested mechanisms underlying WMH include chronic ischemia, hypoperfusion due to endothelial dysfunction and impaired cerebral autoregulation, increased pulsatility of the cerebral vessels as a result of arterial stiffening, blood brain barrier leakage, edema, inflammation, and degeneration [15, 28]. Histopathological correlates of WMH include cortical atrophy, loss of myelinated fibers and axonal disruption. WMH typically accumulate in regions supplied by direct penetrating branches of the cerebral circulation which are susceptible to increased flow pulsatility and increased pressure due to wave reflection. In support of the hypoxic-ischemic mechanism, increased levels of protein markers of hypoxia have also been associated with the prevalence of WMH in a cohort of elderly people [15].

The link between WMH and clinical outcomes such as physical function and cognition has been demonstrated in a number of studies. In a multi-center LADIS study, WMH was shown to be an independent determinant of transition to disability in subjects between 65–84 years [29]. Decline in gait, walking speed and balance performances were directly correlated with the severity of WMH. Similar findings were also reported by investigators examining gait variables using a composite score [30]. In this study, subjects with poor gait scores and higher occurrences of falls were shown to have greater volumes of WMH. Another group observed that WMH, predominantly in the centrum semiovale and periventricular frontal regions, were associated with lower gait speed, shorter stride length, and broader stride width [31]. They also utilized diffusion tensor imaging to examine the microstructural integrity of normal-appearing white matter and demonstrated that in elderly subjects with WMH, there was widespread disruption in white matter microstructural integrity as indicated by a lower fractional anisotropy and higher mean diffusivity. Disrupted normal white matter microstructural integrity was associated with impaired gait measures. Similar relationships between brain structure and cognition have also been observed with aging. Individuals with better cognition as demonstrated by better performance on executive tasks also had lower volume of WMH in the frontal brain regions [32]. Increased WMH burden predicted poor performance on cognitive task involving executive function and processing speed. Among healthy older adults, individuals with poor cognition especially in the executive domain have also been shown to be more prone to falls [33]. Although the etiology of age related WMH is yet to be established, several studies have highlighted the relationship between the hemodynamic changes and clinical manifestations of WMH on the aging brain. These studies are summarized below.

### Cerebral blood flow

Gradual decline in CBF over time is linked to increased risk of developing WMH. In a population based study using TCD and MRI in 628 elderly individuals WMH was strongly associated with low CBF velocity [34]. This study reported a fourfold increase in the risk of severe WMH in subjects with low CBF velocity in the middle cerebral artery compared to subjects with high CBF velocity. Decline in CBF velocity emerged to be a stronger risk factor for the presence of WMH than age and high blood pressure in this population. Another study utilizing arterial spin labeling to measure regional CBF reported that CBF was lower in areas of WMH relative to normal appearing white matter in healthy older individuals [35].

### Pulse wave velocity and pulsatility index

In a community based cohort of elderly people ranging between 69–93 years, increased carotid PI and carotid-femoral PWV were both related to increased risk of subcortical infarcts with a hazard ratio of 1.62 and 1.71 per standard deviation, respectively [36]. Carotid femoral PWV was also associated with higher WMH volume and carotid PI was associated with lower whole brain grey and white matter volumes. Both these hemodynamic indices were also associated with lower scores in multiple cognitive domains. Similar relationships between middle cerebral artery PI and severity of WMH volumes have also been reported in

a community dwelling group of elderly subjects [37]. It has been hypothesized that aortic stiffness exposes the cerebral microcirculation to abnormal physical forces marked with increased PWV and increased transmission of flow pulsatility to the brain causing microvascular remodeling and ischemic damage to the brain and leading to clinical manifestations of cognitive impairment [38].

### Dynamic cerebral autoregulation

Animal models provide evidence that cerebrovascular dysfunction and vascular changes are key contributors to hypoperfusion and eventually result in white matter damage. In animal models of small vessel diseases, impaired cerebral autoregulation is apparent months before the first evidence of white matter damage [39]. In a cross-sectional study of elderly individuals with vascular risk factors, we found that higher WMH volumes and lower microstructural integrity (lower fractional anisotropy and higher mean diffusivity) of the white matter was associated with less effective dCA [40].

### Cerebral vasoreactivity and flow mediated dilatation

WMH are associated with decline in systemic and cerebrovascular endothelial function. In older adults with cardiovascular risk factors, FMD measured in the brachial artery was inversely associated with WMH volume [41]. In elderly subjects from the population-based Rotterdam study, cerebral VR to changes in end-tidal $CO_2$ was found to be inversely associated with deep subcortical and total periventricular WMH [42]. The most robust relationship was between impaired cerebral VR and periventricular WMH which is a watershed territory in the brain, suggesting that hypoperfusion and subsequent ischemia in these regions may be the causal mechanism leading to WMH. Cerebral VR on the other hand has also been associated with impaired mobility in the elderly people. In 419 community dwelling individuals from the MOBILIZE Boston Study, Cerebral VR was linked to gait speed. Subjects in the lowest quintile of VR had lower gait speeds compared to those in the highest quintile. Also, subjects in the highest quintile of VR had significantly lower fall rates [43].

### Neurovascular coupling

NVC has also been linked to WMH and clinical outcomes in the elderly people. Data from the MOBILIZE Boston study, show that changes in CBF velocity responses to an N-Back task (referred to as NVC) was significantly associated with gait speed and that subjects with higher NVC were able to suppress the negative relationship between WMH and gait speed [44]. In other words, individuals with faster gait speed despite increased WMH burden also exhibited higher NVC. In another study involving older individuals, impaired NVC was associated with poor executive function as measured by the Trails making test B [45]. Moreover, higher NVC coupling was associated with greater white matter microstructural integrity as measured by diffusion tensor imaging.

## Summary

Age related changes in the structure and function of the system and cerebral vascular tree have been demonstrated in many studies. A number of age related structural changes in the brain, which clinically manifest with cognitive and mobility impairment, have also been linked to vascular mechanisms. **Figure 1** provides an overview of the relationship between cerebrovascular aging and clinical outcomes.

Future longitudinal studies linking specific age related vascular changes to brain structural changes and age related mobility and cognitive impairment will help identify therapeutic targets for the prevention and treatment of vascular causes of these disorders.

#### Abbreviations

AGE: Advanced glycation end; BOLD: Blood oxygenation level-dependent; CBF: Cerebral blood flow; $CO_2$: Carbon dioxide; dCA: Dynamic cerebral autoregulation; EPC: Endothelial progenitor cells; FMD: Flow-mediated vasodilatation; HIF-1α: Hypoxia-inducible factor-1α; IGF-1: Insulin like growth factor; MRI: Magnetic resonance imaging; NO: Nitric oxide; NVC: Neurovascular coupling; PI: Pulsatility index; PWV: Pulse wave velocity; SIRT-1: Sirtuin-1; TCD: Transcranial Doppler; WMH: White matter hyperintensities; VEGF: Vascular endothelial growth factor; VR: Vasoreactivity

#### Competing interests

The authors declare no conflict of interest.

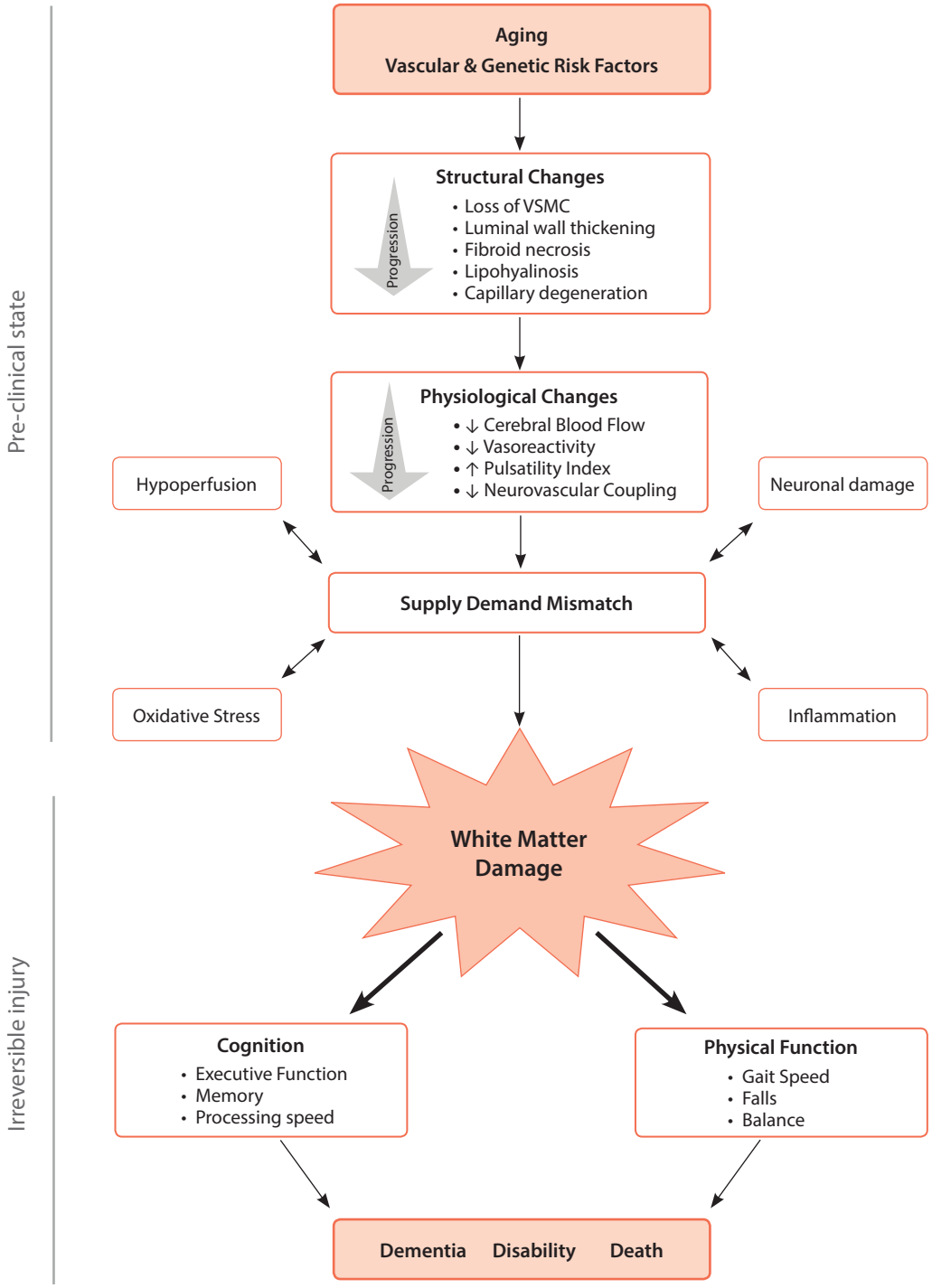


**Figure 1.** Relationship between cerebrovascular aging and clinical outcomes.

## References


1. Lakatta EG, Levy D. Arterial and cardiac aging: major shareholders in cardiovascular disease enterprises: Part I: aging arteries: a "set up" for vascular disease. Circulation 2003; 107(1):139-46.
2. Farkas E, Luiten PG. Cerebral microvascular pathology in aging and Alzheimer's disease. Prog Neurobiol 2001; 64(6):575-611.
3. Kovacic JC, Moreno P, Nabel EG, Hachinski V, Fuster V. Cellular senescence, vascular disease, and aging: part 2 of a 2-part review: clinical vascular disease in the elderly. Circulation 2011; 123(17):1900-10.
4. Jiang L, Wang M, Zhang J, Monticone RE, Telljohann R, Spinetti G, et al. Increased aortic calpain-1 activity mediates age-associated angiotensin II signaling of vascular smooth muscle cells. PLoS One 2008; 3(5):e2231.
5. Kovacic JC, Moreno P, Hachinski V, Nabel EG, Fuster V. Cellular senescence, vascular disease, and aging: part 1 of a 2-part review. Circulation 2011; 123(15):1650-60.
6. Ungvari Z, Kaley G, de Cabo R, Sonntag WE, Csiszar A. Mechanisms of vascular aging: new perspectives. J Gerontol A Biol Sci Med Sci 2010; 65(10):1028-41.

7. Wray DW, Nishiyama SK, Harris RA, Zhao J, McDaniel J, Fjeldstad AS, et al. Acute reversal of endothelial dysfunction in the elderly after antioxidant consumption. Hypertension 2012; 59(4):818-24.
8. Csiszar A, Wang M, Lakatta EG, Ungvari Z. Inflammation and endothelial dysfunction during aging: role of NF-kappaB. J Appl Physiol 2008; 105(4):1333-41.
9. Brown WR, Thore CR. Review: cerebral microvascular pathology in ageing and neurodegeneration. Neuropathol Appl Neurobiol 2011; 37(1):56-74.
10. Bell RD, Winkler EA, Sagare AP, Singh I, LaRue B, Deane R, et al. Pericytes control key neurovascular functions and neuronal phenotype in the adult brain and during brain aging. Neuron 2010; 68(3):409-27.
11. Bakker SL, de Leeuw F-E, den Heijer T, Koudstaal PJ, Hofman A, Breteler MM. Cerebral haemodynamics in the elderly: the Rotterdam study. Neuroepidemiology 2004; 23(4):178-84.
12. Riddle DR, Sonntag WE, Lichtenwalner RJ. Microvascular plasticity in aging. Ageing Res Rev 2003; 2(2):149-68.
13. Iadecola C, Park L, Capone C. Threats to the mind aging, amyloid, and hypertension. Stroke 2009; 40(3 suppl 1):S40-S4.
14. Ito H, Kanno I, Ibaraki M, Hatazawa J. Effect of aging on cerebral vascular response to Paco2 changes in humans as measured by positron emission tomography. Journal of Cerebral Blood Flow & Metabolism 2002; 22(8):997-1003.
15. Sorond FA, Lipsitz LA. Aging and the Cerebral Microvasculature: Clinical Implications and Potential Therapeutic Interventions. Masaro E, Austad S, editors. London: Academic Press; 2011.
16. Kastrup A, Dichgans J, Niemeier M, Schabet M. Changes of cerebrovascular CO2 reactivity during normal aging. Stroke 1998; 29(7):1311-4.
17. Riecker A, Grodd W, Klose U, Schulz JB, Gröschel K, Erb M, et al. Relation between regional functional MRI activation and vascular reactivity to carbon dioxide during normal aging. Journal of Cerebral Blood Flow & Metabolism 2003; 23(5):565-73.
18. Van Beek AH, Claassen JA, Rikkert MGO, Jansen RW. Cerebral autoregulation: an overview of current concepts and methodology with special focus on the elderly. Journal of Cerebral Blood Flow & Metabolism 2008; 28(6):1071-85.
19. Lipsitz LA, Mukai S, Hamner J, Gagnon M, Babikian V. Dynamic regulation of middle cerebral artery blood flow velocity in aging and hypertension. Stroke 2000; 31(8):1897-903.
20. Yam AT, Lang EW, Lagopoulos J, Yip K, Griffith J, Mudaliar Y, et al. Cerebral autoregulation and ageing. Journal of clinical neuroscience 2005; 12(6):643-6.
21. Carey BJ, Eames PJ, Blake MJ, Panerai RB, Potter JF. Dynamic cerebral autoregulation is unaffected by aging. Stroke 2000; 31(12):2895-900.
22. Heckmann JG, Brown CM, Cheregi M, Hilz MJ, Neundorfer B. Delayed cerebrovascular autoregulatory response to ergometer exercise in normotensive elderly humans. Cerebrovasc Dis 2003; 16(4):423-9.
23. Franke WD, Allbee KA, Spencer SE. Cerebral blood flow responses to severe orthostatic stress in fit and unfit young and older adults. Gerontology 2006; 52(5):282-9.
24. Rosengarten B, Aldinger C, Spiller A, Kaps M. Neurovascular coupling remains unaffected during normal aging. J Neuroimaging 2003; 13(1):43-7.
25. Sorond FA, Schnyer DM, Serrador JM, Milberg WP, Lipsitz LA. Cerebral blood flow regulation during cognitive tasks: effects of healthy aging. Cortex 2008; 44(2):179-84.
26. Cabeza R, Anderson ND, Locantore JK, McIntosh AR. Aging gracefully: compensatory brain activity in high-performing older adults. Neuroimage 2002; 17(3):1394-402.
27. Gunning-Dixon FM, Brickman AM, Cheng JC, Alexopoulos GS. Aging of cerebral white matter: a review of MRI findings. Int J Geriatr Psychiatry 2009; 24(2):109-17.
28. Gouw AA, Seewann A, van der Flier WM, Barkhof F, Rozemuller AM, Scheltens P, et al. Heterogeneity of small vessel disease: a systematic review of MRI and histopathology correlations. J Neurol Neurosurg Psychiatry 2011; 82(2):126-35.
29. Baezner H, Blahak C, Poggesi A, Pantoni L, Inzitari D, Chabriat H, et al. Association of gait and balance disorders with age-related white matter changes: the LADIS study. Neurology 2008; 70(12):935-42.
30. Srikanth V, Beare R, Blizzard L, Phan T, Stapleton J, Chen J, et al. Cerebral white matter lesions, gait, and the risk of incident falls: a prospective population-based study. Stroke 2009; 40(1):175-80.
31. de Laat KF, Tuladhar AM, van Norden AG, Norris DG, Zwiers MP, de Leeuw FE. Loss of white matter integrity is associated with gait disorders in cerebral small vessel disease. Brain 2011; 134(Pt 1):73-83.
32. Gunning-Dixon FM, Raz N. Neuroanatomical correlates of selected executive functions in middle-aged and older adults: a prospective MRI study. Neuropsychologia 2003; 41(14):1929-41.
33. Herman T, Mirelman A, Giladi N, Schweiger A, Hausdorff JM. Executive control deficits as a prodrome to falls in healthy older adults: a prospective study linking thinking, walking, and falling. The Journals of Gerontology Series A: Biological Sciences and Medical Sciences 2010; 65(10):1086-92.
34. Tzourio C, Levy C, Dufouil C, Touboul PJ, Ducimetiere P, Alperovitch A. Low cerebral blood flow velocity and risk of white matter hyperintensities. Ann Neurol 2001; 49(3):411-4.
35. Brickman AM, Zahra A, Muraskin J, Steffener J, Holland CM, Habeck C, et al. Reduction in cerebral blood flow in areas appearing as white matter hyperintensities on magnetic resonance imaging. Psychiatry Res 2009; 172(2):117-20.
36. Mitchell GF, van Buchem MA, Sigurdsson S, Gotal JD, Jonsdottir MK, Kjartansson Ó, et al. Arterial stiffness, pressure and flow pulsatility and brain structure and function: the Age, Gene/Environment Susceptibility–Reykjavik study. Brain 2011; 134(11):3398-407.
37. Mok V, Ding D, Fu J, Xiong Y, Chu WW, Wang D, et al. Transcranial Doppler ultrasound for screening cerebral small vessel disease: a community study. Stroke 2012; 43(10):2791-3.
38. Webb AJ, Simoni M, Mazzucco S, Kuker W, Schulz U, Rothwell PM. Increased cerebral arterial pulsatility in patients with leukoaraiosis: arterial stiffness enhances transmission of aortic pulsatility. Stroke 2012; 43(10):2631-6.
39. Joutel A, Monet-Leprêtre M, Gosele C, Baron-Menguy C, Hammes A, Schmidt S, et al. Cerebrovascular dysfunction and microcirculation rarefaction precede white matter lesions in a mouse genetic model of cerebral ischemic small vessel disease. The Journal of clinical investigation 2010; 120(2):433.
40. Purkayastha S, Fadar O, Mehregan A, Salat DH, Moscufo N, Meier DS, et al. Impaired cerebrovascular hemodynamics are associated with cerebral white matter damage. J Cereb Blood Flow Metab 2013.
41. Hoth KF, Tate DF, Poppas A, Forman DE, Gunstad J, Moser DJ, et al. Endothelial function and white matter hyperintensities in older adults with cardiovascular disease. Stroke 2007; 38(2):308-12.
42. Bakker SL, De Leeuw F-E, De Groot J, Hofman A, Koudstaal P, Breteler M. Cerebral vasomotor reactivity and cerebral white matter lesions in the elderly. Neurology 1999; 52(3):578-.
43. Sorond F, Galica A, Serrador J, Kiely D, Iloputaife I, Cupples L, et al. Cerebrovascular hemodynamics, gait, and falls in an elderly population MOBILIZE Boston Study. Neurology 2010; 74(20):1627-33.
44. Sorond FA, Kiely DK, Galica A, Moscufo N, Serrador JM, Iloputaife I, et al. Neurovascular coupling is impaired in slow walkers: the MOBILIZE Boston Study. Ann Neurol 2011; 70(2):213-20.
45. Sorond FA, Hurwitz S, Salat DH, Greve DN, Fisher ND. Neurovascular coupling, cerebral white matter integrity, and response to cocoa in older people. Neurology 2013.

INTERNATIONAL JOURNAL OF
CLINICAL NEUROSCIENCES
AND MENTAL HEALTH

REVIEW

# Multimodal brain monitoring in neurocritical care practice

Celeste Dias[1]

Special Issue on Neurosonology and Cerebral Hemodynamics

## Abstract

The management of severe acute neurological patients is a constant medical challenge due to its complexity and dynamic evolution. Multimodal brain monitoring is an important tool for clinical decision at bedside. The datasets collected by the several brain monitors help to understand the physiological events of acute lesion and to define patient-specific therapeutic targets. We changed from pure neurological clinical evaluation to an era of structure and image definition associated with instrumental monitoring of pressure, flow, oxygenation, and metabolism. At each time, we want to assure perfect coupling between energy deliver and consumption, in order to ensure adequate cerebral blood flow and metabolism, avoid secondary lesion, and preserve normal tissue.

Continuous monitoring of intracranial pressure, cerebral perfusion pressure, and cerebrovascular reactivity with transcranial Doppler, allows us to predict cerebral blood flow. However, adequate blood flow means not only quantity but also quality. To study and avoid tissue hypoxia we start to use methods for evaluation of oxygen extraction, such as oxygen jugular saturation, cerebral transcutaneous oximetry or measurement of oxygen pressure with intraparenchymal probes. To better understand metabolic cascade we use cerebral microdialysis to monitor tissue metabolites such as glucose, lactate/pyruvate, glycerol or cytokines involved in the acute lesion. Multimodal brain monitoring in neurocritical care practice helps neurointensivists to better understand the pathophysiology of acute brain lesion and accomplish the challenge of healing the brain and rescue lives.

**Keywords:** Multimodal brain monitoring, Intracranial pressure, Cerebral oximetry, Cerebral oxygenation, Cerebral blood flow, Cerebral microdialysis, Cerebrovascular reactivity indexes, Neurocritical care.

[1]Neurocritical Care Unit, Intensive Care Department, Hospital São João, Faculty of Medicine, University of Porto, Porto, Portugal

Correspondence: Celeste Dias
Neurocritical Care Unit, Hospital São João
Alameda Professor Hernani Monteiro
4200-319 Porto, Portugal
Email adress: mceleste.dias@gmail.com

Citation: Dias, C. Multimodal brain monitoring in neurocritical care practice. IJCNMH 2014; 1(Suppl. 1):S08

Received: 01 Sep 2013; Accepted: 29 Oct 2013; Published: 09 May 2014

## Introduction

The main purpose of neurocritical care is to fight brain cell death, giving adequate flow, oxygen, and glucose in order to promote neuronal, endothelial, and glial cell recovery to ensure neuronal function. Although clinical evaluation of comatose patients is still one of the foundations of clinical neuroscience, the neurological findings of adverse events appear too late in time. Multimodal brain monitoring may give crucial, real-time information about the dynamic evolution of brain lesion, allowing to avoid secondary injury, recognize adverse events, and improve individualized management of severe acute neurological patients admitted to Neurocritical Care Units (NCCU) [1].

## Basic neuromonitoring

### Intracranial pressure, cerebral perfusion pressure, and autoregulation

Intracranial pressure (ICP) is derived from cerebral blood flow (CBF) and cerebrospinal fluid (CSF) circulation within the stiff skull [2]. The most reliable methods of ICP monitoring are ventricular catheters and intraparenchymal probes. An intraventricular drain connected to an external pressure transducer is still considered to be a "golden standard" method of measure global ICP. Ventricular catheters allow recalibration and therapeutic drainage of CSF but have significant complications, including hemorrhage, occlusion and infection. Intraparenchymal fiberoptic or microtransducer probes have a minimal associated risk of complications, but can be calibrated only before insertion although the sensitivity drift over time is very small. Critical values of ICP may vary between individual patients but current consensus is to treat ICP exceeding the 20 mmHg threshold [3].

International guidelines for traumatic brain injury (TBI) recommend that ICP should be monitored in patients with Glasgow Coma Scale (GCS) score <8, with an abnormal head CT scan; or patients with GCS score <8 with a normal head CT scan if two or more of the following characteristics are present: age over 40 years, systolic blood pressure <90 mmHg or motor posturing [4, 5]. Recently, Chesnut et al. [6] published the results of the first randomized trial of ICP monitoring in patients with severe TBI. Six months after injury, patient groups had similar scores on functional status and cumulative mortality. For intensivists the strongest clinical implication of this trial is that we need to understand that the true value of ICP is more than a number and should become part of a multimodality approach to targeted therapy [7, 8].

ICP beat-to-beat waveform consists of three components named P1, P2, and P3 that are related to arterial pulse and brain compliance (**Figure 1**). P2 over P1 is a sensitive (99%) but not specific (1-17%) predictor of ICP subsequent increase [9]. Continuous ICP and arterial blood pressure monitoring allow calculation of cerebral perfusion pressure (CPP=ABP-ICP). CPP is the driving force of CBF and the principal determinant of cerebrovascular reactivity to pressure, named cerebral autoregulation. The normal cerebral arterial bed actively reacts to small fluctuations in arterial blood pressure in order to maintain constant CBF over a wide range of CPPs (from approximately 50–150 mmHg). When reactivity is normal the changes in ABP produce an inverse change in cerebral blood volume and hence ICP, but when reactivity is disturbed, changes in ABP are passively transmitted to ICP. Computational methods for continuous assessment of cerebral autoregulation were introduced more than a decade ago and they evaluate dynamic relationships between slow waves of ABP or CPP and ICP or flow velocity [10]. Examples of these methods are moving correlation coefficient, phase shift, or transmission (either in time- or frequency-domain).

The pressure reactivity index (PRx) is calculated as the moving correlation coefficient between 30 consecutive, 10 seconds averaged data points of ICP and ABP [11, 12]. A positive PRx (>0.2) signifies passive reactive vascular bed, while a PRx <0.2 means normal autoregulation. PRx may be used to continuous monitoring of autoregulation and define individual lower limit of autoregulation (LLA) and upper limit of autoregulation (ULA), helping target optimal CPP [13, 14] (**Figure 2**). Retrospective studies show that favorable outcome reaches its peak when CPP is maintained close to optimal CPP [15].

### Oxygenation and cerebral blood flow

Brain resuscitation based on basic control of ICP and CPP does not prevent cerebral hypoxia in some patients [16]. Cerebral oxygenation monitoring evaluates the balance between oxygen delivery and consumption [17] and oxygen guided management could lead to improved neurologic outcome [18]. There are several invasive and non-invasive continuous methods of monitoring regional or global brain oxygenation and avoid secondary lesion due to hypoxia (jugular venous bulb oximetry, brain tissue oxygenation, and transcutaneous cerebral oximetry with near infrared spectroscopy).

### Brain tissue oxygen pressure

Brain tissue oxygenation pressure (PbtO2) represents the interaction between plasma oxygen tension and CBF [19]. Direct measurement of local PbtO2 with an intraparenchymal probe is becoming the gold standard for oxygen monitoring in NCCU. PbtO2 probes are placed in the white matter and post-insertion head CT confirmation is needed to interpret readings. The normal range is 25-50 mmHg and PbtO2 <15 mmHg is considered the critical threshold for hypoxia [20, 21]. Algorithms of PbtO2-directed therapy should incorporate the management of the several causes of tissue hypoxia (hypoxic, anemic, ischemic, cytopathic, and hypermetabolic) [22] (**Table 1**). Similarly to PRx, the index of tissue oxygen reactivity (ORx), calculated as the correlation coefficient between PbtO2 and CPP, can be

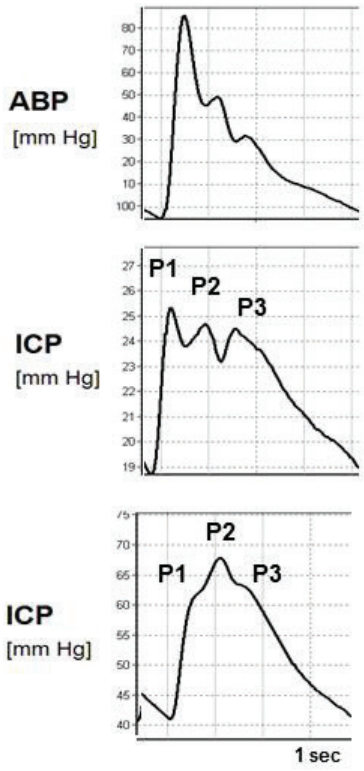


**Figure 1.** Arterial blood pressure (ABP) and Intracranial Pressure (ICP) waveform. P1 (percussion wave) represents systolic arterial pulsation, P2 (tidal wave) reflects intracranial compliance and P3 (dicrotic wave) represents venous wave that result from closure of aortic valve. In normal conditions, P1 > P2 >P3, but when brain compliance starts to decrease, the amplitude of P2 increases and may exceed P1.

used as an indicator of CBF autoregulation [23]. The concepts of cerebrovascular pressure reactivity and oxygen reactivity are related as high CPP should be avoided if it does not yield improvement in brain tissue oxygenation [24].

### Transcranial Doppler and thermal diffusion flowmetry

Continuous direct monitoring of CBF would be helpful to manage acute neurologic patients. Transcranial Doppler ultrasonography (TCD) is a non-invasive method to assess flow velocity as a surrogate of cerebral blood flow. TCD is more frequently used in the diagnosis of vasospasm or hyperemia, but may also be used as a tool to monitor the regulatory reserve of cerebral vasculature to changes in ABP, $CO_2$, and transient hyperemic response test [25-27]. Thermal diffusion flowmetry (TDF) is based on thermal conductivity and provides a quantitative measurement of regional CBF. Probes are inserted in the white matter, 25 mm below the dura and the normal range is 18-25 ml/100g/min [28]. Continuous monitoring of CBF with TDF and CPP allows calculation of flow-related autoregulation index [29].

### Cerebral metabolism and electrical function

Brain metabolism can be assessed by hourly microdyalisis measurement of cell substrates (glucose), metabolites (lactate, pyruvate, glycerol), and neurotransmitters (glutamate) in the extracellular fluid [30]. Normal ranges are described in **Table 2**. Cerebral microdyalisis detects early hypoxia and ischemia and increases the therapeutic window to avoid secondary lesion. However, remains to be established if treatment-related improvement in biochemistry translates into better outcome after acute brain injury [31].

Continuous electroencephalography (cEEG) with or without video surveillance is becoming more widespread in the NCCU [32]. Modern cEEG approaches include quantitative analysis of total power, relative alpha variability and asymmetry detection. The most common indications are: detection of nonconvulsive seizures or status epilepticus, assessment of depth of sedation, detection of ischemia and characterization of clinical signs such as rigidity, tremors, eye deviation, agitation and otherwise unexplained variations of ABP and heart rate [33].

**Table 1.** Causes of brain tissue hypoxia and management.

| Etiology | Pathophysiology | Management of brain tissue hypoxia |
|---|---|---|
| *Hypoxic* | Low $PaO_2$<br>Low $SaO_2$ | Lung recruitment and $FiO_2$ increase<br>Improve $O_2$ delivery and Hb dissociation curve |
| *Anemic* | Low Hb concentration | Red blood cell transfusion |
| *Ischemic* | Hypotension, low CPP<br>Hyperventilation<br>Vasospasm<br>Shunt<br>Low cardiac output<br>Dysperfusion | Increase ABP or CPP<br>Increase $CO_2$<br>Vasodilation (systemic or local)<br>Treat SIRS or sepsis<br>Improve cardiac output<br>Reduce brain edema |
| *Cytotopathic* | Low oxygen extraction<br>Hb high affinity<br>Mitochondrial dysfunction | Improve $O_2$ delivery<br>Improve Hb dissociation curve |
| *Hypermetabolic* | High metabolism | Increase sedation, treat seizures, decrease temperature |

ABP = Arterial blood pressure; CPP = Cerebral perfusion pressure; Hb = Hemoglobin

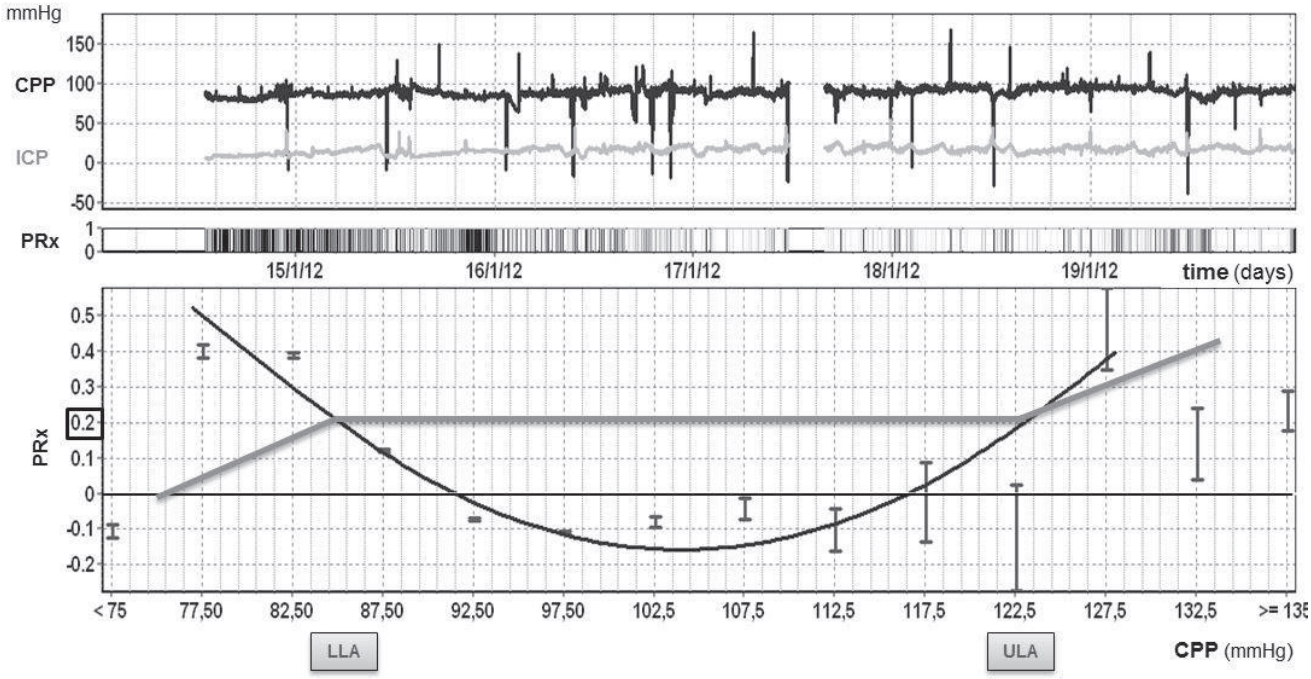


**Figure 2**. Intracranial pressure (ICP), cerebral perfusion pressure (CPP), and pressure reactivity index (PRx). Continuous monitoring of autoregulation and definition of individual lower limit of autoregulation (LLA) and upper limit of autoregulation (ULA) to target optimal CPP during ICU management.

## Conclusion

Multimodal brain monitoring increases the therapeutic window and helps to target treatment avoiding excess or lack of interventions, decreasing cerebral secondary lesions, and systemic complications. Clinical information systems and integrated brain monitoring graphical trends show that pathologic readings precedes clinical deterioration and therefore are an important tool to support proactive medical decision in daily neurocritical care practice.

### Abbreviations

ABP: Arterial blood pressure; CBF: Cerebral blood flow; cEEG: Continuous electroencephalography; CSF: Cerebrospinal fluid; CPP: Cerebral perfusion pressure; GCS: Glasgow coma scale; ICP: Intracranial pressure; LLA: Lower limit of autoregulation; NCCU: Neurocritical care units; ORx: Oxygen reactivity index; PbtO2: Brain tissue oxygenation pressure; PRx: Pressure reactivity index; TBI: Traumatic brain injury; TCD: Transcranial Doppler ultrasonography; TDF: Thermal diffusion flowmetry; ULA: Upper limit of autoregulation

### Competing interests

The authors declare no conflict of interest.

### References

1. Zygun D. Can we demonstrate the efficacy of monitoring? Eur J Anaesthesiol Suppl 2008; 42:94-7.
2. Czosnyka M, Pickard JD. Monitoring and interpretation of intracranial pressure. Journal of Neurology, Neurosurgery, and Psychiatry 2004; 75(6):813-21.
3. Bratton SL, Chestnut RM, Ghajar J, McConnell Hammond FF, Harris OA, Hartl R, et al. Guidelines for the management of severe traumatic brain injury. VIII. Intracranial pressure thresholds. J Neurotrauma 2007; 24 Suppl 1:S55-8.
4. Narayan RK, Kishore PR, Becker DP, Ward JD, Enas GG, Greenberg RP, et al. Intracranial pressure: to monitor or not to monitor? A review of our experience with severe head injury. J Neurosurg 1982; 56(5):650-9.
5. Brain Trauma F, American Association of Neurological S, Congress of Neurological S, Joint Section on N, Critical Care AC, Bratton SL, et al. Guidelines for the management of severe traumatic brain

**Table 2**. Cerebral microdialysis normal range of biomarkers and metabolism failure interpretation.

| Microdialysis concentration | Normal range | Monitoring interpretation |
|---|---|---|
| *Glucose* | 1.5-2.0 mmol/l | Hypoglycemia, cerebral hyperglycolysis<br>Hypoxia, ischemia, |
| *Lactate / Pyruvate ratio* | >20-25 | Cellular redox state, hypoglicemia<br>Hypoxia, ischemia |
| *Glycerol* | >100 µmol/l | Cell membrane degradation<br>Hypoxia, ischemia |
| *Glutamate* | >15-20 µmol/l | Excitotoxicity<br>Hypoxia, ischemia |

injury. VI. Indications for intracranial pressure monitoring. J Neurotrauma 2007; 24 Suppl 1:S37-44.

6. Chesnut RM, Temkin N, Carney N, Dikmen S, Rondina C, Videtta W, et al. A trial of intracranial-pressure monitoring in traumatic brain injury. The New England journal of medicine 2012; 367(26):2471-81.
7. Czosnyka M, Smielewski P, Timofeev I, Lavinio A, Guazzo E, Hutchinson P, et al. Intracranial pressure: more than a number. Neurosurgical Focus 2007; 22(5):E10.
8. Chesnut RM. Intracranial pressure monitoring: headstone or a new head start. The BEST TRIP trial in perspective. Intensive Care Med 2013; 39(4):771-4.
9. Chesnut RM. Intracranial Pressure. In: Roux PDL, Levine J, Kofke WA, editors. Monitoring in Neurocritical Care: Elsevier Saunders; 2013. p. 338-47.
10. Czosnyka M, Brady K, Reinhard M, Smielewski P, Steiner LA. Monitoring of cerebrovascular autoregulation: facts, myths, and missing links. Neurocritical care 2009; 10(3):373-86.
11. Czosnyka M, Smielewski P, Kirkpatrick P, Laing RJ, Menon D, Pickard JD. Continuous assessment of the cerebral vasomotor reactivity in head injury. Neurosurgery 1997; 41(1):11-7; discussion 7-9.
12. Czosnyka M, Pickard JD. Monitoring and interpretation of intracranial pressure. J Neurol Neurosurg Psychiatry 2004; 75(6):813-21.
13. Steiner LA, Czosnyka M, Piechnik SK, Smielewski P, Chatfield D, Menon DK, et al. Continuous monitoring of cerebrovascular pressure reactivity allows determination of optimal cerebral perfusion pressure in patients with traumatic brain injury. Crit Care Med 2002; 30(4):733-8.
14. Brady KM, Lee JK, Kibler KK, Easley RB, Koehler RC, Shaffner DH. Continuous measurement of autoregulation by spontaneous fluctuations in cerebral perfusion pressure: comparison of 3 methods. Stroke 2008; 39(9):2531-7.
15. Lazaridis C, Smielewski P, Steiner LA, Brady KM, Hutchinson P, Pickard JD, et al. Optimal cerebral perfusion pressure: are we ready for it? Neurol Res 2013; 35(2):138-48.
16. Stiefel MF, Udoetuk JD, Spiotta AM, Gracias VH, Goldberg A, Maloney-Wilensky E, et al. Conventional neurocritical care and cerebral oxygenation after traumatic brain injury. J Neurosurg 2006; 105(4):568-75.
17. Zauner A, Daugherty WP, Bullock MR, Warner DS. Brain Oxygenation and Energy Metabolism: PART I—Biological Function and Pathophysiology. Neurosurgery 2002; 51:289-302.
18. Tran-Dinh A, Depret F, Vigue B. [Brain tissue oxygen pressure, for what, for whom?]. Ann Fr Anesth Reanim 2012; 31(6):e137-43. Pression tissulaire cerebrale en oxygene : pour quoi faire et pour qui ?
19. Rosenthal G, Hemphill JC, 3rd, Sorani M, Martin C, Morabito D, Obrist WD, et al. Brain tissue oxygen tension is more indicative of oxygen diffusion than oxygen delivery and metabolism in patients with traumatic brain injury. Crit Care Med 2008; 36(6):1917-24.
20. Brain Trauma F, American Association of Neurological S, Congress of Neurological S, Joint Section on N, Critical Care AC, Bratton SL, et al. Guidelines for the management of severe traumatic brain injury. X. Brain oxygen monitoring and thresholds. J Neurotrauma 2007; 24 Suppl 1:S65-70.
21. Maloney-Wilensky E, Le Roux P. The physiology behind direct brain oxygen monitors and practical aspects of their use. Childs Nerv Syst 2010; 26(4):419-30.
22. Siggaard-Andersen O, Ulrich A, Gothgen IH. Classes of tissue hypoxia. Acta Anaesthesiol Scand Suppl 1995; 107:137-42.
23. Radolovich DK, Czosnyka M, Timofeev I, Lavinio A, Hutchinson P, Gupta A, et al. Reactivity of brain tissue oxygen to change in cerebral perfusion pressure in head injured patients. Neurocritical care 2009; 10(3):274-9.
24. Jaeger M, Dengl M, Meixensberger J, Schuhmann MU. Effects of cerebrovascular pressure reactivity-guided optimization of cerebral perfusion pressure on brain tissue oxygenation after traumatic brain injury. Crit Care Med 2010; 38(5):1343-7.
25. Steiger HJ, Aaslid R, Stooss R, Seiler RW. Transcranial Doppler monitoring in head injury: relations between type of injury, flow velocities, vasoreactivity, and outcome. Neurosurgery 1994; 34(1):79-85; discussion -6.
26. Yoshihara M, Bandoh K, Marmarou A. Cerebrovascular carbon dioxide reactivity assessed by intracranial pressure dynamics in severely head injured patients. J Neurosurg 1995; 82(3):386-93.
27. Smielewski P, Czosnyka M, Kirkpatrick P, Pickard JD. Evaluation of the transient hyperemic response test in head-injured patients. J Neurosurg 1997; 86(5):773-8.
28. Vajkoczy P, Horn P, Thome C, Munch E, Schmiedek P. Regional cerebral blood flow monitoring in the diagnosis of delayed ischemia following aneurysmal subarachnoid hemorrhage. J Neurosurg 2003; 98(6):1227-34.
29. Hecht N, Fiss I, Wolf S, Barth M, Vajkoczy P, Woitzik J. Modified flow- and oxygen-related autoregulation indices for continuous monitoring of cerebral autoregulation. J Neurosci Methods 2011; 201(2):399-403.
30. Bellander BM, Cantais E, Enblad P, Hutchinson P, Nordstrom CH, Robertson C, et al. Consensus meeting on microdialysis in neurointensive care. Intensive Care Med 2004; 30(12):2166-9.
31. Timofeev I, Czosnyka M, Carpenter KL, Nortje J, Kirkpatrick PJ, Al-Rawi PG, et al. Interaction between brain chemistry and physiology after traumatic brain injury: impact of autoregulation and microdialysis catheter location. J Neurotrauma 2011; 28(6):849-60.
32. Wartenberg KE, Mayer SA. Multimodal brain monitoring in the neurological intensive care unit: where does continuous EEG fit in? Journal of clinical neurophysiology : official publication of the American Electroencephalographic Society 2005; 22(2):124-7.
33. Wittman JJ, Jr., Hirsch LJ. Continuous electroencephalogram monitoring in the critically ill. Neurocritical care 2005; 2(3):330-41.

# 03
# Viewpoints

INTERNATIONAL JOURNAL OF
CLINICAL NEUROSCIENCES
AND MENTAL HEALTH

VIEWPOINT

# Usefulness of Doppler ultrasound in ischemic "vertigo plus"

J.M. de Bray[1], J.O. Fortrat[2], L. Laccoureye[3], and C. Verny[1]

Special Issue on Neurosonology and Cerebral Hemodynamics

## Abstract

Vertigo is an illusion of a moving environment. Ischemic "vertigo plus" has additional focal neurological symptoms which are sometimes discrete. Before an initial Doppler examination it is possible to analyze voice, audition, gait, and wave of the hands during history taking.

A patient presenting vertigo plus has to be considered as an emergency case (Stroke Unit).

The following pathologies may present with symptoms of "vertigo plus": (1) Latero-medullar infarction: vertigo and a nasal voice; (2) Infarction in the posterior inferior cerebellar artery (PICA) territory—vertigo and severe ataxia and/or clumsiness of one hand; (3) Progressive infarction of the brainstem with fluctuating symptoms as vertigo, diplopia, and transient hemiparesis; (4) Infarction in the distribution of the anterior inferior cerebellar artery (AICA)—vertigo with unilateral hearing problems in 50% of the cases.

With condition (1) and (2) Doppler Ultrasound (DUS) is likely to find a distal obstruction of the ipsilateral vertebral artery, with (3) and (4) a basilar artery stenosis or occlusion can be suspected and detected by DUS.

In conclusion, DUS is useful in vertigo plus, especially when the hospital does not have immediate access to magnetic resonance with angio. Anyway, DUS can yield additional intracranial and cervical hemodynamic information, even after this technique.

**Keywords:** Vertigo, Vertebrobasilar stroke, Emergency, Doppler ultrasound, Transcranial Doppler sonography.

[1]Department of Neurology, CHU Angers, France
[2]Department of Vascular Investigations, CHU Angers, France
[3]Department of NTP (ORL), CHU Angers, France

Correspondence: J.M. de Bray
Le Pré, Chemin de la Salette,
Avrillé France 49240, France
Email adress: jmdebray@aol.com

Citation: Bray et al. Usefulness of Doppler Ultrasound in ischemic "Vertigo Plus". IJCNMH 2014; 1(Suppl. 1):S09

Received: 03 Sep 2013; Accepted: 08 Feb 2014; Published: 09 May 2014

## Definition of vertigo

Illusion of a moving environment (mainly rotation of the objects). An isolated vertigo is in 95% of patients of a peripheral vestibular origin [1].

Ischemic "vertigo plus" has focal neurological symptoms which can be discrete.

## Diagnosis

During the first contact and history, the following functions may be disturbed indicating "vertigo plus": voice, audition, gait and wave of the hands.

Any patient presenting with a focal neurological sign and vertigo has to be considered as an emergency case (Stroke Unit).

## Types of "vertigo plus"

Four types of vertebrobasilar infarctions with possible "vertigo plus" are described below, concerning underlying vascular pathology and the clinical usefulness of Doppler ultrasound (DUS) [2].

### Lateral medullary infarction:

Lateral medullary infarction, also called Wallenberg syndrome: vertigo with at least a recently appearing nasal voice.

Pathology: Atheroma of 1 to 4 small branches coming from the fourth segment of the vertebral artery (V4), stenosis or dissection involving V3-V4 [1, 3]. DUS can be normal or detect a V4 stenosis, but it does not distinguish a dissection from a stenosis. A cervical MRI allows to assess the presence of a dissection. The main risk is a bronchopneumonia due to disturbed swallowing.

### Posterior inferior cerebellar artery infarction:

Posterior inferior cerebellar artery (PICA) infarction: vertigo (horizontal nystagmus) often associated with a severe ataxia and/or a clumsiness of one hand.

Pathology: Atheromatous stenosis in 50%, involving the PICA, the V4 segment of the vertebral artery (VA) or, more rarely, its origin [2, 3]. Cardioembolic causes represent half of these cases.

DUS can be normal or detect a V4 stenosis. When present, a proximal stenosis can be identified by extracranial DUS, suggested by increased velocities or by indirect signs on the waveform of the distal VA, such as a systolic notch sign or a slow systolic ascending time.

The main risk is a progressive coma occurring in 25% of cases on the second or third day, needing neurosurgical treatment for space occupying edema.

### Progressive infarction of the brainstem:

Progressive infarction of the brainstem due to a thrombosis of the basilar artery, characterized by fluctuating or progressive symptoms.

The main symptoms and signs are intermittent vertigo in 75% of the cases, diplopia, and transient unilateral or bilateral paresis.

An early diagnosis of a basilar artery stenosis by DUS is needed and can reveal a segmental increase of velocities with transoccipital insonation. An intraarterial angiography is useful to confirm basilar artery stenosis, offering the possibility of interventional treatment and thrombolysis. The prognosis is very poor without treatment (death in 80% of the cases).

### Infarction in the distribution of the anterior inferior cerebellar artery:

Vertigo with unilateral hearing loss or pulsatile tinnitus will occur in 50% of the cases.

It is due to an occlusion of a branch of the anterior inferior cerebellar artery (AICA), a main branch of the basilar artery. Sometimes the cause is an atheroma of the basilar artery wall, rarely a significant basilar artery stenosis [3].

DUS is often normal. It is an exception to find a basilar artery stenosis.

The prognosis is in general good.

## Isolated vertigo

An isolated vertigo has mainly a peripheral vestibular cause. An ischemic cause is exceptional, eventually being caused by an atheroma involving the median branch of the PICA, a small vessel which cannot be detected by DUS. In this case, the clinical head trust test is normal; this negative result excludes a vestibular neuritis.

## Conclusion

In the emergency room, DUS is very useful after a CT scanning, when the hospital centre does not provide access to immediate MRI. Otherwise an MRI with angiography (MRA) is the best diagnostic method for a patient with acute onset of "vertigo plus". In such a setting intracranial DUS can add hemodynamic information, and extracranial DUS can be used to precisely quantify extracranial carotid or vertebral artery stenosis.

### Abbreviations

AICA: Anterior inferior cerebellar artery; DUS: Doppler ultrasound; MRA: MRI with angiography; PICA: Posterior inferior cerebellar artery; VA: vertebral artery (VA)

## Competing interests

The authors declare no conflict of interest.

## References

1. Amarenco P. et al.Vertiges d'origine vasculaire. Act Med Angiologie 1998. 14; 247: 4962-4972.
2. Lee and al. Cerebellar infarction presenting isolated vertigo: frequency and vascular topographical patterns. Neurology 2006; 67: 1178-1183.
3. Fisher C.M. and al. Atherosclerosis of the carotid and vertebral arteries. J Neuropathol Exp Neurol. 1965; 24: 455-476.

04

# Original Research

INTERNATIONAL JOURNAL OF
CLINICAL NEUROSCIENCES
AND MENTAL HEALTH

ORIGINAL RESEARCH

# Screening of cerebrovascular diseases in Stroke Prevention Centres in Latvia

Galina Baltgaile[1], Tatjana Timofejeva[2], Ženija Kovaldina[3], Anita Raita[4], and Jelena Pecherska[5]

Special Issue on Neurosonology and Cerebral Hemodynamics

## Abstract

**Background:** To improve stroke prevention, the observation of patients suspected on having cerebrovascular disease (CVD) or stroke risk factors has been carried out in Stroke Prevention Centres (SPC) in Riga. The analysis of the incidence of CVD, correlations of clinical symptoms with diagnostic findings and risk factors was performed.

**Methods:** 1102 outpatients aged 7-89 years (65% female, 35 % male) underwent color-coded duplex sonography of precerebral and cerebral blood vessels (CCDS), had checked brachial blood pressure and blood test. Vascular pathology detected by CCDS was confirmed by CT angiography. Some of patients underwent X-ray, EEG, CT scan or MRI examination.

**Results:** Isolated dyslipidemia was the reason for observation in 2% of cases only, although 56% of surveyed had registered high level of cholesterol at the moment of observation or in the past. Patients with arterial hypertension (14% of all) had atherosclerotic lesions in arteries in 42% of cases. From 22% of patients with vertiginous syndromes and tinnitus CVD was proved in 5% of cases. Vascular pathology in cases of headache (18% of all) was found in only 11%. Silent atherosclerotic process in pre-cerebral arteries was suspected in 15% of patients but proved in 27% of all surveyed.

**Conclusion:** The underestimation of dyslipidemia and arterial hypertension as a stroke risk factors and the mismatch of diagnoses in patients with unspecified vestibular disorders and headache was found. The prevalence of detected silent carotid stenoses from all suspected proved the efficacy of US vascular screening in prevention, detection and follow-up of CVD.

**Keywords:** Stroke prevention, Stroke risk factors, Cerebrovascular diseases, Stenosis of precerebral and cerebral arteries, Vascular ultrasound screening, Vestibular disorders, Headache.

[1]Department of Neurology, Medical clinic "ARS", Latvia
[2]Department of Neurology, Medical Centre "VC-4", Latvia
[3]Department of Functional Diagnostic, Austrumu Clinical Hospital, Latvia
[4]Department of Neurology, Pauls Stradins Clinical University Hospital, Latvia
[5]Department of Modelling and Simulation, Riga Technical University, Latvia

Correspondence: Galina Baltgaile
Medical Hospital "ARS", Skolas 5, Riga, Latvia
Email adress: baltgaile@gmail.com

Citation: Baltgaile et al. Screening of cerebrovascular diseases in Stroke Prevention Centres in Latvia. IJCNMH 2014; 1(Suppl. 1):S10

Received: 09 Sep 2013; Accepted: 25 Nov 2013; Published: 09 May 2014

## Introduction

Diseases of the heart and circulatory system (cardiovascular disease or CVD) are the main cause of death in developed countries, an important cause of disability and a source of large economic and social cost to the society. In the Central and East European (CEE) countries, coronary heart disease (CHD) and stroke were responsible for 49 percent and 32 percent of all CVD deaths, respectively [1]. In the period from the 1980s through the 1990s, Europe experienced a large political transformation which worsened significantly health indicators in Western Europe as a whole and in Latvia in particular, creating a large life expectancy gap between the West and East of the continent [2]. Despite the fact that after 1998 CVD mortality started to decrease in Latvia, it is still one of the highest in European Union [3]. A recent study of neurological stroke care in Europe based on statistic data has provided evidence that stroke as a cause of death ranks second in the Baltic States. Stroke mortality rate in Latvia is one of the highest in EU [4].

There were no epidemiological studies of cerebrovascular diseases based on standardized methods of data collection in Latvia. The only source of information about some risk factors of CVD in Latvian population was the European Health For All Database [3]. Incomplete data about arterial hypertension, obesity and dyslipidemia in Latvian population from the World Health Organization (WHO) statistics database are limited to the year 2004. The only national cross-sectional survey of cardiovascular risk factors based on computerized random sampling from the registry of Latvian population was carried out in 2012 by Latvian Research Institute of Cardiology [5].

The levels of cardiovascular risk factors in Latvia were found to be relatively high. Of all the respondents, 75.2% had an increased total cholesterol level. Hypercholesterolemia was found in almost 56% of men and 41% of women in the age group of 25-34 years. Arterial hypertension was identified in 44.8% of the respondents. This study showed that control of hypertension and dyslipidemia was definitely below expectations, which was mainly due to a combined effect of poor population awareness and poor compliance with medication.

With such high frequency of dyslipidemia and arterial hypertension, high rates of arterial atherosclerotic lesions can be expected. There were no available data on the incidence of silent atherosclerotic disease of coronary and brain supplying arteries in Latvian population, although regular ultrasound vascular examinations revealed frequent occurrence of arterial atherosclerotic lesions. All above mentioned facts prove the insufficiency and inadequacy of stroke and coronary artery diseases prevention in Latvia.

One way to improve stroke prevention in Latvian population was to determine the incidence of cerebrovascular diseases, the correlation of clinical symptoms with arterial atherosclerotic lesions in brain supplying arteries and cerebrovascular risk factors.

The first and important part of study was to discover and analyze the weaknesses in recognition of stroke and other cerebrovascular diseases symptoms by family doctors, other medical specialists and among the public. Despite the fact that knowledge of the nature of atherosclerotic disease, its prevention and treatment increased in recent decades, the recognition of this disease still remains poor. For that purpose the analysis of clinical and diagnostic data of patients observed and followed in Stroke Prevention Centres (SPC) in Riga has been performed in the period of September 2012-March 2013

## Methods

Four stroke prevention centres in Riga were based on the two biggest out-patient clinics and out-patient departments in two clinical hospitals. The requirements for stroke prevention centres were: availability of consultant neurologist experienced in cerebrovascular diseases, experienced neurosonologist, up-to-date ultrasound Duplex scan diagnostic, easy access to X-Ray, CT scan, MRI, EEG diagnostic and clinical laboratory, common protocol of patients observation and program database in all centres.

Due to the mass media advertising campaign for stroke prevention, patients suspected of having cerebrovascular disorders or stroke risk factors have been sent to SPC not only by family doctors or other medical specialists but also through direct patient access.

All out-patients consulted by neurologist underwent US examination of precerebral and cerebral blood vessels by routine extra and transcranial Color Coded Duplex Doppler Scan program performed by using premium class machines ("iE-33" Philips and "Applio" Toshiba). Standard US examination protocol was supplemented by monitoring of cerebral circulation during half an hour in cases of suspected microemboli and registration of arterial wall elastic properties by M-mode scan. Some patients with suspected pathology in brain or spine underwent X-ray, CT scan or MRI examination. Vascular pathology was confirmed by CT angiography in 97% of cases with significant degree of arterial stenosis or cerebral arteries pathology. EEG was performed in all cases of seizures. Almost all observed patients had checked brachial blood pressure and blood test for cholesterol fractions.

From 1400 observed patients 288 had been excluded from analysis because of incomplete data. Statistical analysis of clinical-diagnostic correlations of 1102 patients has been performed.

## Results

The age distribution between 772 observed women and 330 men showed a small prevalence of men in younger age groups (**Figure 1**). There was a larger number of male

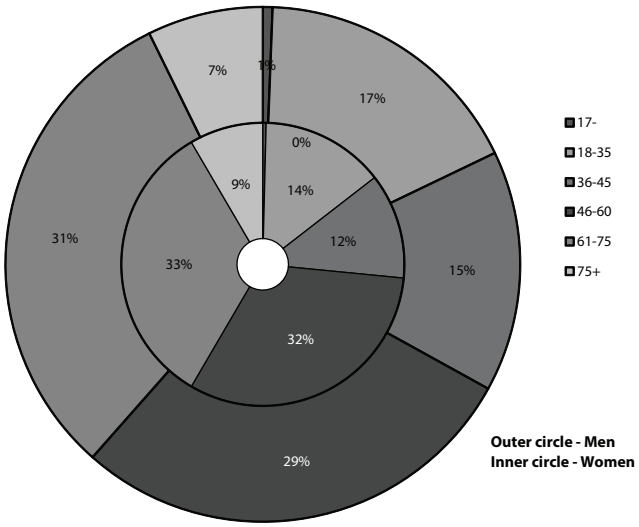


**Figure 1**. Patients distribution by sex and age.

patients aged 18-45 years referred to SPC compared to the group of 46-60 years.

The main complaints from younger patients (18-35 years) were headache, vertigo and vertiginous syndromes, tinnitus. The incidence of cerebrovascular pathologic findings in this group was low: increased intima media thickness (IMT) was found in 6% and premature atherosclerosis manifested as insignificant atherosclerotic plaques (<30% of lumen) in 2% of cases (**Figure 2**). Interestingly, increased levels of cholesterol and triglycerides accompanied these findings in only 4% of cases. Arterial hypertension was found in 12% of young patients and was accompanied by changes in arterial wall elastic properties in most cases (78%).

The progression of IMT and atherosclerotic plaques in neck arteries with age was observed in all patients except the eldest. The incidence of increased IMT and insignificant atherosclerotic plaques in older age patients (more than 75 years) was slightly lower than in patients aged 61-75 years. Incidence of dyslipidemia was proportionally increased with age, except age group 46-65 years where the frequency of increased cholesterol and triglycerides was the highest (**Figure 2**).

This proportional increase of plaques size with age was not found in cases of cerebral stenoses. The occurrence of cerebral stenotic lesions was the same in three first age groups and slightly higher in patients older than 60 years (**Figure 2**). This disproportion could be partly explained by technical inaccuracy of US measurement of degree of stenoses in cerebral arteries.

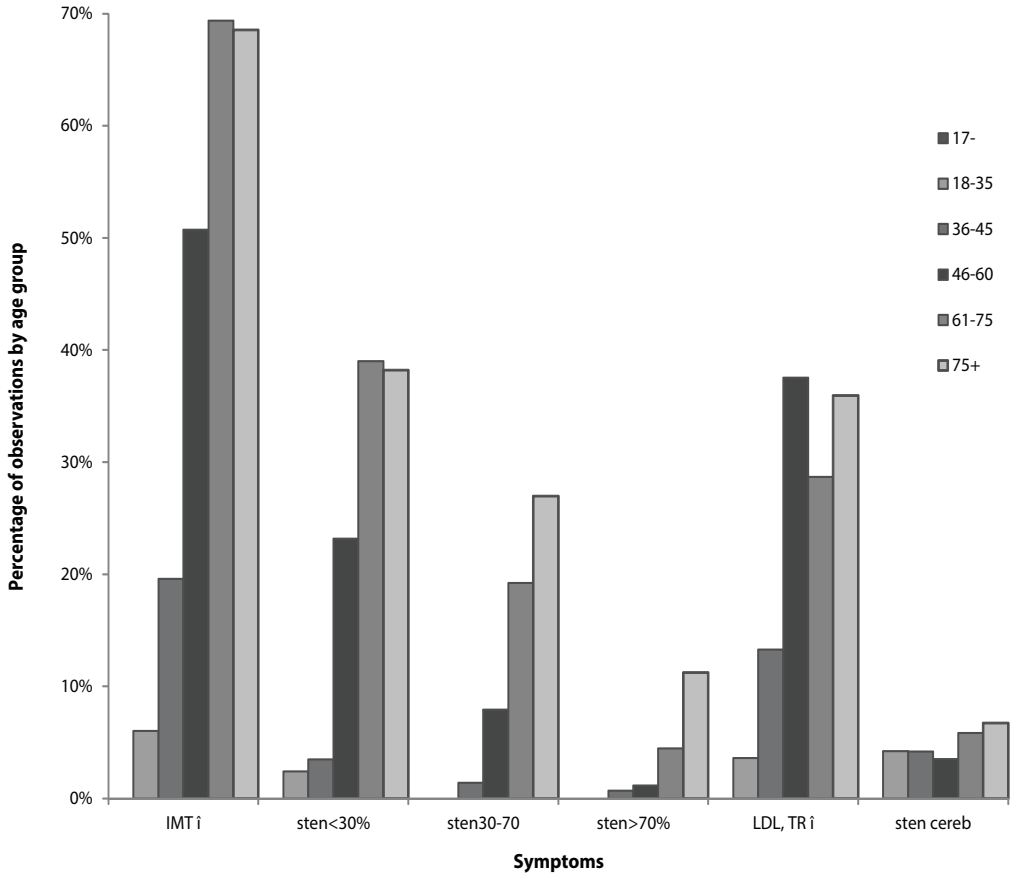


**Figure 1**. Distribution of increased intima-media thickness, stenotic lesions in pre-cerebral and cerebral arteries, dyslipidemia between patients of different age groups (from 17 to 75+ years).

IMT î = Increased intima media thickness; sten <30% = Stenoses less than 30% of arterial lumen; sten 30-70% = Stenoses 30-70% of arterial lumen; sten >70% = Stenoses more than 70% of arterial lumen; LDL, TR î = Increased low-density lipoproteins and triglycerides; sten cereb. = Stenoses of cerebral arteries

The analysis of suspected and proved cerebrovascular pathology showed the main mismatches (**Figure 3**). Dyslipidemia as the isolated pathology was the reason to send patients to observation in 2% of cases only. Meanwhile it was found as the only pathology in 6% of patients and as accompanying sign of atherosclerotic arterial lesions in 26% of patients. Additionally, 24% of all surveyed had registered high level of cholesterol and triglycerides in the past. Surprisingly low number of patients with primary or secondary hypertension was sent to SPC (in 14% of surveyed), although the vascular pathology was found quite frequently in this group—arterial hypertension accompanied atherosclerotic arterial lesions in 42% of cases. The silent atherosclerotic process in precerebral arteries was suspected in 15% of patients but proven in 27% (**Figure 3**).

One of the most represented group in the survey consisted of patients complaining on disorders of vestibular function as the only symptoms (22%): vertigo and vertigi-

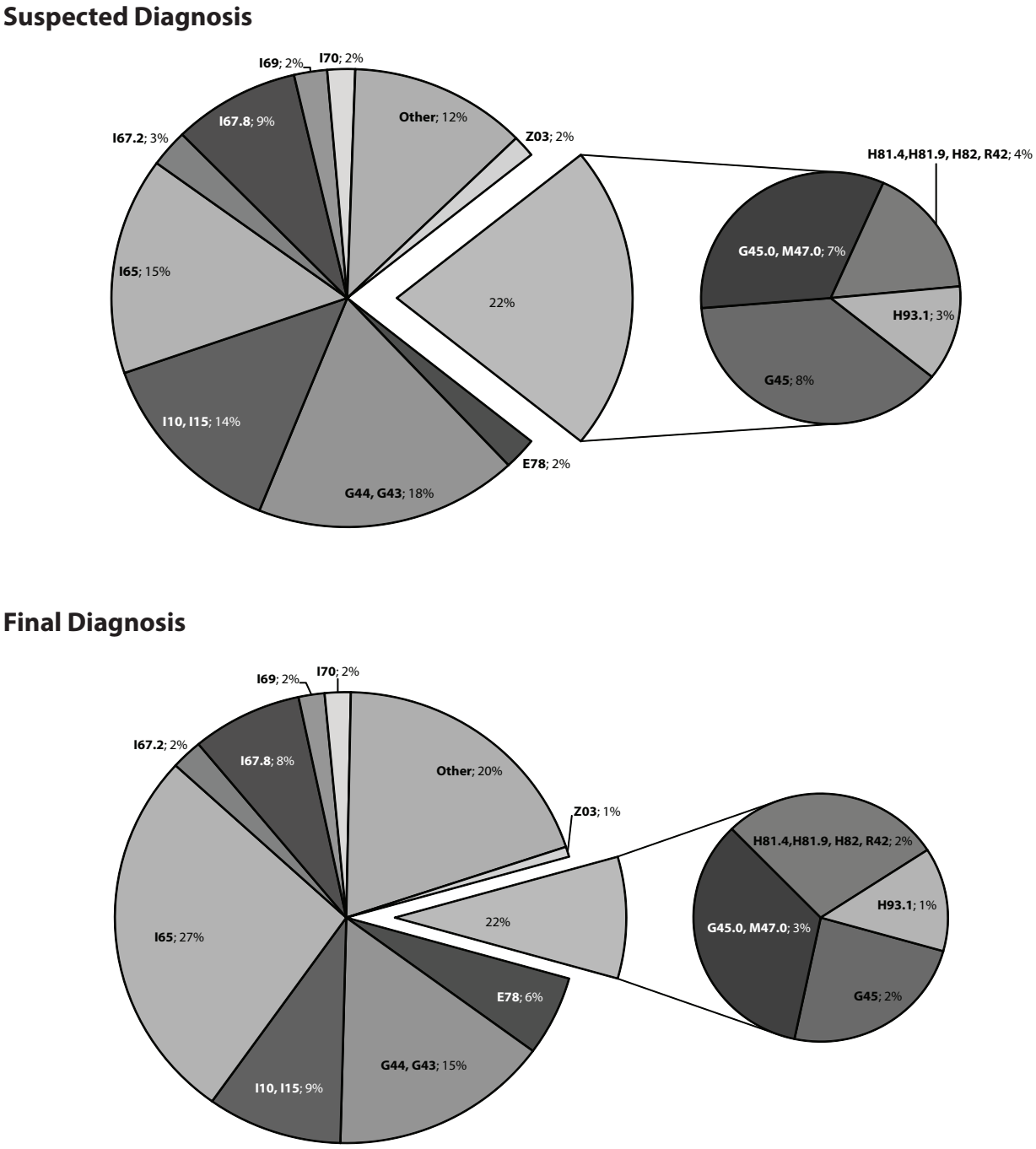


**Figure 3**. Suspected and confirmed disease or pathologic condition.
International codes of diseases [6]: E78 - Dyslipidemia – as an only suspected and found pathological condition; G43, G44 - Migraine and other headache syndromes; G45 - Vertebrobasilar artery syndrome; G45.0, M47.0 - Anterior spinal and vertebral artery compression syndromes; H81.4, H81.9, H82, R42 -Disorders of vestibular function, Vertiginous syndromes, Dizziness and giddiness; I10, I15 - Essential (primary) hypertension, Secondary hypertension; I65 - Occlusion and stenosis of precerebral arteries, not resulting in cerebral infarction; I67.2 - Cerebral atherosclerosis; I67.8 - Other specified cerebrovascular diseases; I69 - Sequelae of cerebrovascular disease; I70 – Atherosclerosis; Z03 - Medical observation and evaluation for suspected diseases and conditions; Other - Other.

nous syndromes, dizziness, giddiness and tinnitus. Vertebro-basilar artery syndrome, transitory ischemic attacks and stroke in vertebrobasilar territory, as well as vertebral artery compression syndromes were suspected in 15% of cases. These suspicions were proven in a surprisingly rare number of patients—5% (**Figure 3**). Different degrees of significant stenotic lesions in vertebrobasilar arteries separately or combined with hypoplasy were found in 20% of patients with proven pathology, and insignificant arterial stenotic lesions in 37% of cases (**Figure 4**). Vertebral artery compression was proven just in 2 cases, subclavian steal syndrome in 3 cases. The rest of patients with vestibular disorders had a wide spectrum of variable pathological conditions—from iron deficit anemia to benign paroxysmal postural vertigo without documented abnormality in arterial and venous cerebral circulation.

Another widely represented group consisted of patients with acute or chronic headache (18% of all surveyed subjects). Vascular pathology was found in 11% only (**Figure 3**). There were a few quite significant findings detected like arteriovenous malformation in posterior artery territory, venous sinus thrombosis and vertebral artery dissection. Altered cerebral blood flow without local lesion was observed in a minority of patients with headache (7%). These findings were accompanied by arterial hypotension or iron deficiency anemia or abnormality in electrical brain activity. Increased cerebral blood flow velocity remained unexplained in 4 cases.

Good correlation between suspected and found stenotic lesions of the precerebral and cerebral vessels was observed in patients sent to SPC with suspected stenosis of precerebral arteries, not resulting in cerebral infarction, as well as cerebral atherosclerosis and sequels of cerebrovascular diseases (**Figure 4**).

## Discussion

The higher prevalence of young male patients aged 18-45 years compared to the 46-60 years males, more suspicious of having CVD, could be partly explained by increased awareness of the disease and as a consequence, a greater concern for their health .The further analysis of complaints and findings in a group of young people aged 18-35 years frequent occurrence of symptoms mistakenly considered as signs of CVD.

Large number of surveyed subjects registered high level of cholesterol in the past or at the moment of observation. All together these findings (56%) were less frequent than previously reported [5], which could be partly explained by difference in cohorts (selected patients with a small proportion of self-referred in this study contrary to population based cross sectional study). Another explanation is the surprisingly small number of patients with dyslipidemia as an only sign (2%) sent for observation. The fact that from the majority of the 32% of observed patients with dyslipidemia had different degrees of atherosclerotic

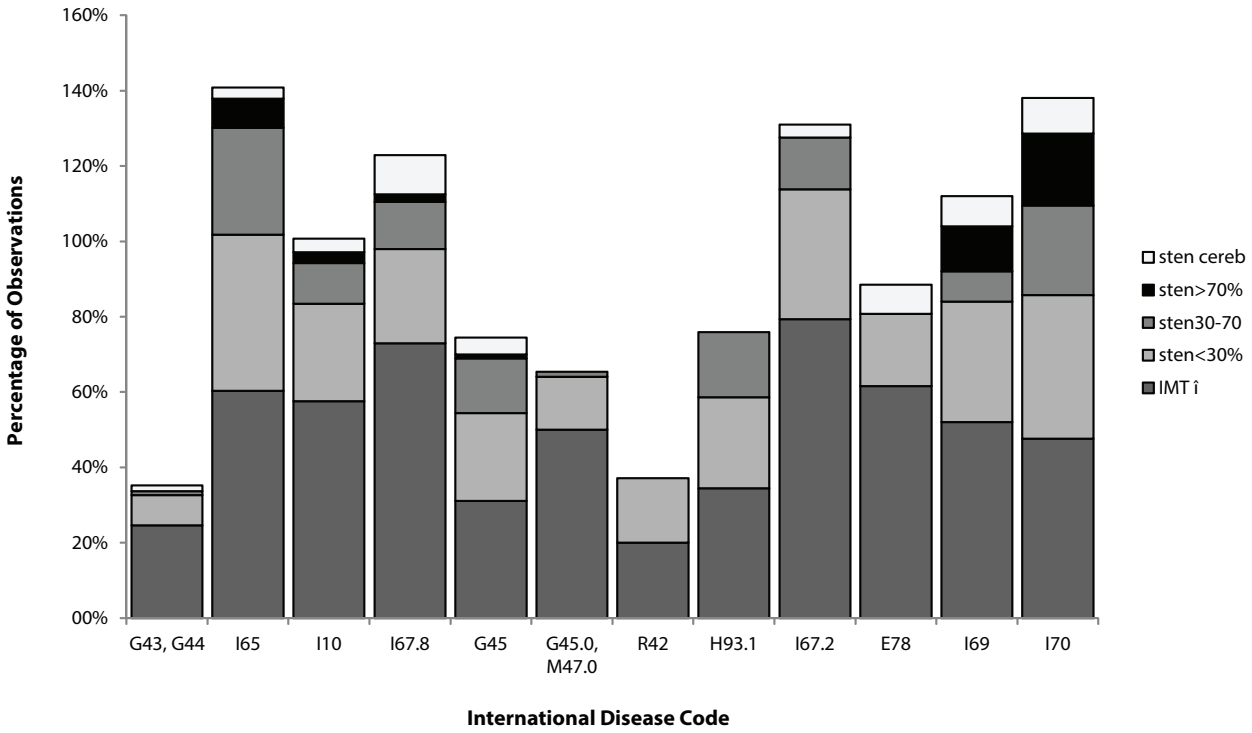


**Figure 4**. Distribution of increased IMT and vascular sclerotic lesions according to suspected disease or pathological condition.
International Diseases codes are the same as in Figure 3. Notations are the same as in Figure 2.

lesions in arteries must prompt more awareness and suspicion on the role of this risk factor in silent vascular pathology. Especially concerning the group aged 45-60 years, with the highest frequency of dyslipidemia.

Arterial hypertension was found in the youngest patients with the same frequency as arterial hypotension. In both conditions changes in arterial wall elastic properties presented as impaired dystensibility/stiffness of arterial wall were found in most cases, which could help as an early risk factor for vascular pathology. The growing frequency of arterial hypertension in patients aged 36-60 years, together with high level of dyslipidemia matched with growing occurrence of stenotic lesions in precerebral arteries, proving the important role of these pathologic conditions as main factors for developing vascular pathology. The only disagreement was found in older patients aged 61-75 years where occurrence of arterial hypertension and hypercholesterolemia was less than that found in age group 46-60 years, but the presence of high-grade atherosclerotic stenotic lesions in precerebral and cerebral arteries was much higher. These findings have to be analyzed in comparison with the course of antihypertensive therapy and use of statins.

The main mismatch between suspected and confirmed vascular pathology was found in patients with unspecific disorders of vestibular function, vertigo and vertiginous syndromes sent to SPC by family doctors with suspicions of transient ischemic attack (TIA) in vertebrobasilar territory and vertebral artery compression due to cervical spondylosis. Vestibular function disorder as well as tinnitus and headache were the main complaints of who patients contacted SPC themselves. The low frequency of documented vascular pathology in this group indicated the need of more educational programs for medical professionals and population with the description of initial symptoms and the course of stroke and cerebrovascular diseases. Rare serious vascular pathology manifested as headache, accompanied by vestibular disorders which proves the benefit of transcranial color-coded duplex (TCCD) screening of arteries in these patients.

The highest correlation between suspected and found arterial stenotic lesions was defined in a well represented group of patients with occlusion and stenosis of precerebral arteries without cerebral infarction, with chronic cerebral ischemia and stroke or TIA. This match proves the role in screening and follow-up of cerebral hemodynamics by TCCD in cases of silent carotid stenoses, chronic cerebral ischemia, TIA and stroke.

Only 5% of all patients having vascular pathology and 2% of those who underwent endovascular procedures or endarterectomy revisited Stroke Prevention Centres to control the atherosclerotic stenoses of precerebral and cerebral arteries and revise the treatment. Most of these patients had controlled arterial tension and level of cholesterol and stable vascular condition with no further progression. The follow-up of therapy resistant growing atherothrombotic plaques allowed to send patients for surgical treatment in time.

All our data demonstrate the need to control the dynamics of arterial pathology apart from the control of risk factors. The easily performed and non-invasive TCCD is quite often the only source of information on the dynamics of the pathological process, therapeutical effect on cerebral circulation and collateral compensating flow, which is extremely important for the prognosis and treatment tactic.

## Abbreviations

CEE: Central and East European; CHD: Coronary heart disease; CVD: Cardiovascular disease; IMT: Intima media thickness; SPC: Stroke Prevention Centres; TCCD: Transcranial color-coded duplex; TIA: Transient ischemic attack; WHO: World Health Organization

## Competing interests

The authors declare no conflict of interest.

## References

1. Allender S, Scarborough P, Peto V, Rayner M, Leal J, Luengo-Fernandez R, Gray A. European cardiovascular disease statistics, 2008 edition. British Heart Foundation; 2008. Available from: http://www.bhf.org.uk/publications/view-publication.aspx?ps=1001443 (Accessed 23 April, 2012).
2. Pająk A, Kozela M. Cardiovascular Disease in Central and East Europe. Public Health Reviews 2012; 33:416-35.
3. World Health Organization Regional Office for Europe. European Health for All Database (HFA-DB). WHO Europe; 2011. Available from: http://www.euro.who.int/en/what-we-do/data-and-evidence/databases/european-health-for-all-database-hfa-db2 (Accessed 23 April, 2012).
4. Branin M, Bornstein N, Boysen G, Demarin V. Acute neurological stroke care in Europe; results of the European Stroke Care Inventory. Eur J Neurol 2000; 7(1):5-10.
5. Ērglis A, Dzērve V, Pahomova-Strautiņa J, Narbute I, Jēgere S, Mintāle I, Ligere R, Apinis P, Lejnieks A, Misiņa D, Rozenbergs A. A Population-Based Cross-sectional study of Cardiovascular Risk Factor in Latvia. Medicina (Kaunas) 2012; 48(6).
6. World Health Organization. WHO classifications, International classification of diseases (ICD), ICD -10 online version:2010. Available from: http://www.who.int/classifications/icd/en.

INTERNATIONAL JOURNAL OF
CLINICAL NEUROSCIENCES
AND MENTAL HEALTH

ORIGINAL RESEARCH

# Carotid ecodoppler and transesophageal echocardiography: complementary methods for evaluation of atherosclerosis?

Joana Chin[1], Ana Camacho[1], Patrícia Guilherme[1], Pedro Sousa[1], Vasco Marques[1], Paula Gago[1], Nelson Tavares[1], Rui Ferrinha[1], Sandra Cunha[1], Ana P. Silva[2], and Ilídio Jesus[1]

Special Issue on Neurosonology and Cerebral Hemodynamics

## Abstract

**Background:** The purpose of this study was to assess the relationship between carotid ultrasonography (CU) and transesophageal echocardiography (TEE), regarding atherosclerotic disease findings, the presence of carotid plaques (CP), proximal aortic plaques (AP), carotid intima-media thickness (CIM), and the aortic intima-media thickness (AIM).

**Methods:** Sixty one patients (57.4% men, mean age 62.7 ± 14 years) were evaluated with CU and TEE with an interval inferior to one month. CIM was measured at the common carotid artery (CCA); CP was defined as a localizaed protrusion in the arterial lumen larger than 1.5 mm, in the CCA or the internal carotid, without uniform wall involvement. AIM was measured at the aortic arch; AP was defined as a hyperechogenic area with >2 mm of thickness.

**Results:** Thirty seven patients had CP and 19 had AP. Seventeen patients had plaques in both locations (p=0.002). There was a difference between the medians of AIM (1.4; IQR=0.5) and CIM (1.0; IQR=0.3) (p<0.001). There was a linear correlation between CIM and AIM (coef =0.378, p=0.003). The presence of CP was a predictor (OR 6.28, p=0.03) of AP. CIM (coef=0.52, p=0.05) and gender (coef=0.22, p=0.02) were predictors of AIMs.

**Conclusion:** The presence of CP was related to the presence of AP. There was a positive association between CIM and AIM. CU results can be used as surrogate markers of aortic atherosclerotic disease. Evaluation of thoracic aorta with TEE is important, since it provides additional information on the extent of atherosclerotic disease.

**Keywords:** Atherosclerosis, Transesophageal echocardiography, Carotid, Aorta, Intima-media, Plaque

[1]Department of Cardiology, Algarve Hospital Center, Faro, Portugal
[2]Department of Nephrology, Algarve Hospital Center, Faro, Portugal

Correspondence: Joana Chan Chin
Department of Cardiology, Centro Hospitalar do Algarve
Rua Leão Penedo, 8000 Faro, Portugal
Email adress: joanachin@yahoo.com

Citation: Chin et al. Carotid ecodoppler and transesophageal echocardiography: complementary methods for evaluation of atherosclerosis? IJCNMH 2014; 1(Suppl. 1):S11

Received: 30 Aug 2013; Accepted: 08 Fev 2014; Published: 09 May 2014

Open Access Publication Available at http://ijcnmh.arc-publishing.org



ARC Publishing

## Introduction

Atherosclerosis is a generalized process that may involve the entire vasculature. Although it mainly manifests in medium-sized vessels, it is also present in the great vessels, such as the thoracic or abdominal aorta and the carotid artery[1].

Some authors suggest that the carotid intima-media thickness (CIM), assessed by high resolution carotid ultrasound, can be considered an indicator of generalized atherosclerotic disease [2]. The presence of an atherosclerotic stenotic lesion in the carotid bulb or in the internal carotid artery (ICA) has been associated with an increased risk of stroke and it may account for up to 20% of all ischaemic strokes [3].

Atherosclerosis of the proximal aorta (ascending aorta and aortic arch), as evaluated by transesophageal echocardiography (TEE), also represents a potential source of emboli [4]. It has been established that stroke risk is associated with increasing thickness of the arch plaque, as well as with the extension of the atherosclerotic process to the brachio-cephalic arteries [5]. However, the precise relationship between the extension of asymptomatic atherosclerotic disease in the carotid artery and ascending aorta, is still not completely understood [2, 5]. We used carotid artery ultrasonography (CU) to study the predictive value of carotid atherosclerotic plaque and CIM thickening to determine the presence of aortic atherosclerotic plaques and AIM thickening.

## Methods

Between July 2011 and July 2012, 120 consecutive patients were referred for TEE study at the echocardiography laboratory of our institution. All patients that did not meet the exclusion criteria were proposed to perform a CU within one month of the TEE.

The exclusion criteria were: prior history or clinical evidence of cerebrovascular disease, previous carotid endarterectomy or carotid angioplasty, and history of aortic dissection or aortic aneurysm. Furthermore patients with poor ultrasonographic recording quality with no clear delineation of the intima-media complex or incomplete examination of the proximal aorta were also excluded from the study.

A standard cardiac examination and aortic assessment was performed by TEE, using an ultrasonograph (General Electrics, ViVid 7) and a multiplane 5 MHz probe. The proximal aorta (aortic arch and ascending aorta) was imaged in short and long axis and the aortic intima media thickness (AIM) was measured in the aortic arch, in both views, in telediastole; the final value was obtained by averaging four measurements. Aortic plaque (AP) was defined as a hyperecogenic thickened area causing protrusion in the arterial lumen with more than 2 mm. Plaques were classified as small (<4 mm) or large (≥4mm) [6]. Recordings of all patients were reviewed in a work-station EchoPac 7 and measurements made offline by a single experienced cardiologist, blinded to the carotid ultrasound results.

Carotid atherosclerosis was assessed by ultrasound Doppler, using a GE Vivid 4 ultrasonograph, with a 10 MHz Linear probe. The distal common carotid artery (CCA), and ICA were evaluated. CIM was measured in the far wall, 1 cm bellow the bifurcation of the CCA on a plaque free site. The final value was obtained by averaging two measurements of both right and left CCA. Carotid plaque (CP) was defined as a localized thickening of the CCA or ICA, making a protrusion in the arterial lumen greater than 1.5 mm, without uniform wall involvement, which resulted or not in an increased speed, as evaluated by pulsed Doppler.

The degree of stenosis at the ICA, was determined according to the criteria of the Society of Radiologists in Ultrasound consensus conference [7], and the patients categorized in the respective groups: no stenosis; less than 50% stenosis; ≥50% and <70%; ≥70% and less than near occlusion; near occlusion; and occlusion.

All CU examinations were performed by the same qualified vascular technician of the neurology department of our institution and reviewed offline by one independent senior echocardiographer who was blinded to patients demographics as well as to TEE data.

Regarding the vascular risk factors, hypercholesterolemia was defined as previous blood test with plasma LDL cholesterol >100 mg/dL or prior prescription of cholesterol lowering drugs. Hypertension was defined as blood pressure >140 mmHg (systolic) or >90mmHg (diastolic) measured twice in the hospital, or previous history of high blood pressure or prior prescription of pressure lowering drugs. Diabetes Mellitus was defined as previous history of the disease and taking glucose lowering drugs.

### Statistical analysis

Descriptive statistics was performed and data is presented as mean values ± standard deviation for continuous variables with normal distribution, as median and interquartile range (IQR) for continuous variables with non-normal distribution and as proportions for categorical variables.

Differences between groups were assessed using the unpaired Student t-test or two-tailed Mann-Whitney test as required. Chi-square test was used to compare differences between proportions. To evaluate the strength of the linear correlation between variables the Spearman's coefficient was used.

In a second step, to identify independent variables related to the presence of AP and to the thickness of the AIM, the variables with a significant association in the univariate analysis were entered into a multivariate stepwise logistic or linear regression model. For all statistical analyses, a two-tailed p-value <0.05 was considered significant. The data was analyzed using IBM SPSS Statistics, version 20.

## Results

Sixty one (61) patients met the inclusion criteria. The patients mean age was 62.7 ± 14 years and 35 (57.4%) patients were men. The motives for referral to TEE were: exclusion of intracardiac thrombus in 24 (39.3%) patients, evaluation of valvular heart disease in 23 (37.7%) patients, evaluation of endocarditis in 7 (11.5%) patients, and other motives in 7 (11.5%) patients.

The demographic and clinical characteristics, as well as reasons for the TEE of the entire study population, are presented in **Table 1**. Regarding vascular risk factors, 37 (60.7%) patients had hypertension, 21 (34.4%) dyslipidaemia, 10 (16.4%) diabetes mellitus, and 12 (19.7%) were current smokers (**Table 1**).

A summary of the carotid ultrasonography and transesophageal echocardiography data of the study population is presented in **Table 2**.

### Carotid ultrasonography data

Carotid artery atherosclerotic plaques were present in 37 (60.7%) patients. 20 (32.8%) patients had bilateral plaques. In detail, 33 patients (54.1%) had plaques with stenosis <50%, 2 (3.3%) had plaques with stenosis ≥50% and <70%, 1 (1.6%) had a plaque with near occlusion and 1 (1.6%) patient had an occlusion of the carotid artery. The median value of the CIM was 1 mm (IQR = 0.3) (**Table 2**).

### Transesophageal echocardiography data

Proximal AP was found in 19 (31.1%) patients. 17 (89.5%) of those had small plaques and 2 (10.5%) had large plaques. The median value of AP thickness was 2.5 mm (IQR = 1.2). The median value of AIM thickness was 1.4 mm (IQR = 0.5).

Comparing within the same patient, the measure of the AIM with the CIM, a significant difference was found, the first being significantly thicker (p<0.001), and with a positive linear correlation between them (Spearman's Rho = 0.378, p=0.003), as seen in **Figure 1**.

**Table 1.** Baseline characteristics of the study population and transoesophageal echocardiography indications.

| | Study population (*n* = 61) |
|---|---|
| *Baseline characteristics* | |
| Age (years) | 62.7±14 |
| Men, n (%) | 35 (57.4) |
| Hypertension, n (%) | 37 (60.7) |
| Diabetes, n (%) | 10 (16.4) |
| Dyslipidemia, n (%) | 21 (34.4) |
| Smokers, n (%) | 12 (19.7) |
| *TEE indications* | |
| Exclusion of thrombus, n (%) | 24 (39.3) |
| Evaluation of valve, n (%) | 23 (37.7) |
| Evaluation of endocarditis, n (%) | 7 (11.5) |
| Other, n (%) | 7 (11.5) |

TEE = Transesophageal echocardiography; n = Number of patients

**Table 2.** Carotid ultrasonography and transesophageal echocardiography data of the study population.

| | Study population (*n* = 61) |
|---|---|
| *Characterization of carotid plaques* | |
| Patients with plaques, n (%) | 37 (60.7) |
| Bilateral plaques, n (%) | 20 (54.0) |
| Plaques without hemodynamic repercussion, n (%) | 28 (75.7) |
| Plaques < 50% stenosis, n (%) | 5 (13.5) |
| Plaques 50%-70% stenosis, n (%) | 2 (5.4) |
| Plaques 70% stenosis to near occlusion, n (%) | 0 (0) |
| Near occlusion, n (%) | 1 (2.7) |
| Occlusion, n (%) | 1 (2.7) |
| *Characterization of aortic plaques* | |
| Patients with plaques, n (%) | 19 (31.1) |
| Plaques 2-4 mm, n (%) | 17 (89.5) |
| Plaques ≥ 4 mm, n (%) | 2 (10.5) |
| Dimension of plaques (mm), median (IQR) | 2.5 (1.2) |
| *Intima-media thickness* | |
| CIM (mm), median (IQR) | 1.0 (0.3) |
| AIM (mm), median (IQR) | 1.4 (0.5) |

n = number; mm = millimetres; IQR = Interquartile range; CIM = Carotid intima media thickness; AIM = Aortic intima media thickness

**Table 3** shows the baseline characteristics of the study population according to CP presence. Compared with the patients without plaques, patients with carotid atherosclerotic plaques were older (p = 0.001) and had a higher prevalence of AP (p = 0.002). Both CIM and AIM were thicker in patients with CP (p = 0.02).

### Association between carotid and aortic atherosclerosis

**Table 4** shows the variables associated with AP in the logistic univariate and multivariate analysis. Age (p = 0.01), male gender (p = 0.03), and CP (p = 0.006) were related to the presence of AP. In logistic multivariate analysis the presence of CP was related (OR 6.28, 95% CI [1.16 to 34.1]) (p = 0.03) with the presence of AP, when adjusted for age, male gender, and CIM, with a square R = 0.327.

To evaluate the predictors of the AIM thickness, univariate and multivariate linear regression were performed; the results are shown in **Table 5**. CIM (p<0.001), age (p<0.001), gender (p = 0.002) and CP (p = 0.03), were univariate predictors of increasing AIM thickness. In the multivariate linear regression model CIM (coefficient = 0.52, 95% CI [0.001 to 1.03]) (p = 0.05) and gender (coefficient = 0.22, 95% CI [0.027 to 0.4]) (p = 0.02) were found as predictors of AIM, when adjusted for age and hypertension, with a square R = 0.31.

## Discussion

In the present study we evaluated the relationship of atherosclerotic disease (plaque and intima-media thickness (IMT)) in the carotid arteries and proximal aorta, in patients without clinical evidence of atherosclerotic vascu-

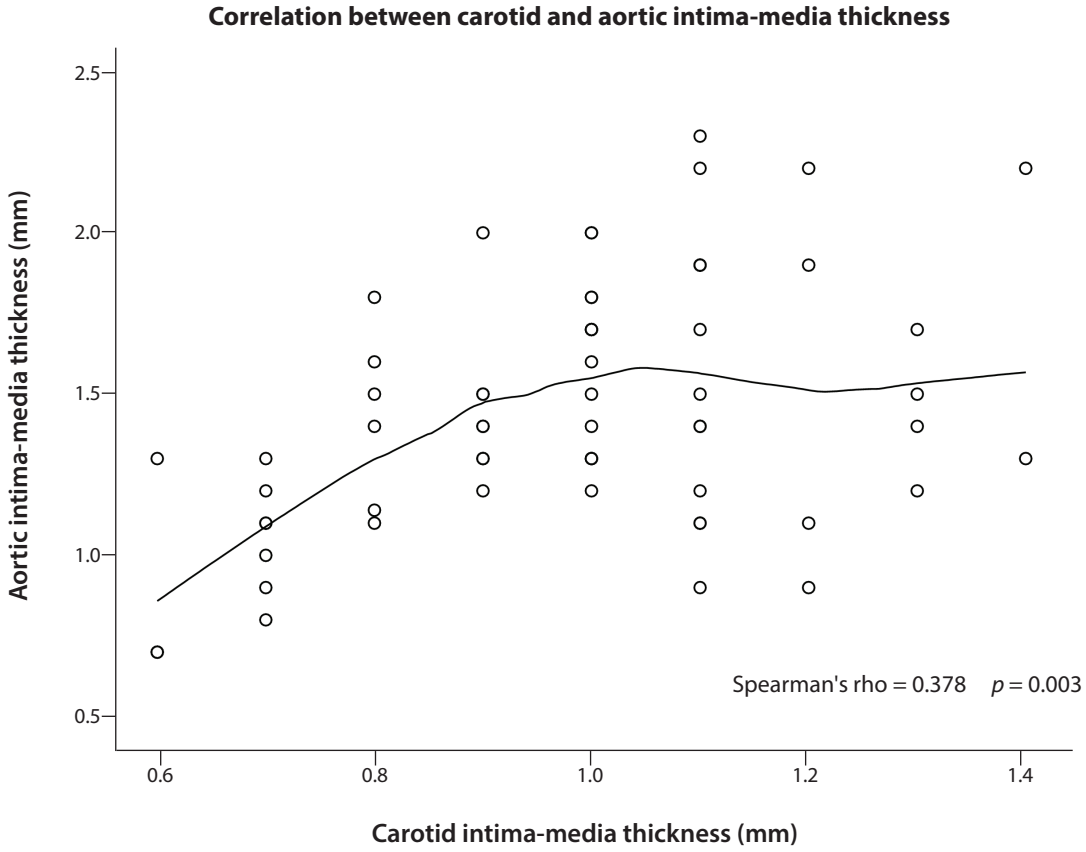


**Figure 1.** Measurements of intima-media thickness. Relationship between carotid intima-media thickness and aortic intima-media thickness, as measured by carotid ultrasound and transesophageal echocardiography, respectively.

lar disease, referred for evaluation by TEE.

In our study population, we found that the presence of asymptomatic carotid atherosclerotic plaques could indicate the presence of aortic atherosclerotic plaques, whereas the absence of carotid plaques may not reflect the absence of aortic plaques.

When comparing the group of patients with and without carotid plaques, we found that the patients with carotid plaques had more often, plaques in the proximal aorta (p = 0.002), and higher values of CIM (p = 0.02) and of AIM (p = 0.02). The patients with plaques in the carotid artery were also significantly older (p < 0.001).

In the multivariate analysis we found that the presence of plaques in the carotid artery, was related to the presence of plaques in the proximal aorta, these results are in agreement with previous studies [2, 8, 9].

The awareness of the association between carotid and aortic atherosclerosis may have preventive, therapeutic and prognostic implications, because aortic arch plaques are a risk factor for stroke [5]. Unnoticed proximal aortic plaques are related to stroke in patients undergoing cardiac surgery or invasive procedures that involve the proximal segment of the aorta, like a coronary angiogram [5].

TEE is one of the exams of choice for evaluating the aorta and although it is not considered an invasive exam, it can cause anxiety and discomfort in some patients, and it is not without risk for the patients [10]. So it is desirable to find another way to diagnose aortic atherosclerotic disease, using a non-invasive and easily available test, like the carotid ultrasonography Doppler [11]. According to the results of our study there is an association between the presence of carotid plaques, diagnosed by carotid ultrasonography and the presence of proximal aortic plaques. Therefore, we suggest that it is possible to use the findings of the carotid ultrasonography as a surrogate marker for the presence of plaques in the proximal aorta.

**Table 3.** Characteristics of the study population according to the presence of carotid plaque.

| Characteristic | No carotid plaque (n =24) | Carotid plaque (n= 37) | *p* |
|---|---|---|---|
| Age, (years) | 54.5±2.9 | 68±1.8 | 0.001 |
| Men, n (%) | 11 (45.8) | 24 (64.9) | 0.18 |
| Hypertension, n (%) | 12 (50) | 25 (67.6) | 0.19 |
| Diabetes, n (%) | 2 (8.3) | 8 (21.6) | 0.29 |
| Dyslipidaemia, n (%) | 5 (20.8) | 16 (43.2) | 0.10 |
| Smokers, n (%) | 6 (25) | 6 (16.2) | 0.30 |
| Aortic plaques, n (%) | 2 (8.3) | 17 (45.9) | 0.002 |
| CIM (mm), (IQR) | 0.8 (0.4) | 1.0 (0.2) | 0.02 |
| AIM (mm), (IQR) | 1.25 (0.5) | 1.5 (0.5) | 0.02 |

n = Number; CIM = Carotid intima media thickness; AIM = Aorta intima media thickness; IQR = Interquartile range

**Table 4.** Univariate and multivariate predictors of aortic plaque presence.

| Characteristic | Odds ratio | 95% CI | *p* |
|---|---|---|---|
| *Univariate predictors of aortic plaque presence* | | | |
| Age | 1.06 | 1.01 - 1.120 | 0.01 |
| Men | 4.13 | 1.17 - 14.52 | 0.03 |
| Hypertension | 1.16 | 0.38 - 3.60 | 0.78 |
| Diabetes | 2.64 | 0.66 - 10.54 | 0.17 |
| Dyslipidemia | 0.58 | 0.17 - 1.91 | 0.37 |
| Smokers | 1.40 | 0.35 - 5.62 | 0.62 |
| CIM | 8.90 | 0.49 - 161.90 | 0.14 |
| Carotid plaques | 9.35 | 1.91 - 45.60 | 0.006 |
| *Multivariate predictors of aortic plaques presence* | | | |
| Age | 1.03 | 0.97 - 1.10 | 0.25 |
| Men | 3.05 | 0.77 - 12.13 | 0.12 |
| CIM | 0.99 | 0.016 - 62.7 | 0.99 |
| Carotid plaques (yes) | 6.28 | 1.16 - 34.1 | 0.03 |

CIM = Carotid intima media thickness

The IMT is a validated marker of atherosclerotic disease, as well as a known marker of coronary atherosclerotic disease [12]. The most frequent location to measure the IMT is at the CCA, because it is more reproducible and has a capability to predict ischemic events comparable to the invasive methods [13]. The CIM value is a continuum and according to the Manheim consensus [14], the values considered normal for the age group in our study population are between 0.75 and 0.85 mm. The majority of our patients had an increased CIM (median 1.0 mm). This could be explained in part because we examined a population of patients referred for the study of cardiac disease.

**Table 5.** Univariate and multivariate analysis of predictors of aorta intima media thickness.

| Characteristic | Coefficient | 95% CI | *p* |
|---|---|---|---|
| *Univariate predictors of aortic intima media thickness* | | | |
| CIM | 0.83 | 0.38 - 1.29 | 0.001 |
| Age | 0.01 | 0.005 - 0.018 | 0.001 |
| Gender | 2.99 | 0.11 - 0.48 | 0.002 |
| Hypertension | 0.18 | 0.15 - 0.38 | 0.07 |
| Diabetes | 0.07 | 0.19 - 0.34 | 0.59 |
| Dyslipidaemia | 0.01 | 0.19 - 0.22 | 0.89 |
| Smokers | - 0.03 | 0.17 - 0.11 | 0.66 |
| Carotid plaque | 0.21 | 0.02 - 0.41 | 0.03 |
| *Multivariate predictors of aortic intima media thickness* | | | |
| CIM | 0.52 | 0.001 - 1.03 | 0.05 |
| Age | 0.003 | 0.004 - 0.011 | 0.39 |
| Gender | 0.22 | 0.027 - 0.40 | 0.02 |
| Hypertension | 0.12 | 0.06 - 0.29 | 0.21 |

CIM = Carotid intima media thickness

In our study population we found a positive linear correlation between the CIM and the AIM, measured in the same patient. In multivariate analysis both CIM and gender were independently related to AIM.

Here, the classical vascular risk factors weren't predictors of the presence of proximal aortic plaques or of increased AIM.

In view of our results, when evaluating the presence and/or extension of atherosclerotic disease, one should consider carotid ultrasonography as surrogate for proximal aorta atherosclerosis. Carotid ultrasonography is a non-invasive, easy, and reliable method for the diagnosis of atherosclerotic disease, directly in the carotid artery territory and indirectly, as a predictor, of the proximal aorta artery atherosclerosis.

### Limitations of the study

There were several limitations to our study. First, the study population was small, which limited the power of the statistical analysis.

The population was composed of patients referred to TEE to study some form of heart disease, whether it was detection of thrombus or valve disease, which limits the use of these findings in the general population.

Data collection was only done in the proximal portion of the aortic artery (ascending aorta and aortic arch). The descending aorta was not studied, which may underestimate the number of patients with atherosclerosis of the aorta. Moreover, in 31 patients (25.8%) no quality ultrasound reading was obtained from the proximal aorta, which further confirms the technical limitations in the assessment of AIM. Also, the authors could not find standardized values for the thickness of aorta intima-media

## Conclusions

In our study population, the presence of carotid artery plaques was related to the presence of proximal aortic plaques. We found a positive association between CIM and AIM. In view of these results, when evaluating the presence and/or extension of atherosclerotic disease, one should consider that the information of carotid ultrasonography Doppler can be a surrogate marker of proximal aorta atherosclerosis.

Evaluation of the thoracic aorta with TEE is important when performing echocardiography, because it provides additional information of the extension of atherosclerotic disease.

### Abbreviations

AIM: Aortic intima media; AP: Aortic plaque; CCA: Common carotid artery; CIM: Carotid intima-media; CP: Carotid plaque; CU: Carotid artery ultrasonography; ICA: Internal carotid artery; IMT: intima-media thickness; IQR: Interquartile range; TEE: Transesophageal echocardiography

## Competing interests

The authors declare no conflict of interest.

## References


1. Fuster V, Weinberger J, Kohler T, et al. Pathology: clinical correlation of carotid, aortic and peripheral vascular disease. In: Fuster V, ed. Syndromes of Atherosclerosis. New York, NY: Futura Publishing Co; 1996.
2. Kallikazaros I, Tsioufis C, Stefanadis C, et al. Closed relation between carotid and ascending aortic atherosclerosis in cardiac patients. Circulation 2000; 102:Iii-263-Iii-268.
3. Lovrencic-Huzjan A, Rundek T, Katsnelson, M. Review Article - Recommendations for Management of Patients with Carotid Stenosis. Stroke Research and Treatment 2012; 2012:175869.
4. Kronzon I, Tunik P, Aortic atherosclerotic disease and stroke, Circulation 2006; 114:63-75.
5. American Heart Association/American Stroke Association: Guidelines for the Primary Prevention of Stroke. Circulation 2006; 113:e409-e449.
6. Tessitore E, Rundek T, Zhezhen, J. Association Between carotid intima-media thickness and aortic arch plaques. J Am Soc Echocardiogr 2010; 23(7): 772-777.
7. Grant EG, Benson CB, Moneta GL, et al. Society of Radiologists in Ultrasound. Carotid artery stenosis: grayscale and Doppler ultrasound diagnosis—Society of Radiologists in Ultra Ultrasound consensus conference. Ultrasound Q. 2003; 19(4):190-8.
8. Harloff, A, Handke, M, Geibel, A, et al. Do stroke patients with normal carotid arteries require TEE for exclusion of relevant aortic plaques?.J Neurol Neurosurg Psychiatry 2005; 76:1654–1658.
9. Fasseas P, Brilakis ES, Leybishkis B, et al. Association of carotid artery intima-media thickness with complex aortic atherosclerosis in patients with recent stroke. Angiology 2002; 53:185–189.
10. Daniel W, Erbel R, Kasper w, et al. Safety of transesophageal echocardiography. A multicenter survey of 10,419. Circulation 1991; 83:817-821.
11. Russo, C, Zhezhen, J, Rundek, T, et al; Atherosclerotic disease of the proximal aorta and the risk of vascular events in a population-based cohort: the aortic plaques and risk of isquemic stroke (APRIS) study. Stroke 2009; 40:2313-2318.
12. Ibáñez, B, Pinero, A, Orejas, M, et al. Novel imaging techniques for quantifying overall atherosclerosis burden. Rev Esp Cardiol 2007; 60(3):299-309.
13. Lorenz M, Markus H, Bots M, et al. Prediction of Clinical Cardiovascular Events With Carotid Intima-Media Thickness: A Systematic Review and Meta-Analysis. Circulation 2007;115:459-467.
14. Touboul P, Hennerici M, Meairs S. Mannheim Carotid Intima-Media Thickness Consensus (2004–2006). Cerebrovascular Disease 2007; 23:75–80.

INTERNATIONAL JOURNAL OF
CLINICAL NEUROSCIENCES
AND MENTAL HEALTH

ORIGINAL RESEARCH

# Modifying effect of aortic atheroma on ischemic events recurrence in stroke patients with cervical and intracranial steno-occlusive disease

Liliana Pereira[1], Carina Fernandes[1], and Miguel Rodrigues[1]

Special Issue on Neurosonology and Cerebral Hemodynamics

## Abstract

**Background:** Large artery atherosclerosis is a major cause of ischemic stroke. Ultrasound can assess aortic, supra-aortic and intracranial vessels. We describe the recurrence rate in patients with cervical/intracranial disease and aortic atheroma.

**Methods:** We performed a retrospective review of patients' charts admitted to a Neurology ward with ischemic stroke/transient ischemic attack in a 5-year period. We collected clinical data, aortic, supra-aortic, and intracranial atherosclerotic changes whenever transesophageal echocardiogram was also available. Follow-up data was obtained from charts. Group comparison and recurrence risk estimates were done by Kaplan-Meier curves with Log Rank (LR) and Cox regression with Hazard Ratio (HR), with 95% confidence intervals (95% CI).

**Results:** Of 1300 patients, 337 underwent transesophageal echocardiogram (mean age 55.7 years; 62.9% male). Stenosis >50% or occlusion was found in 8.0% of carotid arteries, 4.2% of vertebral arteries, and 14.2% of intracranial vessels. Aortic complex plaques were found in 18.2%. Recurrence rate was 10.3% and lethality 1.3%, in 604.7 days of mean follow-up. No difference was found between risk factors of patients with or without recurrence. After 1-year of follow-up more events were seen with cervical/intracranial disease (11.7% vs 2.8%, LR p=0.006). However, cervical/intracranial disease is not predictive of recurrent events in patients without aortic atheroma (LR p=0.607), while the association is strong if aortic atheroma is present (LR p=0.013; HR=4.9; 95% CI 1.2-19.5).

**Conclusion:** In stroke patients investigated with transesophageal echocardiogram, cervical/intracranial disease had higher 1-year recurrence risk, but not in subjects without aortic atheroma. Presence of aortic atheroma slightly further increases recurrences.

**Keywords:** Ischemic stroke, Stroke recurrence, Aortic atherosclerosis, Carotid atherosclerosis, Intracranial atherosclerosis.

[1]Neurology Department, Hospital Garcia de Orta, Almada, Portugal

Correspondence: Liliana Pereira
Neurology Department, Hospital Garcia de Orta
Av Torrado da Silva, Pragal, 2801-951 Almada, Portugal
Email adress: lipereira@yahoo.com

Citation: Pereira et al. Modifying effect of aortic atheroma on ischemic events recurrence in stroke patients with cervical and intracranial steno-occlusive disease. IJCNMH 2014; 1(Suppl. 1):S12

Received: 27 Aug 2013; Accepted: 18 Nov 2013; Published: 09 May 2014

Open Access Publication Available at http://ijcnmh.arc-publishing.org



ARC Publishing

## Introduction

Large artery atherosclerosis has long been identified as one of the most frequent causes of ischemic stroke (IS). Recent epidemiological studies in the European population have shown a prevalence of this stroke etiology ranging from 8.2% to 15.7% [1-3]. Palm et al. [3] identified a further 13.4% of their patients with 'probable atherothrombotic stroke', a subgroup introduced to account for those patients with extracranial or intracranial atherosclerosis without significant stenosis in the absence of alternative stroke etiologies. These cases may reflect atherosclerotic changes at a more proximal site in the arterial tree, not routinely imaged.

The major sites for extracranial large vessel atherosclerosis are the carotid bifurcations, particularly near or at the origin of the internal carotid artery, and the proximal segments of the vertebral arteries. The most commonly affected intracranial sites are: the terminal internal carotid bifurcation, the distal segment of the vertebral arteries, the basilar artery and the middle cerebral artery bifurcation [4]. At the aortic level atherosclerotic changes are also a frequent finding. A population based study by Russo et al. [5] identified a high prevalence of aortic plaques of any size, both in the aortic arch (62.2%) and in the descending aorta (60.9%).

Ultrasound imaging, through cervical triplex ultrasound and transcranial Doppler ultrasound, can be used to assess the arterial patency and the presence of atherosclerotic lesions in the extracranial and intracranial vasculature, and should be available for the evaluation of every stroke patient [6]. Another ultrasound technique, the transesophageal echocardiogram (TEE), is the gold standard for evaluation of cardiac sources of embolism and also assessment of atherosclerotic disease at the level of the aorta [7].

The role of TEE in the evaluation of embolism sources has been questioned, because of its limited benefit in modifying the therapeutic approach [8]. Our aim was to evaluate the modifying effect of the presence of aortic atheroma on the recurrence rate of ischemic events in ischemic stroke patients with cervical and intracranial steno-occlusive disease. We describe the recurrence rate of cerebrovascular events and identify associated risk factors.

## Methods

This study was carried out at the Stroke Unit of a Portuguese tertiary hospital, which has a direct influence area of 381,799 habitants and receives acute stroke patients from an area of almost 500,000 inhabitants.

### Patients

In the present study we retrospectively screened all consecutive patients with a final diagnosis of acute IS or transient ischemic attack (TIA), admitted to our Neurology ward during a period of 5 years—from the 1st of July of 2007 until 30th of June of 2012. Patients with cerebral venous thrombosis, subarachnoid hemorrhage, or intracerebral bleeding on admission were excluded. To reach a final diagnosis of stroke or TIA, all patients were assessed by a neurologist to determine the diagnosis of stroke (neurological deficit of cerebrovascular cause that persists beyond 24 hours or is interrupted by death within 24 hours) with imaging evidence of ischemia or no other likely diagnosis, and TIA (defined as a transient episode of neurologic dysfunction caused by focal brain, spinal cord, or retinal ischemia, without acute infarction). Stroke subtype was categorized according to the Oxfordshire Community Stroke Project classification [9]. Stroke etiology was classified according to the Trial of Org 10172 in Acute Stroke Treatment (TOAST) criteria [10]. Patients were included in the study if they underwent TEE as part of the vascular event etiological investigation.

### Cervical and transcranial color ultrasound technique

Cervical carotid and vertebral color ultrasonography examinations were performed with a GE Vivid 7 Ultrasound System equipped with an 8-MHz linear probe. Transcranial color-coded sonography examinations were performed with the same equipment, fitted with a 3.5-MHz sectorial probe, without ultrasound contrast material. A standardized evaluation protocol was employed and images from all vessels were obtained and stored.

Carotid stenosis was estimated using flow velocities and Doppler spectrum analysis, according to the criteria defined by von Reutern et al. [11]. For vertebral evaluation, peak systolic velocities, artery morphology and symmetry with the contralateral vertebral artery were considered.

The peak systolic flow velocity thresholds considered for a ≥50% intracranial artery stenosis were 220 cm/s for the middle cerebral artery, 155 cm/s for the anterior cerebral artery, 145 cm/s for the posterior cerebral artery, 140 cm/s for the basilar artery and 120 cm/s for the vertebral artery [12].

### Transesophageal echocardiography

TEE was performed with a Hewlett-Packard multiF plane probe at 5 MHz, rotating the image plane by up to 180°. Images with the significant findings for each patient were printed.

Aortic atherosclerosis was classified as simple or complex considering the size and morphology of the plaques. Simple aortic plaques were defined as an intimal thickening of less than 4 mm. Complex aortic plaques were defined as plaques protruding more than 4 mm, with visible surface ulceration, or presence of mobile components regardless of atheroma size [13].

### Stroke risk factors

The medical records were reviewed for risk factor information. Arterial hypertension was defined as current

treatment with antihypertensive medication or a history, or present diagnosis, of hypertension according to the 2003 World Health Organization criteria as systolic blood pressure ≥140 mmHg and/or diastolic blood pressure ≥90 mmHg. Dyslipidemia was defined as on lipid-lowering medication or total cholesterol level ≥190 mg/dL, low-density lipoprotein level ≥110 mg/dL, or triglycerides level ≥150 mg/dL. Diabetes mellitus was defined as treated with oral anti-diabetic drugs or insulin or a history, or present diagnosis, according to the 1999 World Health Organization criteria as fasting plasma glucose ≥126 mg/dL. A patient was defined as a smoker if currently smoking, or past history of regular smoking of ≥1 cigarettes per day or daily use of tobacco (cigar or pipe). Recorded cardiovascular diseases included coronary heart disease, previous myocardial infarction, and atrial fibrillation.

All patients underwent a routine range of laboratory and other diagnostic testing. On admission laboratory tests were ordered, including serum glucose, serum creatinine, hematocrit, platelet count, and International Normalized Ratio (INR). Other baseline variables that were obtained for each patient included fasting serum glucose, fasting serum cholesterol (total, HDL, and LDL), and fasting triglycerides, among other routine blood tests. Systolic and diastolic blood pressures were both recorded on admission and daily per established nursing protocol. All patients had brain imaging with either computed tomography (CT) and/or magnetic resonance imaging (MRI), and systemic investigation including chest X-ray, 12-lead ECG, and transthoracic echocardiogram.

If any new information on vascular risk factors was obtained in the follow-up and if the risk factors were considered relevant in the etiology of the baseline stroke, that information was also incorporated in the baseline risk profile.

### Evaluation of outcome

Patients were followed-up through the information available from registries of medical appointments in the outpatient clinic or emergency room admissions. Study outcomes were assessed at maximum follow-up time available. Subsequent vascular events, their type (IS, TIA), and time of occurrence were recorded. TIA and IS as outcome events were diagnoses according to the same definitions as the baseline TIA or stroke. If the outcome was fatal, both the date and cause of death were recorded. The causes of death were divided into neurological (recurrence of stroke), and other causes. Death after stroke was defined as case-fatality in the following 30 days after the event. We defined combine vascular events as any of TIA, IS of fatal stroke.

### Statistical analysis

The statistical analyses were performed using the software SPSS version 19.0 and MedCalc version 12.3. We report descriptive statistics with rates and 95% confidence intervals (95% CI). Comparisons between groups were made with chi-square test, with a two-tailed level of significance of 0.05. We calculated recurrence risk by Kaplan-Meier curves with Log Rank (LR), and Cox proportional hazards model was used for univariate and multivariate risk factor analyses. Hazard Ratios (HR) are presented, along with 95% CI.

## Results

### Study cohort

From 1300 patients screened, 337 (25.9%) had underwent TEE examination and were entered in the study. Clinical characteristics of the study cohort are shown in **Table 1**. Stroke etiologies according to the TOAST criteria are shown in **Table 2**.

Atherosclerotic disease of the carotid arteries was found in 170 patients (50.4%), of which 9 had ulcerated lesions (2.7%), 9 had hemodynamically significant stenosis (2.7%), and 18 patients had unilateral carotid occlusion (5.3%). The vertebral arteries were involved in the atherosclerotic process in 14 patients (4.2%), with 7 cases of occlusion (2.1%). The intracranial vessels showed significant disease in 48 patients (14.2%), with 31 cases of severe stenosis (9.2%), and 17 cases of occlusion (5.0%). Globally, 69 patients (20.5%) presented with stenosis ≥50% of either carotid, vertebral or intracranial arteries.

Aortic atherosclerotic plaques of any size were found in 157 patients (46.6%). Thickness equal to or above 4 mm was seen in 34 subjects (10.1%) and other complex plaque morphology (ulcerations and/or mobile components) was observed in 27 subjects (8.1%). Aortic atheroma was more frequently seen in the aortic arch (108 patients, 32.1% of the total population, 68.8% of the patients with plaques), irrespective of other sites being affected. In 43 patients

**Table 1.** Baseline characteristics of the study cohort.

| Characteristic | Overall Population (n=337) |
|---|---|
| Age, years | 55.7±11.8 |
| Men, n (%) | 212 (62.9%) |
| Hypertension, n (%) | 214 (63.5%) |
| Dyslipidemia, n (%) | 232 (68.8%) |
| Diabetes, n (%) | 69 (20.5%) |
| Smokers, n (%) | 170 (50.4%) |
| Coronary heart disease, n (%) | 33 (9.8%) |
| Atrial fibrillation, n (%) | 33 (9.8%) |
| Medications | |
| Antiplatelet drugs, n (%) | 57 (16.9%) |
| Anticoagulants, n (%) | 10 (3.0%) |
| Antihypertensive drugs, n (%) | 139 (41.2%) |
| Lipid-lowering drugs, n (%) | 77 (22.8%) |
| Anti-diabetic drugs, n (%) | 45 (13.4%) |

**Table 2.** Stroke etiologies by the TOAST classification of subtypes of acute ischemic stroke.

| Characteristic | Overall Population (n=337) |
|---|---|
| Large-artery atherosclerosis, n (%) | 79 (23.4%) |
| Cardioembolism, n (%) | 57 (16.9%) |
| Small-vessel occlusion, n (%) | 31 (9.2%) |
| Stroke of other determined etiology, n (%) | 25 (7.4%) |
| Stroke of undetermined etiology | |
| Two or more causes identified, n (%) | 12 (3.6%) |
| Negative or incomplete evaluation, n (%) | 133 (39.5%) |

(12.8%) the plaques were exclusively located on the descending portion of the aorta.

Combined disease of the aorta and supra-aortic vessels was present in 47 patients (13.9%).

Table 3 shows the cohort clinical characteristics by presence of atherosclerotic disease of either the supra-aortic and intracranial vessels, or aortic atheroma.

Diabetes loosely associated with the presence of cerebral and pre-cerebral arteries stenosis and occlusion (p=0.082), while other risk factors didn't.

Increasing plaque thickness occurred with advancing age and men more often had complex plaques. Patients with complex plaques had higher prevalence of traditional risk factors. On multivariate analysis, age equal or above 55 years (OR=7.1; 95% CI 3.2-15.6) and smoking (OR=4.7; 95% CI 2.1-10.3) remained associated with complex atheroma, and age alone to simple atheroma (OR=3.5; 95% CI 2.0-6.2%).

No differences in antiplatelet treatment were observed between different arch plaque groups or regarding the presence of cervical and intracranial significant atherosclerotic disease. Anticoagulant treatment was more frequent in subjects with cervical and intracranial stenosis or occlusion (p=0.013). Antihypertensive drugs were more frequently used in those with aortic atheroma and anti-diabetic drugs in those with complex aortic plaques compared to those with no or simple plaques respectively (p=0.032 and p=0.036).

### Risk of combined vascular events

Mean follow-up was 604.7 days (median 468 days, interquartile range 702 days, total range 15 to 1901 days) in 310 patients, while 27 patients were lost to follow-up. Losses to follow-up occurred when patients missed their scheduled appointments, when contacts were missing or were unreliable and no vital information could be retrieved from record linkage with other hospitals. The median survival time was not significantly different in all the presented comparisons. Overall, 32 endpoints (10.3%) occurred, of which 3 were fatal (lethality rate of 1.3%). No difference was found between risk factors prevalence for patients with or without recurrence. Two-thirds of the recurrent events happened during the first year of follow-up. Recurrences according to TOAST classification are shown in Table 4.

In this first year of follow-up more new events happened in the group with cervical and intracranial arteries stenosis or occlusion, with a recurrence rate of 11.7%, compared with 2.8% in the group without supra-aortic disease. This difference is significant, with a LR p=0.006,

**Table 3.** Baseline characteristics of the study cohort by presence of site specific atherosclerotic disease.

| Characteristic | Aortic Atheroma | | | | Cervical or Intracranial Stenosis/Occlusion | | |
|---|---|---|---|---|---|---|---|
| | Without (n=181) | Simple plaques (n=95) | Complex plaques (n=61) | *P* value | Without (n=268) | With (n=69) | *P* value |
| Age, years | 50.9 ± 11.0 | 60.2 ± 11.1 | 62.8 ± 8.9 | <0.001 | 54.3 ± 12.0 | 55.7 ± 11.0 | 0.406 |
| Men, n (%) | 105 (58.3%) | 59 (62.1%) | 47 (77.0%) | 0.032 | 126 (47.0%) | 39 (56.5%) | 0.179 |
| Hypertension, n (%) | 97 (53.9%) | 68 (71.6%) | 49 (80.3%) | <0.001 | 112 (41.8%) | 48 (69.6%) | 0.1 |
| Dyslipidemia, n (%) | 112 (62.2%) | 71 (74.7%) | 48 (78.7%) | 0.019 | 127 (47.4%) | 52 (75.4%) | 0.157 |
| Diabetes, n (%) | 27 (15.0%) | 20 (21.1%) | 22 (36.1%) | 0.002 | 34 (12.7%) | 19 (27.5%) | 0.082 |
| Smokers, n (%) | 78 (43.3%) | 47 (49.5%) | 44 (50.3%) | 0.005 | 99 (36.9%) | 35 (53.0%) | 0.946 |
| Coronary heart disease, n (%) | 14 (7.8%) | 9 (9.5%) | 10 (16.4%) | 0.147 | 16 (6.0%) | 4 (5.8%) | 0.497 |
| Atrial fibrillation, n (%) | 16 (8.9%) | 13 (13.7%) | 4 (6.6%) | 0.285 | 15 (5.6%) | 5 (7.2%) | 0.879 |
| Medications | | | | | | | |
| Antiplatelet drugs, n (%) | 26 (14.4%) | 22 (23.2%) | 9 (14.8%) | 0.273 | 30 (11.2%) | 12 (17.4%) | 0.557 |
| Anticoagulants, n (%) | 7 (3.9%) | 0 (0%) | 3 (4.9%) | 0.239 | 1 (0.4%) | 4 (5.8%) | 0.013 |
| Anti-hypertensive drugs, n (%) | 62 (34.4%) | 46 (48.4%) | 31 (50.8%) | 0.032 | 71 (26.5%) | 30 (43.5%) | 0.326 |
| Lipid-lowering drugs, n (%) | 33 (18.3%) | 28 (29.5%) | 16 (26.2%) | 0.150 | 37 (13.8%) | 20 (29.0%) | 0.123 |
| Anti-diabetic drugs, n (%) | 18 (10.0%) | 12 (12.6%) | 15 (24.6%) | 0.036 | 21 (7.8%) | 13 (18.8%) | 0.131 |

**Table 3.** Stroke Recurrences by the TOAST classification of subtypes of acute ischemic stroke.

| Characteristic | Patients without recurrent events (n=278) | Patients with recurrent events (n=32) |
|---|---|---|
| Large-artery atherosclerosis, n (%) | 60 (21.6%) | 10 (31.2%) |
| Cardioembolism, n (%) | 52 (18.7%) | 3 (9.4%) |
| Small-vessel occlusion, n (%) | 27 (9.7%) | 2 (6.2%) |
| Stroke of other determined etiology, n (%) | 21 (7.6%) | 3 (9.4%) |
| Stroke of undetermined etiology | | |
| Two or more causes identified, n (%) | 10 (3.6%) | 1 (3.1%) |
| Negative or incomplete evaluation, n (%) | 108 (38.8%) | 13 (40.7%) |

TOAST = Trial of Org 10172 in Acute Stroke Treatment

and remains so even after adjustment for diabetes (HR=4.4, 95% CI 1.4-13.9).

After 1 year of follow-up, more new events were also seen in the aortic atheroma group (7.1% in the presence of complex plaques, 5.7% if simple plaques and 1.8% in the group without plaques, LR p=0.097). The difference between groups with and without plaques is significant at 1 year (6.3% vs 1.8%, LR p=0.013), but fades with time until end of follow-up. Kaplan–Meier curves for vascular events are showed in the **Figure 1**.

### Events in patients with cervical and intracranial steno-occlusive disease by aortic atheroma status

To address the influence of aortic atheroma in the survival of patients with cervical and intracranial arteries stenosis or occlusion, we performed a stratified analysis using aortic atheroma presence to define each stratum.

Considering only the patients without aortic atheroma, disease at the cervical and intracranial level no longer predicts recurrent events (1.9% in those without disease compared to 3.7% with cervical/intracranial disease, LR p=0.607). Considering the group of patients with aortic atherosclerotic disease, the recurrence of events is greater in the presence of important stenosis or occlusion of the cervical and intracranial arteries (4.0% in those with only aortic disease paralleled to 18.2% for those with disease at both sites, LR p=0.013; HR=4.9; 95% CI 1.2-19.5). In this last group of patients women had more supra-aortic steno-occlusive disease (p=0.021), while other risk factors were balanced. Adjustment for gender did not change this risk estimate (HR=4.7; 95% CI 1.1-19.7). **Figure 2** shows the Kaplan–Meier curves for vascular events.

## Discussion

We report on the risk of recurrent cerebral vascular events in ischemic stroke and TIA patients with cervical and intracranial steno-occlusive disease, analyzing the modifying

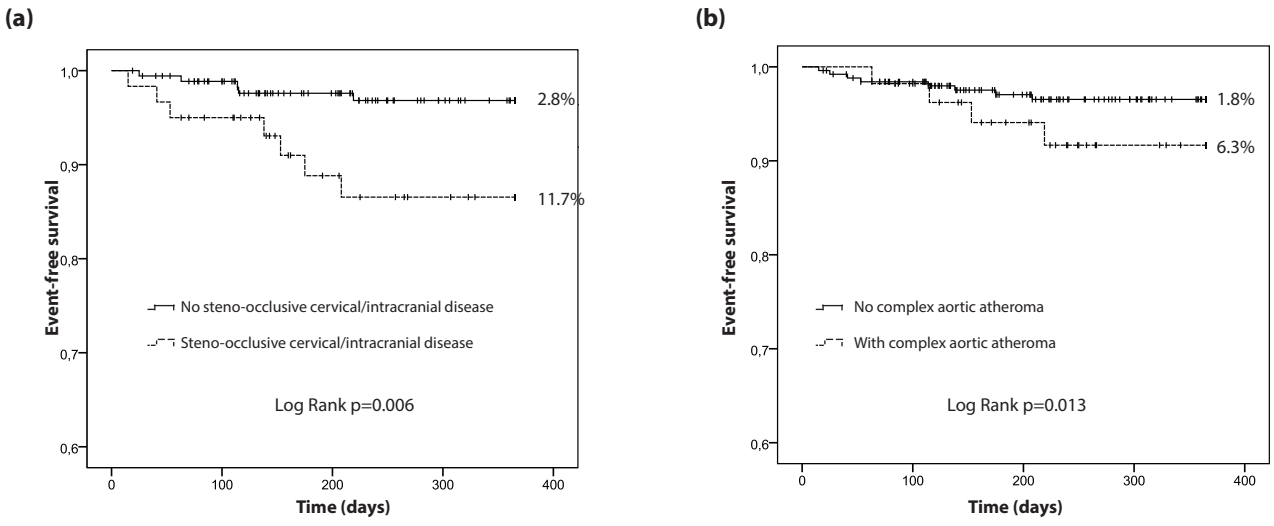


**Figure 1**. Kaplan–Meier curves for time-to-event by presence of cervical or intracranial stenosis or occlusion **(a)** and aortic atherosclerotic disease **(b)**.

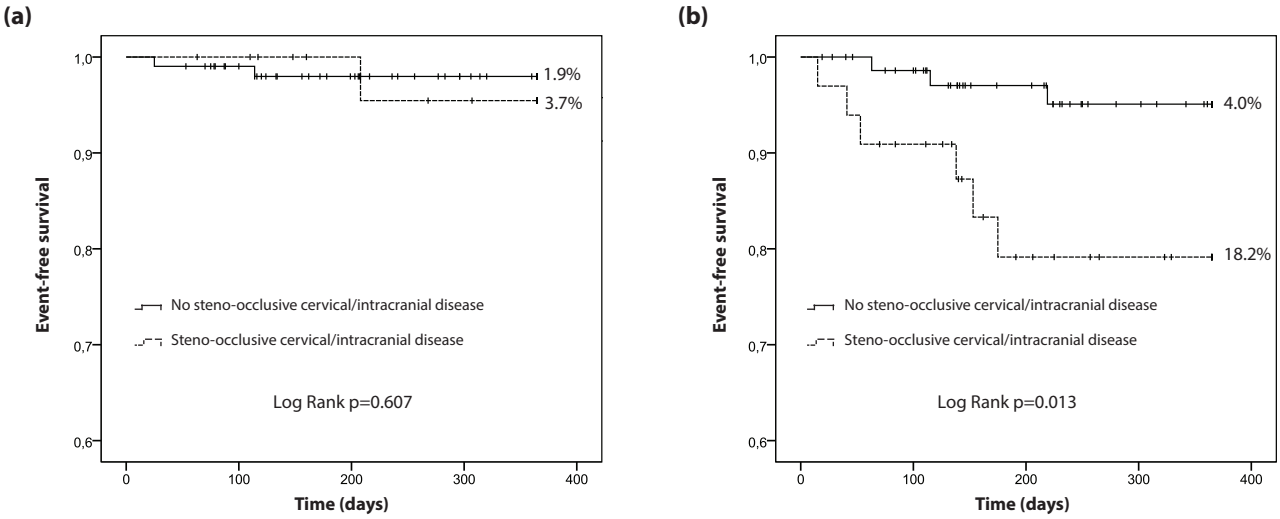


**Figure 2**. Kaplan–Meier curves for time-to-event by presence of cervical or intracranial stenosis or occlusion, according to absence **(a)** or presence of aortic atherosclerotic disease **(b)**.

effect of aortic atheroma in this outcome. We investigated the presence of plaques in the carotid, vertebral and intracerebral arteries causing hemodynamically significant stenosis (≥50%) or occlusion, which have been associated with high early recurrence risk [14]. Likewise, we examined for the presence of aortic atheroma, another well known risk factor for stroke, independent from the traditional vascular risk factors, but which pathophysiology remains uncertain. It is hypothesized that aortic plaques may cause stroke via an atheroembolic mechanism, while other authors consider atherosclerosis at the aortic level as just another marker of generalized atherosclerosis [15-16]. Controversy remains as there is continuing evidence for increased risk of recurrent stroke and death in patients with stroke and large aortic plaques, with plaques of complex morphology conferring a slight additional increase in risk [17]. There are also population-based studies where the incidental detection of plaques in the aortic arch or proximal descending aorta was not associated with future vascular events [5].

In our cohort, the individual presence of either cervical and intracranial steno-occlusive disease or complex aortic atheroma was an independent predictor of subsequent vascular events, including stroke, during the first year of follow-up. But when combining these subgroups of patients, predictive value for recurrence only remains significant in patients with cervical and intracranial significant stenosis or occlusion if there is concomitant disease at the aortic level. This means that the presence of aortic atheroma slightly further increased the number of future recurrences, supporting its pathological role as a stroke mechanism, as opposed to a plain atherosclerotic marker.

Our study has some limitations. The main limitation is the relatively small sample size, which may have affected the statistical power to detect significant risk factors associated with vascular events recurrence. Moreover, given the small number of events, we could not prove an association with atherosclerotic changes at any site beyond the first year of follow-up.

Regarding medication with antihypertensive, antidiabetic or anticoagulant drugs, we also had important unbalances between groups. Nevertheless, these drugs were more frequent in patients with vessel stenosis or occlusion, or aortic atheroma and that should have decreased the risk of recurrence. We found the opposite results, so if any confounding effect of medication is to be expected; it would be to decrease the strength of our estimates and not to increase it.

Our study shows that aortic atheroma interacts with cervical or intracranial atherosclerotic changes, increasing the risk of recurrent events. However we cannot determine with this type of study if the aortic plaques are themselves implied causally in the etiology of recurrences or if they are a signal of more advanced and/or aggressive atherosclerotic systemic disease. Further studies are needed to evaluate whether systematic screening for aortic atheroma or more aggressive treatment strategies in patients with vascular atherosclerotic disease at multiple sites diminish recurrences, and to establish better preventive strategies to limit the occurrence of repeated events

## Abbreviations

CT: Computed tomography; HR: Hazard Ratios; INR: International Normalized Ratio; IS: Ischemic stroke; LR: Log Rank; TEE: Transesophageal echocardiogram; TIA: Transient ischemic attack; TOAST: Trial of Org 10172 in Acute Stroke Treatment

## Competing interests

The authors declare no conflict of interest.

## References


1. Putaala J, Curtze S, Hiltunen S, Tolppanen H, Kaste M, Tatlisumak T. Causes of death and predictors of 5-year mortality in young adults after first-ever ischemic stroke: the Helsinki Young Stroke Registry. Stroke 2009; 40(8):2698-703.
2. Hajat C, Heuschmann PU, Coshall C, Padayachee S, Chambers J, Rudd AG, Wolfe CD. Incidence of aetiological subtypes of stroke in a multi-ethnic population based study: the South London Stroke Register. J Neurol Neurosurg Psychiatry 2011; 82(5):527-33.
3. Palm F, Urbanek C, Wolf J, Buggle F, Kleemann T, Hennerici MG, Inselmann G, Hagar M, Safer A, Becher H, Grau AJ. Etiology, risk factors and sex differences in ischemic stroke in the Ludwigshafen Stroke Study, a population-based stroke registry. Cerebrovasc Dis 2012; 33(1):69-75.
4. Hass WK, Fields WS, North RR, Kircheff II, Chase NE, Bauer RB. Joint study of extracranial arterial occlusion. II. Arteriography, techniques, sites, and complications. JAMA 1968; 203(11):961-8.
5. Russo C, Jin Z, Rundek T, Homma S, Sacco RL, Di Tullio MR. Atherosclerotic disease of the proximal aorta and the risk of vascular events in a population-based cohort: the Aortic Plaques and Risk of Ischemic Stroke (APRIS) study. Stroke 2009; 40(7):2313-8.
6. Martínez-Sánchez P, Tsivgoulis G, Lao A, Sharma V, Alexandrov AV. Ultrasound in acute ischemic stroke. Neurologia 2009; 24(1):59-68.
7. Cho HJ, Choi HY, Kim YD, Nam HS, Han SW, Ha JW, Chung NS, Heo JH. Transoesophageal echocardiography in patients with acute stroke with sinus rhythm and no cardiac disease history. J Neurol Neurosurg Psychiatry 2010; 81(4):412-5.
8. Galougahi KK, Stewart T, Choong CY, Storey CE, Yates M, Tofler GH. The utility of transesophageal echocardiography to determine management in suspected embolic stroke. Intern Med J 2010; 40(12):813-8.
9. Bamford J, Sandercock P, Dennis M, Burn J, Warlow C. Classification and natural history of clinically identifiable subtypes of cerebral infarction. Lancet 1991; 337(8756):1521-6.
10. Adams HP Jr, Bendixen BH, Kappelle LJ, Biller J, Love BB, Gordon DL, Marsh EE 3rd. Classification of subtype of acute ischemic stroke. Definitions for use in a multicenter clinical trial. TOAST. Trial of Org 10172 in Acute Stroke Treatment. Stroke 1993; 24(1):35-41.
11. von Reutern GM, Goertler MW, Bornstein NM, Del Sette M, Evans DH, Hetzel A, Kaps M, Perren F, Razumovky A, von Reutern M, Shiogai T, Titianova E, Traubner P, Venketasubramanian N, Wong LK, Yasaka M; Neurosonology Research Group of the World Federation of Neurology. Grading carotid stenosis using ultrasonic methods. Stroke 2012; 43(3):916-21.
12. Baumgartner RW, Mattle HP, Schroth G. Assessment of >/=50% and <50% intracranial stenoses by transcranial color-coded duplex sonography. Stroke 1999; 30(1):87-92.
13. Sharma U, Tak T. Aortic atheromas: current knowledge and controversies: a brief review of the literature. Echocardiography 2011; 28(10):1157-63.
14. Momjian-Mayor I, Burkhard P, Murith N, Mugnai D, Yilmaz H, Narata AP, Lovblad K, Pereira V, Righini M, Bounameaux H, Sztajzel RF. Diagnosis of and treatment for symptomatic carotid stenosis: an updated review. Acta Neurol Scand 2012; 126(5):293-305.
15. Meier B, Frank B, Wahl A, Diener HC. Secondary stroke prevention: patent foramen ovale, aortic plaque, and carotid stenosis. Eur Heart J 2012; 33(6):705-13, 713a, 713b.
16. Sharma U, Tak T. Aortic atheromas: current knowledge and controversies: a brief review of the literature. Echocardiography 2011; 28(10):1157-63.
17. Di Tullio MR, Russo C, Jin Z, Sacco RL, Mohr JP, Homma S; Patent Foramen Ovale in Cryptogenic Stroke Study Investigators. Aortic arch plaques and risk of recurrent stroke and death. Circulation 2009; 119(17):2376-82

INTERNATIONAL JOURNAL OF
CLINICAL NEUROSCIENCES
AND MENTAL HEALTH

ORIGINAL RESEARCH

# Internal carotid artery stenosis: validation of Doppler velocimetric criteria

Ana Monteiro[1], Rosa Santos[1], Carmen Ferreira[1], Andreia Costa[1], and Elsa Azevedo[1]

Special Issue on Neurosonology and Cerebral Hemodynamics

## Abstract

**Background:** Carotid endarterectomy is effective in reducing recurrent stroke in patients with carotid stenosis. Duplex sonography is widely used for diagnosing internal carotid artery (ICA) stenosis. Surgeons often base management decisions solely on this technique. Published velocimetric criteria should be validated in each laboratory. This study aims to validate Doppler velocimetric criteria for different grades of ICA stenosis and evaluate intracranial collateralization circuits.

**Methods:** Duplex scans from 10,435 consecutive patients routinely referred to our Neurosonology Unit from 2003 to 2011 were reviewed. Cases with ICA stenosis ≥50% (ultrasonographic morphologic criteria) were grouped by percentage of stenosis (ECST method). Mean ICA peak-systolic (PSV) and end-diastolic velocities (EDV), carotid index and presence of collateral flow were recorded. Pearson's coefficient was used to correlate percentage of stenosis and velocity parameters. One-way ANOVA was performed for the presence of collateralization.

**Results:** Nine-hundred and sixty cases of ICA stenosis ≥50% were identified. The Pearson's correlation values were R=0.802, p<0.001; R=0.724, p<0.001 and R=0.769, p<0.001 for the PSV, EDV and carotid index, respectively. The presence of collateral flow increased significantly for a stenosis ≥70% (p<0.001). For stenosis ≥70%, PSV >182 cm/s showed a sensibility of 80%, specificity of 82% and accuracy of 88%, EDV >61 cm/s showed a sensibility of 76%, specificity of 80% and accuracy of 86%, and carotid index >2.3 showed a sensibility of 82%, specificity of 82% and accuracy of 89%. These velocities were superior to the recently published consensus criteria for diagnosing stenosis ≥70%. Collateral blood flow increased significantly for stenosis ≥70% (p<0.001).

**Conclusion:** This work defined optimal velocimetric criteria for ICA stenosis in our laboratory, enabling the correct diagnosis when morphological criteria are lacking. The presence of collateralization was important to identify hemodinamically significant stenosis.

**Keywords:** Internal carotid artery stenosis, Velocimetric criteria, ECST, NASCET; Endarterectomy, Collateral blood flow.

[1]Neurosonology Unit, Department of Neurology, São João Hospital Center and Department of Clinical Neurosciences and Mental Health, Faculty of Medicine of University of Porto, Porto, Portugal

Correspondence: Ana Monteiro
Department of Neurology, Faculty of Medicine of University of Porto
Alameda Prof. Hernani Monteiro, 4200-319 Porto, Portugal
Email adress: ana.mg.monteiro@gmail.com

Citation: Monteiro et al. Internal carotid artery stenosis: validation of Doppler velocimetric criteria. IJCNMH 2014; 1(Suppl. 1):S13

Received: 03 Nov 2013; Accepted: 20 Dec 2013; Published: 09 May 2014

Open Access Publication Available at http://ijcnmh.arc-publishing.org



ARC Publishing

## Introduction

The efficacy of carotid endarterectomy (CEA) in reducing recurrent stroke in patients with carotid stenosis has been well established [1-4] and this technique remains the gold standard for the management of carotid artery disease [5]. The benefits of this intervention, however, are largely dependent on the degree of stenosis [2, 4, 5] and all efforts should be made in order to accurately identify patients who will benefit from this intervention.

Doppler ultrasonography (DUS) is now widely used for the diagnosis of internal carotid artery (ICA) stenosis. The diagnostic accuracy of ultrasonographic duplex imaging has been demonstrated for both moderate and high-grade ICA stenosis, using angiography as a reference [6-11]. This imaging method is commonly the only diagnostic technique performed in patients at risk for atherosclerotic carotid artery disease. DUS has widely replaced preoperative carotid angiography in clinical routine and surgeons often base management decisions solely on this technique [2-4, 8, 10, 12-14]. Patient selection for CEA should be based on a combination of both ultrasound imaging (US) and velocity measurement of carotid stenosis [9]. Several studies have demonstrated the accuracy of B-mode imaging in predicting the grade of stenosis [15-20]. However, in severe disease, adequate B-mode images may be difficult to obtain, as more complex and heavily calcified plaques create shadowing and other artifacts that impair correct plaque measurements. In fact, for severe stenosis hemodynamic criteria are prevailing [9]. The correlation between degree of stenosis and velocity is demonstrated by the "Spencer's curve"[21], which has proven to be a reliable criterion for grading stenosis [9, 12, 22]. Nonetheless, there is considerable variability in published velocimetric criteria for stenosis. This variability is caused, along with other factors, by differences in Doppler protocol and equipment in each laboratory and operator differences in measurement acquisition [9, 23, 24]. Therefore, internal validation of carotid duplex interpretation criteria is essential [10, 25, 26]. The preferred method for validation of Doppler velocimetric criteria would be comparing the grade of stenosis obtained by this method with measurements obtained by arteriography [8, 10, 27-30]. However, it is not always feasible to obtain angiographic correlation for quality assessment of ultrasonography (US) studies especially in centers where US is the main diagnostic technique chosen.

Although DUS is an efficient diagnostic tool to identify moderate to severe (<80% ECST – European Carotid Surgery Trial) stenosis [31], velocity measurements alone are not sufficient to differentiate moderate from severe (≥80% ECST) stenosis [9]. The presence of collateral blood flow may increase post-stenotic blood pressure in the ICA, reducing blood pressure gradients over the stenosis, thus leading to an underestimation of the degree of stenosis and, perhaps, exclusion from surgical treatment. Established collateral blood flow identified by transcranial Doppler can help recognizing stenosis of hemodynamic significance, especially when blood flow velocity criteria combined with plaque morphology are inconclusive [32]. Thus, it is recommended that a search for transcranial collateral flow is made [9].

The purpose of this study was to validate ultrasound velocimetric criteria in our Neurosonology Unit for different grades of ICA stenosis measured by US imaging in our laboratory, as well as to evaluate the presence of intracranial collateralization circuits as a mean of distinguishing moderate and high-grade stenosis.

## Methods

From January 2003 through December 2011, a total of 10,435 patients were routinely referred to our laboratory for clinically driven US evaluation of carotid artery disease. Duplex ultrasonography examinations were performed by two experienced neurosonology technicians using a Philips (Bothell, WA) HDI 5000 scanner. Each study was reviewed by neurosonology dedicated neurologists.

Complete examination of the common (CCA), internal (ICA) and external carotid arteries, as well as the vertebral arteries, was performed. Standard techniques were used as part of the examination protocol: aligning the cursor parallel to the vessel wall, obtaining waveforms using a small sample volume ideally placed in the center of the flow, and maintaining the Doppler beam angulated at 60º or less to the blood flow vector. The grade of ICA disease was assessed by analysis of plaque morphology and blood flow velocity measurements, namely peak systolic velocity (PSV) and end-diastolic velocity (EDV) at the point of highest stenosis, and internal carotid artery/common carotid artery peak systolic velocity ratio (carotid index). The maximal diameter reduction, measured morphologically at the most severely stenotic site of the ICA, was recorded by US imaging and used to calculate percentage diameter stenosis according to ECST method [3]. The cerebral basal arterial segments were also examined, using a pulsed 2-4 MHz Doppler transducer: the middle, anterior and posterior cerebral arteries were investigated using the transtemporal approach, whereas the ophthalmic arteries (OA) were insonated through the transorbital window, and intracranial vertebral arteries, as well as basilar artery, through the suboccipital window. Blood flow velocity signals were analyzed to determine direction and velocity. The presence of collateral blood flow through the anterior communicating, posterior communicating and ophthalmic arteries was assessed.

Cases with ICA stenosis ≥50% graded by US imaging morphologic criteria in our Unit were retrospectively selected for analysis. Groups were defined by percentage of stenosis, measured as diameter narrowing, as follows: (1) 50-59%; (2) 60-69%; (3) 70-79%; (4) 80-89% and (5) 90-99%. Patients with occlusion of the ICA, previous carotid endarterectomy or stenting, isolated parietal thrombus,

arterial dissection, incomplete or inadequate morphologic imaging were excluded from analysis.

The Pearson's correlation coefficient (R) was used to correlate percentage of stenosis and velocity parameters. Receiver operating characteristic (ROC) curves were constructed to compare DUS stenosis with PSV, EDV and carotid index and to establish optimal criteria for each stenosis range. The overall accuracy of each velocity criterion was expressed in terms of the area under the ROC curve (AUC), ranging from 0.5 (poor) to 1.0 (perfect). The confidence intervals (CI), sensitivity and specificity were calculated. One-way ANOVA followed by Bonferroni's post-hoc comparison tests were performed for the presence of collateralization in each stenosis range. Microsoft Excel (MS Office 2010) was used to collect all data and perform descriptive statistics. SPSS Statistics version 20 (IBM, Armonk, NY, USA) was used to perform the remaining analysis.

## Results

Between January 2003 and December 2011, carotid duplex sonography and transcranial Doppler (TCD) were performed in 10,435 consecutive patients. In 783 patients (551 men and 232 women aged 68 ± 11 years) stenosis ≥50% was identified in 977 internal carotid arteries. Data concerning velocity measurements was available for 960 exams (960 for PSV, 946 for EDV, and 929 for the carotid index). For 17 cases, data concerning velocity measurements was not available; 187 patients had bilateral ICA stenosis ≥50%, and 66 patients had contralateral ICA occlusion. TCD flow data was available in 481 arterial systems. Missing collateral TCD flow data were mostly attributable to acoustic difficulties to insonate the temporal bone.

The number of examined ICA in each range of stenosis, as measured by US imaging, is presented in **Figure 1**. In 32% (304 vessels), an ICA stenosis with diameter reductions of ≥70% was found. As expected, exams with less severe stenosis were found more often. There were only 24 ICA with stenosis in the 90-99% stenosis range. Since sample size for the 90-99% range was too small for the ROC curve analysis, the last two ranges (80-89% and 90-99%) were merged.

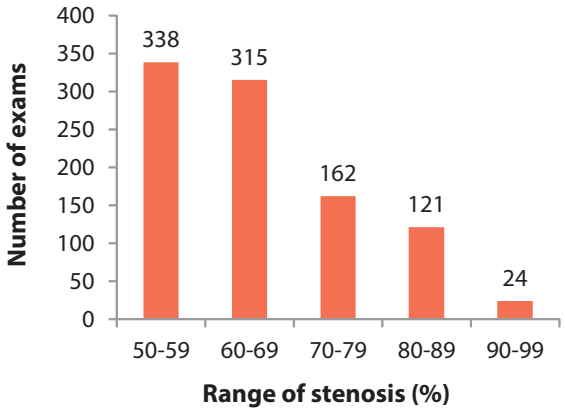


**Figure 1.** Distribution of the exams by range of stenosis as measured by US imaging (ECST method).
US = Ultrasound imaging; ECST = European Carotid Surgery Trial

Mean velocities and carotid index for the different ranges of stenosis were: for 50-59%, 111/35 cm/s, carotid index: 1.3; for 60-69%, 161/51 cm/s, carotid index: 2.1; for 70-79%, 218/78 cm/s, carotid index: 2.8; for 80-89%, 377/151 cm/s, carotid index: 5.3; for ≥90%, 409/191 cm/s, carotid index: 7.0.

The Pearson's correlation coefficient for the different velocimetric criteria were 0.802 for PSV, 0.724 for EDV and 0.769 for carotid index ($p<0.001$), indicating a strong correlation between these velocity measurements and the range of stenosis (**Table 1**).

Scatterplots of US measured stenosis versus the 3 parameters (PSV, EDV, and carotid index ratio) were generated to demonstrate the distribution of severity of ICA disease (**Figure 2**).

**Table 1** depicts the velocimetric criteria for PSV, EDV and carotid index ratio in the different ranges of stenosis, as established by ROC curve analysis, as well as the presence of intracranial collateralization in those ranges. **Figure 3** portrays the ROC curves for the different ranges of stenosis, with the respective sensitivities, specificities and accuracies (represented by the area under the curve—AUC).

As shown in **Figure 4**, the presence of collateral flow increased significantly for stenosis ≥70% ($p<0.001$). For

**Table 1.** Velocimetric criteria for the different ranges of stenosis.

| Range stenosis | PSV | EDV | Carotid index | Collateral flow |
|---|---|---|---|---|
| 50-59% | <152 | <50 | <1.9 | - |
| 60-69% | 152-182 | 50-61 | 1.9-2.3 | - |
| 70-79% | 182-251 | 61-81 | 2.3-3.3 | + |
| 80-99% | >251 | >81 | >3.3 | + |
| Pearson's correlations | 0.802* | 0.724* | 0.769* | |

*p<0.001: + present; - absent.

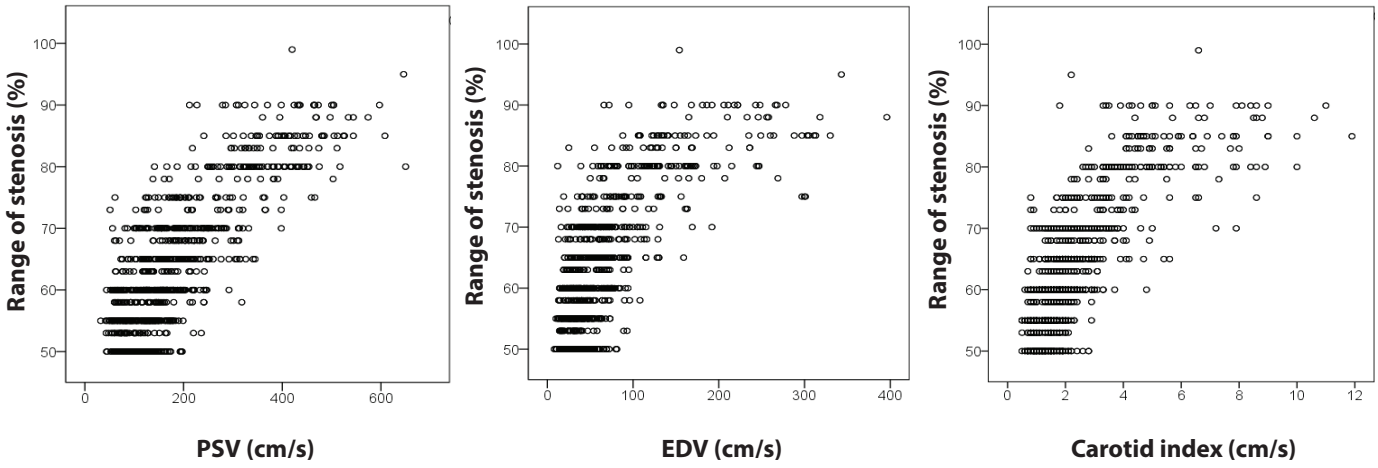


**Figure 2.** Scatterplots the diameter percentage stenosis measured by B-mode and the internal carotid artery (ICA) peak-systolic velocity (PSV), end-diastolic velocity (EDV) and ICA/common carotid artery PSV ratio.

stenosis 50-59%, no collateral flow was identified and for stenosis 60-69%, 1% of the exams presented collateral flow. For stenosis of 70-79%, 80-89%, and 90-99%, collateral flow was identified in 14%, 61%, and 92% of the exams, respectively. There was high specificity, positive predictive value (PPV), negative predictive value (NPV) and accuracy for predicting stenosis ≥70%, although sensitivity was low (**Table 2**).

The specificity, sensitivity and overall accuracy using the consensus criteria for diagnosing stenosis ≥70% (PSV >125 cm/s; EDV >40 cm/s and carotid index >2) and ≥80% (PSV >251 cm/s; EDV >81 cm/s and carotid index >3.3) (ECST method)[12] are presented in **Table 3**. Sensitivity, specificity and accuracy of our criteria are also depicted in **Table 3**. As shown in the table, for stenosis ≥70% ECST, sensitivity would be higher, but specificity and overall accuracy would be lower using the consensus criteria. For stenosis ≥80% ECST, sensitivity would be higher for PSV, but specificity and overall accuracy would be lower using the consensus criteria; for EDV and carotid index, on the other hand, sensitivity was lower and specificity and overall accuracy were higher with the consensus criteria.

Considering the criteria defined for our laboratory for stenosis ≥70% ECST, a PSV >182 cm/s would erroneously define 6% of stenosis as <70%, 11.5% of which would be correctly diagnosed by the presence of collateral blood flow on TCD. Similarly, considering EDV >61 cm/s and carotid index >2.3, 8% and 6% would be erroneously defined as having stenosis <70%, 7% and 8% of which, respectively, would be correctly diagnosed by the presence of collateral blood flow on TCD.

Established collateral blood flow was not observed in cases with <70% ICA stenosis, except in 2 patients with stenosis range 60-69%. In one patient, stenosis was defined

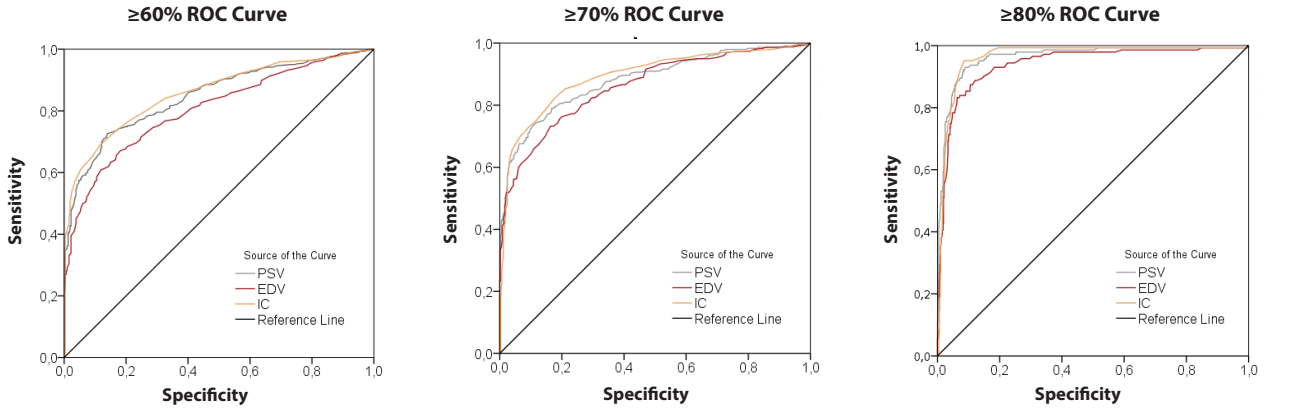


| ≥60% ROC Curve | | | ≥70% ROC Curve | | | ≥80% ROC Curve | | |
|---|---|---|---|---|---|---|---|---|
| PSV | EDV | ICA/CCA | PSV | EDV | ICA/CCA | PSV | EDV | ICA/CCA |
| AUC: 0.848 | AUC: 0.806 | AUC: 0.858 | AUC: 0.881 | AUC: 0.861 | AUC: 0.893 | AUC: 0.963 | AUC: 0.941 | AUC: 0.964 |
| CI: 0.824-0.872 | CI: 0.778-0.833 | CI: 0.835-0.882 | CI: 0.855-0.906 | CI: 0.834-0.888 | CI: 0.869-0.917 | CI: 0.946-0.981 | CI: 0.918-0.963 | CI: 0.948-0.981 |
| Sensitivity: 0.726 | Sensitivity: 0.671 | Sensitivity: 0.731 | Sensitivity: 0.796 | Sensitivity: 0.763 | Sensitivity: 0.823 | Sensitivity: 0.923 | Sensitivity: 0.874 | Sensitivity: 0.951 |
| Specificity: 0.860 | Specificity: 0.818 | Specificity: 0.838 | Specificity: 0.822 | Specificity: 0.801 | Specificity: 0.823 | Specificity: 0.916 | Specificity: 0.894 | Specificity: 0. 915 |

**Figure 3**. ROC curves comparing PSV, EDV and carotid index for ≥60%, ≥70% and ≥80% stenosis.

AUC = Area under the curve; CI = Confidence interval; EDV = End-diastolic velocity; PSV = Peak systolic velocity; ROC = Receiver operating characteristic

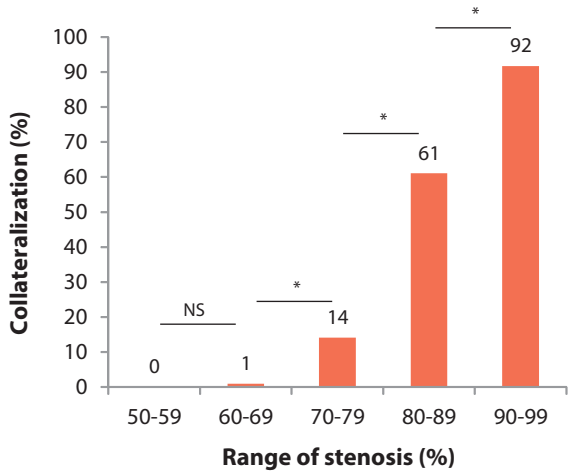


**Figure 4.** Percentage of cases presenting intracranial collateral flow on transcranial Doppler ultrasonography.
*p<0.001; NS = Not significant (p>0.05)

**Table 2.** Presence of collateral flow for predicting stenosis ≥70%.

| | |
|---|---|
| Sensitivity | 39.2% |
| Specificity | 99.5% |
| PPV | 97.4% |
| NPV | 78.0% |
| Accuracy | 80.4% |

PPV = Positive predictive value; NPV = Negative predictive value

as 68% by morphological criteria, but the established velocimetric criteria enabled the diagnosis of stenosis ≥70% (PSV/EDV: 238/102 cm/s and carotid index 2.5). Absence of collateral blood flow was observed in 18% cases (174 vessels) of high-grade (≥70% stenosis) ICA stenosis.

## Discussion

This work aimed to establish the optimal velocimetric criteria for the diagnosis of stenosis grade in our Neurosonology Unit. Our results showed that for diagnosing stenosis ≥70% ECST our criteria were more accurate than the consensus criteria. For stenosis ≥80% ECST, the PSV criterion was superior to the consensus. However, the consensus criteria for EDV and carotid index were superior to our criteria. The presence of collateral blood flow was highly specific for stenosis ≥70% and was helpful in the diagnosis of stenosis is those ranges when velocity criteria pointed to a lower range of stenosis.

Carotid endarterectomy (CEA) guidelines in symptomatic carotid artery stenosis are based on ECST and NASCET (North American Symptomatic Carotid Endarterectomy Trial) criteria of ≥70% carotid stenosis as estimated from angiography [3]. A NASCET 50% to 69% stenosis is equivalent to an ECST ≥70%, while a NASCET 70% to 99% stenosis equates to an ECST ≥80% [33]. Morphologic criteria are prevailing in low-degree disease, but for more severe stenosis velocimetric criteria should be used to define stenosis degree, especially when plaque characteristics impair a correct measurement [9]. These criteria

**Table 3.** Specificity, sensitivity and accuracy of the consensus criteria and our Neurosonology unit criteria for diagnosing stenosis ≥70 and ≥80% (ECST method).

| Range stenosis | Criteria | Duplex variable | Sensitivity | Specificity | Accuracy |
|---|---|---|---|---|---|
| ECST ≥70% (NASCET ≥50%) | Consensus criteria | PSV | 93.3% | 43.1% | 60.8% |
| | | EDV | 92.3% | 50.6% | 65.6% |
| | | Carotid index | 88.6% | 70.0% | 78.9% |
| | Local criteria | PSV | 79.6% | 82.2% | 88.1% |
| | | EDV | 76.3% | 80.1% | 86.1% |
| | | Carotid index | 82.3% | 82.3% | 89.3% |
| ECST ≥80% (NASCET ≥70%) | Consensus criteria | PSV | 94.5% | 87.6% | 88.6% |
| | | EDV | 79.2% | 94.5% | 92.2% |
| | | Carotid index | 92.7% | 93.0% | 93.0% |
| | Local criteria | PSV | 92.4% | 91.8% | 91.9% |
| | | EDV | 93.9% | 84.6% | 85.4% |
| | | Carotid index | 97.6% | 87.4% | 88.3% |

ECST = European Carotid Surgery Trial; EDV = End-diastolic velocity; PSV = Peak systolic velocity; NASCET = North American Symptomatic Carotid Endarterectomy Trial

may, however, lead to underestimation of stenosis owing to reduced maximal flow velocities caused by increased resistance or turbulence, serial stenosis or low flow caused by high distal collateral pressure [34]. Without adequate detection of plaque burden, patients with severe stenosis may be excluded from surgical treatment. Overestimation, on the other hand, may occur in the presence of compensatory increase in volume flow owing to contralateral severe stenosis/occlusion [35]. Also, there is considerable overlap in velocity measurements between moderate and high-degree stenosis [9]. TCD can help determine whether stenosis defined to be high grade with DUS has hemodynamic significance more distally. Conversely, signs of established collateral flow indicate a hemodynamically relevant stenosis that can, therefore, be classified as high grade and can help identify patients with severe plaque burden and no significant increase in ICA blood flow velocities [32, 36]. TCD has been demonstrated to accurately detect stenosis ≥70% [9, 32, 37] and is, hence, an invaluable tool, especially when plaque assessment and velocity criteria combined are inconclusive [32]. Nevertheless, a significant discrepancy between cervical ICA stenosis and signs of intracranial collateral flow might be due to intracranial ICA stenosis prior to the emergence of the ophthalmic artery.

Most DUS velocity thresholds were defined using angiography estimates of stenosis and the reliability of these thresholds has been questioned [3, 36]. A wide variability among laboratories was found with regard to the relationship between carotid angiographic stenosis and Doppler velocity [12, 23, 25, 29, 30, 38-43]. This variability is caused not only by intrinsic factors, such as plaque characteristics, but also by differences in operator technique and experience and device related factors [23]. It has been demonstrated that velocimetric criteria should be validated separately for each piece of equipment [38]. Other groups have analyzed the performance of their standard criteria against the consensus criteria, and found theirs to be more accurate in defining the range of stenosis [10, 44, 45].

There is good correlation of both the NASCET and the ECST methods of calculating percentage stenosis with DUS and both have similar sensitivity and specificity [46]. The NASCET method was used to overcome the lack of direct visualization of the contour of the artery at the stenosis in angiographic measurements, as in the ECST this contour is guessed. With US, the residual lumen and the artery diameter can be directly measured at the point of interest. Therefore, the ECST method is favored in our laboratory, since it can better illustrate plaque burden and is less prone to underestimation when severe stenosis and low post-stenotic flow lead to distal segment involution [9, 47].

In this work, PSV was used as the primary parameter in assessing the percentage of carotid stenosis. It has been shown to be reproducible and to have high sensitivity, specificity, and positive predictive value across most studies [10, 12, 45, 48, 49]. EDV and the carotid index were used as secondary criteria, as proposed by the consensus criteria [12]. These criteria have been shown to be accurate in the diagnosis of ≥70% stenosis, but were less so in detecting 50-69% stenosis [10]. In our study, the parameter with the highest Pearson's correlation was the PSV (0.802) in contrast to both the EDV (0.724) and the carotid index (0.769) ($p<0.001$), which is in agreement with findings from other series [10, 12, 44, 45, 49]. The values defined in our Neurosonology Unit were superior when compared to the consensus criteria of PSV >125 cm/s, EDV >40 cm/s and carotid index >2.0 for detecting ≥70% stenosis (ECST method), with overall accuracy of 88%, 86% and 89% versus 60%, 65%, and 79% for the consensus criteria. Although some sensitivity was lost, the specificity of our criteria was higher than the consensus criteria. For diagnosing stenosis ≥80% ECST, however, although our PSV criterion was superior to the consensus, with overall accuracy of 92% vs 88%, the consensus criteria for EDV and carotid index were superior to ours, with overall accuracy of 92% and 93% against 85%, and 88%, respectively. In order to base the decision of a carotid intervention on DUS, it has been recommended that specificity must be high, avoiding performing an invasive technique without sufficient benefit to the patient [50]. Additionally, TCD was invaluable in identifying hemodinamically significant stenosis, enabling the reappraisal and correct diagnosis of a significant percentage of patients defined as having <70% stenosis by velocimetric and morphologic criteria. Established collateral flow to the middle cerebral artery virtually always indicated pre-cerebral vessel disease with stenosis ≥70%.

Using diameter reduction instead of area reduction, the anatomic parameter for the hemodynamic effect, can be considered a limitation of this work. The relation between the two parameters is not linear, since it depends on the shape of the stenosis (concentric or eccentric). Our decision was based on the fact that, diameter reduction was the method chosen for NASCET and ECST and is widely considered to be the gold standard for decision-making [9].

Over the years, the characteristics of the atherosclerotic plaques, namely the approximated stenosis degree, have also been validated against the plaque observed in surgery by the vascular surgeon of our stroke group. This fact has contributed to the choice of ultrasound as the main diagnostic method in our center.

Another potential limitation is the fact that our criteria are derived from DUS only, as angiography was not available to confirm the US measurements and performing carotid angiography in all of our patients did not seem feasible or justified. However, there is evidence that US imaging can accurately measure ICA diameter reductions independent of velocimetric criteria [16-18, 44, 51, 52]. MacKenzie and co-workers have shown that US imaging correlates closely with angiographic measurements [16] and it has been shown that DUS correlates strictly with histological endarterectomy specimens [22, 51, 52]. Moreover, many studies indicate that DUS is sufficient for safely determining the need for surgery in patients being considered for CEA [53-56].

To our knowledge, this is the first work establishing optimal Doppler velocimetric criteria based only on US imaging. Although this study served as an internal validation of velocimetric criteria in our Neurosonology unit, its results may be extrapolated to other neurovascular laboratories. It enabled the definition of the optimal velocimetric criteria for each stenosis range in our laboratory, allowing a better estimation of the stenosis when plaque characteristics prevent an accurate morphological measurement. As only one device was used and there are only two technicians and three interpreting physicians in our laboratory, there was minimal variability in performing the exams and interpreting the results. DUS is a powerful tool for diagnosing and grading severe stenosis, especially when there are established and validated criteria. Experienced technicians and physicians, as well as continuous internal validation of the accuracy of DUS, are critical in any institution that uses DUS as the sole diagnostic method before surgical intervention.

## Abbreviations

AUC: Area under the ROC curve; CCA: Common carotid artery; CEA: Carotid endarterectomy; CI: Confidence interval; DUS: Doppler ultrasonography; ECST: European Carotid Surgery Trial; EDV: End-diastolic velocity; ICA: Internal carotid artery; NASCET: North American Symptomatic Carotid Endarterectomy Trial; OA: Ophthalmic arteries; PPV: Positive predictive value; PSV: Peak systolic velocity; NPV: Negative predictive value; ROC: Receiver operating characteristic; TCD: Transcranial Doppler; US: Ultrasound imaging

## Acknowledgments

The authors acknowledge Prof. Rita Gaio, from the Faculty of Sciences of University of Porto, for her important contribution to statistical data analysis.

## Competing interests

The authors declare no conflict of interest.

## References

1. Liapis CD, Bell PR, Mikhailidis D, Sivenius J, Nicolaides A, Fernandes e Fernandes J, et al. ESVS guidelines. Invasive treatment for carotid stenosis: indications, techniques. Eur J Vasc Endovasc Surg 2009; 37(4 Suppl):1-19.
2. MRC European Carotid Surgery Trial: interim results for symptomatic patients with severe (70-99%) or with mild (0-29%) carotid stenosis. European Carotid Surgery Trialists' Collaborative Group. Lancet 1991; 337(8752):1235-43.
3. Randomised trial of endarterectomy for recently symptomatic carotid stenosis: final results of the MRC European Carotid Surgery Trial (ECST). Lancet 1998; 351(9113):1379-87.
4. North American Symptomatic Carotid Endarterectomy Trial Collaborators. Beneficial effect of carotid endarterectomy in symptomatic patients with high-grade carotid stenosis. N Engl J Med 1991; 325(7):445-53.
5. Kakisis JD, Avgerinos ED, Antonopoulos CN, Giannakopoulos TG, Moulakakis K, Liapis CD. The European Society for Vasc Surg guidelines for carotid intervention: an updated independent assessment and literature review. Eur J Vasc Endovasc Surg 2012; 44(3):238-43.
6. Blakeley DD, Oddone EZ, Hasselblad V, Simel DL, Matchar DB. Noninvasive carotid artery testing. A meta-analytic review. Ann Intern Med. 1995; 122(5):360-7.
7. Jahromi AS, Cina CS, Liu Y, Clase CM. Sensitivity and specificity of color duplex ultrasound measurement in the estimation of internal carotid artery stenosis: a systematic review and meta-analysis. J Vasc Surg 2005; 41(6):962-72.
8. Jogestrand T, Lindqvist M, Nowak J, Swedish Quality Board for Carotid S. Diagnostic performance of duplex ultrasonography in the detection of high grade internal carotid artery stenosis. Eur J Vasc Endovasc Surg 2002; 23(6):510-8.
9. von Reutern GM, Goertler MW, Bornstein NM, Del Sette M, Evans DH, Hetzel A, et al. Grading carotid stenosis using ultrasonic methods. Stroke. 2012 Mar;43(3):916-21.
10. AbuRahma AF, Srivastava M, Stone PA, Mousa AY, Jain A, Dean LS, et al. Critical appraisal of the Carotid Duplex Consensus criteria in the diagnosis of carotid artery stenosis. J Vasc Surg 2011; 53(1):53-9; discussion 9-60.
11. Bonig L, Weder B, Schott D, Keel A, Nguyen T, Zaunbauer W. Prediction of angiographic carotid artery stenosis indexes by colour Doppler-assisted duplex imaging. A critical appraisal of the parameters used. Eur J Neurol 2000; 7(2):183-90.
12. Grant EG, Benson CB, Moneta GL, Alexandrov AV, Baker JD, Bluth EI, et al. Carotid artery stenosis: grayscale and Doppler ultrasound diagnosis--Society of Radiologists in Ultrasound consensus conference. Ultrasound Q 2003; 19(4):190-8.
13. Goldstein LB, Bushnell CD, Adams RJ, Appel LJ, Braun LT, Chaturvedi S, et al. Guidelines for the primary prevention of stroke: a guideline for healthcare professionals from the American Heart Association/American Stroke Association. Stroke 2011; 42(2):517-84.
14. AbuRahma AF, Robinson PA, Strickler DL, Alberts S, Young L. Proposed New Duplex Classification for Threshold Stenoses Used in Various Symptomatic and Asymptomatic Carotid Endarterectomy Trials. Ann Vasc Surg1998; 12(4):349-58.
15. Sprouse LR, 2nd, Meier GH, Parent FN, Demasi RJ, Lesar CJ, Nelms C, et al. Are we undertreating carotid stenoses diagnosed by ultrasound alone? Vasc Endovascular Surg 2005; 39(2):143-51.
16. MacKenzie KS, French-Sherry E, Burns K, Pooley T, Bassiouny HS. B-mode ultrasound measurement of carotid bifurcation stenoses: is it reliable? Vasc Endovascular Surg 2002; 36(2):123-35.
17. Beebe HG, Salles-Cunha SX, Scissons RP, Dosick SM, Whalen RC, Gale SS, et al. Carotid arterial ultrasound scan imaging: A direct approach to stenosis measurement. J Vasc Surg 1999; 29(5):838-44.
18. Rotstein AH, Gibson RN, King PM. Direct B-mode NASCET-style stenosis measurement and Doppler ultrasound as parameters for assessment of internal carotid artery stenosis. Australas Radiol 2002; 46(1):52-6.
19. Gaitini D, Soudack M. Diagnosing carotid stenosis by Doppler sonography: state of the art. J Ultrasound Med 2005; 24(8):1127-36.
20. de Bray JM, Glatt B. Quantification of atheromatous stenosis in the extracranial internal carotid artery. Cerebrovasc Dis 1995; 5:414–26.
21. Alexandrov AV. The Spencer's Curve: clinical implications of a classic hemodynamic model. J Neuroimaging 2007; 17(1):6-10.
22. Alexandrov AV, Bladin CF, Maggisano R, Norris JW. Measuring carotid stenosis. Time for a reappraisal. Stroke 1993; 24(9):1292-6. 23.Beach KW, Leotta DF, Zierler RE. Carotid Doppler velocity measurements and anatomic stenosis: correlation is futile. Vasc Endovascular Surg 2012; 46(6):466-74.
24. Hadlock J, Beach KW, Sonographers DESVL. Velocity variability in ultrasonic Doppler examinations. Ultrasound Med Biol 2009; 35(6):949-54.
25. Shakhnovich I, Kiser D, Satiani B. Importance of validation of accuracy of duplex ultrasonography in identifying moderate and severe carotid artery stenosis. Vasc Endovascular Surg 2010; 44(6):483-8.

26. Riles TS, Lee V, Cheever D, Stableford J, Rockman CB. Clinical course of asymptomatic patients with carotid duplex scan end diastolic velocities of 100 to 124 centimeters per second. J Vasc Surg 2010; 52(4):914-9, 9 e1.
27. Moneta GL, Edwards JM, Chitwood RW, Taylor LM, Jr., Lee RW, Cummings CA, et al. Correlation of North American Symptomatic Carotid Endarterectomy Trial (NASCET) angiographic definition of 70% to 99% internal carotid artery stenosis with duplex scanning. J Vasc Surg 1993; 17(1):152-7; discussion 7-9.
28. Hansen F, Bergqvist D, Lindblad B, Lindh M, Matzsch T, Lanne T. Accuracy of duplex sonography before carotid endarterectomy--a comparison with angiography. Eur J Vasc Endovasc Surg 1996; 12(3):331-6.
29. Carpenter JP, Lexa FJ, Davis JT. Determination of duplex Doppler ultrasound criteria appropriate to the North American Symptomatic Carotid Endarterectomy Trial. Stroke 1996; 27(4):695-9.
30. Alexandrov AV, Brodie DS, McLean A, Hamilton P, Murphy J, Burns PN. Correlation of peak systolic velocity and angiographic measurement of carotid stenosis revisited. Stroke 1997; 28(2):339-42.
31. Nowak J, Jogestrand T. Duplex ultrasonography is an efficient diag nostic tool for the detection of moderate to severe internal carotid artery stenosis. Clin Physiol Funct Imaging 2007; 27(3):144-7.
32. Zachrisson H, Fouladiun M, Blomstrand C, Holm J, Volkmann R. Functional assessment of high-grade ICA stenosis with duplex ultrasound and transcranial Doppler. Clin Physiol Funct Imaging 2012; 32(3):241-6.
33. Rothwell PM, Gibson RJ, Slattery J, Sellar RJ, Warlow CP. Equivalence of measurements of carotid stenosis. A comparison of three methods on 1001 angiograms. European Carotid Surgery Trialists' Collaborative Group. Stroke 1994; 25(12):2435-9.
34. Zachrisson H, Berthelsen B, Blomstrand C, Holm J, Volkmann R. Influence of poststenotic collateral pressure on blood flow velocities within high-grade carotid artery stenosis: differences between morphologic and functional measurements. J Vasc Surg 2001; 34(2):263-8.
35. van Everdingen KJ, van der Grond J, Kappelle LJ. Overestimation of a stenosis in the internal carotid artery by duplex sonography caused by an increase in volume flow. J Vasc Surg 1998; 27(3):479-85.
36. de Bray JW, Glatt B. Quantification of atheromatous stenosis in the extracranial internal carotid artery. Cerebrovasc Dis 1995; (5):414–26.
37. Byrd S, Wolfe J, Nicolaides A, Stansby G, Cheshire N, Thomas D, et al. Vascular surgical society of great britain and ireland: transcranial doppler ultrasonography as a predictor of haemodynamically significant carotid stenosis. Br J Surg 1999; 86(5):692-3.
38. Fillinger MF, Baker RJ, Jr., Zwolak RM, Musson A, Lenz JE, Mott J, et al. Carotid duplex criteria for a 60% or greater angiographic stenosis: variation according to equipment. J Vasc Surg 1996; 24(5):856-64.
39. Eliasziw M, Rankin RN, Fox AJ, Haynes RB, Barnett HJ. Accuracy and prognostic consequences of ultrasonography in identifying severe carotid artery stenosis. North American Symptomatic Carotid Endarterectomy Trial (NASCET) Group. Stroke 1995; 26(10):1747-52.
40. Heijenbrok-Kal MH, Nederkoorn PJ, Buskens E, van der Graaf Y, Hunink MG. Diagnostic performance of duplex ultrasound in patients suspected of carotid artery disease: the ipsilateral versus contralateral artery. Stroke 2005; 36(10):2105-9.
41. Moneta GL, Taylor DC, Zierler RE, Kazmers A, Beach K, Strandness DE, Jr. Asymptomatic high-grade internal carotid artery stenosis: is stratification according to risk factors or duplex spectral analysis possible? J Vasc Surg 1989; 10(5):475-82; discussion 82-3.
42. Neschis DG, Lexa FJ, Davis JT, Carpenter JP. Duplex criteria for determination of 50% or greater carotid stenosis. J Ultrasound Med 2001; 20(3):207-15.
43. Schwartz SW, Chambless LE, Baker WH, Broderick JP, Howard G. Consistency of Doppler parameters in predicting arteriographically confirmed carotid stenosis. Asymptomatic Carotid Atherosclerosis Study Investigators. Stroke 1997; 28(2):343-7.
44. Shaalan WE, Wahlgren CM, Desai T, Piano G, Skelly C, Bassiouny HS. Reappraisal of velocity criteria for carotid bulb/internal carotid artery stenosis utilizing high-resolution B-mode ultrasound validated with computed tomography angiography. J Vasc Surg 2008; 48(1):104-12; discussion 12-3.
45. Braun RM, Bertino RE, Milbrandt J, Bray M, Society of Radiologists in Ultrasound Consensus Criteria to a Single Institution Clinical P. Ultrasound imaging of carotid artery stenosis: application of the Society of Radiologists in Ultrasound Consensus Criteria to a Single Institution Clinical Practice. Ultrasound Q 2008; 24(3):161-6.
46. Hwang C-S, Liao K-M, Lee J-H, Tegeler CH. Measurement of Carotid Stenosis: Comparisons Between Duplex and Different Angiographic Grading Methods. J Neuroimaging 2003; 13(2):133-9.
47. Rothwell PM, Warlow CP. Low risk of ischemic stroke in patients with reduced internal carotid artery lumen diameter distal to severe symptomatic carotid stenosis: cerebral protection due to low poststenotic flow? On behalf of the European Carotid Surgery Trialists' Collaborative Group. Stroke 2000; 31(3):622-30.
48. Fell G, Phillips DJ, Chikos PM, Harley JD, Thiele BL, Strandness DE, Jr. Ultrasonic duplex scanning for disease of the carotid artery. Circulation 1981; 64(6):1191-5.
49. Sabeti S, Schillinger M, Mlekusch W, Willfort A, Haumer M, Nachtmann T, et al. Quantification of internal carotid artery stenosis with duplex US: comparative analysis of different flow velocity criteria. Radiology 2004; 232(2):431-9.
50. Moneta GL, Edwards JM, Papanicolaou G, Hatsukami T, Taylor LM, Jr., Strandness DE, Jr., et al. Screening for asymptomatic internal carotid artery stenosis: duplex criteria for discriminating 60% to 99% stenosis. J Vasc Surg 1995; 21(6):989-94.
51. Schulte-Altedorneburg G, Droste DW, Felszeghy S, Csiba L, Popa V, Hegedus K, et al. Detection of carotid artery stenosis by in vivo duplex ultrasound: correlation with planimetric measurements of the corresponding postmortem specimens. Stroke 2002; 33(10):2402-7.
52. Jmor S, El-Atrozy T, Griffin M, Tegos T, Dhanjil S, Nicolaides A. Grading internal carotid artery stenosis using B-mode ultrasound (in vivo study). Eur J Vasc Endovasc Surg 1999; 18(4):315-22.
53. Melissano G, Castellano R, Mazzitelli S, Zoppei G, Chiesa R. Safe and cost-effective approach to carotid surgery. Eur J Vasc Endovasc Surg 1997; 14(3):164-9.
54. Ranaboldo C, Davies J, Chant A. Duplex scanning alone before carotid endarterectomy: a 5-year experience. European J Vasc Surg 1991; 5(4):415-9.
55. Melissano G, Castellano R, Zucca R, Chiesa R. Results of carotid endarterectomy performed with preoperative duplex ultrasound assessment alone. Vasc Surg 2001; 35(2):95-101.
56. Mattos MA, Hodgson KJ, Faught WE, Mansour A, Barkmeier LD, Ramsey DE, et al. Carotid endarterectomy without angiography: is color-flow duplex scanning sufficient? Surgery 1994; 116(4):776-82; discussion 82-3.

INTERNATIONAL JOURNAL OF
CLINICAL NEUROSCIENCES
AND MENTAL HEALTH

ORIGINAL RESEARCH

# Reversal of ophthalmic artery blood flow direction and severe ipsilateral carotid stenosis

Miguel Grilo[1], Ana Monteiro[1], Rosa Santos[1], Carmen Ferreira[1], Andreia Costa[1], and Elsa Azevedo[1]

Special Issue on Neurosonology and Cerebral Hemodynamics

## Abstract

**Background:** The assessment of ophthalmic artery flow direction by transcranial Doppler sonography has become part of the cerebrovascular routine examination in stroke patients. It provides helpful information for the investigation of collateral circulation and can evaluate the hemodynamic significance of high-grade internal carotid artery (ICA) stenosis. Our aim was to determine the value of assessing the direction of ophthalmic artery blood flow in the setting of routine color flow duplex ultrasonography examination of patients with ipsilateral carotid disease.

**Methods:** We reviewed 967 ultrasound carotid scans performed in our Neurosonology Unit from January 2003 to December 2011 with ICA stenosis ≥50%, and assessed ophthalmic artery flow direction.

**Results:** Ophthalmic artery flow reversal was seen in 73 cases, 62 (85%) of which were in cases of ICA stenosis ≥80%. Flow reversal in ophthalmic artery had a sensitivity of 43%, specificity of 99%, negative predictive value of 91% and positive predictive value of 85% for ICA stenosis ≥80%.

**Conclusion:** We found a significant association between reversal of ophthalmic artery flow and carotid stenosis ≥ 80% with an excellent specificity and negative predictive value. Assessing ophthalmic artery can be especially important in patients with difficult duplex scans or with stenosis in the pre-ophthalmic artery intracranial segment of internal carotid artery, where duplex scan may fail to detect the lesion. Evaluation of ophthalmic artery blood flow direction is therefore feasible and accurate with Doppler ultrasound, and it brings very useful information to better assess intracranial hemodynamic status that can influence treatment decisions.

**Keywords:** Carotid stenosis, Ophthalmic artery, Reversed ophthalmic artery flow, Cerebral collateral flow pathways, Transcranial Doppler, Carotid duplex ultrasonography.

[1]Department of Neurology, São João Hospital Centre and Faculty of Medicine of University of Porto, Portugal

Correspondence: Miguel Grilo
Department of Neurology, Faculty of Medicine of University of Porto
Alameda Prof. Hernâni Monteiro, 4200-319 Porto, Portugal
Email adress: miguel.rgrilo@gmail.com

Citation: Grilo et al. Reversal of ophthalmic artery blood flow direction and severe ipsilateral carotid stenosis. IJCNMH 2014; 1(Suppl. 1):S14

Received: 07 Nov 2013; Accepted: 20 Dec 2013; Published: 09 May 2014

## Introduction

Doppler ultrasonography is now widely used for the diagnosis of internal carotid artery (ICA) stenosis. Its diagnostic accuracy, if performed by experienced sonographers, has shown to be >90% when compared with angiography [1, 2].

A significant number of previous studies have shown that transcranial Doppler examination can add important information to carotid duplex scanning [3-7]. Some have used a transcranial Doppler battery to assess the hemodynamic significance of ICA stenosis and reported that reversed ophthalmic artery flow (ROAF) has low sensitivity but a specificity of 100% in ≥70% carotid stenosis on cerebral angiography or in lesions with a residual lumen diameter of less than 1.5 mm from "en bloc" endarterectomy [3, 4]. A more recent study specifically focused on the ophthalmic collateral pathway in patients with internal carotid artery disease has also established that the frequency of ROAF increases with worsening severity of stenosis. Moreover, the authors found that ROAF was strictly associated with high-grade (≥80%) ICA stenosis or occlusion, with excellent positive predictive value and decent negative predictive value [7].

The ROAF in the setting of significant ICA (≥70%) is not infrequent, with some reports estimating an incidence of approximately 25% [8, 9]. However, its role in cerebral collateralization is somewhat controversial [9-18]. The ophthalmic artery (OA) is traditionally regarded as an important source of cerebral blood supply in patients with ICA occlusion [10, 11]. Some authors have demonstrated that intracranial hemodynamic status is associated with overall collateral blood supply available to the brain not depending on specific patterns of collateralization, namely via anterior and posterior communicating arteries, or OA [12, 13]. Moreover, Vernieri and co-workers suggested that the prognosis of patients with carotid artery occlusion was significantly influenced by the number of collateral pathways and by vasomotor reactivity. Notably, in patients with only one or two intracranial collateral pathways, the functional aspect of cerebral hemodynamics appeared to overhang individual anatomic characteristics in influencing their outcome [13]. Conversely, other studies show conflicting results and are not clear about the specific role of OA as an important source of blood to the brain. Anzola and colleagues suggested that this pathway, although important for the intraorbital structures, was probably of limited functional significance to the hemispheric blood supply [14]. Accordingly, others proposed an hierarchy in cerebral collateralization, relegating the OA as a collateral of last resort [15, 16]. Hu and co-workers reported in a prospective 4-year follow-up study that asymptomatic patients with ≥75% carotid artery stenosis or occlusion and ROAF had an elevated risk of occurrence of ischemic event, in contrast to patients with forward OA flow [17]. Furthermore, Reinhard and colleagues found that dynamic cerebral autoregulation is substantially impaired when secondary collateral pathways (ophthalmic or leptomeningeal arteries) are activated [18]. In line with these findings, Tsai and co-workers observed that the presence of ROAF was associated with a shunt to an area of low-resistance intracranial circulation due to impaired intracranial hemodynamic status or insufficient collateral blood flow via the circle of Willis. Moreover, it was demonstrated that ROAF was highly associated to the combination of stenosis of the cervical and intracranial segments and less well correlated to high-grade cervical carotid stenosis/occlusion alone. Additionally, similarly to the presence of intracranial stenosis and previous stroke, ROAF was shown to be associated with a poorer functional outcome [9].

The objective of our study was to determine the value of assessing the direction of ophthalmic artery blood flow in the setting of color flow duplex ultrasonography examination of symptomatic or asymptomatic patients, in order to better characterize the hemodynamics related to ipsilateral carotid stenosis.

## Methods

All records from patients referred to the Neurosonology Unit at São João Hospital Centre between January 2003 and December 2011 were reviewed. Duplex scanning was performed using Philips HDI 5000 ultrasound device, with a 4-7 MHz linear array transducer for cervical carotid evaluation and a pulsed 2-4 MHz transducer via transorbital approach for OA exam, with adapted power. The grade of ICA stenosis was assessed using the European Carotid Surgery Trial (ECST) method and combined with velocimetric criteria [19, 20]. We selected duplex scans with ≥50% ICA stenosis in which orbital color flow duplex ultrasonography examination was available. Cases with carotid occlusions, previous endarterectomy or stenting, isolated parietal carotid thrombus, arterial dissection or incomplete data were excluded. The range of carotid stenosis was correlated with OA flow direction using the one-way analysis of variance (ANOVA) followed by Bonferroni's post-hoc comparisons tests. Sensitivity, specificity, positive predictive value, negative predictive value and accuracy were then calculated. Microsoft Excel (MS Office 2010) was used to collect all data and perform descriptive statistics. SPSS Statistics version 20 (IBM, Armonk, NY, USA) was used to perform the remaining analysis.

## Results

We have selected duplex scans of 967 ICA stenosis: 346 with 50-59%, 316 with 60-69%, 162 with 70-79%, 119 with 80-89%, and 24 with 90-99% stenosis (**Figure 1**). Seventy-three of these stenotic cases had ipsilateral ROAF. We did not find collateralization from this artery in any of the cases with 50-59% stenosis. However, with worsening severity of stenosis, the frequency of ROAF increased, as can

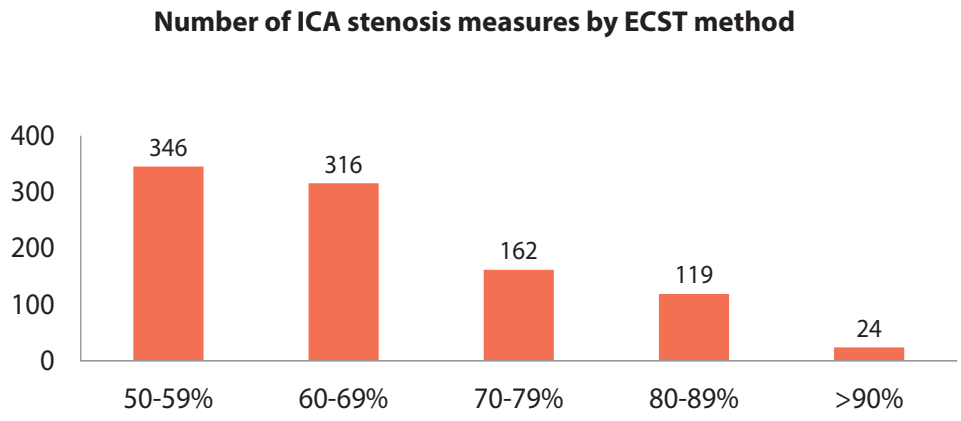


**Figure 1.** Number of ICA stenosis measured by the ECST method.
ICA = Internal carotid artery; ECST = European Carotid Surgery Trial

be seen in **Figure 2**, being 43% (62 cases) when carotid stenosis was ≥80%. There was a significant increase in collateralization from this artery for stenosis 80-89% comparing to 70-79% and in the 90-99% group comparing to 80-89%. Overall, when ROAF was detected, there was a sensitivity of 43%, a specificity of 99%, a negative predictive value of 91%, a positive predictive value of 85%, and an accuracy of 91% for a high-grade stenosis of ≥80% (**Table 1**).

## Discussion

Our study has shown an increase of the frequency of ROAF with the worsening severity of cervical ICA stenosis. Detection of ROAF had a sensitivity of 43%, a specificity of 99%, a negative predictive value of 91%, a positive predictive value of 85%, and an accuracy of 91% for a high-grade stenosis of ≥80% (**Table 1**).

To our knowledge, this study is one of the largest series correlating the flow direction of the OA and ipsilateral ICA stenosis, and according to the data previously reported by Reynolds and colleagues [7], we confirm that ROAF has a high specificity for severe ipsilateral ICA stenosis.

One possible limitation of the study is the lack of comparison with digital angiography. Despite duplex scan acknowledged as having a high diagnostic accuracy, we accept that the presence of ROAF associated with <80% stenosis could be related to distal ICA stenosis/occlusions not detected by this technique. Another issue that should be referred is that in this study the presence of other intracranial collateralization systems was not analyzed, which could interfere with the existence of ROAF in each patient.

The present study shows that the analysis of the OA flow as common practice in any Neurosonology laboratory constitutes a powerful tool. It can be especially im-

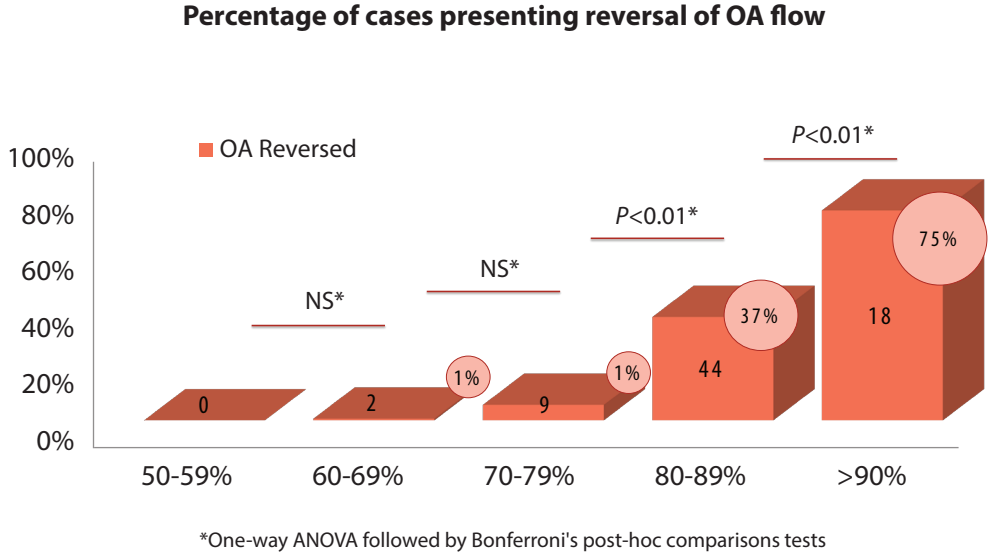


*One-way ANOVA followed by Bonferroni's post-hoc comparisons tests

**Figure 2.** Percentage of cases presenting ROAF according to the grade of ipsilateral ICA stenosis.
OA = ophthalmic artery ICA = Internal carotid artery; ECST = European Carotid Surgery Trial; ROAF = Reversed ophthalmic artery flow

**Table 1.** Statistical measures for the presence of ROAF.

| **High-grade stenosis (≥80)** | |
|---|---|
| Sensitivity | 43% |
| Specificity | 99% |
| Negative predictive value | 91% |
| Positive predictive value | 85% |
| Accuracy | 91% |

ROAF = Reversed ophthalmic artery flow

portant in patients with difficult duplex scans that may limit the effectiveness of the exam, bringing advantage in better characterizing the hemodynamic significance of ipsilateral ICA stenosis. Additionally, ROAF might be the only ultrasound exam clue in the case of a severe stenosis in the pre-ophthalmic artery intracranial segment of internal carotid artery, where duplex scan may miss the lesion. More importantly, ROAF may indicate inadequate collaterals through the circle of Willis and poor cerebral hemodynamic status [9].

In conclusion, evaluation of ophthalmic artery blood flow direction is feasible and accurate with Doppler ultrasound, and it brings very useful information to better assess intracranial hemodynamic status that can influence treatment decisions.

## Abbreviations

ANOVA: Analysis of variance; ECST: European Carotid Surgery Trial; ICA: Internal carotid artery; OA: Ophthalmic artery; ROAF: Reversed ophthalmic artery flow

## Competing interests

The authors declare no conflict of interest.

## References


1. Jogestrand T, Lindqvist M, Nowak J. Diagnostic Performance of Duplex Ultrasonography in the Detection of High Grade Internal Carotid Artery Stenosis. European Journal of Vascular & Endovascular Surgery 2002; (6):510–8.
2. AbuRahma AF, Srivastava M, Stone PA, Mousa AY, Jain A, Dean LS, et al. Critical appraisal of the Carotid Duplex Consensus criteria in the diagnosis of carotid artery stenosis. J Vasc Surg. 2011; 53(1):53–60.
3. Wilterdink JL, Feldmann E, Furie KL, Bragoni M, Benavides JG. Transcranial Doppler ultrasound battery reliably identifies severe internal carotid artery stenosis. Stroke 1997; (1):133–6.
4. Can U, Furie KL, Suwanwela N, Southern JF, Macdonald NR, Ogilvy CS, et al. Transcranial Doppler Ultrasound Criteria for Hemodynamically Significant Internal Carotid Artery Stenosis Based on Residual Lumen Diameter Calculated From En Bloc Endarterectomy Specimens. Stroke 1997; 28(10):1966–71.
5. Nuzzaci G, Righi D, Borgioli F, Nuzzaci I, Giannico G, Pratesi C, et al. Duplex Scanning Exploration of the Ophthalmic Artery for the Detection of the Hemodynamically Significant ICA Stenosis. Stroke 1999; 30(4):821–6.
6. Christou I, Felberg RA, Demchuk AM, Grotta JC, Burgin WS, Malkoff M, et al. A broad diagnostic battery for bedside transcranial Doppler to detect flow changes with internal carotid artery stenosis or occlusion. J Neuroimaging 2001; 11(3):236–42.
7. Reynolds PS, Greenberg JP, Lien L-M, Meads DC, Myers LG, Tegeler CH. Ophthalmic artery flow direction on color flow duplex imaging is highly specific for severe carotid stenosis. J Neuroimaging 2002; 12(1):5–8.
8. Costa VP, Kuzniec S, Molnar LJ, Cerri GG, Puech-Leão P, Carvalho CA. Collateral blood supply through the ophthalmic artery: a steal phenomenon analyzed by color Doppler imaging. Ophthalmology 1998; 105(4):689–93.
9. Tsai CL, Lee JT, Cheng CA, Liu MT, Chen CY, Hu HH, et al. Reversal of ophthalmic artery flow as a predictor of intracranial hemodynamic compromise: implication for prognosis of severe carotid stenosis. European Journal of Neurology 2012; 20(3):564–70.
10. Countee RW, Vijayanathan T. External carotid artery in internal carotid artery occlusion. Angiographic, therapeutic, and prognostic considerations. Stroke 1979; 10(4):450–60.
11. Schneider PA, Rossman ME, Bernstein EF, Ringelstein EB, Otis SM. Noninvasive assessment of cerebral collateral blood supply through the ophthalmic artery. Stroke 1991; 22(1):31–6.
12. van Everdinge KJ, Visser GH, Klijn C, Kappelle LJ, Van der Grond J. Role of collateral flow on cerebral hemodynamics in patients with unilateral internal carotid artery occlusion. Ann Neurol. Wiley Online Library; 1998;44(2):167–76.
13. Vernieri F, Pasqualetti P, Matteis M, Passarelli F, Troisi E, Rossini PM, et al. Effect of Collateral Blood Flow and Cerebral Vasomotor Reactivity on the Outcome of Carotid Artery Occlusion. Stroke 2001; 32(7):1552–8.
14. Anzola GP, Gasparotti R, Magoni M, Prandini F. Transcranial Doppler Sonography and Magnetic Resonance Angiography in the Assessment of Collateral Hemispheric Flow in Patients With Carotid Artery Disease. Stroke 1995; 26(2):214–7.
15. Müller M, Schimrigk K. Vasomotor reactivity and pattern of collateral blood flow in severe occlusive carotid artery disease. Stroke 1996; 27(2):296–9.
16. Ringelstein EB, Weiller C, Weckesser M, Weckesser S. Cerebral vasomotor reactivity is significantly reduced in low-flow as compared to thromboembolic infarctions: the key role of the circle of Willis. J Neurol Sci. 1994; 121(1):103–9.
17. Hu HH, Wang S, Chern CM, Yeh HH, Sheng WY, Lo YK. Clinical significance of the ophthalmic artery in carotid artery disease. Acta Neurol Scand 1995; 92(3):242–6.
18. Reinhard M, Müller T, Guschlbauer B, Timmer J, Hetzel A. Dynamic cerebral autoregulation and collateral flow patterns in patients with severe carotid stenosis or occlusion. Ultrasound in Medicine & Biology 2003; 29(8):1105–13.
19. Farrell B, Fraser A, Sandercock P, Slattery J, Warlow CP. Randomised trial of endarterectomy for recently symptomatic carotid stenosis: final results of the MRC European Carotid Surgery Trial (ECST). Lancet 1998; 351(9113):1379–87.
20. Grant EG, Benson CB, Moneta GL, Alexandrov AV, Baker JD, Bluth EI, et al. Carotid artery stenosis: gray-scale and Doppler US diagnosis--Society of Radiologists in Ultrasound Consensus Conference. Radiology 2003; 340–6.

INTERNATIONAL JOURNAL OF
CLINICAL NEUROSCIENCES
AND MENTAL HEALTH

ORIGINAL RESEARCH

# Simulated hemodynamics in human carotid bifurcation based on Doppler ultrasound data

Luísa C. Sousa[1], Catarina F. Castro[1], Carlos C. António[1], João M.R.S. Tavares[2], André M.F. Santos[2], Rosa M. Santos[3], Pedro Castro[3], and Elsa Azevedo[3]

Special Issue on Neurosonology and Cerebral Hemodynamics

## Abstract

**Background:** Atherosclerotic lesions commonly develop at arterial branch sites. Non-invasive carotid artery ultrasound is a well-established and effective method that allows real-time imaging and measurement of flow velocities. We aimed to develop a methodology for patient-specific computational 3D reconstruction and blood flow simulation based on ultrasound image data.

**Methods:** Subject-specific studies based on the acquisition of a set of longitudinal and sequential cross-sectional ultrasound images and Doppler velocity measurements at common carotid artery (CCA) bifurcation were performed at a university hospital. A developed simulation code of blood flow by the finite element method (FEM) that includes an adequate structured meshing of the common carotid artery bifurcation was used to investigate local flow biomechanics.

**Results:** Hemodynamic simulations of CCA bifurcations for six individuals were analyzed. Comparing pairs (Doppler, FEM) of velocity values, Lin's concordance correlation coefficient analysis demonstrated an almost perfect strength of agreement ($\rho_c = 0.9911$), in patients with different degrees of internal carotid artery (ICA) stenosis. Numerical simulations were able to capture areas of low wall shear stress correlated with stagnation zones.

**Conclusion:** Simulated hemodynamic parameters can reproduce the disturbed flow conditions at the bifurcation of CCA and proximal ICA, which play an important role in the development of local atherosclerotic plaques. This novel technology might help to understand the relationship between hemodynamic environment and carotid wall lesions, and have a future impact in carotid stenosis diagnosis and management.

**Keywords:** Doppler image-based analysis, Carotid bifurcation, Computational fluid dynamics, Wall shear stress.

[1]Institute of Mechanical Engineering (IDMEC-FEUP), Faculty of Engineering, University of Porto, Porto, Portugal

[2]Institute of Mechanical Engineering and Industrial Management, Faculty of Engineering, University of Porto, Porto, Portugal

[3]Department of Neurology, Hospital São João, Faculty of Medicine, University of Porto, Porto, Portugal

Correspondence: Luisa Costa Sousa

Institute of Mechanical Engineering (IDMEC-FEUP), Faculty of Engineering, University of Porto

Rua Dr. Roberto Frias, s/n, 4200 - 465 Porto, Portugal

Email adress: lcsousa@fe.up.pt

Citation: Sousa et al. Simulated hemodynamics in human carotid bifurcation based on Doppler ultrasound data. IJCNMH 2014; 1(Suppl. 1):S15

Received: 13 Sep 2013; Accepted: 20 Nov 2013; Published: 09 May 2014

Open Access Publication Available at http://ijcnmh.arc-publishing.org



ARC Publishing

## Introduction

It is widely accepted that, in large arteries, regions of disturbed flow like arterial bifurcations or curvatures correspond closely those locations where atherosclerosis develops. Atherosclerosis results from an accumulation of lipids and other materials in arterial walls, and can cause a focal luminal narrowing as well as loss of elasticity in the arteries. This disease often leads to heart attack and brain stroke, leading causes of death in the industrial world. Although the precise hemodynamic determinants of atherosclerotic disease are not yet completely understood, different studies have shown that atherosclerotic sites correlate strongly with regions of disturbed flow [1-3].

Doppler ultrasound imaging has been widely used in clinical practice to image blood vessels and to quantify arterial blood flow. B-mode ultrasound allows direct visualization of both vessel wall and lumen and, subsequently, detection of early atherosclerosis, beginning with intima-media thickening [4-6]. Such information is a prerequisite for accurate diagnosis and assessment of the severity of arterial disease, with all that this implies in terms of the treatment that individual patients receive.

Computational fluid dynamics (CFD) models have become very effective tools for predicting the flow field within the carotid bifurcation, and for understanding the relationship between local hemodynamics, and the initiation and progression of vascular wall pathologies. CFD, applied to realistic, three-dimensional arterial geometries derived from clinical imaging, provides an accurate assessment of flow patterns and shear stress in complex geometries [7, 8].

Recent work has demonstrated differences in carotid artery blood flow dynamics between individuals [9, 10] and the use of a suitable-scaled characteristic waveform is reasonable when subject-specific flow conditions are unavailable. Although for large-scale studies of common carotid artery (CCA) bifurcation hemodynamics the use of a typical flow waveform shape is likely sufficient, for a detailed patient study a subject-specific waveform collected in clinical practice, as in our study, yields a more accurate assessment of flow characteristics [9, 11, 12].

The aim of the present investigation was to study of the image-based CFD of stenozed carotid bifurcations. Selecting patient specific stenozed carotid artery as diagnosed by ultrasound imaging, the complexity of the hemodynamic environment of five diseased CCA bifurcations is addressed and compared with a stenosis-free case.

## Methods

Modeling a carotid bifurcation starting from medical images requires four serial steps: image acquisition, image-based definition of the carotid bifurcation model, computational simulation, and post-processing as described below.

In this study ultrasound data from six CCA bifurcations, referred in this study as P1 to P6, were analyzed. Patient ages ranged from 50 to 84 years. The present research received favorable opinion by the institutional Ethics Committee, and all subjects gave written informed consent.

### Acquisition of anatomical in vivo data

The ultrasound imaging examinations were performed by an experienced certified sonographer, dedicated to neurovascular ultrasound at the Neurosonology Unit of the Department of Neurology of São João Hospital Centre, Oporto, Portugal. For each volunteer, a set of B-mode and pulsed-wave Doppler images of the CCA, its bifurcation, and proximal segments of the internal carotid artery (ICA) and the external carotid artery (ECA) was obtained. High-Resolution B-Mode Ultrasound scanner (Vivid e; GE, Milwaukee, WI, USA) was used to examine the extracranial carotid arteries. This system, equipped with a linear array transducer probe (GE 8L-RS) with pulsed-wave Doppler and spectrum analysis capabilities, provides high-resolution ultrasonic images with a resolution of 614×820 pixels and 256 degrees of gray scale. Three-dimensional (3D) models of the lumen and wall boundaries were reconstructed from B-mode longitudinal images completed by B-mode cross-sectional images registered at the end of diastolic phase to control physiologic variations of vessel diameter along cardiac cycle. Carotid stenosis was measured according to the percentage of luminal diameter narrowing at the most stenotic point, according to ECST grading method [13]. An example of longitudinal and cross-sectional B-mode images for volunteer (P1) are presented in **Figure 1**.

Using pulsed wave mode, blood flow velocity spectral waveforms were obtained at several specific locations identified on B-mode imaging, from approximately 2 cm before CCA bifurcation, until post-bulbar ICA and ECA, including the bifurcation entrance (APEX). Angle correction was activated as appropriated, with angle of insonation ≤60° [14]. Ultrasound images were stored to hard disc for later offline analysis.

### Geometrical 3D surface reconstruction

We developed a semi-automatic methodology for reconstruction and structured meshing based on the images obtained with ultrasound. DICOM files were imported into a specific program developed in MATLAB (The Mathworks Inc. Natick, MA, USA). Then B-mode images were segmented to produce smooth lumen and plaque contours by using purpose-developed software [15-17], which automatically segments the lumen and bifurcation boundaries of the carotid artery based on the hypoechogenic characteristics of the lumen. Using this software each input image was initially processed with the application of an anisotropic diffusion filter for speckle noise removal, and morphologic operators were employed in the detection of the relevant ultrasound data regarding the artery. The information obtained was then used to define initial contours, corresponding to the lumen and to the bifurcation

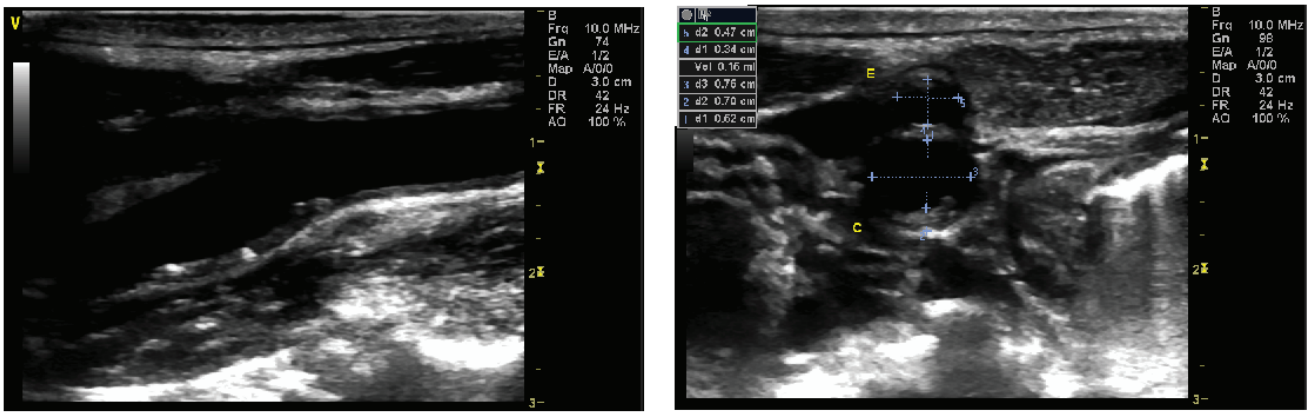

**Figure 1.** Ultrasound images of the volunteer P1 common carotid artery bifurcation region: longitudinal (left) and cross-sectional (right) images.

boundaries, for the application of the Chan-Vese level set segmentation model [18, 19].

Geometric lumen boundaries for CCA, ICA, and ECA were obtained importing the segmented 2D images into the modeling software FEMAP (FEMAP, Siemens PLM, USA & Canada). Specific points of the lumen-intima and media-adventitia boundaries were identified in order to construct splines A, B, C and D for ICA, ECA and CCA boundary definition, as shown is **Figure 2(a)**.

The centerlines of CCA, ECA and ICA were defined by creating a curve associated to equidistant points from splines A to B, A to C and D to B. Segmented transverse contours were then positioned and oriented in 3D space; each contour was then realigned so that its centroid coincided with the defined arteries centerlines. **Figure 2(b)** and **Figure 2(c)** show the specific 3D surface reconstruction for patient P1 defining the reconstructed bifurcation shape.

## Blood flow model

Subject-specific 3D hemodynamics were determined using an in-house CFD code, which has been extensively validated [20, 21]. Eight-node hexahedral isoparametric element meshes constructed with software FEMAP were employed to discretize each bifurcation volume. Cylindrical flow extensions were extruded from the lower boundary in CCA (inlet) and the upper boundary in ICA and ECA (outlet) to facilitate the imposition of velocity boundary conditions as described below. Vessel walls were assumed to be rigid and blood was approximated by an isotropic, incompressible, homogeneous and Newtonian viscous fluid with a density of 1060 kg/m$^3$. The rheological behavior of blood was simulated considering a constant dynamic viscosity value of 0.0035 kg/(m.s), a reasonable assumption for bulk flow metrics [22, 23]. Newtonian rheology is reasonable in the context of fluid precision and uncertainties related to boundary conditions [11, 23-25].

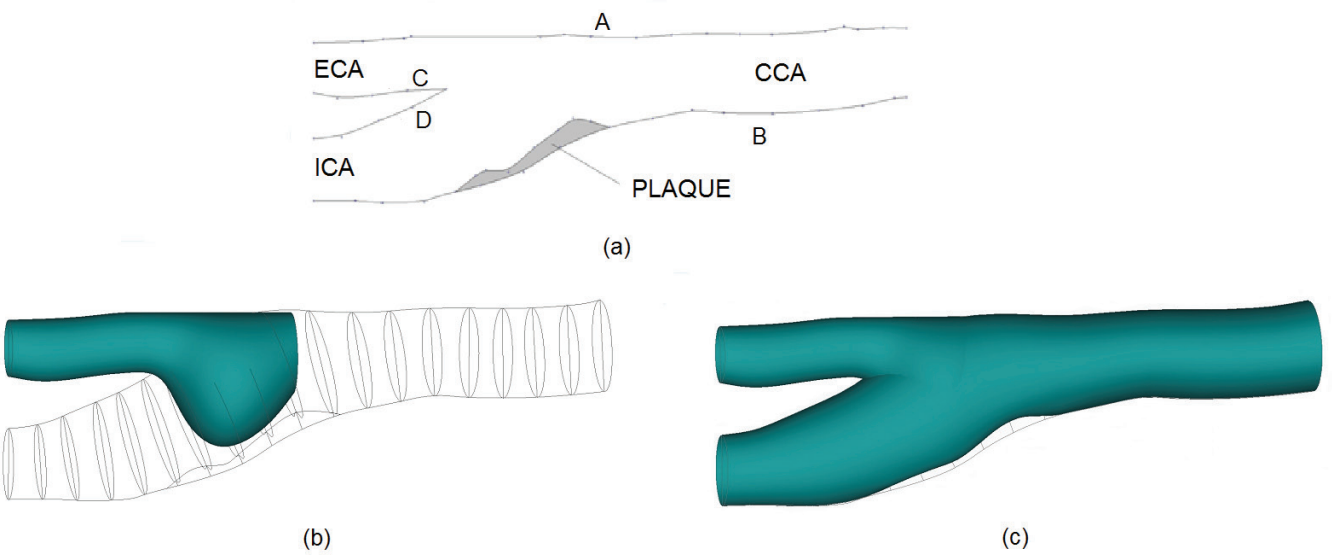


**Figure 2.** 3D model reconstruction: **(a)** definition of CCA, ICA and ECA lumen boundaries; **(b)** definition of cross-sections; **(c)** reconstructed surface of bifurcation P1.

The volume-filling finite element meshes consisted of nearly 60000 quadratic hexahedral finite elements. The nonlinear system of equations derived from the discretization of the flow equations was solved using the upwinding method. The backward Euler implicit time integration scheme was implemented to obtain the solution at each time step of the time-dependent problem. Based upon mesh and time-step refinement studies [21], this mesh density and constant time-step equal to $2.5\times10^{-3}$s were deemed sufficient for the purposes of characterizing velocities and wall shear stress (WSS) patterns.

For each bifurcation analysis, subject-specific velocity boundary conditions were prescribed at CCA inlet and ICA outlet using Womersley velocity profiles derived from pulsatile spectral waveforms obtained by pulsed Doppler and traction-free boundary condition was defined at ECA outlet [9, 26-28]. **Figure 3** presents the volume hexahedral mesh (left) and the distal CCA velocity waveform (right) used for solving the hemodynamics of subject P1.

## Results

Pulsatile hemodynamics were computed for six patients (ages 50 to 84 years; 4 males and 2 females) identified in **Figure 4.** The local degree of stenosis (ECST) was registered. For patient P3 no ICA plaque was observed and for the others, an ICA stenosis from 30 to 70% was registered. Peak systole velocities at ICA are presented in **Figure 4.** Comparing pairs (Doppler, FEM) of velocity values, Lin's concordance correlation coefficient analysis demonstrated an almost perfect strength of agreement ($\rho_c$ = 0.9911) between ultrasound data and simulated FEM values.

Velocity field at peak systolic phase is shown in **Figure 5** for patients P1 to P6. Bifurcation P3 is the non-stenotic carotid of the analyzed set and P4 to P6 present a higher degree of stenosis. For most patients a strongly skewed axial velocity in the proximal internal carotid artery due to enlarged bulb region was observed. For all patients a stagnation zone was detected near the outer bulb wall (opposite to the divider wall), as expected. At systole, patients P2 to P4 exhibit higher velocities at ECA as compared to the other patients, which present higher velocities at ICA.

At ECA, during systolic peak, high velocity gradients were detected for patients P3 and P4, due to the sharp unevenness of the vessel wall. At ICA, the highest velocity gradients were detected during peak systole for patients P1 and P4 to P6.

WSS contours near peak systole for all the volunteers (P1 to P6) are shown in **Figure 6**, exhibiting regions of low shear stress located on the lateral surface of proximal ICA. The main features expected from fluid dynamics, such as low WSS values in the bulb region of the ICA and high WSS in proximal ECA were successfully captured. Nevertheless, different WSS patterns were found for each individual, mainly due to the effect of patient-specific artery morphology variability. For the non-stenotic bifurcation P3, low WSS patches in CCA were contiguous with the carotid bulb low WSS region. For patients P1, P2, and P3, maximum values of WSS, equal to 32, 35, and 22 Pa respectively, were found at inner wall of ECA proximal to bifurcation. For the other patients presenting higher stenosis degree, maximum WSS were located at ICA within stenosis. The maximum value of WSS was 42 Pa and it was observed for patient P4.

## Discussion

A noninvasive approach for simultaneously quantifying flow and WSS fields at CCA bifurcation was presented. Inter-individual variation in flow dynamics was analyzed considering six different models based on ultrasound morphologic and velocimetric acquisitions.

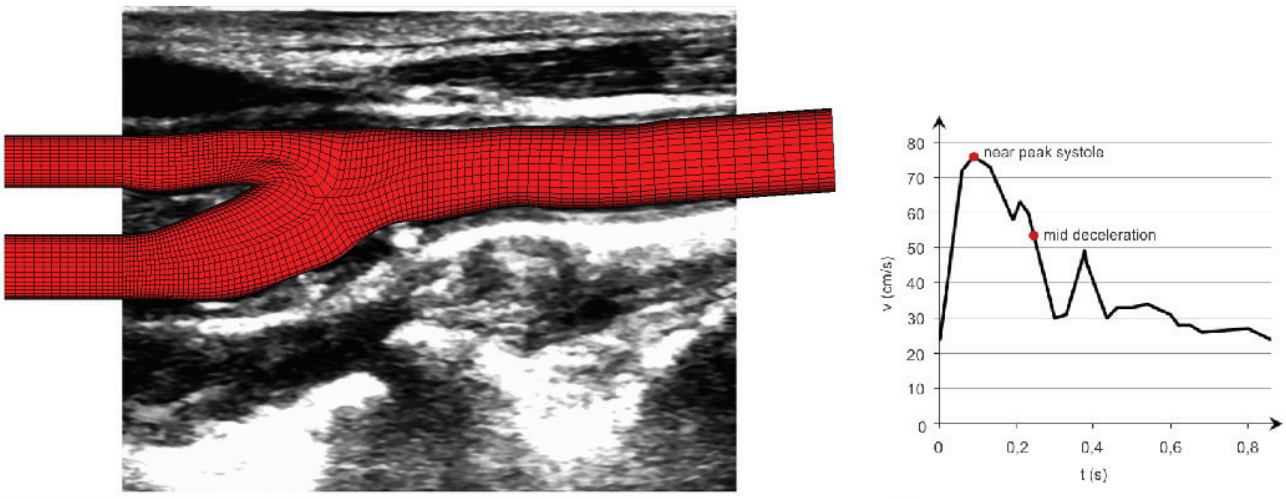


**Figure 3.** Volume discretization and distal CCA velocity waveform used for hemodynamics simulation of patient P1 bifurcation.

| Ultrasound Image | Identification and Data |
|---|---|
| 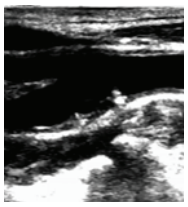 | **P1**<br>Age: 73<br>Gender: Male<br>Stenosis degree: 30%<br>ICA velocity:<br>• Doppler: 103.4 cm/s<br>• FEM: 102.6 cm/s |
| 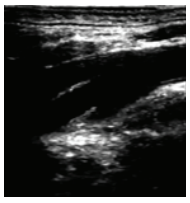 | **P2**<br>Age: 50<br>Gender: Male<br>Stenosis degree: 40%<br>ICA velocity:<br>• Doppler: 68.2 cm/s<br>• FEM: 68.9 cm/s |
| 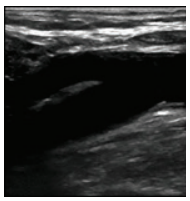 | **P3**<br>Age: 63<br>Gender: Male<br>Stenosis degree: No<br>ICA velocity:<br>• Doppler: 33.2 cm/s<br>• FEM: 38.0 cm/s |
|  | **P4**<br>Age: 57<br>Gender: Male<br>Stenosis degree: 50%<br>ICA velocity:<br>• Doppler: 103.4 cm/s<br>• FEM: 103.4 cm/s |
|  | **P5**<br>Age: 78<br>Gender: Female<br>Stenosis degree: 55%<br>ICA velocity:<br>• Doppler: 104.6 cm/s<br>• FEM: 99.3 cm/s |
| 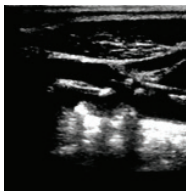 | **P6**<br>Age: 84<br>Gender: Female<br>Stenosis degree: 70%<br>ICA velocity:<br>• Doppler: 160.0 cm/s<br>• FEM: 153.5 cm/s |

**Figure 4.** Longitudinal images and identification of patients P1 to P6.

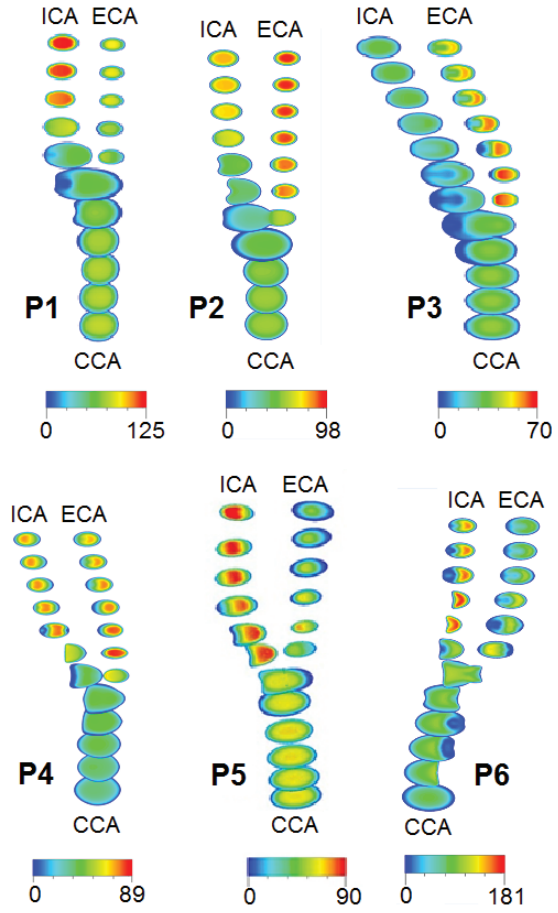


**Figure 5.** Velocity field (cm/s) at systolic peak for patients P1 to P6.

Each patient exhibits a different velocity pattern, associated with its morphology. When the bulb atherosclerotic plaques did not cause relevant stenosis, as in patients P1 and P2, maximum velocities at ICA appeared more distally, similarly to the P3 non-stenotic case, while for patients P4 to P6 maximum velocities were detected within stenosis, presenting high gradients.

Different WSS fields were found for the six volunteers as reported in Figure 6. For all patients with stenozed ICA, high WSS values were observed within the stenosis and low WSS values were detected in the non-stenotic or near normal ICA bulb region, and also in ICA distally to stenosis. For the non-stenotic bifurcation P3, low WSS patches in the common carotid artery (CCA) were contiguous with the carotid bulb low WSS region.

Since real artery morphology and flow velocities were employed, an obvious question arises if variations were attributable to morphology or flow velocity differences or both [12, 29, 30]. The analyzed bifurcations indicate that morphology, as the curvature of the in vivo models, may play the key role in determining the wall shear stress patterns. These findings could help to explain why some individuals develop more pronounced ICA stenosis than others, although vascular risk factors may be similar.

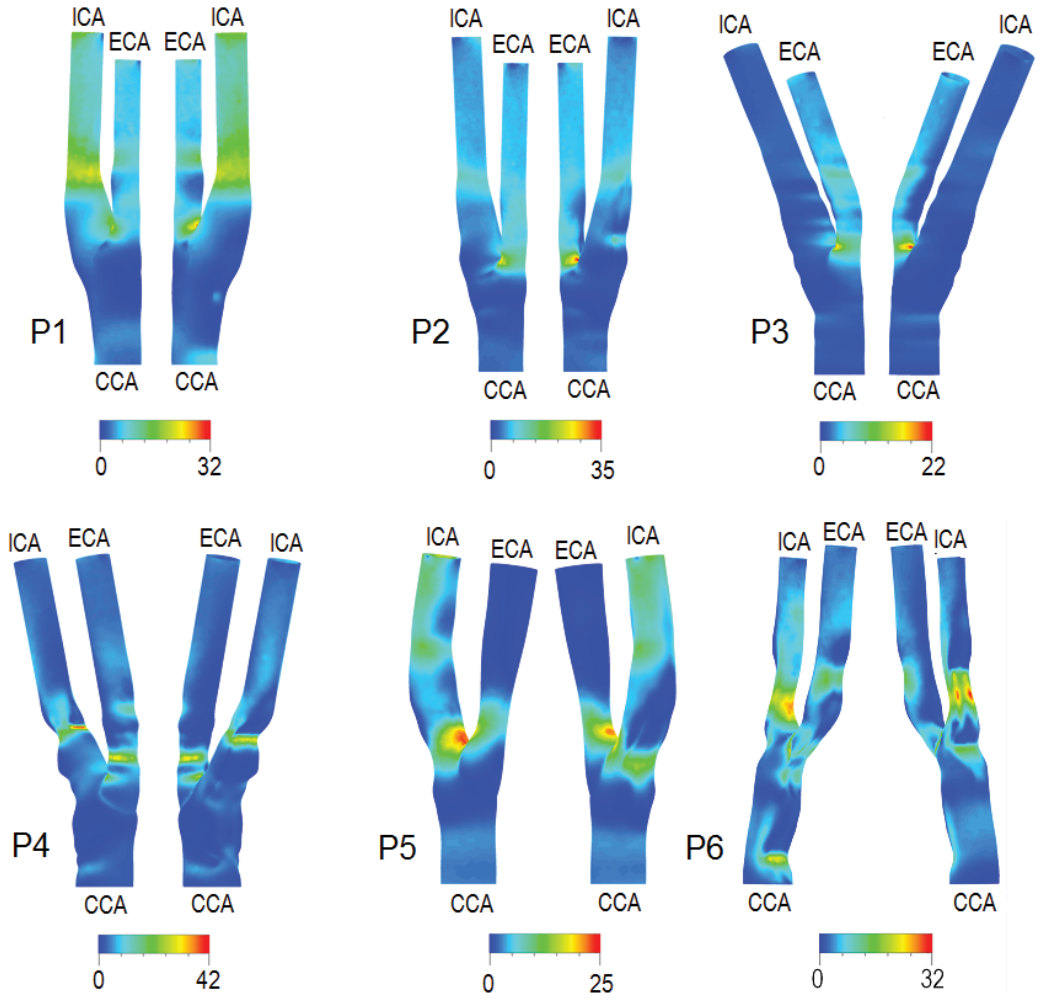


**Figure 6.** WSS contours (Pa) near peak systole for carotid bifurcations P1 to P6.

A full understanding of hemodynamic changes caused by the carotid bifurcation and stenosis is meaningful for clinical research. In this study we presented a noninvasive approach for simultaneously quantifying subject-specific flow patterns and wall shear stress distributions of human carotid bifurcation using a combination of ultrasound data and CFD modeling. Application of this novel approach to a normal volunteer and five subjects with atherosclerosis demonstrated a qualitative association between low WSS and recirculation zones at the carotid bulb where plaques were detected. This is consistent with many reports (e.g. [10, 29-31]) relating such hemodynamic factors to the localization of atherosclerosis at the carotid bifurcation.

This study indicates that morphology plays an important role on the hemodynamic behavior of the carotid artery bifurcation. It is imperative to include subject-specific morphology and flow velocities in modeling in vivo flow patterns. This novel technology might help to understand the relationship between hemodynamic environment and carotid wall lesions, and have a future impact in carotid stenosis diagnosis and management.

## Abbreviations

3D: Three-dimensional; CCA: Common carotid artery; CFD: Computational fluid dynamics; DICOM: Digital imaging and communications in medicine; ECA: External carotid artery; ECST: European Carotid Surgery Trial; ICA: Internal carotid artery; WSS: Wall shear stress

## Acknowledgments

This work was partially done in the scope of project PTDC/SAU-BEB/102547/2008, "Blood flow simulation in arterial networks towards application at hospital", financially supported by FCT – Fundação para a Ciência e a Tecnologia, Portugal.

## Competing interests

The authors declare no conflict of interest.

## References

1. Chiu JJ, Chien S. Effects of disturbed flow on vascular endothelium: pathophysiological basis and clinical perspectives. Physiol Rev 2011; 91(1):327-87.
2. Krams R, Wentzel JJ, Oomen JA, Vinke R, Schuurbiers JC, de Feyter PJ, et al. Evaluation of endothelial shear stress and 3D geometry as factors determining the development of atherosclerosis and remodeling in human coronary arteries in vivo. Combining 3D reconstruc-

tion from angiography and IVUS (ANGUS) with computational fluid dynamics. Arterioscler Thromb Vasc Biol 1997; 17(10):2061-5.

3. Wang C, Baker BM, Chen CS, Schwartz MA. Endothelial cell sensing of flow direction. Arterioscler Thromb Vasc Biol 2013; 33(9):2130-6.
4. Chandran KB, Vonesh MJ, Roy A, Greenfield S, Kane B, Greene R, et al. Computation of vascular flow dynamics from intravascular ultrasound images. Med Eng Phys 1996; 18(4):295-304.
5. Staub D, Schinkel AF, Coll B, Coli S, van der Steen AF, Reed JD, et al. Contrast-enhanced ultrasound imaging of the vasa vasorum: from early atherosclerosis to the identification of unstable plaques. JACC Cardiovasc Imaging 2010; 3(7):761-71.
6. Swillens A, De Santis G, Degroote J, Lovstakken L, Vierendeels J, Segers P. Accuracy of carotid strain estimates from ultrasonic wall tracking: a study based on multiphysics simulations and in vivo data. IEEE Trans Med Imaging 2012; 31(1):131-9.
7. Antiga L, Piccinelli M, Botti L, Ene-Iordache B, Remuzzi A, Steinman DA. An image-based modeling framework for patient-specific computational hemodynamics. Med Biol Eng Comput 2008; 46(11):1097-112.
8. Botnar R, Rappitsch G, Scheidegger MB, Liepsch D, Perktold K, Boesiger P. Hemodynamics in the carotid artery bifurcation: a comparison between numerical simulations and in vitro MRI measurements. J Biomech 2000; 33(2):137-44.
9. Hoi Y, Wasserman BA, Lakatta EG, Steinman DA. Carotid bifurcation hemodynamics in older adults: effect of measured versus assumed flow waveform. J Biomech Eng 2010; 132(7):071006.
10. Ku DN. Blood Flow in Arteries. Annual Review of Fluid Mechanics 1997; 29(1):399-434.
11. Lee SE, Lee SW, Fischer PF, Bassiouny HS, Loth F. Direct numerical simulation of transitional flow in a stenosed carotid bifurcation. J Biomech 2008; 41(11):2551-61.
12. Zhao SZ, Ariff B, Long Q, Hughes AD, Thom SA, Stanton AV, et al. Inter-individual variations in wall shear stress and mechanical stress distributions at the carotid artery bifurcation of healthy humans. J Biomech 2002; 35(10):1367-77.
13. ECST Collaborators. Randomised trial of endarterectomy for recently symptomatic carotid stenosis: final results of the MRC European Carotid Surgery Trial (ECST). Lancet 1998; 351(9113):1379-87.
14. Gill JD, Ladak HM, Steinman DA, Fenster A. Accuracy and variability assessment of a semiautomatic technique for segmentation of the carotid arteries from three-dimensional ultrasound images. Med Phys 2000; 27(6):1333-42.
15. Santos A, Sousa L, Tavares J, Santos R, Castro P, Azevedo E. Computer simulation of the carotid artery. Cerebrovasc Dis 2012; 33(suppl 1):77.
16. Santos A, Tavares J, Sousa L, Castro C, António C, Santos R, et al. Carotid artery bifurcation modelling from patient CT angiography and ultrasound technics. Cerebrovasc Dis 2013; 35(suppl 2):47.
17. Santos AMF, dos Santos RM, Castro PMAC, Azevedo E, Sousa L, Tavares JMRS. A novel automatic algorithm for the segmentation of the lumen of the carotid artery in ultrasound B-mode images. Expert Systems with Applications 2013; 40(16):6570-9.
18. Chan TF, Vese LA. Active contours without edges. IEEE Trans Image Process 2001; 10(2):266-77.
19. Lankton S, Tannenbaum A. Localizing region-based active contours. IEEE Trans Image Process 2008; 17(11):2029-39.
20. Sousa L, Castro C, António C. Blood Flow Simulation and Applications. In: Natal Jorge RM, Tavares JMRS, Pinotti Barbosa M, Slade AP, editors. Technologies for Medical Sciences: Springer Netherlands; 2012. p. 67-86.
21. Sousa LC, Castro CF, Antonio CC, Chaves R. Blood flow simulation and vascular reconstruction. J Biomech 2012; 45(15):2549-55.
22. Lee SW, Steinman DA. On the relative importance of rheology for image-based CFD models of the carotid bifurcation. J Biomech Eng 2007; 129(2):273-8.
23. Morbiducci U, Gallo D, Massai D, Ponzini R, Deriu MA, Antiga L, et al. On the importance of blood rheology for bulk flow in hemodynamic models of the carotid bifurcation. J Biomech 2011; 44(13):2427-38.
24. De Santis G, Conti M, Trachet B, De Schryver T, De Beule M, Degroote J, et al. Haemodynamic impact of stent-vessel (mal)apposition following carotid artery stenting: mind the gaps! Comput Methods Biomech Biomed Engin 2013; 16(6):648-59.
25. De Santis G, Mortier P, De Beule M, Segers P, Verdonck P, Verhegghe B. Patient-specific computational fluid dynamics: structured mesh generation from coronary angiography. Med Biol Eng Comput 2010; 48(4):371-80.
26. Kim HJ, Figueroa CA, Hughes TJR, Jansen KE, Taylor CA. Augmented Lagrangian method for constraining the shape of velocity profiles at outlet boundaries for three-dimensional finite element simulations of blood flow. Computer Methods in Applied Mechanics and Engineering 2009; 198(45–46):3551-66.
27. Lee SW, Antiga L, Spence JD, Steinman DA. Geometry of the carotid bifurcation predicts its exposure to disturbed flow. Stroke 2008; 39(8):2341-7.
28. Morbiducci U, Gallo D, Massai D, Consolo F, Ponzini R, Antiga L, et al. Outflow conditions for image-based hemodynamic models of the carotid bifurcation: implications for indicators of abnormal flow. J Biomech Eng 2010; 132(9):091005.
29. Markl M, Wegent F, Zech T, Bauer S, Strecker C, Schumacher M, et al. In vivo wall shear stress distribution in the carotid artery: effect of bifurcation geometry, internal carotid artery stenosis, and recanalization therapy. Circ Cardiovasc Imaging 2010; 3(6):647-55.
30. Meng H, Wang Z, Hoi Y, Gao L, Metaxa E, Swartz DD, et al. Complex hemodynamics at the apex of an arterial bifurcation induces vascular remodeling resembling cerebral aneurysm initiation. Stroke 2007; 38(6):1924-31.
31. Malek AM, Alper SL, Izumo S. Hemodynamic shear stress and its role in atherosclerosis. JAMA 1999; 282(21):2035-42.

INTERNATIONAL JOURNAL OF
CLINICAL NEUROSCIENCES
AND MENTAL HEALTH

ORIGINAL RESEARCH

# Transcranial color coded sonography: advanced approach using ultrasound fusion imaging

Stephan J. Schreiber[1], José M Valdueza[2], and Florian Doepp[1]

Special Issue on Neurosonology and Cerebral Hemodynamics

## Abstract

**Background:** Transcranial color-coded sonography (TCCS) is a well established method to study intracranial parenchymal and vascular structures. It is, however, limited by the need to insonate through available bone windows, resulting in oblique imaging planes, which can hinder easy allocation, particularly within the brain parenchyma and limit the opportunity for direct comparison with other imaging techniques. The objective of this study was to analyze the diagnostic yield of the ultrasound fusion imaging (UFI) technique using standard diagnostic approaches.

**Methods:** UFI is a new technique, permitting an online matching and comparison of live ultrasound images with preregistered CT or MRI images by means of a local electromagnetic field. The principles and setup of the technique for transcranial UFI is demonstrated and examples of its use in assessing established insonation planes given.

**Results:** UFI is suitable for transcranial insonation and allows easy combination of live ultrasound with routine diagnostic CT or MRI image datasets in the classical TCCS transtemporal and transforaminal insonation planes. System setting and matching is fast and movement artifacts are eliminated by the use of a motion tracker correction. First application in patients demonstrates easy identification and comparison of structural lesions like dilated ventricles, arachnoid cyst, or subdural hematoma.

**Conclusions:** UFI offers a unique opportunity to study transcranial ultrasound and CT or MRI anatomy simultaneously. It seems therefore particularly promising to be further analyzed concerning its potentials in teaching and education as well as in any intracranial condition in which repetitive intracranial imaging is required.

**Keywords:** Ultrasound, Virtual navigation, Transcranial color-coded sonography, Duplex ultrasound, Imaging planes.

[1]Charité – Universitätsmedizin Berlin, Department of Neurology, Charitéplatz 1, 10117 Berlin, Germany

[2]Segeberger Kliniken, dept. of Neurology, Am Kurpark, 23795 Bad Segeberg, Germany

Correspondence: Stephan J Schreiber
Dept. of Neurology, Charité - Universitätsmedizin Berlin
Charitéplatz 1, 10117 Berlin, Germany
Email adress: stephan.schreiber@charite.de

Citation: Schreiber et al. Transcranial color coded sonography: advanced approach using ultrasound fusion imaging. IJCNMH 2014; 1(Suppl. 1):S16

Received: 04 Sep 2013; Accepted: 12 Nov 2013; Published: 09 May 2014



ARC Publishing

## Introduction

Transcranial color-coded sonography (TCCS) is a modern, non-invasive diagnostic method to study intracranial parenchymal and vascular structures. The method has been well described and well established in routine clinical practice, particularly focusing on cerebrovascular disease and ischemic stroke [1, 2]. However, applied in adults, the technique has some limitations compared to other available diagnostic modalities like CT or MRI, because ultrasound waves are absorbed by the scull bone. Only two major transcranial bone windows exist that allow visualization of intracranial structures with ultrasound. For orientation within the resulting images, different imaging planes have been defined. For the transtemporal approach there is the midbrain plane, the thalamic plane, the cella media plane, the upper and lower pontine planes; for the transforaminal approach there is the lower and higher axial planes. More recently, coronal and oblique imaging planes have come into use. However, landmarks for orientation are not well defined and, particularly within brain parenchymal structures orientation is often difficult. Besides, a simple direct comparison with other imaging techniques has so far not been possible.

Recently, a new technique—ultrasound fusion imaging (UFI)—has been developed, which permits an online matching and comparison of live ultrasound images with preregistered CT or MRI images. While first attempts for clinical use have been focused on abdominal or rectal insonation, we describe in the following manuscript the principles and setup of the technique for transcranial insonation of brain parenchyma and vessels and give examples for its use in physiological conditions as well as in the identification of intracranial pathology.

## Methods

UFI combines the simultaneous online analysis of TCCS ultrasound images in combination with pre-registered CT or MRI image datasets. While performing a routine transcranial TCCS examination, the system provides an exactly matched image slice of the CT or MRI modality which adapts instantly and online to any movement of the ultrasound probe (**Video 1**).

The following cases have been studied with an ESAOTE Mylab Twice Virtual Navigator® ultrasound system (Genoa, Italy) using the systems Virtual Navigator® software. Prior to UFI analysis the preregistered CT or MRI DICOM datasets are loaded onto the ultrasound system. The system then performs a recalculation of these images into a 3D-dataset including a 3D-surface-rendered head image in which external marker points (e.g. ear, nose, forehead) can manually be defined (**Figure 1**). During the matching process and the actual TCCS analysis, the patient is positioned in a standard supine position with the investigator sitting at the side of the patients head. Fixed to the stretcher, an antenna is continuously emitting a local electromagnetic field aimed towards the study region. Prior to matching, a small electromagnetic field sensor (motion control sensor, online correcting for any head movement) is fixed to the patients forehead and remains in place until the end of the study. A second electromagnetic field sensor, attached to a registration pen, is used for the matching process by touching all prior defined external marker points with the pen. Afterwards, the electromagnetic field sensor is detached from the registration pen and attached to the standard TCCS-ultrasound insonation probe of the system (**Figure 1**). Then the ultrasound study can be started. The whole above described positioning and matching process takes approximately 10 minutes of time.

On screen imaging during UFI permits simultaneous visualization of ultrasound and corresponding CT or MRI image as well as gradual overlay between both imaging modalities (**Figure 2**).

## Results

Compared to CT or MRI imaging techniques, TCCS is limited by the need to insonate intracranial structures and vessels through one of the 3 main ultrasound access pathways, the transtemporal, the transforaminal, and the transorbital bone window. Applying this "keyhole" technique, the resulting images are mostly oblique slices and therefore variations of the classical axial or coronal imaging planes. Orientation subsequently requires a good 3-dimensional understanding of intracranial structures to compensate for the tilted images. In addition to the established use of B-mode and vessel landmarks the simultaneous projection

*Video accessible at http://ijcnmh.arc-publishing.org*

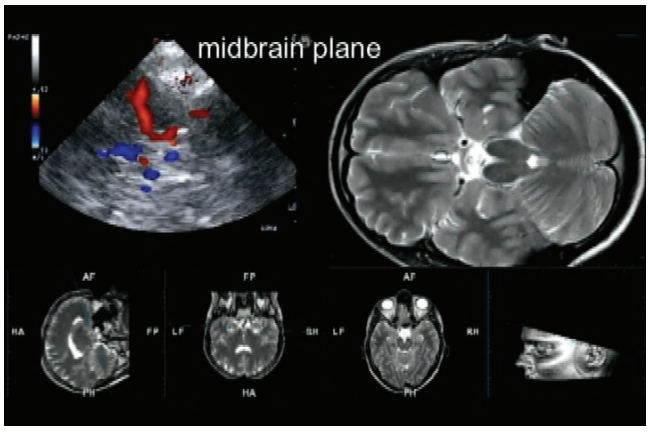


**Video 1.** Ultrasound fusion imaging (UFI) with a T2-weighted MRI dataset. The video demonstrates an UFI example of color-mode ultrasound matched with a T2-weighted MRI dataset in a patient with no pathological findings. The sequence, using the axial transtemporal approach starts with the classical midbrain plane moving downwards to the upper and lower pons plane. Please note the simultaneous movements in both imaging modalities and the excellent correlation of color-mode ultrasound signal and the corresponding arterial flow-void in the MRI dataset.

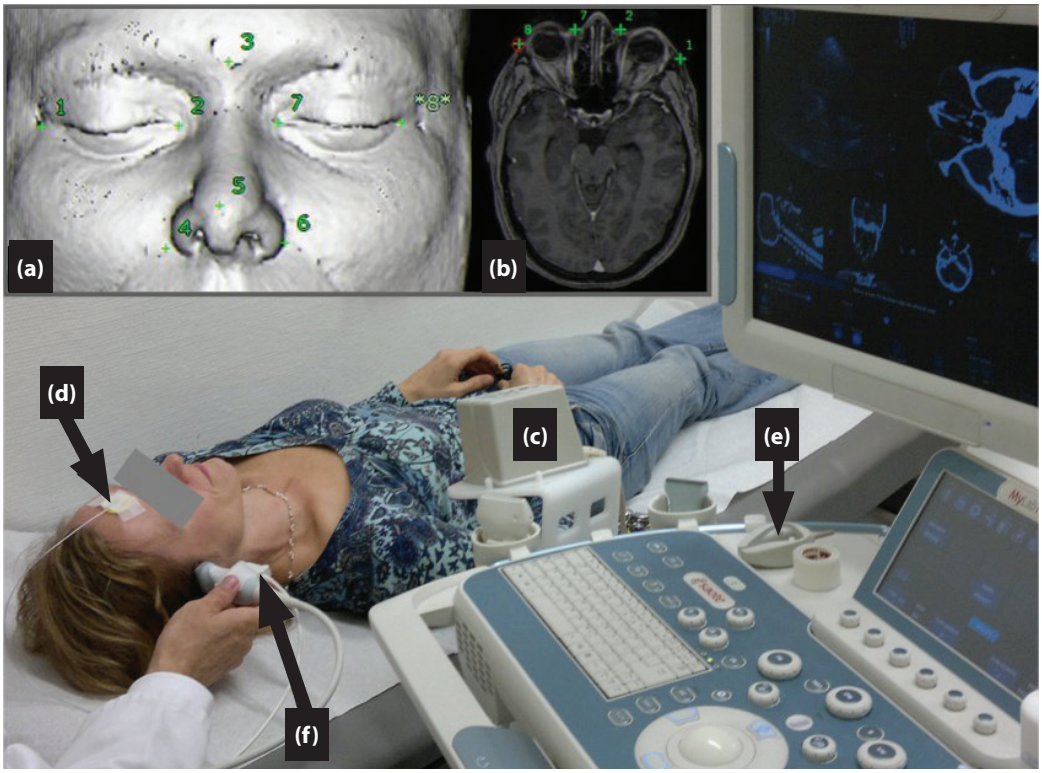


**Figure 1.** Ultrasound fusion imaging (UFI) system setup and matching: patient and investigator position for routine transcranial UFI. **(a)** 3D-surface-rendered head image: green numbered stars indicate the chosen external marker points of a T1-MRI-dataset derived from a conventional 1.5 Tesla MRI scanner (outer and inner eye corners, nose and forehead); **(b)** single MRI image of a 3D-reconstructed dataset with localization of external marker points; **(c)** electromagnetic field emitter orientated towards the patients head; **(d)** motion control sensor fixed by adhesive tape to the patient's forehead; **(e)** registration pen with slot for temporary attachment of the second electromagnetic field sensor; **(f)** Conventional transcranial color-coded sonography (TCCS) probe with attached electromagnetic field sensor during examination .

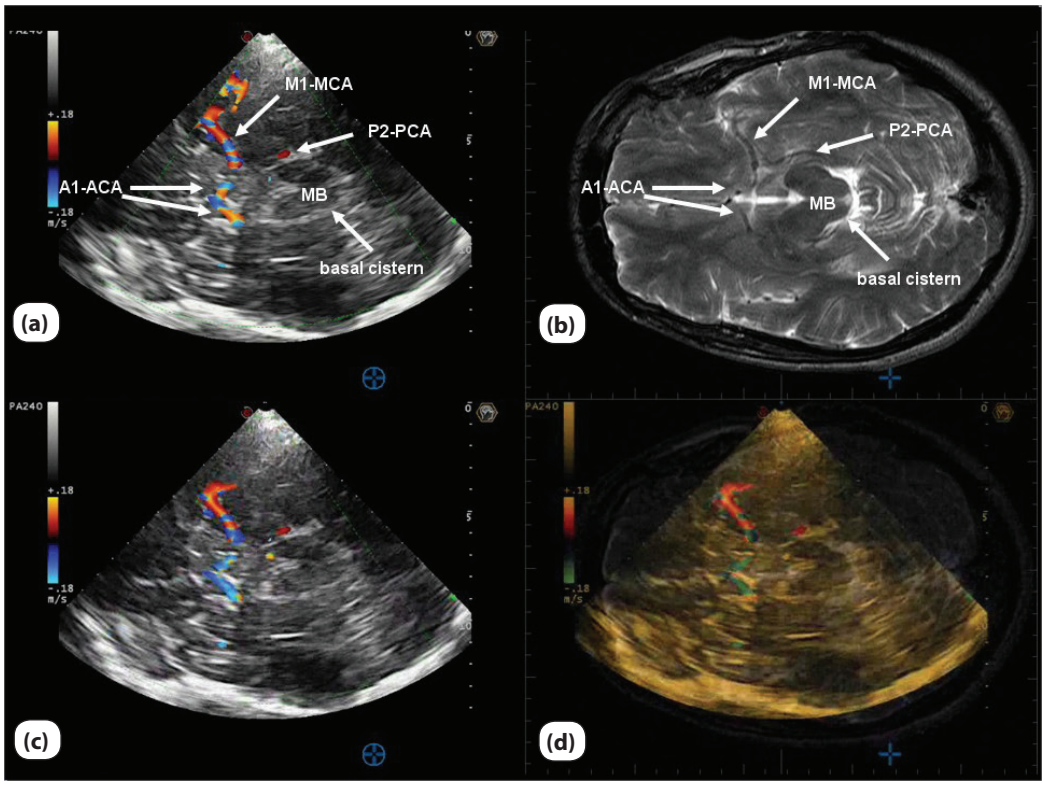


**Figure 2.** Ultrasound fusion imaging (UFI) overlay function. **(a)** transcranial color-coded sonography (TCCS) image of the midbrain plane demonstrating the butterfly-shaped midbrain (MB), the hyperechogenic basal cisterns, the ipsilateral P2-PCA, and M1-MCA-segment as well as both A1-ACA segments; **(b)** corresponding T2-weighted MR image with exactly corresponding structures; **(c)** identical TCCS image; **(d)** fused overlay image showing exact match between both image modalities.

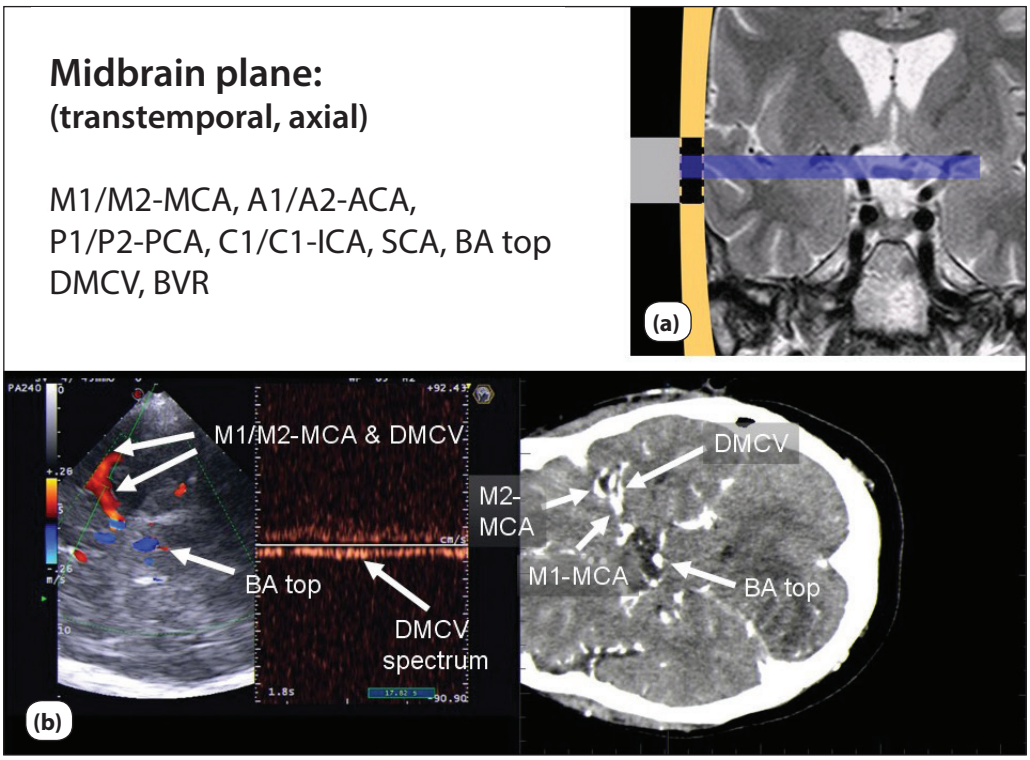


**Figure 3.** Example of the midbrain plane. **(a)** Vessel segments which can be identified by transcranial color-coded sonography (TCCS) and schematic visualization of the plane direction; **(b)** Ultrasound fusion imaging (UFI) color-mode and Doppler spectrum of the midbrain plane matched with a CT-angiography (CTA) dataset of a subject without pathological findings. Note, that one out of the three presumed middle cerebral artery (MCA) branches seen on the CTA is actually derived from the deep middle cerebral vein (DMCV) which is located slightly posterior to the MCA. The MCA color-mode signal usually overturns the weaker blue-coded signal of the DMCV.

of a corresponding CT or MRI image simplifies the process of image plane recognition and might even yield additional information. The most frequently used access pathway is the transtemporal bone window located just anterior to the external acoustic meatus. Using an axial imaging approach, 5 image planes can be identified: **Figures** 3-7.

Orientation within the transtemporal coronal imaging plane is more difficult as the typical B-mode guiding structures of the axial planes, like the butterfly-shaped midbrain or the bone structures of the base of the scull are missing. However, apart from the arterial vessels like the carotid-T in the anterior coronal plane and the basilar-T in the posterior coronal plane (**Figure 8**), other B-mode structures can be identified (**Figure 9**).

Transforaminal insonation through the foramen magnum requires the patient to antevert the head. If the insonation is performed in the supine body position the head is usually rotated by approximately 45 degrees. Until now, only two B-mode landmarks, the rim of the foramen magnum and the clivus have been recognized for this insonation approach. However, using UFI these landmarks can be extended by a number of other structures, that can be identified (**Figure 10**). For insonation of the proximal part of the VA entering the foramen, the lower transforaminal plane is used with the probe aimed towards the subject's nasion. For insonation of the basilar artery the upper transforaminal plane, aimed towards the forehead is needed (**Figure 11**).

## Discussion and conclusions

Ultrasound fusion imaging is a technique that allows a direct comparison of ultrasound images with preregistered images of other diagnostic modalities like MRI, CT, or PET. Its first clinical use was reported for analysis of lesions or tumours of the liver [3], breast [4], and prostate [5]. Since then an increasing number of reports have been published, primarily aiming to use a combined image modality approach for improvement of ultrasound-guided biopsies [6].

The application of the technique in neurosonology has only recently emerged. Two authors particularly addressed the specific issue of sonographic identification of intracranial veins [7, 8] using an unconventional transcondylar ultrasound bone window. One further publication of the former group has since reported on a specific 3D-panoramic ultrasound approach in three healthy volunteers [9]. However an analysis of the technique and it's potential in routine TCCS diagnostic does not yet exist.

Our cases give a first impression about possible applications of UFI in neurosonology. Concerning potential disadvantages of the technique it is important to notice, that patients with a pacemaker device should not be exposed to the systems electromagnetic field and hence can not be studied. A particular advantage of the transcranial insonation approach, compared to the above cited applications

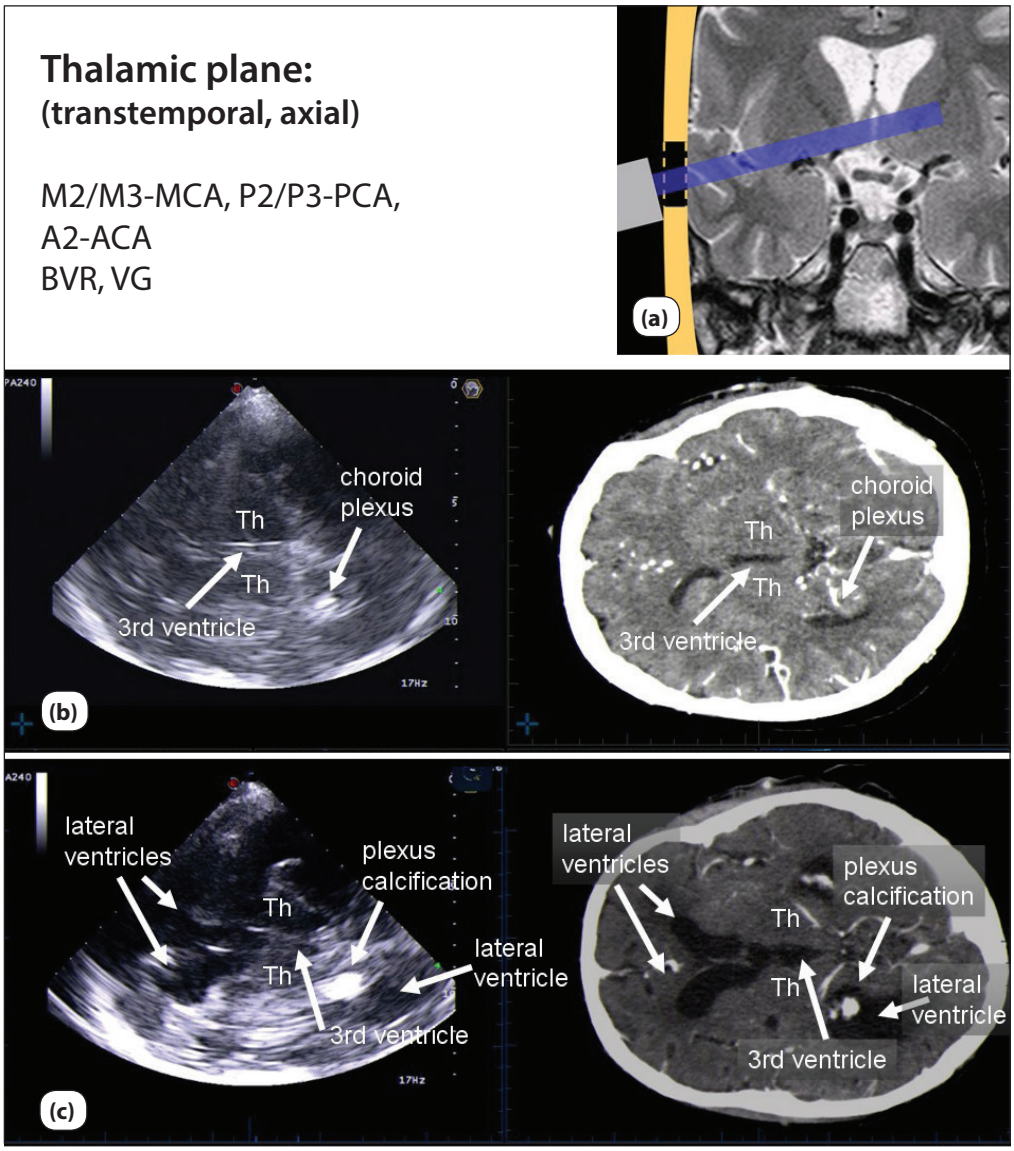


**Figure 4.** Example of thalamic plane. **(a)** Vessel segments which can be identified by transcranial color-coded sonography (TCCS) and schematic visualization of the plane direction; **(b)** Ultrasound fusion imaging (UFI) color-mode imaging of the thalamic plane, matched with a CT-angiography dataset of a subject without pathological findings. Note the double lineation of the third ventricle, both hypoechogenic thalami (Th) and hyperechogenic calcification of the choroid plexus, **(c)** hydrocephalus: UFI - B-mode imaging of the thalamic plane, matched with a CT-angiography dataset of a patient with hydrocephalus. Note the enlarged anterior horns of the lateral ventricles as well as the contralateral hypoechogenic posterior horn.

is that matching of image modalities is easy and simple. As external surface markers at the patients head can be used, the extra time of aproximately 10 minutes needed for the study preparation seems reasonable. Also, no specific MRI or CT sequences are required, as the system is able to calculate its 3D-datasets from any routine DICOM image series and can even compensate for changing slice thickness within a given dataset.

Concerning the transcranial approach a further advantage is that insonation is not restricted by breathing artifacts and any movements of the patients head after matching are automatically corrected by the motion tracker of the systems Virtual Navigator software®. As limited head movements are permitted and do not affect the quality of the results, transcranial UFI is similarly convenient for patient and sonographer as performing a "normal" routine TCCS analysis.

Concerning the diagnostic yield—even using only the presented standard insonation approach—our example cases already demonstrate that the technique facilitates the three-dimensional orientation and may be of particular help to identify or match specific regions of interest. Furthermore, it seems to be promising in helping to avoid false assignments of structures and vessels as demonstrated in **Figure 11**. It seems therefore especially suitable in any ultrasound training constellation, e.g. in ultrasound courses or a training ultrasound laboratory.

In addition, our few cases already demonstrate that the technique might help to add some further structural information, especially concerning parenchymal B-mode imag-

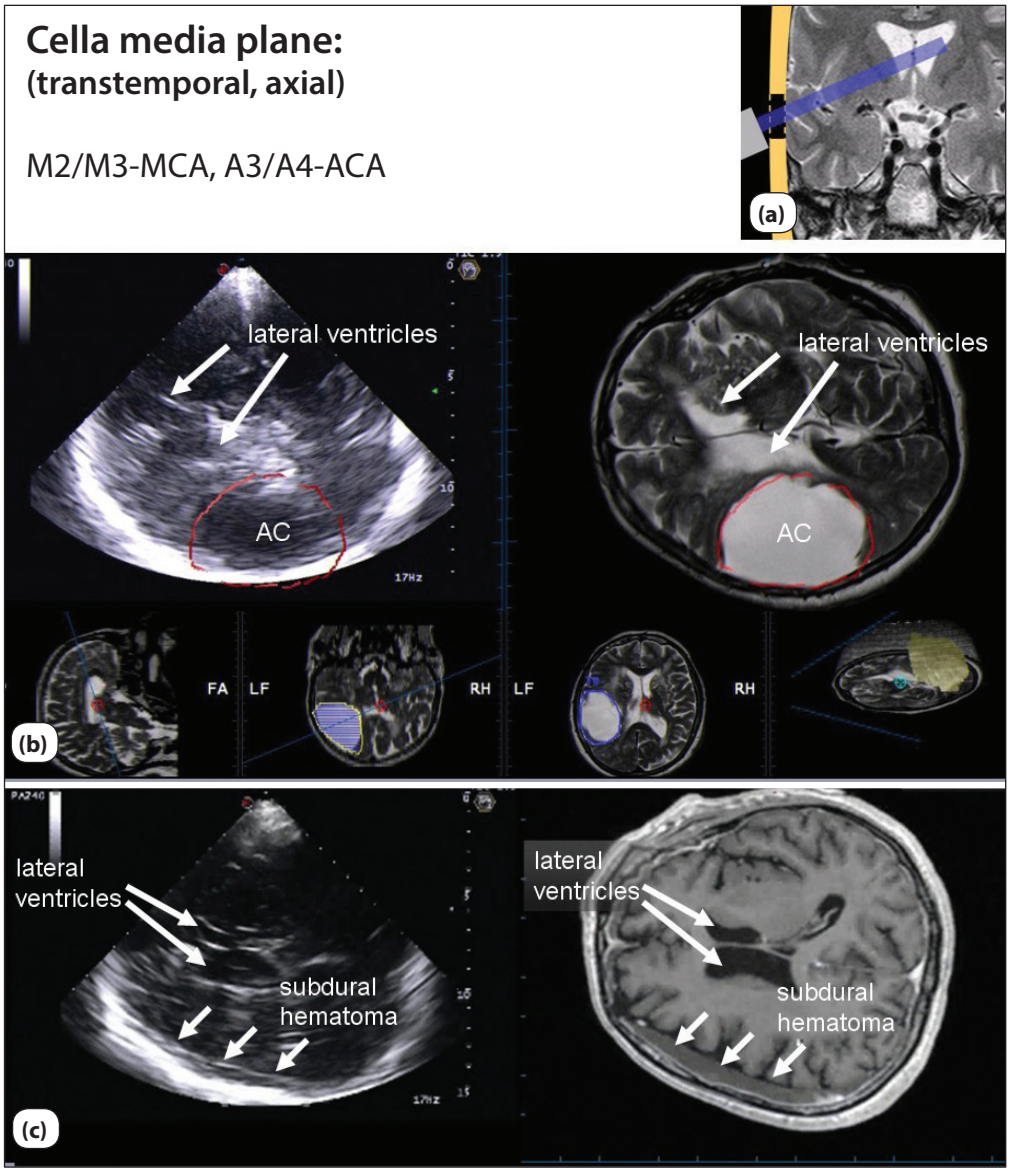


**Figure 5.** Example of the cella media plane. **(a)** Vessel segments which can be identified by transcranial color-coded sonography (TCCS) and schematic visualization of the plane direction; **(b)** Ultrasound fusion imaging (UFI) B-mode imaging of the cella media plane, matched with a T2-weighted MRI dataset of a patient with headaches. Note the oblique plane with ipsilateral prominent frontal horn and contralateral prominent middle part of the lateral ventricle. Contralateral to the probe, a large hypoechogenic arachnoid cyst (AC) can be identified. Borders of the cyst were manually delineated as a 3D-object within MRI dataset and online projected onto the ultrasound image; **(c)** subdural hematoma: UFI B-mode imaging of the cella media plane, matched with a T1-weighted MRI dataset of a patient with a subdural hematoma. Note the hyperechogenic delineation of the hematoma close to the contralateral skull bone.

ing. Very promising seems to us the use of the technique in conditions with a need of repetitive measurements over time, as for instance our patients with subdural hematoma, hydrocephalus or arachnoidal cyst. As lesions can be delineated in the CT or MRI dataset, they can be identically overlayed onto the real-time ultrasound images each time the patient returns for a follow-up study. However, up to now no systematic analysis of such use has been performed and its applicability and reliability has yet to be studied.

In summary, UFI is a promising new tool for the use in neurosonology and deserves fast further exploration concerning its specific advantages in teaching and training as well as its use as an advanced diagnostic tool.

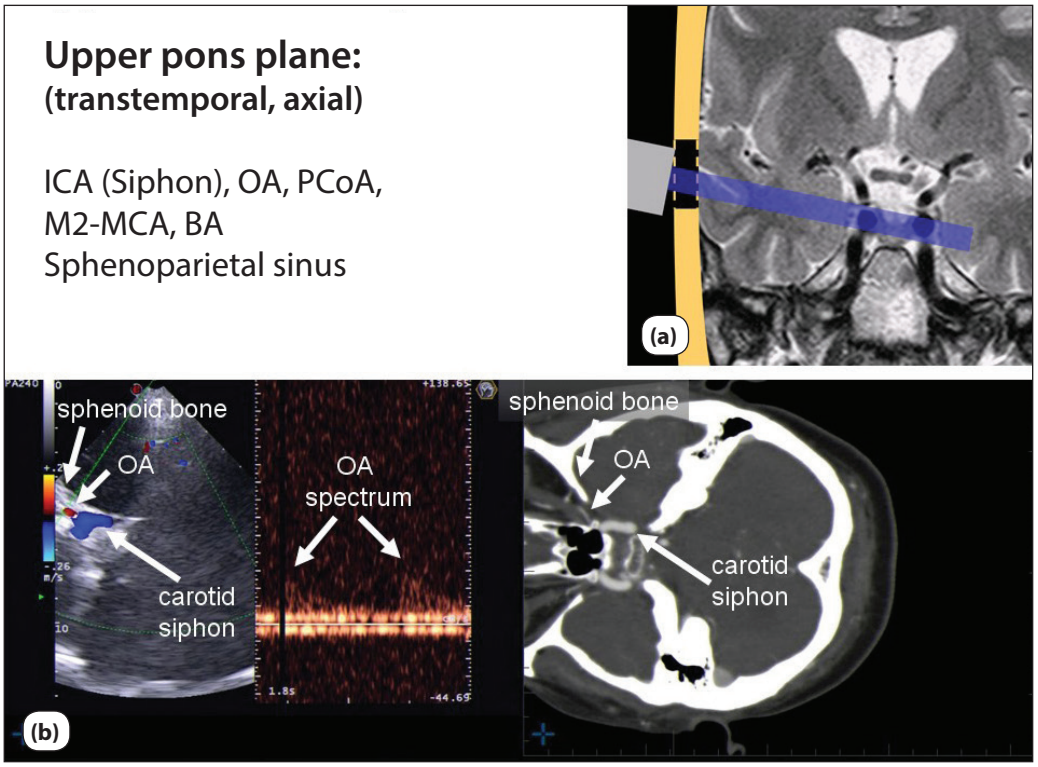


**Figure 6.** Example of the upper pons plane. **(a)** Vessel segments which can be identified by transcranial color-coded sonography (TCCS) and schematic visualization of the plane direction; **(b)** Ultrasound fusion imaging (UFI) color-mode and Doppler spectrum imaging of the upper pons plane, matched with a CTA dataset of a patient without pathological findings. Note the OA signal that can be located slightly medial to the hyperechogenic sphenoid bonebone.

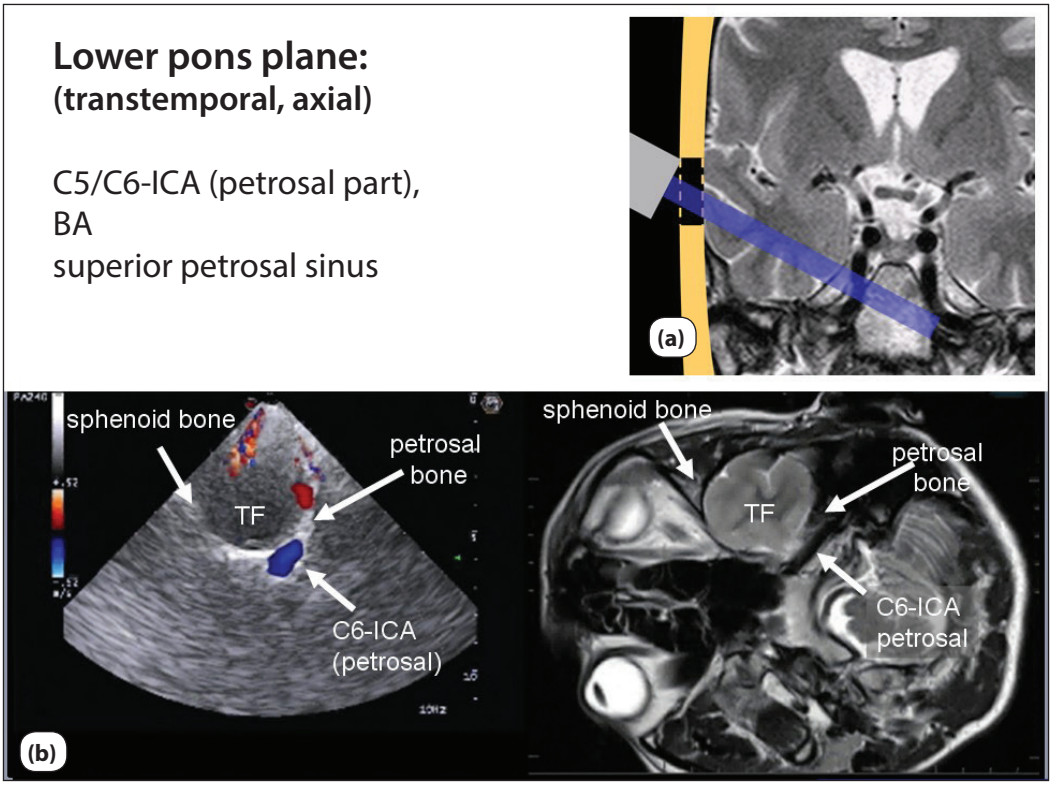


**Figure 7.** Example of the lower pons plane. **(a)** Vessel segments which can be identified by transcranial color-coded sonography (TCCS) and schematic visualization of the plane direction; **(b)** Ultrasound fusion imaging (UFI) color-mode imaging of the lower pons plane, matched with a T2-weighted MRI dataset of a patient without pathological findings. Note the petrosal part of the ICA which can easily be depicted with a flow direction away from the probe on the posterior border of the temporal fossa (TF).

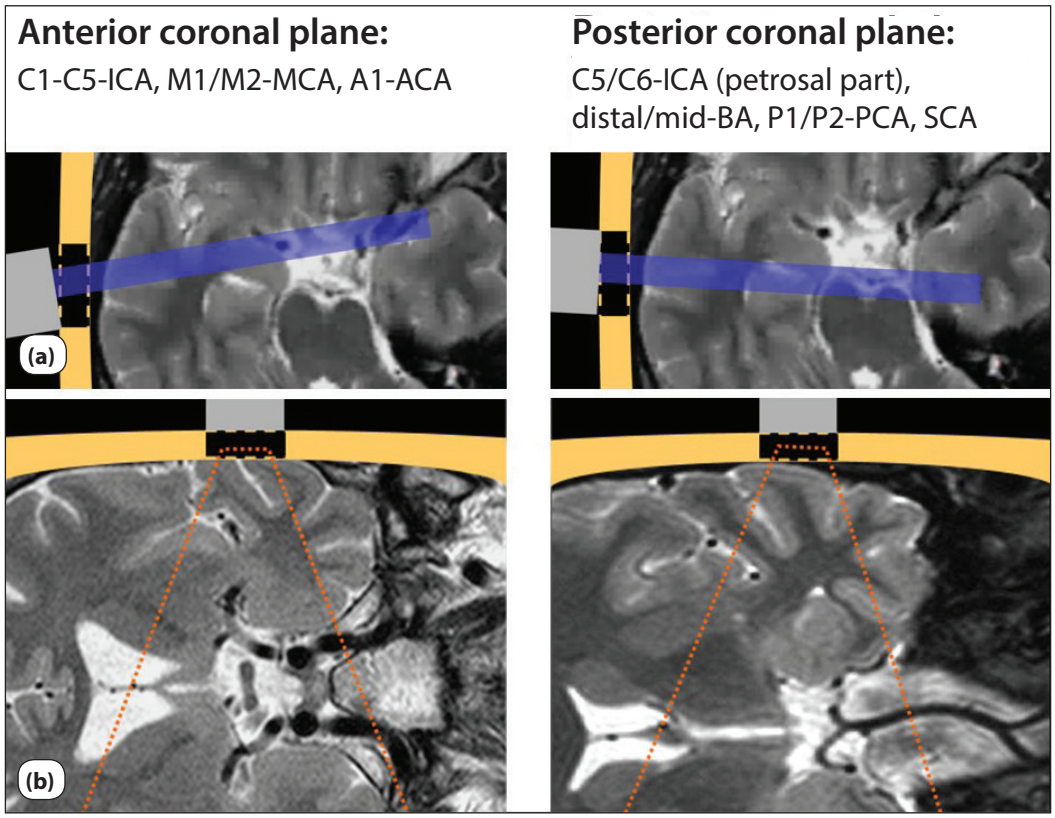


**Figure 8.** Anterior and posterior coronal plane. **(a)** Schematic axial visualization of the probe positioning to identify the anterior and posterior coronal plane and the corresponding vessel segments which can be identified by transcranial color-coded sonography (TCCS); **(b)** Schematic images of the ultrasound field of view in the two coronal imaging planes.

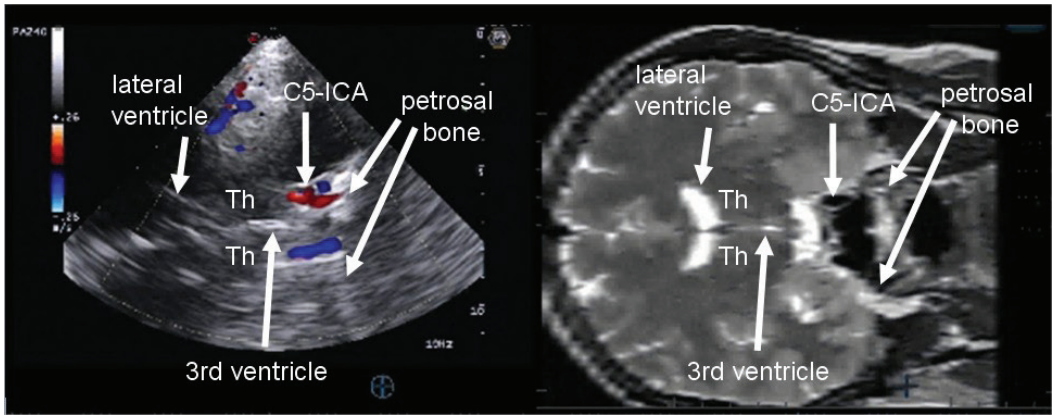


**Figure 9.** Example of the anterior coronal imaging plane. Ultrasound fusion imaging (UFI) color-mode imaging matched with a T2-weighted MRI dataset of a patient without pathological findings. Note the symmetrical hyperechogenicity of the petrosal bone and the B-mode signal of the third ventricle.

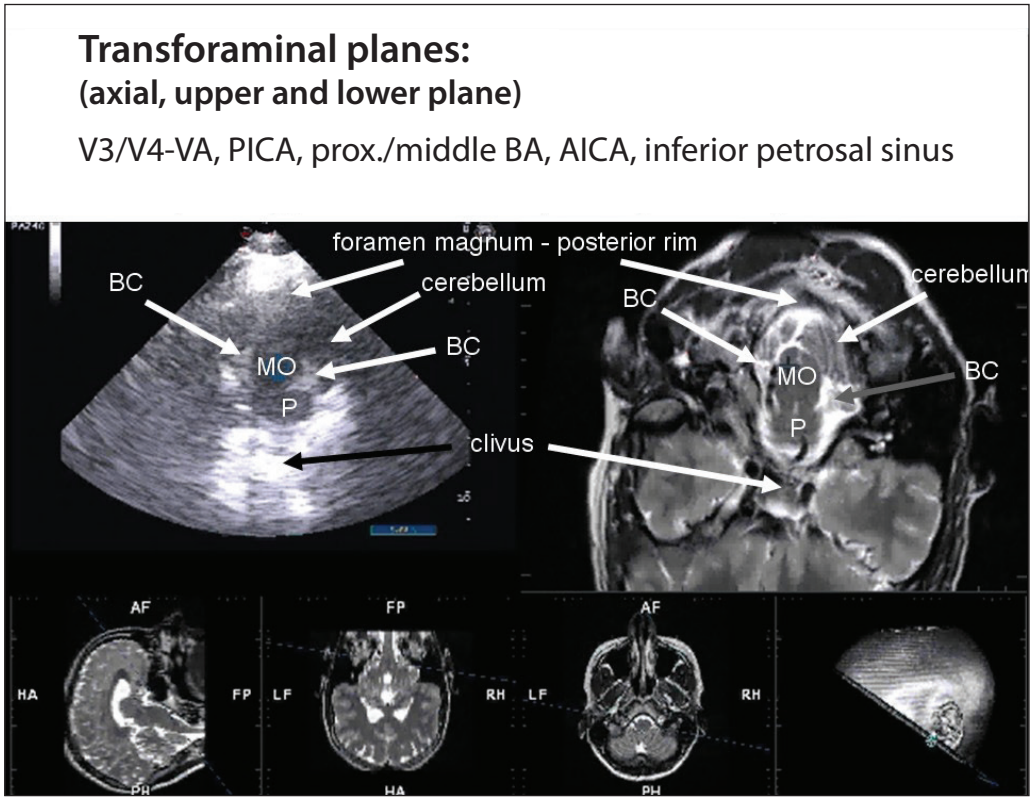


**Figure 10.** Transforaminal plane: B-mode. Vessel segments which can be identified by transcranial color-coded sonography (TCCS) via the transforaminal approach. Example of UFI (ultrasound fusion imaging) B-mode imaging of the upper transforaminal plane, matched with a T2-weighted MRI dataset of a patient without pathological findings. Note the clear delineation of the medulla oblongata (MO), the partial imaging of the lower pons (P) and the hyperechogenic appearance of the basal cisterns, differing from the echogenicity of the bone rim of the foramen magnum.

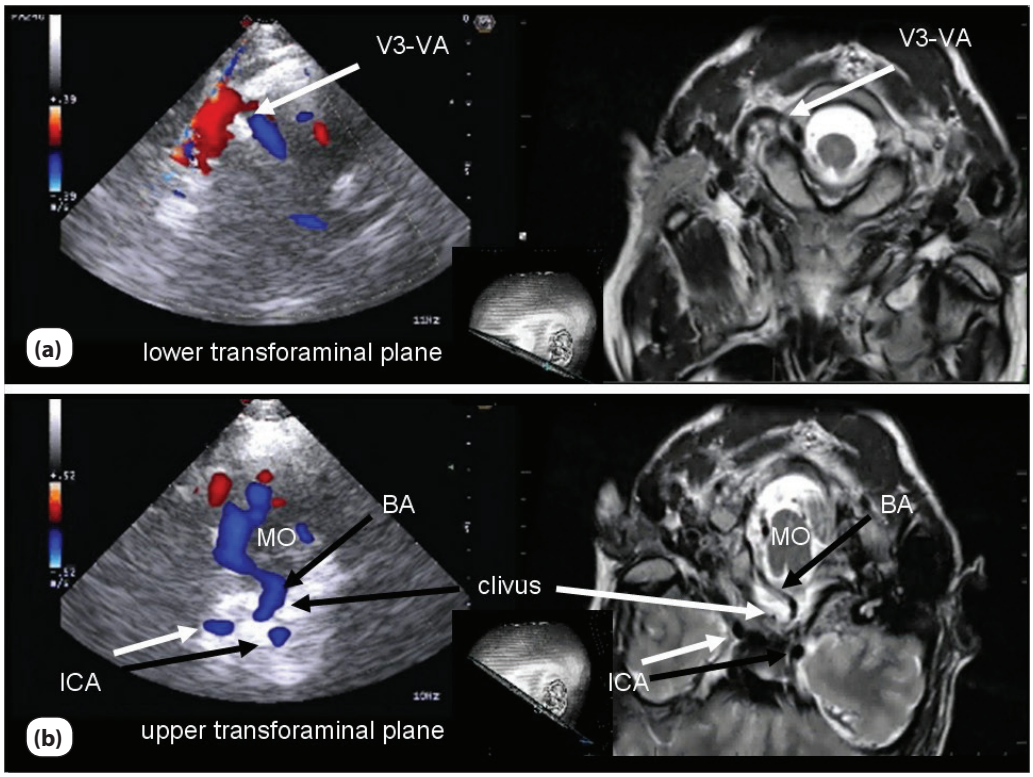


**Figure 11.** Examples of upper and lower transforaminal planes. Ultrasound fusion image (color-mode) matched with a T2-weighted MRI dataset of a patient without pathological findings **(a)** visualization of the V3-VA and proximal V4-V-segment. Note the angle of the insonation plane aiming for the nasion of the subject; **(b)** visualization of an elongated basilar artery (BA). Note, that the two blue-coded signals distal to the BA are derived from the ICA and not the PCA.

## Abbreviations

AC: Arachnoid cyst; ACA: Anterior cerebral artery; BA: Basilar artery; BC: Basal cistern; BVR: Basal vein of Rosenthal; DMCV: Deep middle cerebral vein; ICA: Internal carotid artery; MB: Midbrain; MCA: Middle cerebral artery; MO: Medulla oblongata; OA: Opthalmic artery; P: Pons; PCA: Posterior cerebral artery; SCA: Superior cerebellar artery; TF: Temporal fossa; Th: Thalamus; TL: Temporal lobe; VG: Vein of Galen

## Competing interests

Dr. Schreiber was supported by Esaote by providing a fusion imaging Duplex ultrasound system used for the current study.

## References

1. Valdueza JM, Schreiber S, Roehl JE, Klingebiel R.Neurosonology and Neuroimaging of Stroke, Thieme International. New York 2008
2. Alexandrov AV. Cerebrovascular ultrasound in stroke prevention and treatment. Blackwell Publishing Ltd. Oxford 2011
3. Tatsugami F, Matsuki M, Nakai G, et al. Hepatic computed tomography for simultaneous depiction of hepatocellular carcinoma, intrahepatic portal veins, and hepatic veins in real-time virtual sonography: initial experience. J Ultrasound Med 2007; 26:1065–1069
4. Nakano S, Yoshida M, Fujii K, et al. Fusion of MRI and sonography image for breast cancer evaluation using real-time virtual sonography with magnetic navigation: first experience. Jpn J Clin Oncol 2009; 39:552–559
5. Singh AK, Kruecker J, Xu S, et al. Initial clinical experience with real-time transrectal ultrasonography-magnetic resonance imaging fusion-guided prostate biopsy. BJU Int 2008; 101:841–845
6. Ewertsen C, Săftoiu A, Gruionu LG et al. Real-time image fusion involving diagnostic ultrasound. AJR Am J Roentgenol. 2013 Mar; 200(3):W249-55.
7. Laganà MM, Forzoni L, Viotti S et al. Assessment of the cerebral venous system from the transcondylar ultrasound window using virtual navigator technology and MRI. Conf Proc IEEE Eng Med Biol Soc. 2011; 2011:579-82.
8. Zamboni P, Menegatti E, Viselner G, Morovic S, Bastianello S. Fusion imaging technology of the intracranial veins. Phlebology. 2012 Oct; 27(7):360-7.
9. Forzoni L, D'Onofrio S, Beni SD, et al. Virtual Navigator Tridimensional Panoramic Imaging in Transcranial Application. Biomed Tech (Berl). 2012 Aug 24.

INTERNATIONAL JOURNAL OF
CLINICAL NEUROSCIENCES
AND MENTAL HEALTH

ORIGINAL RESEARCH

# Clinical predictors of increased middle cerebral artery pulsatility

Ana Gouveia[1], João Sargento-Freitas[2], João Madaleno[3], Joana Penetra[4], Fernando Alves-Silva[2], Cristina Machado[2], Gustavo Cordeiro[2], and Luís Cunha[2]

Special Issue on Neurosonology and Cerebral Hemodynamics

## Abstract

**Background:** Transcranial Doppler Pulsatility Index (PI) has traditionally been interpreted as a descriptor of distal cerebrovascular resistance. Many authors have investigated its usefulness in the context of traumatic brain injury (TBI), subarachnoid hemorrhage (SAH) and hydrocephalus. Nonetheless, many doubts remain about its interpretation in cerebrovascular prevention. The aim of our study is to identify the clinical predictors of increased PI.

**Methods:** We conducted an analysis of a prospective database including all patients undergoing cerebrovascular ultrasonographic evaluation during 2011. We excluded patients with ≥70% stenosis or occlusion in any intra or extracranial artery, stenosis in middle cerebral artery (MCA), atrial fibrillation, patients without transtemporal sonographic window and all evaluations performed in context of TBI, SAH, acute ischemic stroke or intracranial hypertension. The mean PI of both MCA, measured in its middle third after a minimum of 10 minutes of rest in the supine position, was registered. Vascular risk factors and clinical conditions were analyzed.

**Results:** Of the 947 patients analyzed, 446 were included, of which 287 (64.3%) were male. The mean age was 62.7 years (SD = 14.92) and the mean PI was 0.995 (SD = 0.240). In multivariate analysis, age (regression coefficient Beta (B):0.007, 95% CI: 0.005-0.009, p<0.001), hypertension (B:0.056, 95% CI: 0.003-0.108, p=0.037) and diabetes mellitus (B:0.064, 95% CI: 0.006-0.121, p=0.030) were identified as predictors of increased PI.

**Conclusion:** These results suggest that PI is associated with vascular risk factors classically responsible for small vessel disease. We discuss the pathophysiology of elevation of PI and its possible usefulness in cerebrovascular prevention.

**Keywords:** Pulsatility Index, Transcranial Doppler, Cerebrovascular resistance, Small vessel disease, Cerebrovascular prevention.

[1]Neurology Department, Coimbra University Hospital, Coimbra, Portugal
[2]Stroke Unit, Coimbra University Hospital, Coimbra, Portugal
[3]Internal Medicine Department, Coimbra University Hospital, Coimbra, Portugal
[4]Faculty of Medicine of the University of Coimbra, Coimbra, Portugal

Correspondence: Ana Gouveia
Neurology Department, Coimbra University Hospital
Praceta Prof. Mota Pinto, 3000-075 Coimbra, Portugal
Email adress: anargouveia86@gmail.com

Citation: Gouveia et al. Clinical predictors of increased middle cerebral artery pulsatility. IJCNMH 2014; 1(Suppl. 1):S17

Received: 31 Aug 2013; Accepted: 12 Nov 2013; Published: 09 May 2014

## Introduction

Gosling's Pulsatility Index (PI) and Pourcelot's Resistance Index, as derived from transcranial Doppler ultrasound (TCD), have long been proposed to reflect the degree of downstream vascular resistance caused by small vessel ischemic disease [1, 2]. PI characterizes the shape of a TCD spectral waveform and is calculated as the ratio of the difference between peak systolic and end diastolic velocities and the mean velocity (**Figure 1**). The index, being a ratio of velocities, does not rely on the knowledge of the diameter nor insonation angle of the vessel and thus can be directly compared between patients.

Its usefulness has been investigated for the last decades in the noninvasive assessment of intracranial pressure and cerebral perfusion pressure in the context of traumatic brain injury (TBI) [3], hydrocephalus [3] and subarachnoid hemorrhage (SAH) [4]. In cerebrovascular disease research, PI, measured in middle cerebral artery (MCA), was found to be associated with the presence and the severity of white matter lesions in magnetic resonance imaging (MRI), suggesting a role as a screening tool for cerebral small vessel disease [5, 6]. Nonetheless, the value of PI in these fields remains controversial.

The aim of our study was to identify the clinical predictors of increased MCA PI.

## Methods

We performed a cross-sectional study including all patients undergoing cerebrovascular ultrasonographic evaluation in our hospital's neurosonology laboratory during 2011. We excluded subjects with ≥70% stenosis or occlusion in any intra or extracranial artery, stenosis in MCA, atrial fibrillation, patients without transtemporal sonographic window and all evaluations performed in context of TBI, SAH, acute ischemic stroke or intracranial hypertension.

We analyzed a prospective database including mean MCA PI and presence of several vascular risk factors.

PI was measured by two neurosonologists using transcranial color-coded Doppler with a handheld 3-MHz probe (General Electrics Logiq 7®). After a minimum of 10 minutes of rest in the supine position, both MCAs were insonated through transtemporal window using color Doppler technique and PI was measured in its middle third.

Vascular risk factors and clinical conditions registered were age, gender, hypertension, diabetes, dyslipidemia, hyperuricaemia, obesity, smoking, congestive heart failure (CHF), and history of stroke.

For univariate analysis of nominal variables we performed independent-samples t-tests and for age Pearson's correlation coefficient. Considering the high number of patients included and the potential for confounding regarding the pathological relationship between the variables analyzed we decided to perform a multivariate analysis using a linear regression model that included all clinical factors. We present the results of the multivariate analysis as regression coefficient Beta (B) and 95% Confidence Interval (CI). Values of $p<0.05$ were regarded as significant.

## Results

We analyzed 947 subjects. Of those, 501 were excluded for presenting ≥70% stenosis or occlusion in an intra or extracranial artery (72), stenosis in MCA (101), atrial fibrillation (169), missing transtemporal sonographic window (155), and evaluations performed in context of TBI, SAH, acute ischemic stroke or intracranial hypertension (43). Of the 446 patients included, 287 (64.3%) were male, mean age was 62.7 years (SD = 14.92) and mean MCA PI was 0.995 (SD = 0.240).

In univariate analysis, the clinical factors associated with elevated PI were male gender (0.94±0.21 vs. 1.02±0.25; $p<0.001$), hypertension (0.92±0.20 vs. 1.06±0.25; $p<0.001$), diabetes (0.98±0.24 vs. 1.07±0.22; $p=0.001$) and hyperuricaemia (0.99±0.23 vs. 1.06±0.22; $p<0.031$). Age ($r=0.440$; $p<0.001$) was correlated with elevated PI (**Table 1**).

In multivariate analysis the predictors of increased PI were age (B:0.007, 95% CI: 0.005-0.009, $p<0.001$), hypertension (B:0.056, 95% CI: 0.003-0.108, $p=0037$) and diabetes (B:0.064, 95% CI: 0.006-0.121, $p=0.030$) (**Table 2**).

## Discussion

In the present study, the main predictors of elevated PI were vascular risk factors classically responsible for small vessel disease: age, hypertension, and diabetes. Interestingly, dyslipidemia was not a clinical or analytical

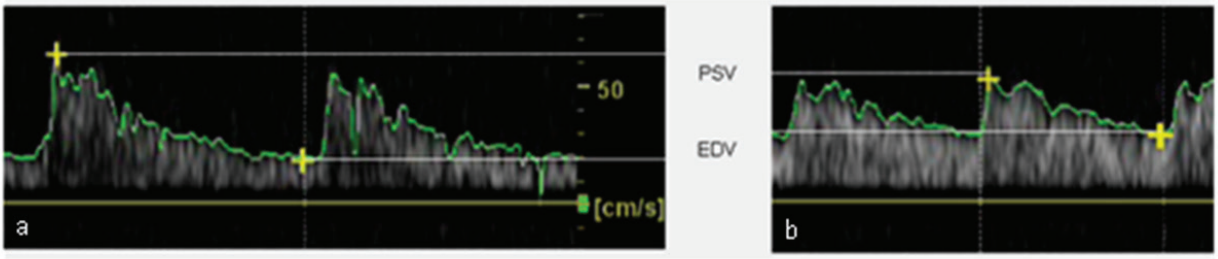


**Figure 1.** Hemodynamic parameters derived from Doppler spectrum analysis: **(a)** elevated PI; **(b)** normal PI.
PSV: Peak systolic velocity; EDV: End diastolic velocity

**Table 1.** Results of univariate analysis.

| *Risk factor* | N | Mean PI (SD) | | *r* | *p* |
|---|---|---|---|---|---|
| | | Absent | Present | | |
| Male gender | 287 | 0.94 (0.21) | 1.02 (0.25) | – | <0.001 |
| Hypertension | 234 | 0.92 (0.20) | 1.06 (0.25) | – | <0.001 |
| Diabetes | 90 | 0.98 (0.24) | 1.07 (0.22) | – | 0.001 |
| Hyperuricaemia | 59 | 0.99 (0.23) | 1.06 (0.22) | – | 0.031 |
| Dyslipidemia | 271 | 0.99 (0.27) | 1.00 (0.22) | – | 0.505 |
| Obesity | 31 | 0.99 (0.24) | 1.00 (0.25) | – | 0.858 |
| Smoking | 40 | 1.00 (0.24) | 0.98 (0.24) | – | 0.757 |
| CHF | 16 | 0.99 (0.24) | 1.09 (0.22) | – | 0.113 |
| Previous stroke | 30 | 0.99 (0.24) | 1.06 (0.20) | – | 0.098 |
| Age | – | – | – | 0.440 | <0.001 |

CHF = Congestive Heart Failure; PI = Pulsatility Index

predictor of increased PI. In fact, dyslipidemia has shown a strong inverse association with white matter hyperintensities, suggesting a protective role in cerebral small vessel disease [7].

The pathophysiology of MCA PI elevation remains unclear and has been an object of discussion. It appears to be a complex function of various hemodynamics factors, namely cardiac function, vessel radius, blood viscosity, and cerebral perfusion pressure [8]. Increased cerebrovascular resistance, measured by MCA PI, has been interpreted as a direct consequence of the narrowing of small vessels due to lipohialynosis and microatherosclerosis.

Mok et al. [6] conducted a community study where PI was found to be independently associated with white matter lesions severity, evaluated by MRI. Moreover, the negative predictive value of PI was high, suggesting that TCD PI may guide the identification of subjects with subclinical small vessel disease. In a similar study, PI correlated well with a variety of MRI manifestations of small vessel disease: periventricular hyperintensity, deep white matter hyperintensity, lacunar disease, and pontine hyperintensity [9].

Two studies [10, 11] investigated TCD findings of diabetes-related cerebral hemodynamic changes. PI was correlated with the duration of diabetes and was significantly increased in complicated diabetic subjects (with retinopathy and lacunar infarction).

Meanwhile, other authors hypothesized that disproportionate stiffness of proximal aorta with advancing age and in the presence of various vascular risk factors, as compared with peripheral arteries, reduces the Windkessel function of aorta and therefore facilitates transmission of excessive pulsatile energy into cerebral microcirculation. These abnormal physical forces would trigger microvascular damage and remodelling, leading to microvascular ischaemia [12].

Supporting this theory, several studies have proved that MCA PI is strongly correlated with aortic pulsatility and stiffness, suggesting a causative pathophysiological relationship [5, 13].

There are limitations of our study that need to be considered. First, it has a single centered, cross-sectional design, and therefore it examined associations; additional work will be required to ascertain whether these associations represent causal relationships. Second, the time of evolution of each vascular risk factor was not analyzed, nor the possible ongoing treatments. Another natural limitation refers to the population analyzed, including only patients referred to a neurosonology laboratory, therefore with higher prevalence of risk factors. Nonetheless we feel that by selecting consecutive patients without stringent exclusion criteria and considering the multivariate analysis performed, this factor did not influence the results obtained.

**Table 2.** Results of multivariate analysis.

| *Risk factor* | B | 95% CI | | *p* |
|---|---|---|---|---|
| | | *Lower* | *Upper* | |
| Age | 0.007 | 0.005 | 0.009 | <0.001 |
| Hypertension | 0.056 | 0.003 | 0.108 | 0.037 |
| Diabetes | 0.064 | 0.006 | 0.121 | 0.030 |
| Dyslipidemia | -0.091 | -0.112 | 0.008 | 0.089 |
| Hyperuricaemia | 0.078 | -0.160 | 0.109 | 0.148 |
| Obesity | 0.021 | -0.076 | 0.114 | 0.694 |
| Smoking | 0.048 | -0.041 | 0.112 | 0.362 |
| CHF | 0.024 | -0.103 | 0.164 | 0.654 |
| Previous stroke | -0.062 | -0.147 | 0.380 | 0.244 |

B = Regression Coefficient Beta; CI = Confidence Interval; CHF = Congestive Heart Failure

The main strength of our study is its large sample, allowing to observe independent associations in multivariate analysis.

## Conclusion

PI is directly related to higher age, hypertension, and diabetes mellitus. Longitudinal multicenter studies are needed to document its potential role in the development and severity of diffuse small vessel disease and as a measure of the effectiveness of therapeutic interventions.

### Abbreviations

CHF: Congestive heart failure; MCA: Middle cerebral artery; MRI: Magnetic resonance imaging; PI: Pulsatility index; SAH: Subarachnoid hemorrhage; TBI: Traumatic brain injury; TCD: Transcranial Doppler ultrasound

### Acknowledgments

We gratefully acknowledge the support from the all nurses of Coimbra University Hospital's Stroke Unit. This study had no financial support.

### Competing interests

The authors declare no conflict of interest.

### References

1. Gosling RG KD. Arterial assessment by Doppler-shift ultrasound. Proc Roy Soc Med 1974; 67:447-9.
2. Legarth J, Thorup E. Characteristics of Doppler blood-velocity waveforms in a cardiovascular in vitro model. I. The model and the influence of pulse rate. Scandinavian Journal of Clinical & Laboratory Investigation 1989; 49(5):451-7.
3. Bellner J, Romner B, Reinstrup P, Kristiansson K-A, Ryding E, Brandt L. Transcranial Doppler sonography pulsatility index (PI) reflects intracranial pressure (ICP). Surgical Neurology 2004; 62(1):45-51.
4. Soehle M, Chatfield DA, Czosnyka M, Kirkpatrick PJ. Predictive value of initial clinical status, intracranial pressure and transcranial Doppler pulsatility after subarachnoid haemorrhage. Acta Neurochirurgica 2007; 149(6):575-83.
5. Webb AJ, Simoni M, Mazzucco S, Kuker W, Schulz U, Rothwell PM. Increased cerebral arterial pulsatility in patients with leukoaraiosis: arterial stiffness enhances transmission of aortic pulsatility. Stroke 2012; 43(10):2631-6.
6. Mok V, Ding D, Fu J, Xiong Y, Chu WW, Wang D, et al. Transcranial Doppler ultrasound for screening cerebral small vessel disease: a community study. Stroke 2012; 43(10):2791-3.
7. Jimenez-Conde J, Biffi A, Rahman R, Kanakis A, Butler C, Sonni S, et al. Hyperlipidemia and reduced white matter hyperintensity volume in patients with ischemic stroke. Stroke 2010; 41(3):437-42.
8. Riva N, Budohoski K, Smielewski P, Kasprowicz M, Zweifel C, Steiner L, et al. Transcranial Doppler Pulsatility Index: What it is and What it Isn't. Neurocritical Care 2012; 17(1):58-66.
9. Kidwell CS, El-Saden S, Livshits Z, Martin NA, Glenn TC, Saver JL. Transcranial Doppler Pulsatility Indices as a Measure of Diffuse Small-Vessel Disease. Journal of Neuroimaging 2001; 11(3):229-35.
10. Lee KY, Sohn YH, Baik JS, Kim GW, Kim J-S. Arterial Pulsatility as an Index of Cerebral Microangiopathy in Diabetes. Stroke 2000; 31(5):1111-5.
11. Lee KO, Lee KY, Lee SY, Ahn CW, Park JS. Lacunar infarction in type 2 diabetes is associated with an elevated intracranial arterial pulsatility index. Yonsei Med J 2007; 48(5):802-6.
12. Mitchell GF, van Buchem MA, Sigurdsson S, Gotal JD, Jonsdottir MK, Kjartansson O, et al. Arterial stiffness, pressure and flow pulsatility and brain structure and function: the Age, Gene/Environment Susceptibility--Reykjavik study. Brain 2011; 134(Pt 11):3398-407.
13. Kwater A, Gąsowski J, Gryglewska B, Wizner B, Grodzicki T. Is blood flow in the middle cerebral artery determined by systemic arterial stiffness? Blood Pressure 2009; 18(3):130-4.

INTERNATIONAL JOURNAL OF
CLINICAL NEUROSCIENCES
AND MENTAL HEALTH

ORIGINAL RESEARCH

# Impaired autoregulation is associated with mortality in severe cerebral diseases

Bernhard Schmidt[1], Jens J. Schwarze[1], Marco Weinhold[1], Vesna Lezaic[1], Marek Czosnyka[2], and Jürgen Klingelhöfer[1]

Special Issue on Neurosonology and Cerebral Hemodynamics

## Abstract

**Background:** Small cerebral vessels respond to variations of cerebral perfusion pressure (CPP) by changes of vessel diameter inducing changes of blood flow resistance and keeping cerebral blood flow constant. This mechanism is called cerebral autoregulation (CA). An index Mx, observing correlation between cerebral blood flow velocity (CBFV) and CPP has been recently introduced for assessment of state of CA during spontaneous changes of CPP. In the current study, the relationship between lethal outcome during hospitalization and Mx index was investigated.

**Methods:** Thirty patients (18-77 years, mean 53±16 years) with severe cerebral diseases were studied. CBFV, arterial blood pressure (ABP,) and intracranial pressure (ICP) were simultaneously recorded. Assessments were repeated at days 2, 4 and 7. Mx was calculated retrospectively, as averaged correlation between CBFV and CPP (=ABP-ICP). Positive values of Mx indicated impairment of CA.

**Results:** Six of the patients died in-hospital. In this group Mx was significantly higher than in the group of survivors (0.28±0.40 versus 0.03±0.21; $p<0.05$). Changes of Mx during days of monitoring (Mx last day - Mx first day) were not significantly related to mortality. Nine patients showed an Mx >0.2, four of them died, whereas from the 21 patients with Mx <0.2 only two died . The association between increased Mx and death was significant ($p<0.05$, Fisher's exact test). Mx correlated significantly with Glasgow Outcome Score (GOS) in the subgroup of patients with known GOS (N=21; $R=-0.56$, $p<0.05$).

**Conclusion:** Increased Mx indicates impairment of CA and is associated with risk of death in patients with severe cerebral diseases.

**Keywords:** Cerebral autoregulation, Cerebral perfusion pressure, Intracranial pressure, Cerebral disease.

[1]Department of Neurology, Chemnitz Medical Center, Chemnitz, Germany.
[2]Department of Clinical Neurosciences, Neurosurgical Unit, Addenbrooke's Hospital, Cambridge, United Kingdom.

Correspondence: Bernhard Schmidt
Department of Neurology, Chemnitz Medical Center
Dresdner Str. 178, 09131 Chemnitz, Germany
Email adress: B.Schmidt@skc.de

Citation: Schmidt et al. Impaired autoregulation is associated with mortality in severe cerebral diseases. IJCNMH 2014; 1(Suppl. 1):S18

Received: 11 Sep 2013; Accepted: 22 Nov 2013; Published: 09 May 2014

## Introduction

The mechanism of cerebral autoregulation (CA) minimizes variation of cerebral blood flow (CBF) during changes of cerebral perfusion pressure (CPP). Pressure excited dilatation or constriction of small arteries regulates cerebral blood flow resistance and prevents the brain from ischemia during decrease of CPP, as well as from hyperemia during increase of CPP.

Severe cerebral diseases may affect cerebral autoregulation [1, 2] and cause vulnerability of the brain. Therefore, the monitoring of cerebral autoregulation provides important information for patient treatment. Various CA monitoring methods have been introduced so far. They generally rely on the analysis of cerebral blood flow velocity (CBFV) either during controlled induction of pressure changes [3, 4] or during spontaneous oscillations of arterial blood pressure (ABP) or CPP [5-8]. In a former study with traumatic brain injured (TBI) patients [5] an index (so-called Mx index) has been introduced, which evaluated state of CA during spontaneous changes of CPP and corresponded to clinical outcome. In patients with intracranial pressure (ICP) monitoring, Mx was calculated from correlation between CBFV and CPP. In patients without ICP monitoring an iterative, self-adjusting method of non-invasive ICP assessment could be used for estimating CPP and Mx [9].

Several recent studies reported an association between unfavorable clinical outcome and increased values of Mx in patients with TBI [5, 10, 11], intracerebral hemorrhage [12], and ischemic stroke [13]. In the current study the association between Mx and lethal outcome during hospitalization in a population of diverse cerebral diseases (TBI, hemorrhagic and ischemic stroke, and others) was investigated.

## Methods

### Patient population

In a retrospective study, signal data of thirty patients with severe cerebral diseases (age 18–77 years, mean 53±16 years, 20 male/10 female) were analyzed. Patients were treated in Chemnitz Medical Centre between 2006 and 2008. The patients suffered from TBI (n=15), subarachnoidal hemorrhage (n=9: traumatic n=5, spontaneous n=4), MCA infarction (n=2), intracerebral hemorrhage (n=11: traumatic n=3, spontaneous n=8), intracranial hematoma (n=9), sinus venous thrombosis, hypoxic encephalopathy, and encephalitis.

At the time of data recording, all the patients were sedated, paralyzed, and mechanically ventilated. Their arterial partial pressure of $CO_2$ ($PaCO_2$) ranged from 30–35 mmHg. During signal recording, ventilator settings were unchanged in order to keep $PaCO_2$ constant.

### Monitoring

Transcranial Doppler (TCD) measurements were taken using 2 MHz pulsed Doppler device (Multidop-P, DWL, Sipplingen, Germany). The envelope curve of CBFV in the middle cerebral artery (MCA) was continuously recorded in the hemisphere ipsilateral to brain lesion in most cases. The ultrasound probe was fixed mechanically with a holder frame or elastic headband. TCD recording was performed during stable periods free from nursing, physiotherapy, or tracheal suction. The clinical objective of recording was to assess the state of cerebral autoregulation [5].

ABP was measured with a standard manometer line inserted into the radial artery. ICP was measured using either implanted intraparenchymal or intraventricular microsensors (Raumedic GmbH, Helmbrechts, Germany).

### Computer-assisted recording

Personal computers equipped with data acquisition systems (Daq 112B, Iotech, Inc., Cleveland, OH, USA) and home written software [14] were used for recording and analyzing CBFV, ABP, and ICP signals. Sampling frequencies ranged from 25 Hz to 50 Hz. Signals were assessed during 60 minutes. If possible, recording was repeated at days 2, 4, and 7. Signal data was recorded initially at day 1 from all 30 patients (34 recordings), at day 2 from 28 patients (33 recordings), at day 4 from 19 patients (21 recordings) and at day 7 from 7 patients (8 recordings). In total 96 recordings of 30 patients were acquired.

### Assessment of cerebral autoregulation

Recorded signal data of CBFV, ABP, and ICP was initially filtered by a 0.15 Hertz low-pass filter in order to erase oscillations from breathing. Cerebral autoregulation was assessed in terms of Pearson's correlation coefficients of 60 consecutive samples (in steps of 5 seconds) of CBFV and CPP (=ABP-ICP) values, i.e. during 5-minute periods. These correlation indices were averaged, and resulted in the autoregulation index Mx [5]. Essentially being a correlation coefficient, Mx may take on every value between -1.0 and 1.0. In case of active CA, small cerebral arteries constrict during increase of CPP and dilate during decrease of CPP. That way, changes of CBF resistance compensate or even over-compensate the CPP change, which means that CBFV and CPP are not correlated or are negatively correlated, i.e. Mx becomes zero or negative. In case of impaired CA, CBFV passively follows changes of CPP, i.e. Mx becomes positive.

One Mx value was calculated for each signal recording. If related to a patient, Mx means the average Mx over all recordings of this patient. For dichotomous analysis of CA and survival a cut-off point of Mx above or below 0.2 was used.

All signal monitoring was part of a clinical routine and did not require individual consents. Local ethical committee approved this study.

## Results

Six of the patients died during their hospitalization. Mean age (± SD) in this group (Non-Survivors) was 53±12 years,

while mean age of the remaining 24 patients (Survivors) was 51±16. The difference of age in both groups was not significant (p=0.23).

Mx was significantly higher (p<0.05; students t-test) in the Non-Survivors group than in the Survivors group (0.28±0.40 versus 0.03±0.21). **Figures 1 and 2** present signal recordings from a patient in the non-survivors and a patient in the survivors group, respectively. Change of Mx during consecutive days of monitoring (i.e. Mx last day - Mx first day) was not significantly related to mortality (Non-Survivors: 0.14±0.35 versus Survivors: -0.17±0.38; p=0.17). Nine patients showed an Mx >0.2, four of them died, while in 21 patients Mx was <0.2, only two of them died (**Table 1**). This association between high Mx and mortality was significant (p<0.05; OR=7.6). In 21 patients, the 3-month Glasgow Outcome Score (GOS) could be assessed. In this subgroup, Mx significantly correlated with GOS (R=-0.56, p<0.05). **Figure 3** illustrates the correlation between Mx and GOS. In fourteen patients craniotomy was performed. Craniotomy was neither related to Mx (p=0.42) nor was it related to mortality (p=0.12).

**Table 1.** Relationship between Mx and mortality during hospitalisation.

| | Non-Survival | Survival | Sum |
|---|---|---|---|
| **Mx > 0.2** | 4 | 5 | 9 |
| **Mx < 0.2** | 2 | 19 | 21 |
| **Sum** | 6 | 24 | 30 |

In 9 patients Mx was on average higher than 0.2 (upper line). Four of these patients died. In the group of 21 patients with Mx below 0.2, only two patients died (lower line). Mortality was significantly higher in patients with high Mx, i.e. Mx>0.2 (p<0.05; Odds Ratio [OR] =7.6).

## Discussion

The results showed a moderate but significant association between increased Mx (indicating impairment of CA) and mortality during hospitalization. In addition a relationship between increased Mx index and GOS could be found, i.e. a decline of CA was related to poor clinical outcome. Mortality was neither associated with age nor with craniotomy intervention. A relationship between increased Mx and worse clinical outcome in TBI patients was shown in former studies [5]. Recently an association between unfavorable outcome and secondary increase of Mx in patients with intracerebral hemorrhage was reported [12]. In our study, an association between increased Mx and mortality could be stated in a population with diverse types of cerebral diseases including TBI as well as hemorrhagic and ischaemic stroke. But there was no significant association between secondary increase of Mx and mortality in our

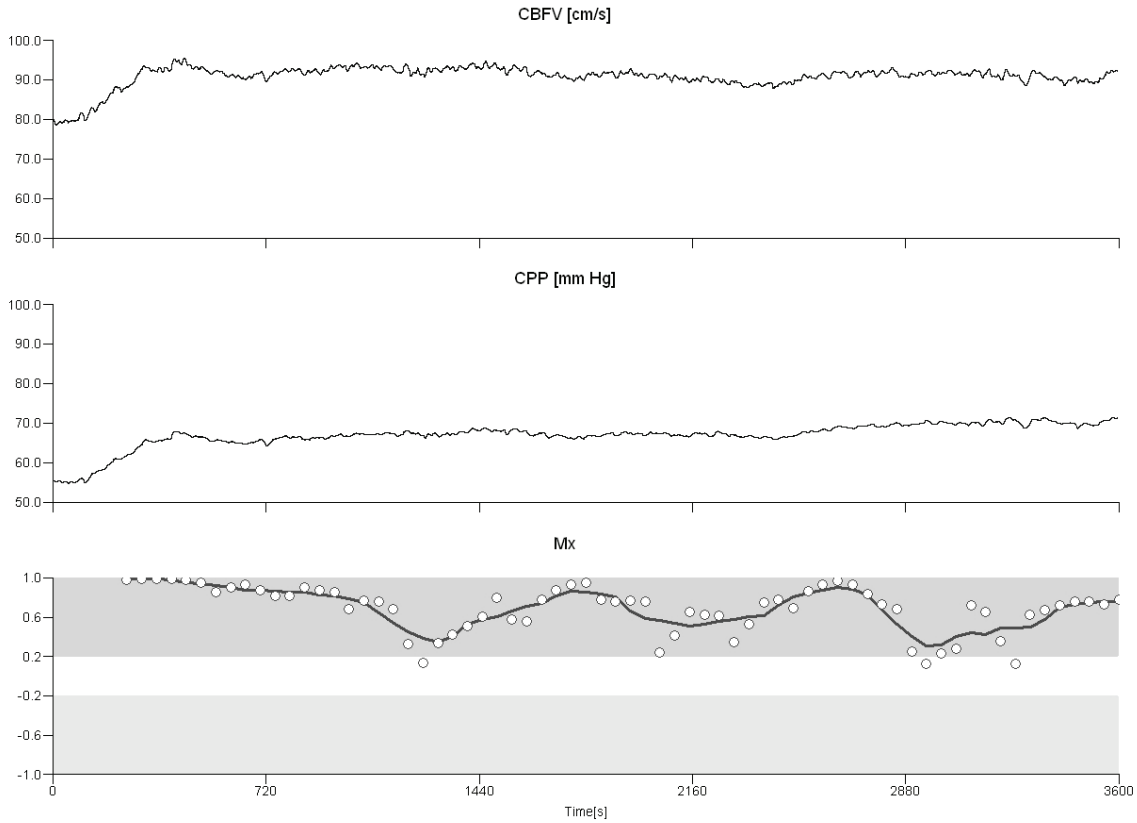


**Figure 1.** Signal recording of a 74 year-old patient with spontaneous subarachnoidal hemorrhage who died during hospitalization. CBFV, ABP, and ICP have been recorded for one hour, CPP has been calculated by means of ABP-ICP. CBFV (upper channel) and CPP (middle channel) signals have been filtered and Mx calculated (lower channel). The circles show the calculated correlation coefficients between CBFV and CPP. The curve is the moving average of five consecutive correlation coefficients. The Mx value related to this recording is 0.61 and was calculated as average over all correlation coefficients of this recording. This value corresponds to the optical impression of parallel curves of CPFV and CPP.

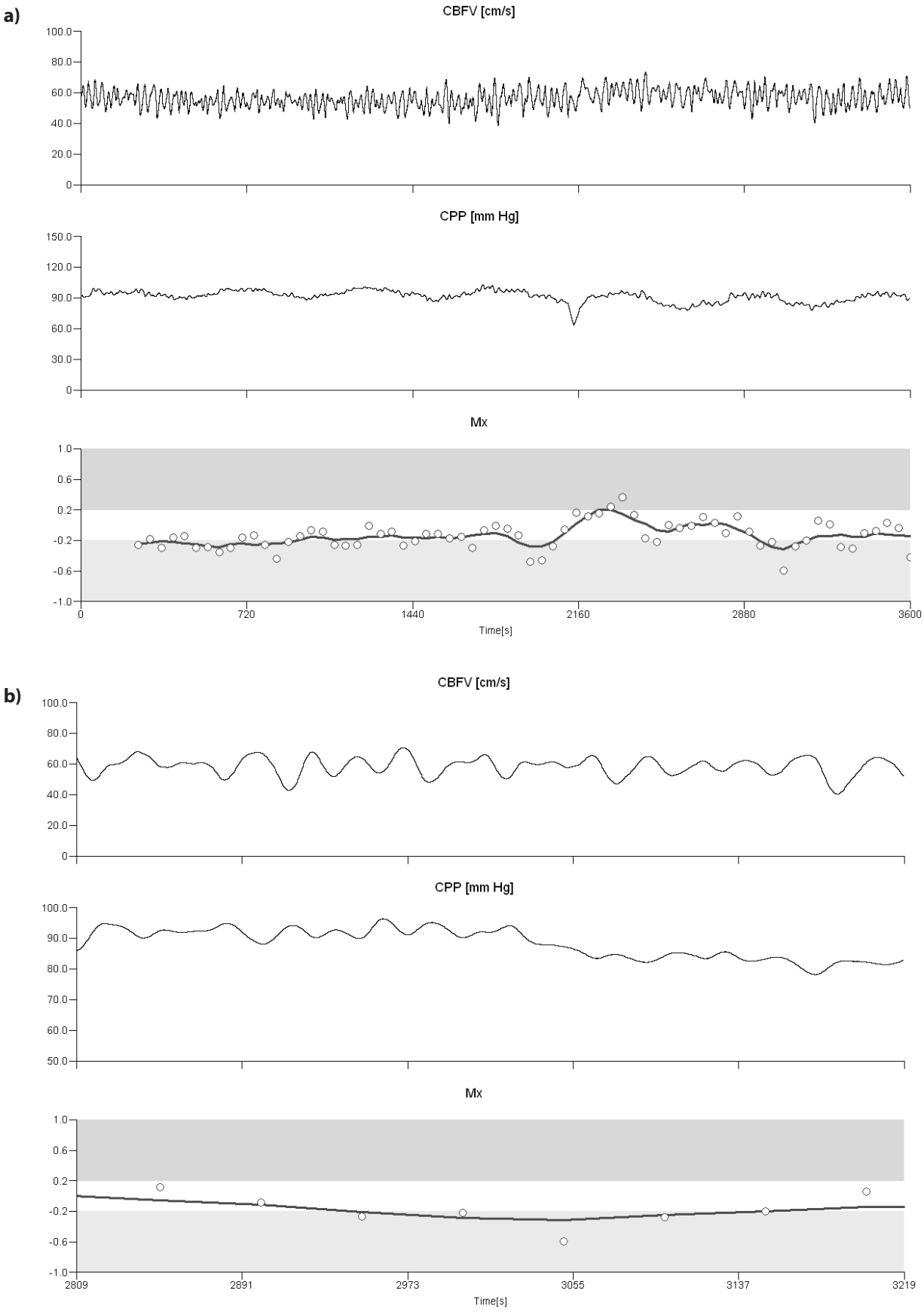


**Figure 2.** Signal recording of a 34-year-old patient with traumatic brain injury, part of the group of survivors, with unknown GOS. Signal processing was same as described under Fig. 1. CBFV (upper channel) and CPP (middle channel) signals have been filtered and Mx calculated (lower channel). The Mx value is -0.20 and was calculated as average over all correlation coefficients of this recording.

**a)** CBFV, CPP and Mx curves over the whole 1-hour time period.

**b)** CBFV, CPP and Mx curves during a 400-sec time subinterval. This graph clearly shows anti-parallel oscillations of CPFV and CPP, which correspond to a negative correlation between both curves.

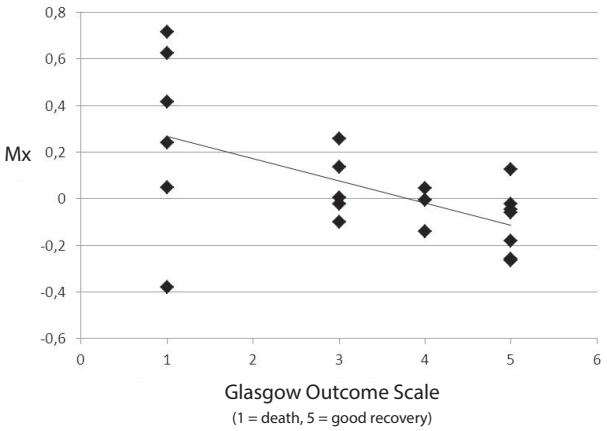


**Figure 3.** Mx versus Glasgow Outcome Score (GOS). In 21 cases with known 3-month GOS, Mx correlated negatively with GOS (R=-0.56, p<0.05). Higher Mx corresponded to a poorer outcome.

study. Especially in the Non-Survivors group Mx showed a high variation (SD=0.40). However, it remains unclear whether this can be explained by the heterogeneity of the population or whether high variability is an intrinsic property of this index.

Our choice of 0.2 as a critical threshold for increased Mx was somewhat arbitrary. However, its interpretation as an indicator of reduced CA was justified by its prognostic potential for outcome prognosis. In a recent study (Sorrentino et al., 2011 [11]) an Mx value of 0.3 was proposed to be the critical threshold for disturbed CA in TBI patients.

Only for 21 patients, we had access to a detailed GOS index. It cannot be ruled out that this might have yielded a bias in this sub-group. One obvious effect was the predominance of fatal outcome during hospitalization, because all fatal cases were registered. However, this could have only affected the analysis of correlation between GOS and Mx. In all other investigations, we restricted on a dichotomic classification of outcome into survival and non-survival. This study was based on a relatively small population of 30 patients. Especially in view of the inclusion of diverse types of cerebral diseases, it would be appropriate to conduct further studies with larger populations. Moreover, a larger population would also allow the analysis of specificity and sensitivity of Mx by means of ROC curve evaluation, which appears unsuitable in this study in view of the small number of events (lethal outcome, n=6).

It is not clear whether Mx was an independent predictor of clinical outcome. Investigation of a possible relationship between Mx and other clinical predictors was not subject of this study.

## Conclusions

Reduced CA with Mx >0.2 is significantly related to lethal outcome in patients with severe cerebral diseases. Increased Mx also corresponds to worse 3-month clinical outcome.

Former results of other centers with plain TBI population could be confirmed in this heterogeneous disease group. Further studies with larger populations and complete outcome information would be appropriate.

### Abbreviations

ABP: Arterial blood pressure; CA: Cerebral autoregulation; CBF: Cerebral blood flow; CBFV: Cerebral blood flow velocity; CPP: Cerebral perfusion pressure; GOS: Glasgow outcome score; ICP: Intracranial pressure; MCA: middle cerebral artery; PaCO2: Partial pressure of CO2; TBI: Traumatic brain injury; TCD: Transcranial Doppler

### Acknowledgments

Dr. M. Czosnyka is on leave from Warsaw University of Technology, Poland.

### Competing interests

The authors declare no conflict of interest.

### References

1. Enevoldsen EM, Jensen FT. Autoregulation and CO2 responses of cerebral blood flow in patients with acute severe head injury. J Neurosurg 1978; 48(5):689-703.
2. Lassen NA. Control of cerebral circulation in health and disease. Circ Res 1974; 34(6):749-60.
3. Aaslid R, Lindegaard KF, Sorteberg W, Nornes H. Cerebral autoregulation dynamics in humans. Stroke 1989; 20(1):45-52.
4. Diehl RR, Linden D, Lucke D, Berlit P. Phase relationship between cerebral blood flow velocity and blood pressure. A clinical test of autoregulation. Stroke 1995; 26(10):1801-4.
5. Czosnyka M, Smielewski P, Kirkpatrick P, Menon DK, Pickard JD. Monitoring of cerebral autoregulation in head-injured patients. Stroke 1996; 27(10):1829-34.
6. Panerai RB, White RP, Markus HS, Evans DH. Grading of cerebral dynamic autoregulation from spontaneous fluctuations in arterial blood pressure. Stroke 1998; 29(11):2341-6.
7. Zhang R, Zuckerman JH, Giller CA, Levine BD. Transfer function analysis of dynamic cerebral autoregulation in humans. Am J Physiol 1998; 274(1 Pt 2):H233-41.
8. Zhang R, Zuckerman JH, Levine BD. Spontaneous fluctuations in cerebral blood flow: insights from extended-duration recordings in humans. Am J Physiol Heart Circ Physiol 2000; 278(6):H1848-55.
9. Schmidt B, Czosnyka M, Raabe A, Yahya H, Schwarze JJ, Sackerer D, et al. Adaptive noninvasive assessment of intracranial pressure and cerebral autoregulation. Stroke 2003; 34(1):84-9.
10. Budohoski KP, Reinhard M, Aries MJ, Czosnyka Z, Smielewski P, Pickard JD, et al. Monitoring cerebral autoregulation after head injury. Which component of transcranial Doppler flow velocity is optimal? Neurocrit Care 2012; 17(2):211-8.
11. Sorrentino E, Budohoski KP, Kasprowicz M, Smielewski P, Matta B, Pickard JD, et al. Critical thresholds for transcranial Doppler indices of cerebral autoregulation in traumatic brain injury. Neurocrit Care 2011; 14(2):188-93.
12. Reinhard M, Neunhoeffer F, Gerds TA, Niesen WD, Buttler KJ, Timmer J, et al. Secondary decline of cerebral autoregulation is associated with worse outcome after intracerebral hemorrhage. Intensive Care Med 2010; 36(2):264-71.
13. Reinhard M, Rutsch S, Lambeck J, Wihler C, Czosnyka M, Weiller C, et al. Dynamic cerebral autoregulation associates with infarct size and outcome after ischemic stroke. Acta Neurol Scand 2012; 125(3):156-62.

14. Schmidt B, Czosnyka M, Schwarze JJ, Sander D, Gerstner W, Lumenta CB, et al. Evaluation of a method for noninvasive intracranial pressure assessment during infusion studies in patients with hydrocephalus. J Neurosurg 2000; 92(5):793-800.

INTERNATIONAL JOURNAL OF
CLINICAL NEUROSCIENCES
AND MENTAL HEALTH

ORIGINAL RESEARCH

# Capability of cerebral autoregulation assessment in arteriovenous malformations perinidal zone

Vladimir Semenyutin[1], Grigory Panuntsev[1], Vugar Aliev[1], Andreas Patzak[2], Dmitry Pechiborsch[1], and Alexandr Kozlov[1]

Special Issue on Neurosonology and Cerebral Hemodynamics

## Abstract

**Background:** Cerebral autoregulation (CA) in the region of an intracranial artery involved in blood supply of arteriovenous malformations (AVM) is impaired. This could be due to pathologic shunting, disguising real state of CA, or brain lesion in perinidal area. It is quite difficult to define the influence of both factors on CA. The purpose of this study was to assess dynamics of CA in patients with AVM in perioperative period.

**Methods:** The radicality of AVM embolization (Hystoacryl or Onyx) was evaluated in 47 patients by cerebral angiography and blood flow index in precerebral arteries with a Vivid E ultrasound scanner. We monitored blood flow velocity (BFV) in basal cerebral arteries with Multi Dop X and blood pressure (BP) with Finapres-2300. CA was assessed with cuff test (autoregulation index – ARI) and phase-shift (PS) between spontaneous oscillations of BP and BFV within the range of Mayer's waves.

**Results:** Preoperative values of ARI and PS were 1.8±0.7 and 0.3±0.2 rad, respectively. In 15 cases with total embolization a significant ($p<0.005$) increase of rate of CA (ARI: 6.0±1.1, PS: 0.9±0.1 rad) was noted. In other two cases with total embolization, CA didn't change significantly after operation. In 14 cases with subtotal embolization postoperative ARI and PS were 3.6±0.5 and 0.7±0.1 rad, respectively ($p<0.05$), and in cases with partial elimination were 2.1±0.6 and 0.4±0.1 rad ($p>0.05$).

**Conclusion:** CA assessment could be used for detection of its real impairment in perinidal zone of AVM during the staged endovascular treatment and for prognostication of postoperative complications.

**Keywords:** Cerebral autoregulation, Cerebral blood flow volume, Arteriovenous malformation, Embolization

[1]Russian Polenov Neurosurgical Institute, St. Petersburg, Russia
[2]Johannes-Mueller Institute of Physiology University Hospital Charité, Humboldt-University of Berlin, Berlin, Germany

Correspondence: Vladimir Semenyutin
Russian Polenov Neurosurgical Institute
191014 Mayakovsky str. 12, St.Petersburg, Russia
Email adress: lbcp@mail.ru

Citation: Semenyutin et al. Capability of cerebral autoregulation assessment in arteriovenous malformations perinidal zone. IJCNMH 2014; 1(Suppl. 1):S19

Received: 09 Sep 2013; Accepted: 06 Nov 2013; Published: 09 May 2014

Open Access Publication Available at http://ijcnmh.arc-publishing.org



ARC Publishing

## Introduction

Comprehension of specific hemodynamic features in cerebral arteriovenous malformations (AVM) is a key to good treatment outcome. Cerebral autoregulation (CA) is an important adaptive mechanism of cerebral hemodynamic stability [1–4]. Introduction of transcranial Doppler (TCD) in clinical practice improved timely diagnosis of cerebral hemodynamic disorders and prognosis of outcome in patients on different stages of endovascular treatment [5–7]. Continuous multichannel monitoring of blood flow velocity (BFV) in intracranial arteries and systemic arterial blood pressure (BP) using advanced TCD technique makes possible noninvasive assessment of CA with cross-spectral analysis as well as thigh-cuff test [8–11].

AVM is a congenital deformity which is characterized by the absence of capillary network and high rate of arteriovenous shunting. The occurrence of AVM is estimated at 18 per 100,000 population per year. The main symptoms of AVM are intracranial hemorrhage and epileptic seizures. Superselective embolization with different kind of embolizing materials (Histoacryl, Onyx) is one of the main methods of AVM treatment aiming at exclusion of abnormal vessels of AVM from circulation.

Due to the absence of normal resistive component in the structure of AVM, the major pathogenic mechanism of disease progression is low vascular resistance, as well as absence of regulation in afferent vessels of AVM and its network. This causes formation of pathologic blood flow shunting through AVM, which is its specific hemodynamic feature.

The vasomotor reactivity and rate of CA has been shown to decrease in cerebral arteries, predominantly in the arteries feeding cerebral AVM [12, 13]. Major cerebral arteries are more accessible for noninvasive insonation of BFV than arteries of second and third order. Hence all used methods allow detection of decreased rate of CA, mostly in a major cerebral artery, which feeds both the shunting structure (nidus) through hypertrophic afferent vessels of an AVM and surrounding brain (perinidal zone) perfused by this artery. Decrease of CA rate in a territory perfused by a major cerebral artery happens due to significant shunting and total CA impairment in AVM's vessels and possible decrease of CA rate in the arteries of perinidal zone. In case of significant shunting process, AVM may disguise true value of CA rate in zones of brain nearby AVM network. In case of less prominent shunting, the data of CA assessment in the region of a major artery would reflect rather true functional value of resistive vessels feeding brain adjacent to AVM.

Thus, investigation of CA in major arteries feeding AVM in staged exclusion of AVM from circulation by embolization (decrease of shunting flow) will promote detection of true impairment of CA in the perinidal zone. The latter will make natural disease progression, surgery, and postoperative period more predictable.

The purpose of this study is to assess the dynamics of CA in patients with cerebral AVM in perioperative period.

## Methods

Forty seven (47) patients (age range 22-63 years) with cerebral AVM were studied. All patients were divided into groups according to the Spetzler-Martin classification [14]. In 12 patients AVM corresponded to I-II grades, in 24 patients had grade III AVM, and 11 patients had grade IV AVM. AVMs were embolized either with Hystoacryl or Onyx through afferent vessels originated from the middle cerebral artery (MCA) and the anterior cerebral artery (ACA). All patients had a standard preoperative workup including CT angiography, cerebral MRI with MR angiography, ultrasound Doppler of cerebral arteries, as well as additional methods of CA evaluation and extent of AVM embolization.

TCD with bilateral monitoring of BFV in basal cerebral arteries, as well as thigh-cuff test were performed by MultiDop X, DWL (Germany). Monitoring of BP by CNAP (Austria) was performed parallel to BFV monitoring. CA was assessed by thigh-cuff test (autoregulation index – ARI) and phase shift (PS) in cross-spectral analysis of spontaneous oscillations of BP and BFV in basal cerebral arteries within the range of Mayer's waves. Data were processed with conventional statistical programs (Statistica 7.0 for Windows, Excel). Parametric (Student) and non-parametric (Kolmogorov-Smirnov) tests were used. Difference was considered to be statistically significant if $p<0.05$.

Extent of embolization was evaluated by intraoperative cerebral angiography. 16 patients had color Doppler of both internal carotid arteries (ICA) and vertebral arteries (VA) before and after surgery with evaluation of total flow index by ultrasound scanner Vivid E (USA). Thus, in patients with cerebral AVMs, flow velocity index ($FVI_{total}$) was calculated. We also investigated 26 healthy volunteers (13 men and 13 women) with color Doppler of both ICA and VA to assess normal total flow index ($FVI_{norm}$), which was 661±91 mL/min for males and 560±82 mL/min for females. Then shunting blood flow was calculated as $FVI_{shunt} = FVI_{total} - FVI_{norm}$. $FVI_{norm}$ was put in accordance with patients' gender.

All patients were divided into three groups depending on the extent of embolization based on angiographic images. Seventeen (17) patients were included in the group with total AVM embolization, in whom 75–100% of AVM volume was excluded. Subtotal embolization (50–75%) was achieved in 14 patients. Partial occlusion of AVM (up to 50%) was performed in 16 patients.

## Results

Preoperative study in all patients revealed decreased CA in basal cerebral artery feeding AVM. ARI was 1.8±0.7, PS was 0.3±0.2 rad.

Endovascular intervention and early postoperative period in all patients were without complications. In general, postoperative investigation showed positive dynamics of CA, the degree of which was different in groups. Patients with total exclusion of AVM from circulation in 15 cases (12 patients – I, II grades, 3 patients – III grade by Spetzler-Martin) had significant ($p<0.05$) increase of CA (ARI after surgery was 6.0±1.1, PS was 0.9±0.1 rad). Other 2 patients with total AVM occlusion (grade III by Spetzler-Martin) did not have significant changes in CA after surgery. Mean values of ARI and PS in entire group of total embolization were 4.6±1.4 and 0.9±0.2 rad respectively ($p<0.05$).

The dynamics of CA in patients with subtotal embolization (14 patients with AVM grade III) was also significant ($p<0.05$): postoperative ARI and PS were 3.6±0.5 and 0.7±0.1 rad, respectively.

Partial embolization was achieved in 5 patients with grade III AVM and in all patients with grade IV AVM (n=11). Changes of CA rate were insignificant ($p>0.05$) in these cases: ARI was 2.1±0.6, PS was 0.4±0.1 rad.

CA dynamics in relation with extent of AVM embolization is shown on the **Figure 1**. In patients with total AVM embolization much more considerable changes in PS and ARI (**Figure 1b**) were observed.

A clear dependence was revealed in 16 patients comparing PS and shunting flow indexes obtained during preoperative investigation: in cases with a higher shunting flow PS in basal cerebral artery on the AVM side was less (**Figure 2a**). The same dependence during investigation of PS on the contralateral side was less significant (**Figure 2b**).

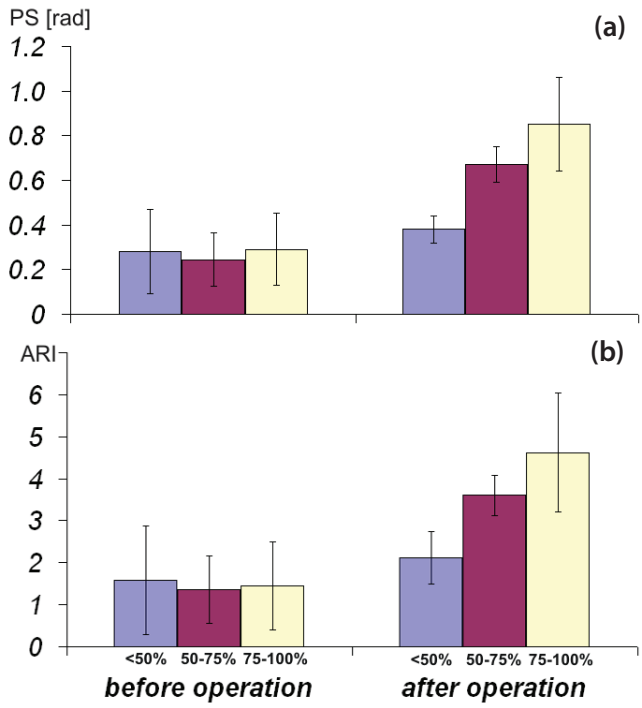


**Figure 1.** Perioperative values of phase shift (PS) **(a)** and autoregulation index (ARI) **(b)** in comparison with extent of arteriovenous malformations (AVM) embolization.

Results of investigation of a female patient (40 years-old) with AVM in left frontal lobe fed through perforating vessels of left ACA are presented on the **Figure 3**. Before surgery PS was 0.4 rad, ARI was 2, $FVI_{total}$ was 947 mL/min. Both PS and ARI increased up to normal values (1.0 rad and 6, respectively) after total AVM embolization in one session of embolization by Onyx. FVI in left ICA decreased from 458 to 233 mL/min.

Results of investigation of a female patient (44 years -old) with AVM in left frontal lobe fed by left ACA are presented in **Figure 4**. Before surgery PS was 0.2 rad, ARI was 2, $FVI_{total}$ was 733 mL/min. PS did not change (0.5 rad) after total AVM occlusion in one session of embolization by Onyx. ARI was also 2. $FVI_{total}$ decreased insignificantly – to 618 mL/min. FVI in left ICA decreased from 316 to 241 mL/min.

Results of investigation of a 41 year old patient with AVM of the right temporal lobe fed by short vessels of the right MCA are presented in **Figure 5**. Before surgery PS in MCA was reduced to 0.5 rad, ARI was 1. $FVI_{total}$ was 1221 mL/min. PS did not change after surgery (0.5 rad), ARI was 2. $FVI_{total}$ decreased significantly, to 920 mL/min. FVI in the right ICA decreased from 493 to 395 mL/min.

## Discussion

There is no consensus in the literature concerning impairment of CA and cerebral perfusion in brain adjacent and distant to AVM, as well as significance of this impairment for presenting clinical symptoms, disease progression and prognosis of complications in the postoperative period.

There are studies in which authors assessed cerebral blood flow in patients with AVM with $Xe^{133}$ inhalation using single photon-emission tomography. Signs of hypoperfusion in structurally intact zones of the brain distant to AVM have been revealed. The reason for decrease of blood flow in the perinidal zone and the contralateral side was explained by decrease of BP in proximal parts of afferent vessels, due to the presence of significant shunt through AVM and consequently a decrease of pressure on the level of arterial cerebral circle of Willis [15–17]. The latter in turn causes decrease of pressure in intact perinidal arteries and on the contralateral side, which in case of impairment of CA and cerebrovascular reactivity may be accompanied by reduction of cerebral blood flow. Young W.L. et al. [18] suggested that chronic hypotension in normal vascular zones adjacent to AVM induces adaptation of lower limit of CA, which provides constancy of blood flow. There is opinion that CA in the afferent vessel's territory feeding both AVM and adjacent brain initially impaired since own AVM vessels lack CA ability due to altered histological structure of the vessel wall [19, 20].

Nowadays endovascular surgery is the preferred method of AVM treatment. Technology improvements, new types of embolizing materials in particular, make embolization more manageable. As a result, multi-stage opera-

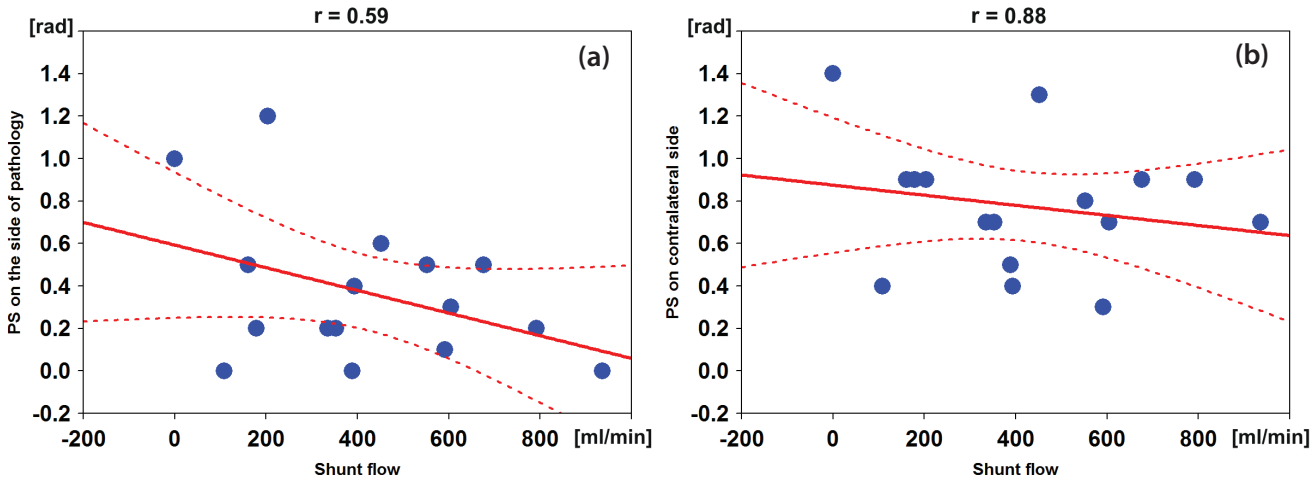


**Figure 2.** Relations between shunting flow and phase shift (PS) **(a)** on the side of arteriovenous malformations (AVM ), **(b)** contralateral side.

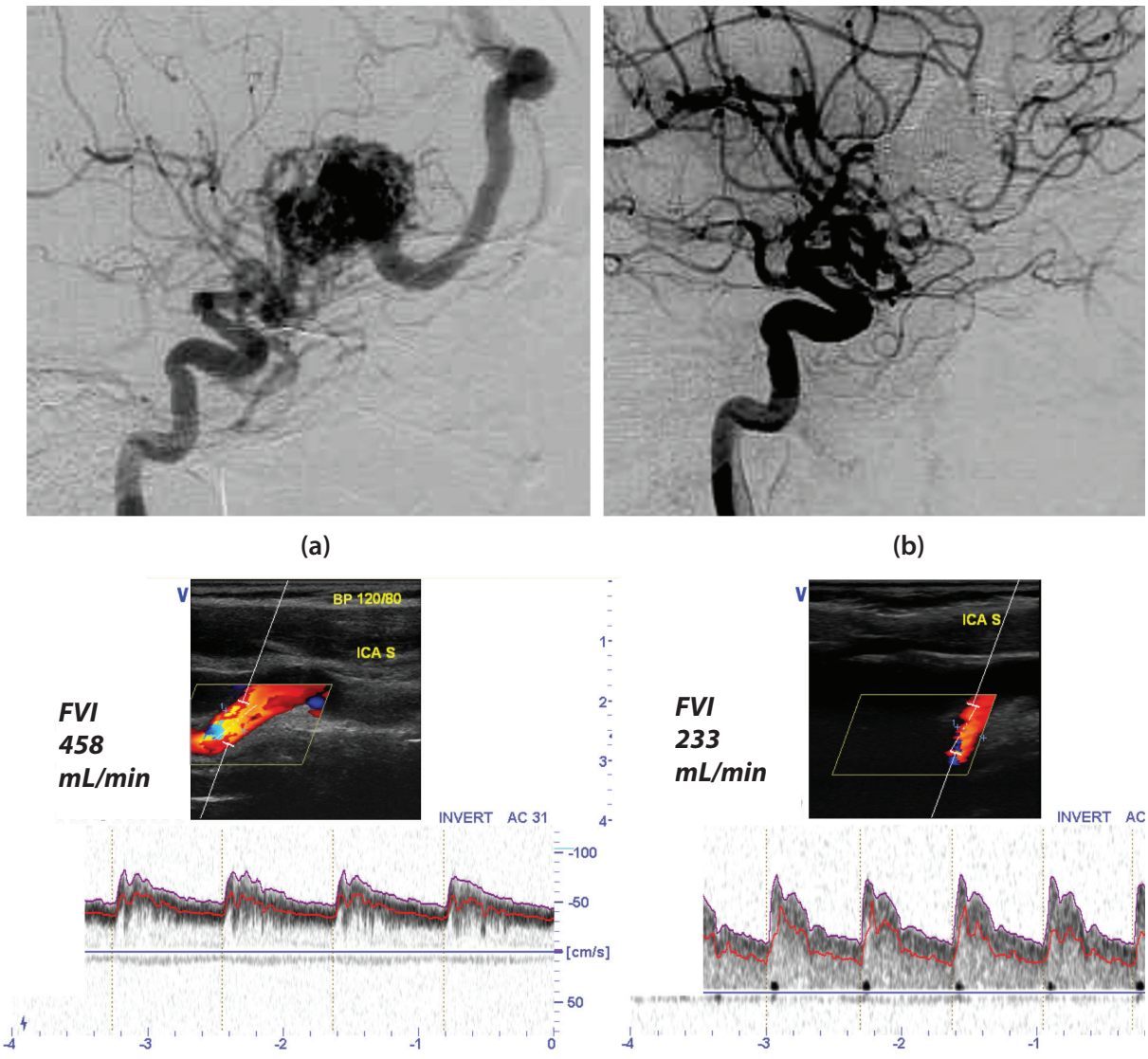


**Figure 3**. Carotid angiograms and results of color Doppler in the left internal carotid arteries (ICA) with calculation of flow index before **(a)** and after **(b)** total arteriovenous malformations (AVM) embolization by Onyx in a 40 year old patient (case 1) with AVM in the left frontal lobe.

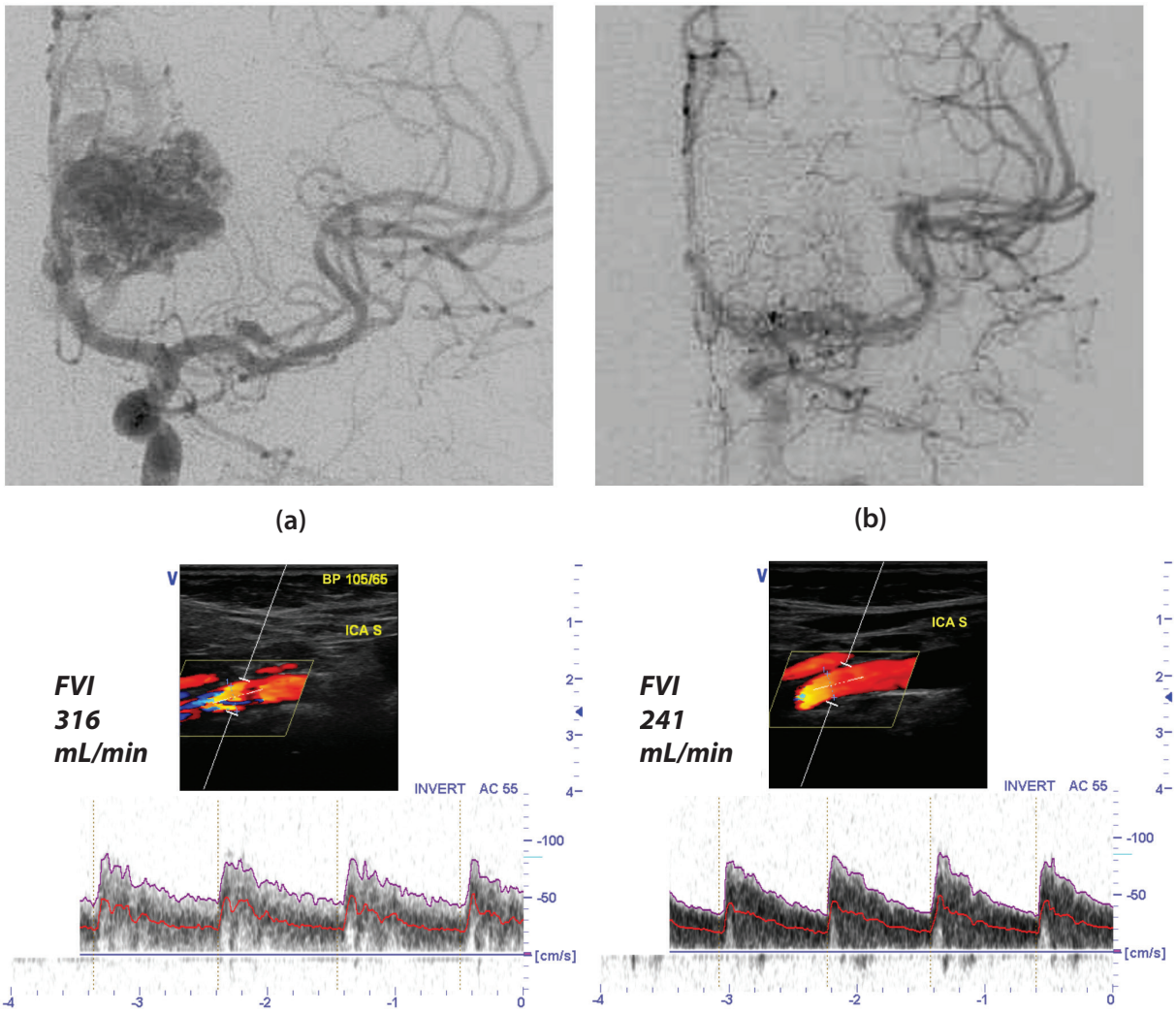


**Figure 4**. Carotid angiograms and results of color Doppler in the left internal carotid arteries (ICA) with calculation of flow index before **(a)** and after **(b)** total arteriovenous malformations (AVM) embolization by Onyx in a 44 year old patient (case 2) with AVM in the left frontal lobe.

tions are performed, which exclude compartments or the whole AVM depending on its size, structure, and number of afferent vessels. Perioperative bilateral monitoring of BFV in basal cerebral arteries with parallel BP monitoring, further cross-spectral analysis and calculation of the PS between the M-waves of BFV and BP, thigh-cuff test with calculation of ARI allow for assessment of CA dynamics after different (in terms of extent of exclusion) embolizations of AVM.

Our data show an increase of CA rate in the early postoperative period after embolization of the pathological process. Changes of CA are most evident after total embolization of AVM. Yet in some patients CA impairment was preserved even after radical exclusion of AVM from the circulation (case 2), which may indicate true CA impairment in the perinidal zone due to shunting.

Cases 1 and 2 have much in common: around the same volume of AVM, carotid origin of blood-supplying, one-stage total embolization. There were differences between these cases as well concerning different degree of shunting flow in both AVMs. In case 1, $FVI_{total}$ before embolization was increased by 2 times in comparison with normal values, which indicates high shunting flow through AVM nidus. In case 2, $FVI_{total}$ before operation differed from normal values much less but was also higher. In case 1, AVM was supplied by MCA, in case 2 by ACA. Possible difference in AVM structure cannot be excluded as reason of dissimilarity of $FVI_{total}$. The aforementioned differences may have various mechanisms of influence on the vascular territory where AVM and perinidal zone are located, which in turn could lead to difference in CA rate dynamics in these cases: full recovery in case 1, and no change in case 2. It is not clear why in latter case CA didn't improve after total embolization of AVM. Possibly there are other factors besides shunting compromising circulation of perinidal zone (e.g. persistent ischemia due to inadequate collateral flow), which are not eliminated after total embolization of AVM and still may affect state of CA postoperatively.

Further investigations should be directed to pathologic mechanisms determining circulation both in AVM

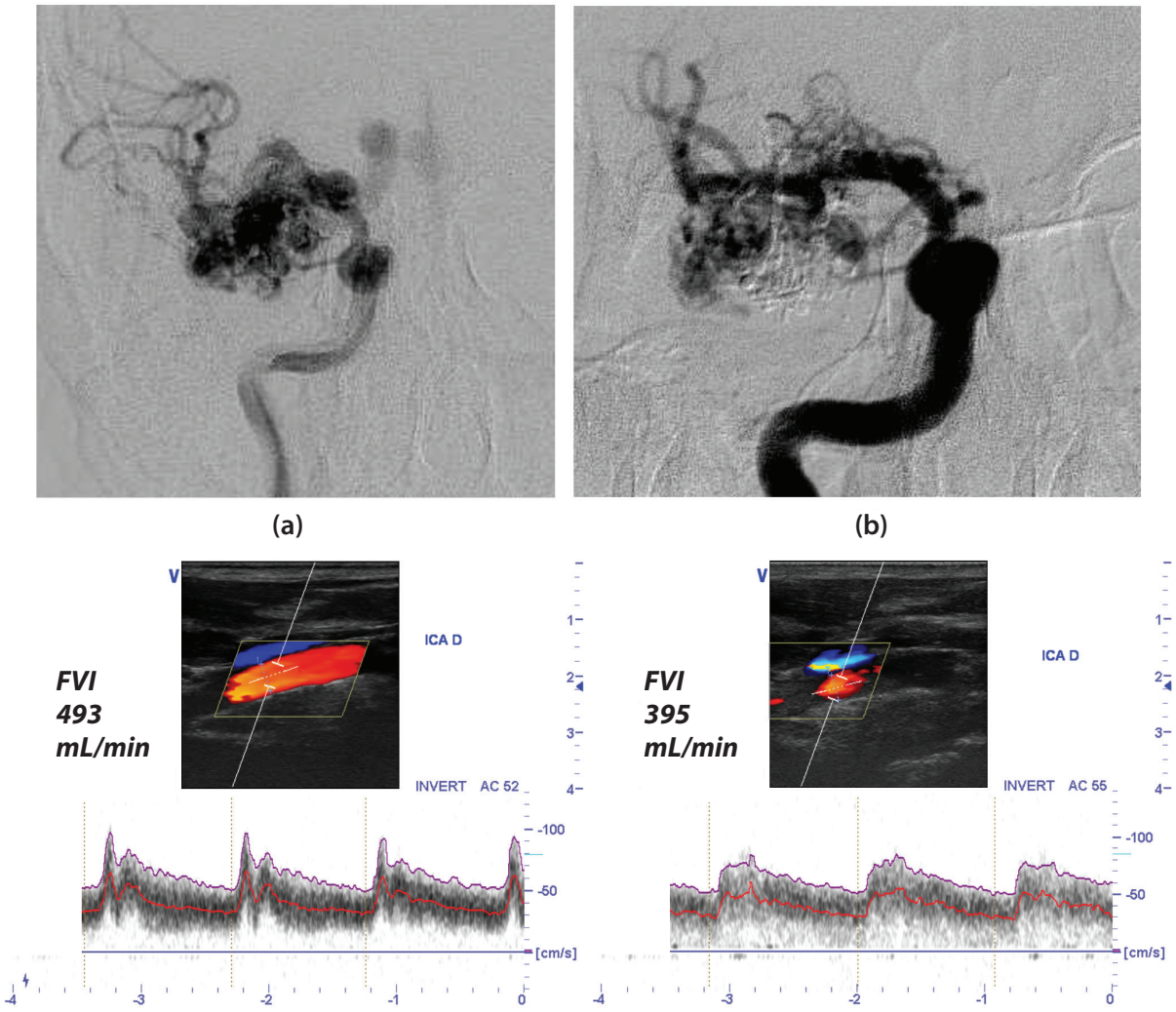


**Figure 4.** Carotid angiograms and results of color Doppler in the left internal carotid arteries (ICA) with calculation of flow index before **(a)** and after **(b)** total arteriovenous malformations (AVM) embolization by Hystoacryl in a 45 year old patient (case 3) with AVM in the right temporal lobe.

and surrounding brain. Detailed analysis of clinical symptoms, hemodynamics, CA dynamics in these patients in the perioperative period will explain causes of different treatment outcomes. The obtained results may be used for determination of surgical strategy, management of patients in the postoperative period, and prognosis of possible neurologic complications.

## Conclusion

Assessment of the CA in AVM major feeding arteries, during staged exclusion of AVM from circulation (stepwise decrease of shunting process), will help to reveal true impairment of CA in the perinidal zone, to find the optimal surgical strategy, and to better predict treatment outcomes.

### Abbreviations

ACA: Anterior cerebral artery; ARI: autoregulation index; AVM: Arteriovenous malformations; BFV: Blood flow velocity; BP: Blood pressure; CA: Cerebral autoregulation; FVI: Flow velocity index; ICA: Internal carotid arteries; MCA: Middle cerebral artery; PS: Phase shift; TCD: Transcranial Doppler; VA: Vertebral arteries

### Competing interests

The authors declare no conflict of interest.

### References

1. Fog M. Cerebral circulation: The reaction of the pial arteries to a fall in blood pressure. Arch Neurol Psychiatry 1937; 37:351-64.
2. Lassen NA. Autoregulation of cerebral blood flow. Circ Res 1964; 15 (suppl 1): 201-4.
3. McHenry L, West J, Cooper E, et al. Cerebral autoregulation in man. Stroke 1974; 5(6):695-706.
4. Strandgaard S, Paulson O. Cerebral autoregulation. Stroke 1984; 15(3):413-6.
5. Aaslid R, Markwalder T, Nornes H. Noninvasive transcranial ultrasound recording of flow velocities in basal cerebral arteries. J Neurosurg 1982; 57(6):769-74.
6. Gaĭdar BV, Parfenov VE, Svistov DV. Dopplerographic assessment of the autoregulation of the blood supply to the brain in neurosurgical pathology. Zh Vopr Neirokhir Im N N Burdenko 1998; (3):31-6.

7. Panerai R. Assessmant of cerebral pressure autoregulation in humans – a review of measurement methods. Physiol Meas 1998; 19(3):305-38.
8. Aaslid R, Lindegaard KF, Sorteberg W, et al. Cerebral autoregulation dynamics in humans. Stroke 1989; 20(1):45-52.
9. Semenyutin V, Aliev V, Nikitin P, et al. The intracranial B-waves amplitude as prognostication criterion of neurological complications in neuroendovascular interventions. Acta Neurochir Suppl 2005; 94:53-8.
10. Zhang R, Zuckerman J, Giller C, et al. Transfer function analysis of dynamic cerebral autoregulation in humans. Am J Physiol 1998; 274:H233-H241.
11. Panerai R, White R, Markus H, et al. Grading of cerebral dynamic autoregulation from spontaneous fluctuations in arterial blood pressure. Stroke 1998; 29(11):2341-6.
12. Diehl R.R, Henkes H, Nahser HC, et al. Blood flow velocity and vasomotor reactivity in patients with arteriovenous malformations. A transcranial Doppler study. Stroke 1994; 25(8):1574-80.
13. Diehl RR, Linden D, Lücke D, et al. Phase relationship between cerebral blood flow velocity and blood pressure: a clinical test of autoregulation. Stroke 1995; 26(10):1801-4.
14. Spetzler RF, Martin NA. A proposed grading system for arteriovenous malformations. J Neurosurg 1986; 65(4):476-483.
15. Homan RW, Devous MD Sr, Stokely EM, et al. Quantification of intracerebral steal in patients with arteriovenous malformation. Arch Neurol 1986; 43(8):779-85.
16. Hacein-Bey L, Nour R, Pile-Spellman J, et al. Adaptive changes of autoregulation in chronic cerebral hypotension with arteriovenous malformations: an acetazolamide-enhanced single-photon emission CT study. AJNR Am J Neuroradiol 1995; 16(9):1865-74.
17. Marks MP, O'Donahue J, Fabricant JI, et al. Cerebral blood flow evaluation of arteriovenous malformations with stable xenon CT. AJNR Am J Neuroradiol 1988; 9(6):1169-75.
18. Young WL, Pile-Spellman J, Prohovnik I, et al. Evidence for adaptive autoregulatory displacement in hypotensive cortical territories adjacent to arteriovenous malformations. Columbia University AVM Study Project. Neurosurgery 1994; 34(4):601-11.
19. Moo LR, Murphy KJ, Gailloud P, et al. Tailored cognitive testing with provocative amobarbital injection preceding AVM embolization. AJNR Am J Neuroradiol 2002; 23(3):416-21.
20. Wakhloo BB, Lieber R, Siekmann DJ, et al. Acute and Chronic Swine Rete Arteriovenous Malformation Models: Hemodynamics and Vascular Remodeling. AJNR Am J Neuroradiol 2005; 26(7):1702-6.

INTERNATIONAL JOURNAL OF
CLINICAL NEUROSCIENCES
AND MENTAL HEALTH

ORIGINAL RESEARCH

# Convergent cross mapping: a promising technique for cerebral autoregulation estimation

Linda Heskamp[1,2], Aisha S.S. Meel-van den Abeelen[1], Joep Lagro[1], and Jurgen A.H.R. Claassen[1]

Special Issue on Neurosonology and Cerebral Hemodynamics

## Abstract

**Background:** Cerebral autoregulation (CA) is the physiological mechanism that keeps the cerebral blood flow velocity (CBFV) relatively constant despite changes in arterial blood pressure (ABP). Currently, transfer function analysis (TFA) is widely used to assess CA non-invasively. TFA is based on the assumption that CA is a linear process, however, in reality CA is a non-linear process. This study explores the usability of convergent cross mapping (CCM) as a non-linear analysis technique to assess CA.

**Methods:** CCM determines causality between variables by investigating if historical values of a time-series X(t) can be used to predict the states of a time-series Y(t). The Pearson correlation is determined between the measured Y(t) and the predicted Y(t) and increases with increasing time-series length to converge to a plateau value. When used for CA, normal and impaired CA should be distinguishable by a different plateau value. With impaired CA, ABP will have a stronger influence on CBFV, and therefore the CBFV signal will contain more information on ABP. As a result, the correlation converges to a higher plateau value compared to normal CA. The CCM method was validated by comparing normal CA (normocapnia: breathing 0-2% $CO_2$) with a model of impaired CA (hypercapnia: breathing 6-7% $CO_2$).

**Results:** CCM correlation was higher (p=0.01) during hypercapnia (0.65 ± 0.16) compared to normocapnia (0.51 ± 0.18).

**Conclusion:** CCM is a promising technique for non-linear cerebral autoregulation estimation.

**Keywords:** Cerebral autoregulation, Convergent cross mapping, Non-linear analysis.

[1]Department of Geriatric Medicine, Radboud University Medical Centre, Nijmegen, The Netherlands

[2]MIRA Institute for Biomedical Technology and Technical Medicine, Faculty of Science and Technology, University of Twente, Twente, The Netherlands

Citation: Heskamp et al. Convergent cross mapping: a promising technique for cerebral autoregulation estimation. IJCNMH 2014; 1(Suppl. 1):S20

Received: 02 Jul 2013; Accepted: 13 Nov 2013; Published: 09 May 2014

Correspondence: Jurgen A.H.R. Claassen
Radboud University Medical Centre
925, PO Box 9101, 6500 HB, Nijmegen, The Netherlands
Email adress: Jurgen.Claassen@radboudumc.nl

## Introduction

The high metabolic demand of the brain requires an adequate cerebral blood flow (CBF). However, changes in arterial blood pressure (ABP) or intracranial pressure may influence CBF. To keep CBF relatively constant and to return CBF to baseline after a fast change in ABP, adaption of the cerebrovascular resistance (CVR) occurs. This process is called cerebral autoregulation (CA) [1]. When CA is disturbed, the brain may become excessively sensitive to fluctuations in ABP, causing hypo- and/or hyperperfusion. Hypo- and hyperperfusion can lead to ischemia or haemorrhages, respectively [2]. CA failure has been associated with increased morbidity and mortality [3]. Therefore, the ability of accurately quantifying the quality of CA may be of great importance in clinical practice.

CA can be determined as static CA or dynamic CA. With static CA, the response of the CBF to changes in ABP is studied in a semi-steady state, i.e. a measurement of CBF is obtained first at a constant baseline ABP and constant CBF, followed by another measurement that is taken after the autoregulatory response to a manipulation of ABP has been completed [4]. However, static CA represents the overall effect of the autoregulatory action, but does not address the time in which this is achieved.

The use of Transcranial Doppler (TCD) ultrasound combined with servo-controlled finger photoplethysmography makes it possible to measure the process of CA itself, the dynamic CA [2, 5]. Ideally, clinical monitoring of CA should be non-invasive, continuous, bedside, and precise. Because static CA measurement only provides steady-state point measurements and therefore is not a continuous measurement, the dynamic approach is preferable.

Despite the importance of measuring dynamic CA, there is no consensus about the best way to analyze dynamic CA [6]. Currently, the most frequently described method in the literature is transfer function analysis (TFA) [6]. However, this method is based on the assumption that the relation between ABP and CBF is linear, while physiologically CA exhibits nonlinear dynamics [7]. In our study, a new non-linear analysis method, convergent cross mapping (CCM) is applied to asses dynamic CA. Originally CCM was proposed to detect causality in complex ecosystems. According to its definition, CA can be quantified as the causal influence of ABP on CBF and this causal influence can be determined with CCM. Therefore the goal of this study is to explore the use of CCM in assessing dynamic CA.

## Methods

### Experimental procedure

The CCM model was validated by comparing normocapnic data with hypercapnic data. Hypercapnia causes vasodilation of the cerebral vasculature and can therefore be used as a model for impaired CA [8]. This study included 19 healthy adults, male and female, with an age of 69 ± 4 (mean ± SD). ABP was measured non-invasively in the middle finger of the right hand using photoplethysmography (Finapres Medical Systems, Amsterdam, the Netherlands). The hand and arm were supported securely and comfortably with a sling, providing a stable position of the hand and arm at the heart level. It has been shown that ABP measured indirectly using the Finapres is a reliable technique to track changes in ABP that correlate well with auscultatory ABP measurements in the upper arm [9]. TCD is used to measure CBF velocity (CBFV) in the middle cerebral artery (MCA) by insonating the left and right MCA using a 2 MHz TCD probe (Multi-Dop, Compumedics DWI, Germany) [10]. It is assumed that changes in CBFV represent changes in CBF, because the diameter of the vessel remains constant [8, 11]. End tidal $CO_2$ ($etCO_2$) was monitored with a nasal cannula using capnography (Biopax Systems, Goleta, Ca, USA). ABP, CBFV and $etCO_2$ were recorded with a 200 Hz sampling frequency.

Subjects were asked to inhale a gas mixture mimicking room air, containing 0% $CO_2$, 21% $O_2$, and 79% $N_2$ through a tightly fitting mouthpiece until a stable plateau of CBFV had been reached. Next, the percentage of $CO_2$ was increased every 30 seconds, until a $CO_2$ concentration of 7% was obtained. The first 90 seconds with a 0-2% $CO_2$ concentration and the last 90 seconds with 6-7% $CO_2$ were selected as normocapnia and hypercapnia, respectively. Beat-to-beat data of the ABP and CBFV were obtained using a low pass fourth-order Butterworth filter with a cut-off frequency of 0.5 Hz. Thereafter, CBFV and ABP were downsampled to a sampling frequency of 10 Hz.

### Data analysis

*Mathematical background of convergent cross mapping*

Sugihara et al. [12, 13] presented CCM as a new non-linear analysis method to determine causality between variables in a dynamical system. CCM is described in detail by Sugihara et al [12, 13]. In short, a dynamical system can be represented by a so called attractor manifold (M). **Figure 1A** depicts as example the manifold of the Lorentz attractor consisting of three variables, represented by the time-series X(t), Y(t) and Z(t). Interestingly, the dynamics of a system can also be represented using only one of the time-series, for example Y(t). Lagged coordinates of this time-series, for example Y(t-τ) and Y(t-2τ) can be used to reconstruct a shadow manifold My. (**Figure 1B**). Tau (τ) is defined as a number of samples. My reproduces the two-lobed butterfly of M, i.e. My represents the dynamics of M. Similarly, shadow manifolds Mx and Mz can be reconstructed using X(t) and Z(t), respectively. CCM consists of two main steps that use these shadow manifolds to determine causality between variables: cross mapping and convergence.

*Cross mapping*

In a dynamical system, consisting of two variables (X(t) and Y(t)), cross mapping investigates if it is possible to

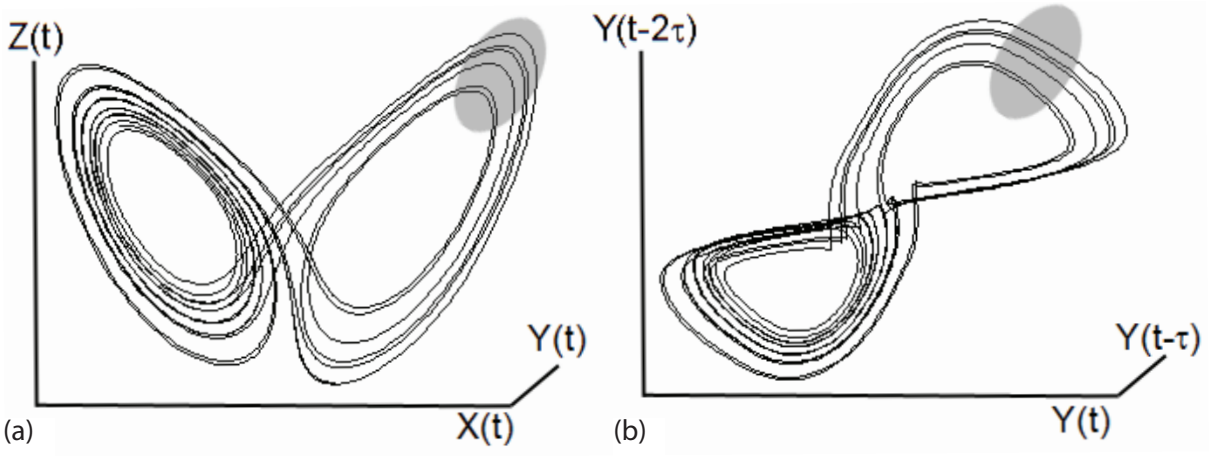


**Figure 1. (a)** Attractor Manifold (M) of the Lorenz attractor. A point of M is defined by X(t), Y(t) and Z(t). **(b)** Shadow manifold My with E=3 dimensions and τ = 1.4 seconds. Each point on the manifold is defined by Y(t), Y(t-τ) and Y(t-2τ). The grey area in A corresponds to the grey area in B. E = dimensions of the shadow manifold, τ = time-lag. Adapted from Sugihara et al. [12].

predict a point on My from Mx using the nearest neighbor principle.

This nearest neighbor principle is depicted in **Figure 2**. Point A is a random point on Mx and A' is the in time corresponding point of A on My. The basic principle is that if nearest neighbors of A on Mx can accurately predict A' on My, it can be stated that historical values of X(t) can be used to estimate states of Y(t). This is only possible if X(t) contains information on Y(t), in other words as Y(t) causally influences X(t).

Cross mapping is applied to each point on Mx resulting in a prediction of Y(t): $Y_{Pred}(t)$. To estimate the accuracy of the $Y_{Pred}(t)$, the correlation between the $Y_{Pred}(t)$ and Y(t) is determined.

*Convergence*

Convergence is based on the fact that the longer the time-series length of X(t) and Y(t), the smaller the distance between the trajectories on the manifold. As a result, the estimation error decreases. Therefore, if Y(t) causally influences X(t), the correlation should increase to a plateau value with increasing time-series length, which is defined as convergence. The faster the convergence the stronger the coupling between the two variables.

**Figure 3** illustrates the convergence principle [13]. The cases that Y(t) does, and Y(t) does not causally influence X(t) are represented by the solid and dashed line, respectively.

*Validation of CCM*

CCM is applied to determine CA quality during normocapnia (0-2% $CO_2$) and hypercapnia (6-7% $CO_2$). As CA quality can be quantified as the causative effect of ABP on CBFV, the shadow manifold of CBFV was used to predict ABP. Generically, the shadow manifold maps 1:1 to the original manifold M. If a 1:1 mapping occurs then the shadow manifold is defined as an embedding [14]. Optimal embedding parameters, embedding dimension E and lag τ, were determined with the method of Gautama et al. [15], which is based on differential entropy. The determined optimal embedding parameters were E is 3 dimensions and τ is 1 sample. In this study, the correlation corresponding to the plateau value was used instead of the rate of convergence. A window of 890 samples was used to calculate the plateau value. Shifting the window of 890 samples through the entire dataset results in 10 correlations of which the mean is determined. The complete algorithm of CCM is described in more detail in the Supplementary materials of Sugihara et al. [13].

### Statistical analysis

Results are presented as means ± standard deviation. Statistical significance was tested using a paired t-test. Significance was set at $p < 0.05$.

## Results

**Figure 4** depicts the correlation results for normocapnia and hypercapnia. The correlation differed between normocapnia (0.51 ± 0.18) and hypercapnia (0.65 ± 0.16), $p = 0.01$.

## Discussion

Our study showed that the non-linear method of CCM is able to distinguish normal dynamic CA from impaired dynamic CA. In clinical practice, the ability to measure CA may be of great importance, as impaired CA can result in hypo- or hyperperfusion of the brain. Impaired CA is also associated with increased morbidity and mortality [3].

Several methods have been developed to measure CA, however no gold standard exists. In literature, TFA is currently the most applied method to quantify CA. However,

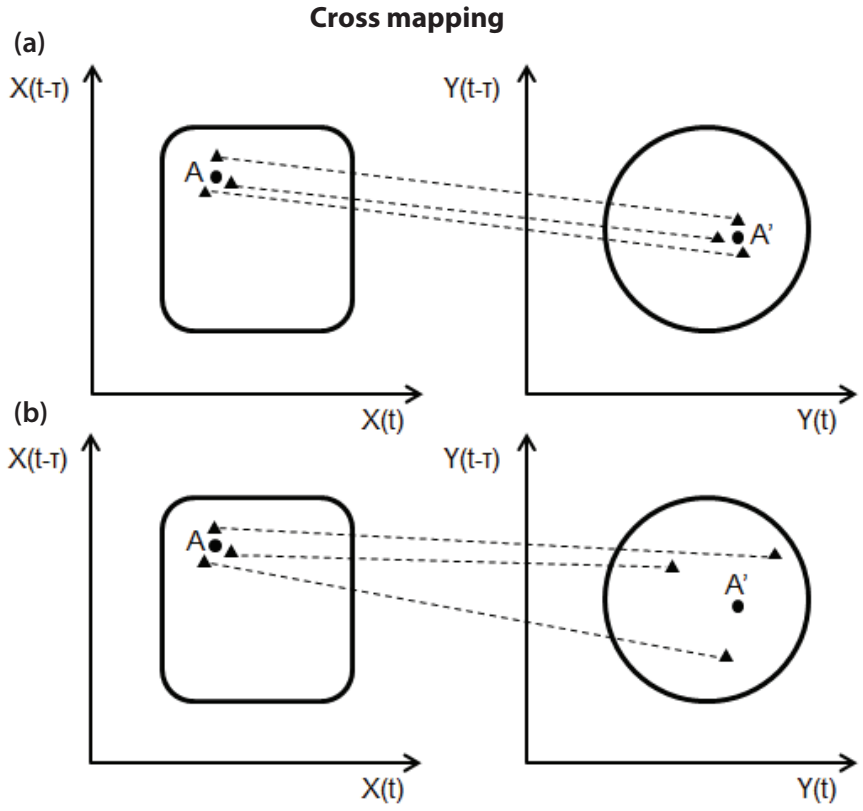


**Figure 2.** The nearest neighbor principle. **(a)** Nearest neighbors (triangles) of point A (dot) on Mx are also nearest neighbors of the in time corresponding point A' on My. Therefore Mx can be used to estimate the states of Y(t), i.e. Y(t) causally influences X(t). **(b)** Nearest neighbors (triangles) of point A (dot) on Mx are not nearest neighbors of point A' on My. Therefore Mx cannot be used to estimate the states of Y(t). Mx: shadow manifold of M with time-lagged coordinates of X(t) (E=2). My: shadow manifold of M with time-lagged coordinates of Y(t) (E = 2). E = dimension of the shadow manifold. Adapted from Sugihara et al. [13].

this technique assumes that CA is a linear process, while in fact CA exhibits non-linear dynamics. Zhang et al. [16] pointed out that a coherence <0.5 in the low frequency range using TFA is an indicator of non-linear behavior of CA. In addition, Mitsis et al. [7] showed that with the use of a non-linear model (Laguerre-Voltera network) a 20% reduction of the normalized mean square error was seen compared to a linear model when predicting CBFV based on the input ABP.

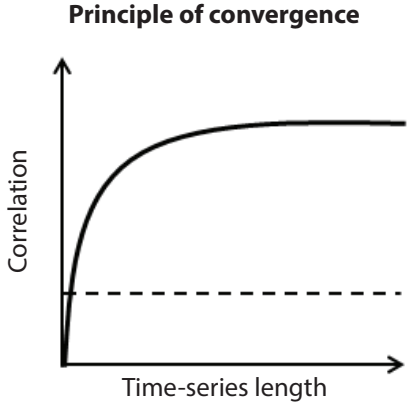


**Figure 3.** Principle of convergence. **Solid line:** Y causally influences X. **Dashed line:** Y does not causally influence X. The solid line shows convergence with increasing time-series length while the dashed line does not. Adapted from Sugihara et al. [13].

CCM is a non-linear analysis technique, which was originally proposed by Sugihara et al. [12] to detect causality in complex ecosystems. They applied CCM on a classic predator-prey dynamic system. In a classic predator-prey dynamic system, there is bidirectional causality between the predator and the prey, i.e. they both causally influence each other. The correlation converged when predicting the state of the prey using the predator data and also when predicting the state of the predator using the prey data. This indicates indeed that both factors causally influence each other. CCM was also applied on a dynamical system of sardines, anchovies and sea surface temperature. CCM showed that anchovies and sardines do not causally influence each other, but are both causally influenced by the sea surface temperature.

As CCM takes non-linear dynamics into account, this technique might also be more accurate for the quantification of CA. A well-functioning CA attenuates the effect of changes in ABP on changes in CBF, i.e. ABP has as only a small causal influence on CBF. During impaired CA the effect of changes in ABP on changes in CBF are less attenuated, i.e. ABP has a larger causal influence on CBF. There-

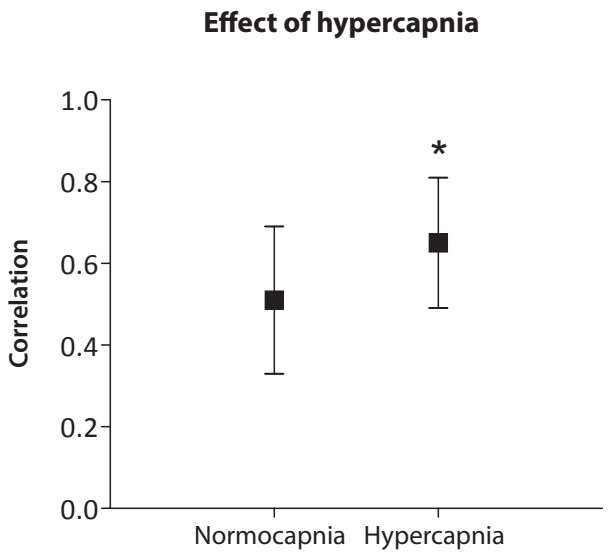


**Figure 4.** Correlation between real ABP and predicted ABP during normocapnia and hypercapnia circumstances (n=19). Correlation is significantly increased during hypercapnia (breathing 6-7% $CO_2$) compared to normocapnia (breathing 0-2% $CO_2$).
* p<0.05. ABP = arterial blood pressure.

fore the causal influence of ABP on CBF is a measure of impairment of CA and CCM can be applied to assess the functioning of CA.

In this study, the ability of CCM to quantify CA was explored using a hypercapnia model. Hypercapnia is a well-known model to simulate impaired CA [17]. Hypercapnia causes vasodilation, reducing the ability of the cerebral vessels to respond to changes in ABP, leading to impaired CA. In our study a significantly higher CCM correlation value was found during hypercapnia which indicates a less efficiently functioning CA. This underlines the potential of CCM to quantify CA.

However, still a large spread is seen in the outcome of CCM. The standard deviation was 0.2 and 0.16 for normo- and hypercapnia, respectively. Therefore, optimization of this technique is necessary before it can be easily applied in clinical practice.

There are several explanations for the large spread in CCM outcomes. First, the degree of impaired CA of each subject during hypercapnia is unknown and might differ between subjects. As a results, the spread in CCM outcome is large. However, breathing 7% $CO_2$ is the physiological limit. Therefore it is likely that all subjects did reach their plateau of impaired CA.

Second, besides the possible difference in effect of the $CO_2$ on CA in subjects during hypercapnia, also the breath-to-breath $etCO_2$ fluctuations in normo- and hypercapnia circumstances between subjects might influence the correlation. Mitsis et al. [18] showed that $etCO_2$ fluctuations have a considerable effect in the lower frequencies, i.e. below 0.04 Hz. Incorporating the breath-to-breath $etCO_2$ fluctuations might therefore reduce the spread in CCM outcome.

Third, the respiratory frequency is below 0.5 Hz and because the respiratory frequency is below the cut-off frequency of 0.5 Hz, it is still present in the ABP and CBFV signal. If the respiratory frequency is very constant, prediction of ABP using CBFV might be easier because the fluctuations caused by respiration are then very predictable. This might result in a high CCM outcome value. On the other hand, if the respiratory frequency is less constant, prediction of ABP using CBFV is harder, because the fluctuations caused by the respiration are less predictable. This results in a lower CCM outcome value. Therefore, differences in variability of the respiratory frequency between subjects might be responsible for the large spread in CCM outcome. Using a low-pass filter with a cut-off frequency of 0.15 Hz might reduce the large spread in CCM outcome, because the breathing frequency is above 0.15 Hz. Because CA is most prominent in frequencies below 0.15 Hz, it can be justified to use a cut-off frequency of 0.15 Hz.

Besides the large spread in CCM outcome values, it should also be noted that in this study the plateau value was used to quantify the causal influence of ABP on CBFV instead of the rate of convergence as suggested by Sugihara et al. [12]. The choice for the plateau value was based on a pilot study in which the validity of the model was investigated using the autoregulatory index of Tiecks et al. [4]. In this pilot study, the plateau value could discriminate the autoregulatory indexes. However, a situation might be possible in which the correlation does not converge, but remains horizontal (dashed line in **Figure 3**). In this case, using only the plateau value, might give inaccurate results. If this correlation is high, the plateau value falsely represents a high influence of the ABP on CBFV while actually there is no influence at all. Using the rate of convergence overcomes this problem. In our study, convergence was seen in all subjects during normo- and hypercapnia. Therefore, using the plateau value was seen as a valid choice in this study. Furthermore, calculating the rate of convergence is more time-consuming than calculating the plateau value. This plateau value is therefore more promising for bedside CA monitoring.

Furthermore it should be noted that the used embedding parameters were E=3 dimensions and $\tau$=1 sample. These embedding parameters were determined using the differential entropy technique [15]. A $\tau$ of 1 sample is a delay of 0.1 seconds, which is within one heartbeat. It is difficult to interpret this $\tau$ physiologically, because a $\tau$ of at least one heartbeat (± 8-10 samples) is expected.

## Conclusions

The ideal clinical monitoring device of CA should be non-invasive, continuous, bedside and precise. CCM is indeed a non-invasive measurement which uses spontaneous fluctuations of the ABP and CBFV to assess CA. The use of spontaneous fluctuations has the additional advantage that

no interventions have to be performed, making continuously measuring CA possible.

Furthermore, CCM can quantify CA using small datasets and the outcome of CCM is a single value, which is very important and practical for bedside monitoring. When the spread in CCM outcome can be reduced, perhaps with the aforementioned optimizations, CCM could be a very promising technique for future bedside monitoring of CA.

## Abbreviations

ABP: Arterial blood pressure; CA: Cerebral autoregulation; CBF: Cerebral blood flow; CBFV: Cerebral blood flow velocity; CCM: Convergent cross mapping; CVR: Cerebrovascular resistance; $etCO_2$: End tidal $CO_2$; MCA: Middle cerebral artery; TCD: Transcranial Doppler; TFA: Transfer function analysis

## Competing interests

The authors declare no conflict of interest.

## References


1. Lassen NA. Cerebral blood flow and oxygen consumption in man. Physiol Rev 1959; 39(2):183-238.
2. Willie CK, Colino FL, Bailey DM, Tzeng YC, Binsted G, Jones LW, et al. Utility of transcranial Doppler ultrasound for the integrative assessment of cerebrovascular function. J Neurosci Methods 2011; 196(2):221-37.
3. Hu K, Peng CK, Czosnyka M, Zhao P, Novak V. Nonlinear assessment of cerebral autoregulation from spontaneous blood pressure and cerebral blood flow fluctuations. Cardiovasc Eng 2008; 8(1):60-71.
4. Tiecks FP, Lam AM, Aaslid R, Newell DW. Comparison of static and dynamic cerebral autoregulation measurements. Stroke 1995; 26(6):1014-9.
5. Aries MJ, Elting JW, De Keyser J, Kremer BP, Vroomen PC. Cerebral autoregulation in stroke: a review of transcranial Doppler studies. Stroke 2010; 41(11):2697-704.
6. van Beek AH, Claassen JA, Rikkert MG, Jansen RW. Cerebral autoregulation: an overview of current concepts and methodology with special focus on the elderly. J Cereb Blood Flow Metab 2008; 28(6):1071-85.
7. Mitsis GD, Zhang R, Levine BD, Marmarelis VZ. Modeling of nonlinear physiological systems with fast and slow dynamics. II. Application to cerebral autoregulation. Ann Biomed Eng 2002; 30(4):555-65.
8. Aaslid R, Lindegaard KF, Sorteberg W, Nornes H. Cerebral autoregulation dynamics in humans. Stroke 1989; 20(1):45-52.
9. Imholz BP, Wieling W, Langewouters GJ, van Montfrans GA. Continuous finger arterial pressure: utility in the cardiovascular laboratory. Clin Auton Res 1991; 1(1):43-53.
10. Aaslid R, Markwalder TM, Nornes H. Noninvasive transcranial Doppler ultrasound recording of flow velocity in basal cerebral arteries. J Neurosurg 1982; 57(6):769-74.
11. Newell DW, Aaslid R, Lam A, Mayberg TS, Winn HR. Comparison of flow and velocity during dynamic autoregulation testing in humans. Stroke 1994; 25(4):793-7.
12. Sugihara G, May R, Ye H, Hsieh CH, Deyle E, Fogarty M, et al. Detecting causality in complex ecosystems. Science 2012; 338(6106):496-500.
13. Sugihara G, May R, Ye H, Hsieh C, Deyle E, Fogarty M, et al. Supplementary Materials for Detecting Causality in Complex Ecosystems. Science 2012; 338(6106):496-500.
14. Takens F. Detecting strange attractors in turbulence. In: Rand D, Young L-S, editors. Dynamical Systems and Turbulence, Warwick 1980: Springer Berlin Heidelberg; 1981. p. 366-81.
15. Gautama T, Mandic DP, Van Hulle MM, editors. A differential entropy based method for determining the optimal embedding parameters of a signal. Acoustics, Speech, and Signal Processing, 2003 Proceedings (ICASSP '03) 2003 IEEE International Conference on; 2003 6-10 April 2003.
16. Zhang R, Zuckerman JH, Giller CA, Levine BD. Transfer function analysis of dynamic cerebral autoregulation in humans. Am J Physiol 1998; 274(1 Pt 2):H233-41.
17. Ainslie PN, Celi L, McGrattan K, Peebles K, Ogoh S. Dynamic cerebral autoregulation and baroreflex sensitivity during modest and severe step changes in arterial PCO2. Brain Res 2008; 1230:115-24.
18. Mitsis GD, Poulin MJ, Robbins PA, Marmarelis VZ. Nonlinear modeling of the dynamic effects of arterial pressure and CO2 variations on cerebral blood flow in healthy humans. IEEE Trans Biomed Eng 2004; 51(11):1932-43.

INTERNATIONAL JOURNAL OF
CLINICAL NEUROSCIENCES
AND MENTAL HEALTH

ORIGINAL RESEARCH

# Continuous monitoring of vertebrobasilar hemodynamics utilizing TCDS transducer holder Sonopod during postural changes

Toshiyuki Shiogai[1], Mayumi Yamamoto[1], Yuka Arima[1], Daichi Yamasaka[2], Kenji Yoshikawa[3], Toshiki Mizuno[4], and Masanori Nakagawa[4]

Special Issue on Neurosonology and Cerebral Hemodynamics

## Abstract

**Background:** The objective was to evaluate continuous monitoring in the vertebrobasilar arteries (VBA), utilizing the transducer holder Sonopod for transcranial color duplex sonography (TCDS), vertebrobasilar hemodynamics and autoregulation, during postural changes.

**Methods:** Subjects were five normal controls and seven patients: two patients with arterial hypertension, three with dizziness (peripheral neuropathy, hepatic cirrhosis, and unknown), one with lacunar infarction and diabetes mellitus (LI/DM), and one with spino-cerebellar degeneration (SCD). TCDS utilizing the transducer holder Sonopod was used to continuously monitor the intracranial VA and BA. Blood pressure (BP), heart and respiration rates were also monitored. During two series of postural changes (supine or sitting to/from standing), a) clinical symptoms, b) BP: systolic, mean, and diastolic pressures (SBP, MBP, and DBP), c) TCDS: time-averaged maximum velocity (Vmax) and pulsatility Index (PI), estimated cerebrovascular resistance (eCVR) = MBP/Vmax, and autoregulation index (ARI) = %ΔeCVR/%ΔMBP, were all calculated on the basis of maximum and minimum values during both series and of separate values from sitting to standing.

**Results:** a) Severe dizziness resulted in an inability to remain standing in two patients (LI/DM and SCD). b) BP: 1) ΔDBP >10mmHg in all cases. 2) ΔSBP>20mmHg in 2 controls and all but one patient (LI/DM). c) TCDS: 1) ΔPI and ΔeCVR tended to increase in the two severe dizziness patients. 2) ARI for both normal control subjects and patients fluctuated in all series and during individual standing.

**Conclusion:** Continuous TCDS monitoring in the VBA during postural changes is capable of evaluating vertebrobasilar autoregulation associated with autonomic regulation.

**Keywords:** Transcranial color duplex sonography, Transducer holder sonopod, Vertebrobasilar artery, Autoregulation, Postural changes.

[1]Department of Clinical Neurosciences, Kyoto Takeda Hospital, Kyoto, Japan
[2]Department of Radiology, Kyoto Takeda Hospital, Kyoto, Japan
[3]Department of Stroke Medicine, Hoshigaoka Kouseinenkin Hospital, Osaka, Japan
[4]Department of Neurology, Kyoto Prefectural University of Medicine, Kyoto, Japan

Correspondence: Toshiyuki Shiogai
Departments of Clinical Neurosciences, Kyoto Takeda Hospital
Minamikinuta-cho 11, Nishinanajo, Shimogyo-ku, Kyoto 600-8884, Japan
Email adress: shiogait@pop11.odn.ne.jp

Citation: Shiogai et al. Continuous monitoring of vertebrobasilar hemodynamics utilizing TCDS transducer holder Sonopod during postural changes. IJCNMH 2014; 1(Suppl. 1):S21

Received: 08 Sep 2013; Accepted: 29 Nov 2013; Published: 09 May 2014

## Introduction

Orthostatic intolerance is associated with various symptoms caused by hypotension during postural changes due to autonomic dysregulation [1]. The hypothesis is that these symptoms result from cerebral dysautoregulation in the vertebrobasilar artery (VBA) system. Autoregulation (AR) in the VBA has been studied in normal subjects utilizing a hand-held probe with conventional transcranial Doppler sonography (TCD) [2-5].

Recently, continuous suboccipital monitoring with a transducer fixation device has been introduced for the evaluation of vasoreactivity [6, 7] and detection of high intensity transient signals [8]. We have introduced and improved a transducer holder, named the Sonopod, for transcranial color duplex sonography (TCDS) monitoring via both temporal/suboccipital windows [9, 10]. However, no AR study has yet been carried out in the VBA utilizing a transducer holder for TCDS.

The objective of this study is to clarify the significance of continuous monitoring in the VBA, utilizing the transducer holder Sonopod for TCDS, and in this way vertebrobasilar hemodynamics and autoregulation were evaluated during postural changes.

## Methods

Subjects were five normal controls and seven patients (aged 23-75, mean 53 years); two patients had hypertension, three had dizziness (peripheral neuropathy, liver cirrhosis, and unknown), one had a lacunar infarction and diabetes mellitus (LI/DM), and one had spino-cerebellar degeneration (SCD). TCDS utilizing the transducer holder Sonopod has monitored continuously the intracranial vertebral artery (VA) and basilar artery (BA). Blood pressure (BP), heart and respiration rates were also monitored. During two series of postural changes (supine or sitting for 3-5 minutes to/from standing for 3-5 minutes), it was registered a) clinical symptoms, b) BP: systolic, mean, and diastolic pressures (SBP, MBP, and DBP), c) TCDS: time-averaged maximum velocity (Vmax) and pulsatility index (PI), estimated cerebrovascular resistance (eCVR) = MBP/Vmax. Autoregulation index (ARI) = %ΔeCVR/%ΔMBP were calculated on the basis of maximum and minimum values during both series: %ΔeCVR = (eCVR maximum - eCVR minimum)/eCVR minimum and %ΔBP = (BP maximum - BP minimum)/BP minimum.

Also individual ARIst during two series of standing (= %ΔeCVR/%ΔMBP) were based on separate values from sitting (or supine) to standing: %ΔeCVR = (eCVR standing - eCVR sitting or supine)/eCVR sitting or supine and %ΔBP = (BP standing - BP sitting or supine)/BP sitting or supine.

## Results

a) Clinical symptoms: Severe dizziness resulted in an inability to remain standing in two patients (LI/DM and SCD). No symptoms during postural changes were observed in the remaining 5 patients or 5 normal control subjects.

b) BP (**Table 1**): DBP increased at least 10mmHg in all cases. SBP increased at least 20 mmHg in 2 normal controls and in all but one patient (LI/DM). Hypotension during standing was remarkable only in the SCD patient.

c) TCDS (**Table 1**): ΔPI and ΔeCVR tended to increase in the two severe dizziness patients. ARIs in both normal control subjects and patients fluctuated in all series and during individual standing.

**Table 1.** Demographic characteristics of the study population.

| Case | Age/ Sex | Diagnosis | Artery | ΔSBP (mmHg) | ΔMBP (mmHg) | ΔDBP (mmHg) | ΔVmax (cm/s) | ΔPI | ΔeCVR | %ΔeCVR | %ΔMBP | ARI | ARIst1 | ARIst2 |
|---|---|---|---|---|---|---|---|---|---|---|---|---|---|---|
| DY | 23M | Normal | BA | 19 | 21 | 10 | 5.3 | 0.33 | 1.00 | 0.56 | 0.33 | 1.70 | 1.62 | -0.05 |
| MY | 24F | Normal | BA | 11 | 10 | 16 | 11.2 | 0.75 | 0.49 | 0.37 | 0.12 | 3.08 | 2.21 | -9.54 |
| RS | 68M | Normal | LVA | 11 | 31 | 13 | 8.2 | 0.61 | 1.55 | 0.66 | 0.39 | 1.69 | 2.18 | 1.94 |
| KI | 23M | Normal | BA | 34 | 32 | 18 | 22.5 | 0.50 | 1.60 | 0.98 | 0.39 | 2.51 | 3.39 | 2.50 |
| YN | 60M | Normal | BA | 20 | 23 | 10 | 16.0 | 0.40 | 0.44 | 0.30 | 0.25 | 1.20 | -9.05 | 1.47 |
| MN | 65F | HT | BA | 22 | 24 | 23 | 6.2 | 0.40 | 0.77 | 0.37 | 0.30 | 1.23 | 0.66 | 2.17 |
| TS | 60M | HT | RVA | 25 | 18 | 17 | 6.1 | 0.26 | 1.03 | 0.31 | 0.20 | 1.55 | 5.46 | 16.20 |
| MY | 67F | SCD | BA | 20 | 16 | 14 | 11.8 | 1.16 | 2.18 | 0.72 | 0.25 | 2.88 | -12.30 | -1.47 |
| MK | 75M | LI/DM | RVA | 15 | 9 | 13 | 1.4 | 1.22 | 1.73 | 0.24 | 0.16 | 1.50 | 0.09 | ND |
| KN | 63M | dizziness/ LC | BA | 40 | 25 | 13 | 8.0 | 0.39 | 1.15 | 0.73 | 0.32 | 2.28 | 0.24 | 0.63 |
| SM | 66M | dizziness | BA | 21 | 14 | 10 | 5.0 | 0.30 | 0.74 | 0.28 | 0.16 | 1.75 | 2.62 | 0.81 |
| HI | 36M | dizziness/ PN | RVA | 25 | 22 | 14 | 9.0 | 0.49 | 0.34 | 0.21 | 0.29 | 0.72 | 0.60 | 4.95 |

HT = Hypertension; SCD = Spino-cerebellar degeneration; LI = Lacunar infarction; DM = Diabetes mellitus; LC = Liver cirrhosis; PN = Peripheral neuropathy; BA = Basilar artery; L = Left; R = Right; VA = Vertebral artery; SBP = Systolic blood pressure; MBP = Mean blood pressure; DBP = Diastolic blood pressure; Vmax = Time-averaged maximum velocity; PI = Pulsatility index; eCVR = Estimated cerebrovascular resistance; Δ = Maximum-minimum; %ΔeCVR = (eCVR maximum- eCVR minimum)/eCVR minimum; %ΔMBP = (MBP maximum-MBP minimum)/MBP minimum; ARI = Autoregulation Index (%ΔeCVR/, %ΔMBP); ARIst = ARI during standing (Vmax sitting or supine/Vmax standing-BP sitting or supine)/BP standing/(1- BP sitting or supine/BP standing); ND = No data

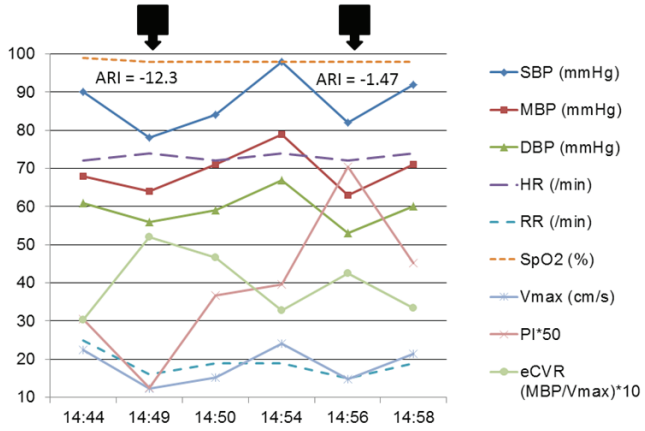


**Figure 1.** Parameters demonstrated during two series of standing (indicated by arrows) in the MY patient with spinocerebellar degeneration. The patient complained of dizziness during standing and could not remain standing. Falling BP and Vmax and increasing PI and eCVR during standing were distinctive. Calculated ARIst during individual standing was -12.3 and -1.47, respectively. However, calculated ARI on the basis of maximum and minimum values during all series was 2.88.

Falling BP and Vmax and increasing PI and eCVR during two series of standing were distinctive in the SCD patient (**Figure 1**). Calculated ARI on the basis of maximum and minimum values was 2.88 during all series. However, ARIst during individual standing was -12.3 and -1.47, respectively.

## Discussion

### Continuous suboccipital monitoring and transducer fixation device

Evaluation of cerebral vasomotor reactivity, such as AR, in the BA, via the suboccipital window, has been evaluated by conventional TCD with a labor-intensive hand-held probe utilizing thigh cuffs [2], phenylephrine infusion [4], and change in position from supine to sitting [5]. In order to perform accurate and reproducible evaluation, continuous monitoring utilizing a transducer fixation device is needed. Recently, continuous suboccipital monitoring with a transducer fixation device has been introduced for evaluation of $CO_2$ reactivity [6], autoregulation in migraines [7], and detection of high intensity transient signals [8].

Compared to conventional TCD, TCDS is able to measure much more accurately on the basis of angle-collected velocities in the intracranial major vessels via both the temporal and suboccipital bone windows. We have introduced and improved a transducer holder, named Sonopod, for TCDS monitoring via both temporal/suboccipital windows [9, 10]. In this study, transducer displacement was not problematic in all cases despite position changes from supine or sitting to standing. However, in order to avoid transducer displacement, it is necessary to use a semi-lateral, lateral or sitting position instead of a pure supine position. Furthermore, in this study, we had to monitor in the VA in 4 out of 12 cases due to a limitation of fixation angle. Future improvement of the Sonopod is necessary in this matter.

### Static and dynamic autoregulation

Calculation of static ARI has been performed as changes of estimated cerebrovascular resistance (eCVR) in relation to the changes in BP: eCVR = BP/Vmax and ARI = %ΔeCVR/%ΔBP with %ΔeCVR = (eCVR2 - eCVR1)/eCVR1 and %ΔBP = (BP2-BP1)/BP1 [11]. Alternatively, static ARI can be calculated as follows: ARI = (initial Vmax/final Vmax - initial BP/final BP)/ (1 - initial BP/final BP) [12]. Our calculation of ARI during two series of standing and sitting (or supine) was based on maximum and minimum values: %ΔeCVR = (eCVR maximum - eCVR minimum)/eCVR minimum and %ΔBP = (BP maximum-BP minimum)/BP minimum. Additionally, individual ARIst during standing was based on values from standing to sitting (or supine): %ΔeCVR = (eCVR standing- eCVR sitting or supine)/eCVR sitting or supine and %ΔBP = (BP standing-BP sitting or supine)/BP sitting or supine.

Normal static ARI values in children were reported as 0.95±0.05 [3] and 0.96±0.09 [5] in the middle cerebral artery (MCA), and 0.94±0.10 [3] and 0.94±0.12 [5] in the BA. Static ARI in normal orthopedic adult patients during sevoflurane anesthesia [4] were much lower, 0.66±0.2 in the MCA and 0.72±0.2 in the BA, than that found in children. It has been considered that static ARI is a dimensionless value ranging between 0-1 [4]. Dynamic ARI is ranged from 0-9 and 5±1 as normal [11].

However, our calculated ARI were variable from -12.3 to 16.20 during position changes based on the previous two equations (**Table 1** and **Figure 1**) [11, 12]. A demonstrated patient with SCD (**Figure 1**) showed that MBP decrease (68 mmHg to 64mmHg), Vmax decrease (22.5 cm/s to 12.3 cm/s), and calculated CVR increase (MVP/Vmax) (3.02 to 5.20) resulted in -12.3 ARI (ΔeCVR/ΔBP) during her first standing. During her second standing, MBP decrease (79 mmHg to 63mmHg), Vmax decrease (24.1 cm/s to 14.8 cm/s), and calculated CVR increase (MVP/Vmax) (3.28 to 4.26) resulted in -1.47 ARI (ΔeCVR/ΔBP).

Our data sampling occurred every 1 minute during all series. The previous study utilizing change in position (from supine to sitting) took five minute intervals between position changes before data collection [5]. Other static AR studies utilizing phenylephrine infusion probably required a much longer period of data sampling, in the period between before and after BP increase [4, 11]. In contrast, dynamic AR studies utilizing the thigh cuff method evaluated the data every second, resulting in higher ARI [2, 11, 13] in comparison with static ARI (**Table 2**). Dynamic AR utilizing spontaneous transient pressor and depressor changes [14] in normal control subjects was much higher, as high as 6.3±1.1 [15]. Data sampling time is probably affecting the ARI results.

**Table 2.** Normal autoregulation index (ARI) in the basilar and middle cerebral arteries (BA and MCA).

| Authors | Year published | Age (range) | n | Dynamic or Static AR | Methods | ARI | |
|---|---|---|---|---|---|---|---|
| | | | | | | BA | MCA* |
| Tiecks et al. | 1995 | 35±10 (27-54) | 10 | Dynamic | Propofol /thigh cuff deflation | – | 4.9±1L<br>4.6±0.9R |
| | | | | Static | Propofol/ pnenylephrine infusion | – | 0.87±0.2L<br>0.82±0.1R |
| | | | | Dynamic | Isoflurane/ thigh cuff deflation | – | 2.2±1.1L<br>2.1±1.1R |
| | | | | Static | Isoflurane/ pnenylephrine infusion | – | 0.33±0.26L<br>0.31±0.27R |
| White and Markus | 1997 | 69±7 (51-81) | 69 | Dynamic | Spontaneous pressor and depressor changes | – | 6.3±1.1 |
| Vavilala et al. | 2002 | 25-45<br>12-17 | 9<br>8 | Dynamic | Thigh cuff deflation | – | 5.3±0.8<br>3.9±2.1 |
| Eames et al. | 2002 | 69±7 (51-81) | 48 | Dynamic | Spontaneous pressor changes | – | 4.5±2 |
| | | | 47 | Dynamic | Spontaneous depressor changes | – | 4.7±2.2 |
| Park et al. | 2003 | 27.4±8.5 (19-46) | 15 | Dynamic | Thigh cuff deflation | 4.62±1.26 | 4.77±1.23 |
| Vavilala et al. | 2005 | Boys:12.9±1.7 (10-16)<br>Girls:12±1.4 (10-16) | 13<br>13 | Static | Change in position (from supine to sitting) | 0.92±0.12<br>0.97±0.06 | 0.98±0.03<br>0.92±0.1 |
| Rozet et al. | 2006 | 30±9 (22-47) | 9 | Static | Sevoflurane/ pnenylephrine infusion | 0.72±0.2 | 0.66±0.2 |
| Tontisirin et al. | 2007 | 6±2 (4-8) | 48 | Static | Change in position (from supine to sitting) | 0.94±0.12 | 0.96±0.09 |

* L = left; R = right

Our data of first and second standing were also variable, there was no definite tendency between series. This variability should be clarified in following analysis.

### Orthostatic hypotension (OH) and autoregulation in the VBA

Our patients of SCD and LI/DM complained of severe dizziness resulting in an inability to remain standing for three minutes. Both patients during the series showed DBP ≥ 10, and there was a SPB ≥ 20 in the SCD patient. The SCD patient showed decreased BP and Vmax during standing, fulfilling the criteria of OH on the basis of the recommendations of active standing [16]. The SCD patient showed ΔPI and ΔeCVR increases and probably disturbed AR in the BA. Older subjects displayed greater vulnerability to reduced perfusion in the posterior cerebral artery (PCA) during orthostatic stress [17]. The head-up tilt table tests indicated that the static AR in the PCA tended to be worse than in the MCA [18]. Further studies in the VBA AR are recommended for those patients with autonomic dysregulation.

In conclusion, continuous TCDS monitoring in the VBA during postural changes is capable of evaluating pathophysiology of vertebrobasilar hemodynamics and autoregulation associated with autonomic regulation.

### Abbreviations

AR: Autoregulation; ARI: Autoregulation index; BA: Basilar artery; BP: Blood pressure; DM: Diabetes mellitus; eCVR: Estimated cerebrovascular resistance; DBP: Diastolic blood pressure; LI: Lacunar infarction; MBP: Mean blood pressure; MCA: Middle cerebral artery; OH: Orthostatic hypotension; PCA: Posterior cerebral artery; PI: Pulsatility index; SBP: Systolic blood pressure; SCD: Spino-cerebellar degeneration; TCD: Transcranial Doppler sonography; TCDS: Transcranial color duplex sonography; VA: Vertebral artery; VBA: Vertebrobasilar artery

### Competing interests

The authors declare no conflict of interest.

### References

1. Naschitz JE, Rosner I. Orthostatic hypotension: framework of the syndrome. Postgrad Med J 2007; 83(983):568-574.
2. Park CW, Sturzenegger M, Douville CM, Aaslid R, Newell DW. Autoregulatory response and CO2 reactivity of the basilar artery. Stroke 2003; 34:34-39.
3. Vavilala MS, Kincaid MS, Muangman SL, Suz P, Rozet I, Lam AM. Gender differences in cerebral blood flow velocity and autoregulation between the anterior and posterior circulations in healthy children. Pediatr Res 2005; 58:574-578.
4. Rozet I, Vavilala MS, Lindley AM, Visco E, Treggiari M, Lam AM. Cerebral autoregulation and CO2 reactivity in anterior and posterior cerebral circulation during sevoflurane anesthesia. Anesth Analg 2006; 102:560-564.

5. Tontisirin N, Muangman SL, Suz P, Pihoker C, Fisk D, Moore A, Lam AM, Vavilala MS. Early childhood gender differences in anterior and posterior cerebral blood flow velocity and autoregulation. Pediatrics 2007; 119:e610-615.
6. Hong JM, Joo IS, Huh K, Sheen SS. Simultaneous vasomotor reactivity testing in the middle cerebral and basilar artery with suboccipital probe fixation device. J Neuroimaging 2010; 20:83-86.
7. Reinhard M, Schork J, Allignol A, Weiller C, Kaube H. Cerebellar and cerebral autoregulation in migraine. Stroke 2012; 43:987-993.
8. Yamaoka Y, Ichikawa Y, Kimura T, Sameshima T, Ochiai C, Morita A. A Novel Method for Transcranial Doppler Microembolic Signal Monitoring at the Vertebrobasilar Junction in Vertebral Artery Dissection Patients. J Neuroimaging 2012; 20:1-4.
9. Shiogai T, Koyama M, Yamamoto M, Yoshikawa K, Mizuno T, Nakagawa M: Brain tissue perfusion monitoring using Sonopod for transcranial color duplex sonography. Perspectives in Medicine 2012; 1: 34—38.
10. Shiogai T, Koyama M, Yamamoto M, Hashimoto H, Yoshikawa K, Nakagawa M: Monitoring of brain tissue perfusion utilizing a transducer holder (Sonopod) for transcranial color duplex sonography. Acta Neurochir (Suppl) 2013; 118: 229-233.
11. Tiecks FP, Lam AM, Aaslid R, Newell DW. Comparison of static and dynamic cerebral autoregulation measurements. Stroke 1995; 26:1014-1019.
12. Strebel S, Lam AM, Matta B, Mayberg TS, Aaslid R, Newell DW. Dynamic and static cerebral autoregulation during isoflurane, desflurane, and propofol anesthesia. Anesthesiology 1995; 83:66-76.
13. Vavilala MS, Newell DW, Junger E, Douville CM, Aaslid R, Rivara FP, Lam AM. Dynamic cerebral autoregulation in healthy adolescents. Acta Anaesthesiol Scand 2002; 46:393-397.
14. Eames PJ, Blake MJ, Dawson SL, Panerai RB, Potter JF. Dynamic cerebral autoregulation and beat to beat blood pressure control are impaired in acute ischaemic stroke. J Neurol Neurosurg Psychiatry 2002; 72:467-472.
15. White RP, Markus HS. Impaired dynamic cerebral autoregulation in carotid artery stenosis. Stroke 1997; 28:1340-1344.
16. Task Force for the Diagnosis and Management of Syncope; European Society of Cardiology (ESC); European Heart Rhythm Association (EHRA); Heart Failure Association (HFA); Heart Rhythm Society (HRS), Moya A, Sutton R, Ammirati F, Blanc JJ, Brignole M, Dahm JB, Deharo JC, Gajek J, Gjesdal K, Krahn A, Massin M, Pepi M, Pezawas T, Ruiz Granell R, Sarasin F, Ungar A, van Dijk JG, Walma EP, Wieling W. Guidelines for the diagnosis and management of syncope (version 2009). Eur Heart J 2009; 30:2631-2671.
17. Sorond FA, Khavari R, Serrador JM, Lipsitz LA. Regional cerebral autoregulation during orthostatic stress: age-related differences. J Gerontol A Biol Sci Med Sci 2005; 60: 1484-1487.
18. Wang YJ, Chao AC, Chung CP, Huang YJ, Hu HH. Different cerebral hemodynamic responses between sexes and various vessels in orthostatic stress tests. J Ultrasound Med 2010; 29: 1299-1304.

INTERNATIONAL JOURNAL OF
CLINICAL NEUROSCIENCES
AND MENTAL HEALTH

ORIGINAL RESEARCH

# Transcranial targeting low frequency ultrasound thrombolysis system: evaluation of the probe fixation devices for blood flow monitoring

Jun Shimizu[1], Hidetaka Mitsumurab[2], Ayumi Arai[2], Jun Kubotaa[1], Takashi Azuma[3], Takeki Ogawa[4], and Hiroshi Furuhata[1]

Special Issue on Neurosonology and Cerebral Hemodynamics

## Abstract

**Background:** We developed the transcranial targeting low frequency ultrasound thrombolysis system (TCTLoFUT) which will be used for an acute ischemic stroke (AIS). TCT-LoFUT can emit the T beam (500 kHz continuous waveform, 0.72 W/cm$^2$) for thrombolysis to a target thrombus with the D beam (2 MHz pulsed waveform, 0.72 W/cm$^2$) for diagnostic TC-CFI. We report the in vitro thrombolytic efficacy by TCTLoFUT and estimate the blood flow monitoring in human with a newly developed head-fixture for TCT-LoFUT using a same aspect of commercial probe.

**Methods:** A) Sonothrombolysis experiment: The 1.25 ml of blood was extracted by the healthy volunteer. The blood in a syringe for 40 min and created a fresh thrombus with a centrifuge (4500 rotation / 5 min). The alteplase concentration in a syringe solution was made to be 358 IU/ml. The intermittent T/D beams were applied under the 60 min of protocol which was described in our studies. The rt-PA independent group (rt-PA, n=39) and the rt-PA + TCT-LoFUT group (rt-PA+US, n=13) were compared. The sound intensity in a syringe was 0.05 W /cm$^2$. B) Blood-flow monitoring evaluation: We evaluated the blood flow monitoring by middle cerebral artery (MCA) detection in 10 healthy volunteers for 30 min. We used the 2.5 MHz TCCFI probe with the fixture which was developed for same aspect of the TCT-LoFUT.

**Results:** A) Sonothrombolysis experiment: The recanalization rate of 60 min after were 64.1% in rt-PA group and 92.3% in rt-PA+US group. Average recanalization time was shortened from 27.2 min in rt-PA group to 21.4 min in rt-PA+ US group ( $p < 0.01$). B) Blood-flow monitoring evaluation: The MCA could be detected using the fixture for TCT-LoFUT.

**Conclusions:** TCT-LoFUT has a function of the blood-flow monitoring simultaneously with a thrombolysis accelerating effect which will be used for AIS patients.

**Keywords:** Sonothrombolysis, Low frequency, Color flow imaging, Fixation.

[1]Medical Engineering Laboratory, Research Center for Medical Sciences, The Jikei University School of Medicine, Tokyo, Japan

[2]Department of Neurology and Radiology, The Jikei University School of Medicine, Tokyo, Japan

[3]Faculty of Engineering, University of Tokyo, Tokyo, Japan

[4]Department of Emergency Medicine, The Jikei University School of Medicine, Tokyo, Japan

Correspondence: Jun Shimizu

Medical Engineering Laboratory, Research Center for Medical Sciences, The Jikei University School of Medicine

3-25-8, Nishi-shinbashi, Minato-ku, Tokyo 105-8461, Japan

Email adress: jun-sh@jikei.ac.jp

Citation: Shimizu et al. Transcranial targeting low frequency ultrasound thrombolysis system: evaluation of the probe fixation devices for blood flow monitoring. IJCNMH 2014; 1(Suppl. 1):S22

Received: 30 Aug 2013; Accepted: 02 Dec 2013; Published: 09 May 2014

Open Access Publication Available at http://ijcnmh.arc-publishing.org



ARC Publishing

## Introduction

We have developed a transcranial targeting low-frequency ultrasound thrombolysis system (TCT-LoFUT) with recombinant tissue plasminogen activator (rt-PA) for use in the treatment of acute ischemic stroke (AIS) [1]. The TCT-LoFUT probe has a laminated ultrasound (US) phased array structure in a single sector scan probe that can emit 490-kHz continuous waveform (CW) US as a T-beam for mid-frequency sonothrombolysis to a target thrombus under navigation by 2.5-MHz pulsed waveform US as a D-beam for diagnostic transcranial color flow imaging (TC-CFI) (**Figure 1**). We have already confirmed the efficacy of sonothrombolysis using this method in monkey and human clot in vitro studies with rt-PA [2, 3] and the biological safety of the approach in macaque monkey brain [4].

To achieve stable sonothrombolysis with blood flow monitoring, an adequate probe fixation device is indispensable. Since 2000, several authors have reported various head frame probe holders for transcranial Doppler (TCD) [5, 6, 7], transcranial color duplex sonography (TCDS) [8] and TC-CFI [9] for stable blood flow monitoring. TC-CFI is more useful for intracranial vessel orientation with navigation under color flow imaging, particularly in Japanese populations, which show a low detection rate for intracranial vessels. We also developed a head frame holder for the TCT-LoFUT probe at first, but motion of the examinee's head disturbed stable blood flow monitoring [10]. We manufactured and developed two types of the probe- fixation device, and evaluated middle cerebral artery (MCA) or posterior cerebral artery (PCA) blood flow monitoring with the same aspect and property with a commercial probe, and identified problems with clinical use.

## Methods

### Subjects

Basic freehand evaluation with a commercial sector scan probe was performed for 16 healthy volunteers (12 males, 4 females; mean age ± standard deviation, 26.3±7.0 years) without hypertension, diabetes mellitus, and dyslipidemia, history of cerebrovascular disease or smoking. MCA blood flow monitoring in AIS was evaluated in 10 patients (9 males, 1 female; mean age, 64.4±15.6 years) with the P-type device. Moreover, using the P-type device, another 7 AIS patients with suspected paradoxical emboli in the MCA or PCA (all male; mean age, 53.9±11.5 years) were examined for right-left shunt (RLS) using the Valsalva maneuver.

After P-type device evaluation, blood flow monitoring in AIS was evaluated in another 6 patients (all male; mean age, 57.2±14.4 years) with the developed BJ-type device. All examinations were performed at the Jikei University Hospital. This study was conducted under the consent and approval of the Ethics Committee of the Jikei University School of Medicine. All volunteers and patients provided informed consent prior to enrollment.

### Study methodology

We evaluated the function of the probe-fixation devices using the same aspect of a commercial 2.5-MHz sector scan probe (S50) with EUB 8500 (Hitachi Medical Corporation, Tokyo, Japan) via the temporal window (TW), as the TCT-LoFUT is not currently approved for clinical use.

**Figure 2** compares the color flow imaging (CFI) function between the commercial and TCT-LoFUT probes. These pictures suggest that the potentiality of CFI function in the TCT-LoFUT probe is equivalent to a commercial probe.

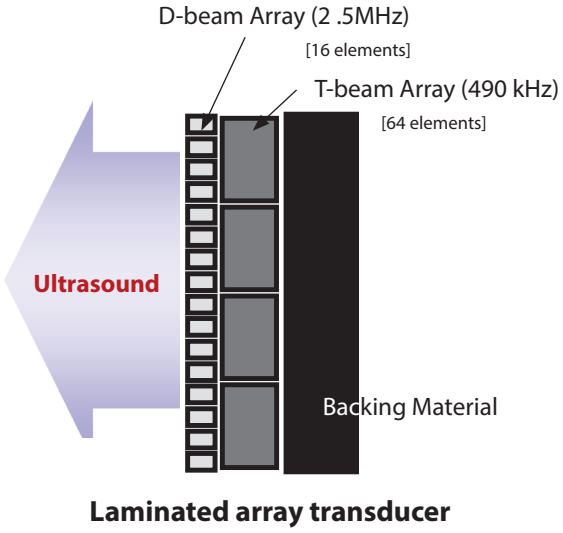


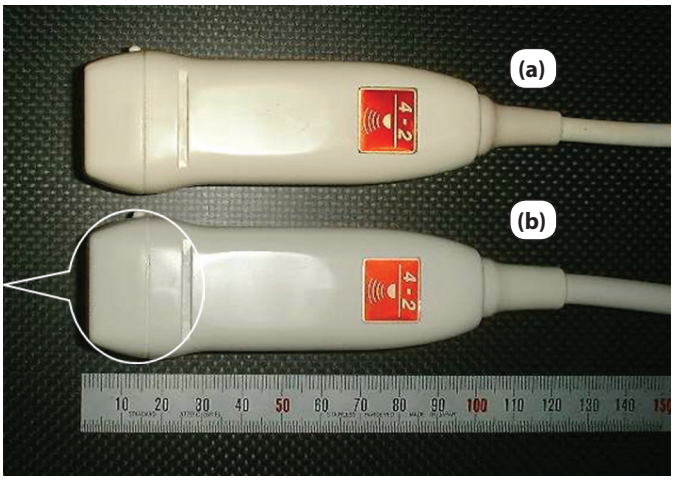


**Figure 1.** Structure of the TCT-LoFUT probe, which has a laminated array structure in the same manner as a commercial probe.
**(a)** Commercial probe (Hitachi S50); **(b)** TCT-LoFUT probe.

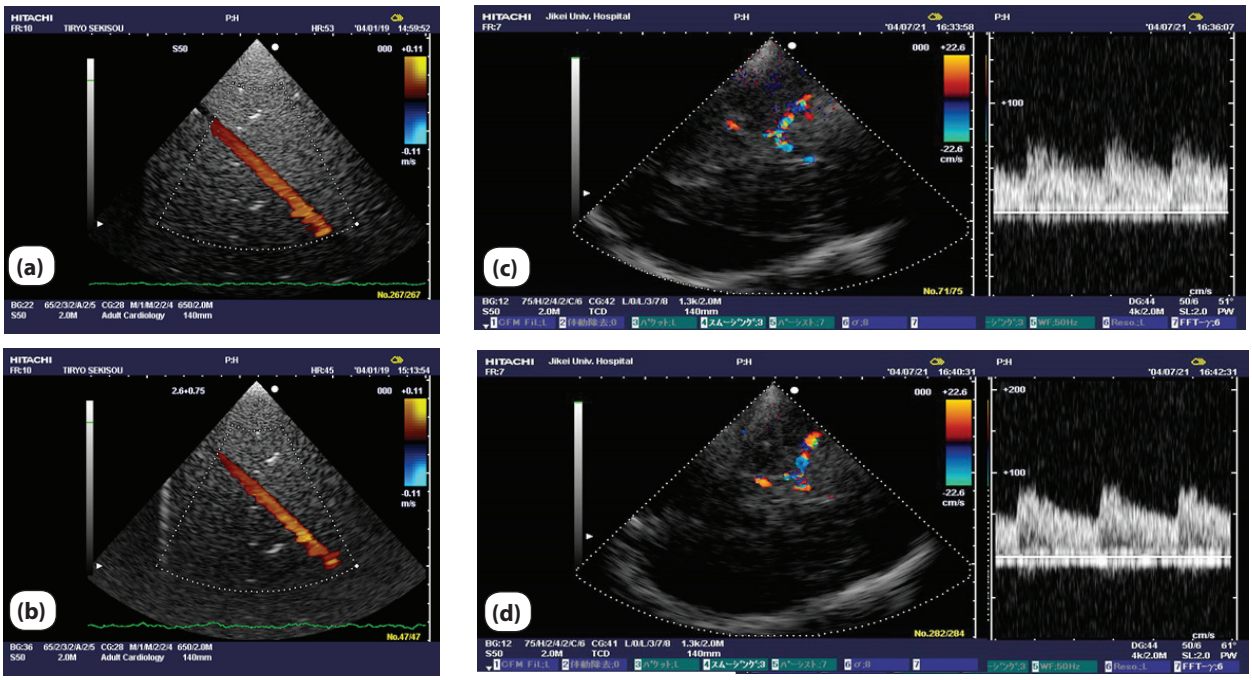


**Figure 2.** Comparison of color flow imaging (CFI) with 2.5 MHz pulsed waveform between the commercial and TCT-LoFUT probes. **(a, b)** Flow phantom CFI with a commercial probe (a) and TCT-LoFUT probe (b); **(c, d)** TC-CFI of the MCA in a 30-year-old female volunteer using a commercial probe (c) and the TCT-LoFUT probe (d).

All blood flow detection was performed by two expert examiners, a neurologist and a sonographer with certification from the Japan Academy of Neurosonology. We first evaluated 16 volunteers to detect bilateral MCA blood flow images via the TW by free hand. Next, we evaluated the high-intensity transient signal (HITS)/micro-embolic signal (MES) at MCA in 9 patients with AIS for 30 min of TC-CFI using P-type fixation via the TW. We also evaluated RLS in 7 patients with suspected paradoxical emboli using P-type device. The manufactured P-type fixation keeps the TCT-LoFUT probe in a holder arm and the opposite side arm pad attached to the head for fixation (**Figure 3a**). The side of each arm is interchangeable. The evaluation points were fixation time, re-fixation and pain from fixation. Finally, we evaluated HITS/MES at the MCA in 6 patients with AIS for 30 min of TC-CFI using BJ-type fixation via the TW. **Figure 3b** shows BJ-type fixation, which was developed from a commercial surgical fixture arm (PointsetterTM; Mitaka-Kohki, Tokyo, Japan). This method uses hydraulic and pneumatics pressure in a ball joint arm that can tightly fix and easily release the probe attachment to the TW with a single-touch button. The degree of freedom is changed more easily than with the P-type for movement of the probe holder arm. The probe holder arm can extend to

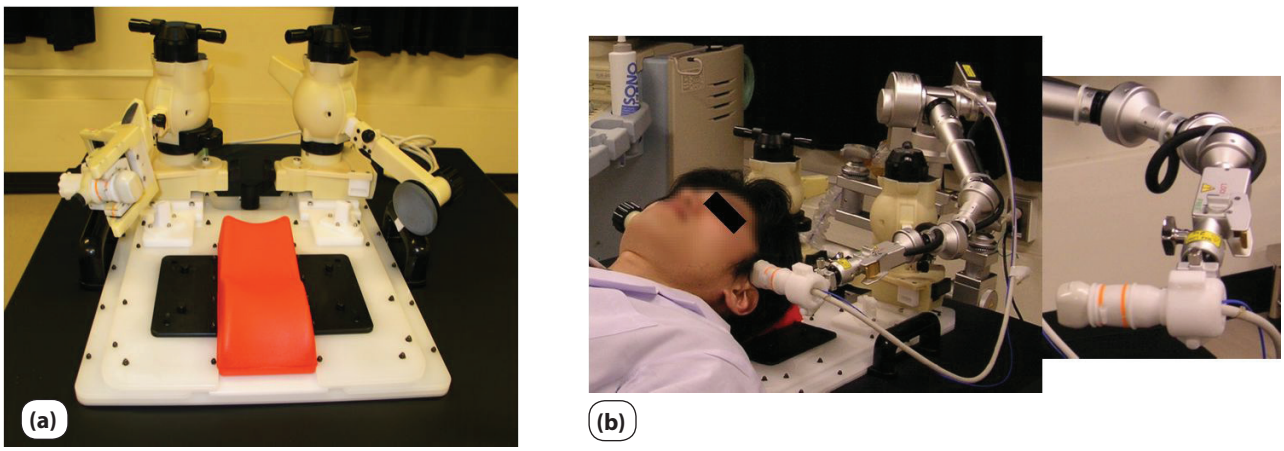


**Figure 3.** Photograph of the probe fixation devices. **(a)** Pillow type; **(b)** Ball joint type.

other types of probe use. The evaluation points were TW permeability, fixation time, number of times for re-fixation, number of times for sample volume re-set up, pain by fixation and body motion.

## Results

### MCA detection in volunteers

MCA detection ratio on 32 sides using the free hand technique was 90.6%. Detection on both sides was impossible in a 53-year-old woman. A 29-year-old man reported poor health during an inspection, and only one side was detectable.

### HITS/MES detection with the P-type fixation device

HITS/MES could be detected in only 1 of 10 cases (10.0%). Two patients needed over 5 min for fixation time and re-fixation. No patients complained of fixation pain (**Table 1**).

### RLS detection with the P-type fixation device

RLS was detected in 2 of 7 cases (28.6%). One patient needed over 5 min for fixation time and re-fixation. No patients complained of fixation pain (**Table 2**).

### HITS/MES detection with the BJ-type fixation device

No patient could be detected any HITS/MES. TW permeability was slightly poor in 4 patients. Fixation time was within 5 min in all patients (mean, 155±121 s), faster than for the P-type device. No patients complained of pain, but 4 patients could not keep quiet for 30 min and we had to fix the head and set the sample volume again (**Table 3**).

## Discussion

The development of US probe fixation devices is one of the most important issues for accurate transcranial ultrasonography. In 1993, Michel et al. reported a multipurpose probe fixation device for newborns via the anterior fontanel [11]. The following year, Woodtli et al. (1994) reported a head and TCD probe-holding technique for monitoring the vertebrobasilar circulation in adult [12]. Three years later, two authors reported probe fixation devices for MCA blood flow monitoring [13, 14].

Since 2000, several authors reported head frame holders for probe fixation. Alexandrov et al. (2000) in a pioneer sonothrombolysis clinical study with rt-PA, reported recanalization blood flow monitoring in MCA using the fixation head frame for power M-mode Doppler (PMD) [5]. Hong et al. (2010) followed MCA and basilar artery vasomotor reactivity tests using a modified head frame for PMD [7]. Mackinnon et al. (2003) reported a unique trial [6]. They developed a long-term ambulatory monitoring head frame with a battery-powered Doppler unit that can servocontrol a 2-MHz transducer probe and store Doppler signal on flash disc drives.

On the other hand, the proposed criteria for judging probe-holding systems include ease of application, stability during patient movement, cost, comfort and durability, and compatibility with multiple probes [8, 14]. We have developed two types of fixation device aimed at recanalization blood flow monitoring in sonothrombolysis. No fixation pain was seen with either device. We could detect RLS in 2 of 7 patients using a P-type device with the Valsalva maneuver. The BJ-type device made up for the shorter set-up time by offering higher functionality.

However, both devices showed some problems in clinical use. First, detection rates of HITS/MES were low with both devices. Next, Mackinnon et al. (2004) pointed out that the embolus detection is a very time-consuming factor even by experts [6]. Nevertheless, skill is required to understand the structure of device and to fix the head, particularly with the P-type device. Third, although ease of application and compatibility with multiple probes is suitable with the BJ-type device, development of a probe fixation device from commercial surgical arms is very expensive. Fourth, the BJ-type device must be connected to

**Table 1.** Blood flow monitoring with the P type fixation device.

| Patient No. | Age | Sex | Target Vessel | HITS/MES | Fixation time | Re-fixation | Pain |
|---|---|---|---|---|---|---|---|
| 1 | 79 | F | lt MCA | (-) | >5 min | (+) | (-) |
| 2 | 63 | M | rt MCA | (-) | <5 min | (-) | (-) |
| 3 | 67 | M | lt MCA | (-) | <5 min | (-) | (-) |
| 4 | 70 | M | rt MCA(M2) | (-) | >5 min | (+) | (-) |
| 5 | 80 | M | lt MCA | (-) | <5 min | (-) | (-) |
| 6 | 60 | M | lt MCA | (-) | <5 min | (-) | (-) |
| 7 | 29 | M | rt MCA | (-) | <5 min | (-) | (-) |
| 8 | 79 | M | rt MCA | (-) | <5 min | (-) | (-) |
| 9 | 67 | M | lt MCA | (-) | <5 min | (-) | (-) |
| 10 | 50 | M | lt MCA | (+) | >5 min | (+) | (-) |

HITS = High intensity transient signal; MES = Micro embolic signal; MCA = Middle cerebral artery

**Table 2.** Blood flow monitoring in RLS suspected patient with the P type fixation device.

| Patient No. | Age | Sex | Target Vessel | RLS | Fixation time | Re-fixation | Pain |
|---|---|---|---|---|---|---|---|
| 1 | 51 | M | bilateral MCA | (-) | <5 min | (-) | (-) |
| 2 | 51 | M | rt MCA | (+) | <5 min | (-) | (-) |
| 3 | 35 | M | lt MCA and PCA | (-) | >5 min | (+) | (-) |
| 4 | 63 | M | rt MCA | (+) | <5 min | (-) | (-) |
| 5 | 67 | M | bilateral MCA | (-) | <5 min | (-) | (-) |
| 6 | 46 | M | rt MCA | (-) | <5 min | (-) | (-) |
| 7 | 64 | M | rt MCA | (-) | <5 min | (-) | (-) |

RLS = Right left shunt; MCA = Middle cerebral artery; PCA = Posterior cerebral artery

a reservoir of compressed air, which may be unsuitable for urgent bedside use. Moreover, we spent a great deal of time and effort in the set-up process before examination, because the BJ-type fixation device was large. Fifth, movement of the patient's body can easily require re-fixation of the probe fixation arm with both devices. To make a probe fixation arm stable, a restoration function like in a weighted toy tumbler is required. Motion of a probe fixation arm can be defined by five parameters: movement of the center of gravity in three dimensions (along x, y and z axes) and surrounding rotation of the center of gravity (latitude θ and longitude Φ). If these five parameters are fixed, the probe holding arm will remain still. Each of these five parameters will be considered stable in response to external force if a self return to the original position like a weighted toy tumbler can be achieved. However, with our two types of fixation device, which have no restoring force on the probe-holding arm, external force by patient movement could easily change the values of the five parameters, resulting in instability. Even if external force on the probe is minute, movement will be amplified by the holding arm. To create a stable probe-fixation device, a design must minimize change in the three-dimensional parameter specifying the stability of probe fixation.

Shiogai et al. (2012) recently reported brain tissue perfusion monitoring with TCDS via both the TW and foraminal window using the Sonopod head frame holder, which is compatible with multiple probes [8]. They also pointed out shifts in the fixed probe due to patient movements during monitoring, but re-adjustment of the probe in the Sonopod was easy. Their setup time for monitoring was usually around 5-10 min. Watt et al. (2012) published preliminary MCA blood flow monitoring data using a probe fixation device in 9 controls and 2 patients with unilateral AIS. Their device was designed to stabilize two 2-MHz TCD probes to sample bilateral MCA blood flow, but the aspects and properties of their fixation device was not described [15]. Ohyama et al. (2013) are currently developing a fixation device to be compatible with multiple probes [9]. That fixation device is a helmet-type device that can achieve long-term blood flow monitoring with stable probe fixation.

To use the TCT-LoFUT at the bedside, improvements in probe-fixation devices must be achieved not only for blood flow monitoring, but also for performing effective thrombolysis acceleration with rt-PA by 490-kHz CW-US with a newly developed safe method of transcranial ultrasonication [16].

## Conclusions

The probe-fixation device for TCT-LoFUT must be further improved to actualize the stable ultrasound supply for sonothrombolysis with monitoring by TC-CFI function.

**Table 3.** MCA blood flow monitoring with the BJ type fixation device.

| Patient No. | Age(y) | Sex | HITS/MES | TW permeability | Fixation Time (sec) | Re-fixation (time) | Re-set SV (time) | Body Motion | Pain |
|---|---|---|---|---|---|---|---|---|---|
| 1 | 58 | M | (-) | F | 20 | 0 | 0 | rare | (-) |
| 2 | 42 | M | (-) | F | 105 | 0 | 1 | often | (-) |
| 3 | 76 | M | (-) | SP | 300 | 1 | 0 | intense | (-) |
| 4 | 39 | M | (-) | SP | 240 | 0 | 1 | often | (-) |
| 5 | 60 | M | (-) | SP | 240 | 3 | 5 | intense | (-) |
| 6 | 68 | M | (-) | SP | 25 | 0 | 0 | rare | (-) |

MCA = Middle cerebral artery; TW = Temporal window; F = fair; SP = Slightly poor; SV = Sample volume

A probe-fixation device must be designed to minimize changes in the three-dimensional parameters specifying the stability of probe fixation.

## Abbreviations

AIS: Acute ischemic stroke; CFI: Color flow imaging; CW: Continuous waveform; HITS: High-intensity transient signa; MES: Micro-embolic signal; MCA: Middle cerebral artery; PCA: Posterior cerebral artery; PMD: Power M-mode Doppler; RLS: Right-left shunt; rt-PA: recombinant tissue plasminogen activator; TCD: Transcranial Doppler; TCDS: Transcranial color duplex sonography; TC-CFI: Transcranial color flow imaging; TCT-LoFUT: Transcranial targeting low-frequency ultrasound thrombolysis system; TW: Temporal window; US: Ultrasound

## Acknowledgments

This study was supported in part by Health and Labor Sciences Research Grants (H17-general-001) from the Ministry of Health, Labor and Welfare of Japan. The authors wish to thank Makoto Ogihara Msc, Hitachi Medical Corporation and Hitachi Ltd. for their help in developing the systems and performing the study, and are grateful to Osamu Saito PhD (physics) for discussions and advices on physical consideration.

## Competing interests

The authors declare no conflict of interests associated with this manuscript.

## References

1. Azuma T, Ogihara M, Kubota J, Sasaki A, Umemura S, Furuhata H. Dual-frequency ultrasound imaging and therapeutic bilaminar array using frequency selective isolation layer. IEEE Trans Ultrason Ferroelectr Freq Control 2010; 57:1211–1224.
2. Ogihara M, Kubota J, Azuma T, Ando K, Tanifuji Y, Umemura S, Furuhata H. Verification of ultrasonic thrombolysis effect by in vitro experiments. J Jpn Appl Phys 2006; 45:4736–4739.
3. Zenitani T, Minamisawa S, Furuhata H. Experimental evaluation of the minimum effective acoustic intensity of sonothrombolysis with whole-blood clots of primates[in Japanese]. Tokyo Jikeikai Medical Journal 2013; 128:35-40.
4. Shimizu J, Fukuda T, Ogihara M, Kubota J, Sasaki A, Sasaki K, Azuma T, Shimizu K, Oishi T, Umemura S, Furuhata H. Ultrasound safety with midfrequency transcranial sonothrombolysis: preliminary study on normal Macaca monkey brain. Ultrasound Med Biol 2012; 38:1040–1050.
5. Alexandrov AV, Demuchuk AF, Felberg RA, Christou I, Barger PA, Burgin WS, Malkoff M, Wojner AW, Grotta JC. High rate of complete recanalization and dramatic clinical recovery during tPA infusion when continuously monitored with 2 MHz transcranial Doppler monitoring. Stroke 2000; 31: 610-614.
6. Mackinnnon AD, Aaslid R, Marks HS. Ultrasound long-term ambulatory monitoring for cerebral emboli using transcranial Doppler. Stroke 2004; 35: 73-78.
7. Hong JM, Joo IS, Huh K, Sheen SS. Simultaneous vasomotor reactivity testing in the middle cerebral and basilar artery with suboccipital probe fixation device. J Neuroimaging 2010; 20: 83-86.
8. Shiogai T, Koyama M, Yamamoto M, Yoshikawa K, Mizuno T, Nakagawa M. Brain tissue perfusion monitoring using Sonopod for transcranial color duplex sonography. Perspective in Medicine 2012; 1:34-38.
9. Ohyama K, Koga M, Endoh K, Suzuki R, Yamamoto H, Toyoda K, Minematsu K. Third generation prototype of a probe holder for transcranial color-corded Doppler. Neurosonology 2013; 26:49.
10. Mitsumura H, Arai A , Ogihara M, Kubota J, Mochio S, Furuhata H. New probe fixation system for transcranial targeting low frequency ultrasonic thrombolysis. Cerebrovasc Dis 2009; 27 (suppl 5):11.
11. Michel E, Zernikow B, Rabe H, Jorch G. Adaptive multipurpose probe fixation device for use on newborn. Ultrasound Med Biol 1993; 19: 581-586.
12. Woodtli M, Müller HR. A head and transducer holding technique for TCD monitoring of the vertebrobasilar circulation. Ultraschall Med 1994; 15: 293-295.
13. Gehring H, Meyer zu Westrup L, Berndt S, Joubert-Hübner E, Eleftheriadis S, Schmucker P. A new probe holding device for continuous bilateral measurements of blood flow velocity in basal brain vessels. Anasthesiol Intensivmed Notfallmed Schmerzther 1997; 32: 355-359.
14. Giller CA, Giller AM. A new method for fixation of probes for transcranial Doppler ultrasound. J Neuroimaging 1997; 7:103-105.
15. Watt BP, Burnfield JM, Truemper EJ, Buster TW, Bashford GR. Monitoring cerebral hemodynamics with transcranial Doppler ultrasound during cognitive and exercise testing in adults following unilateral stroke. Conf Proc IEEE Eng Med Biol Soc 2012; 2310-2013.
16. Furuhata H, Saito O. Comparative study of standing wave reduction methods using random modulation for transcranial ultrasonication. Ultrasound Med Biol 2013; 39:1440–1450.

INTERNATIONAL JOURNAL OF
CLINICAL NEUROSCIENCES
AND MENTAL HEALTH

ORIGINAL RESEARCH

# Improving uniformity of intensity distribution of ultrasound passing through a human-skull fragment by random modulation

Osamu Saito[1] and Hiroshi Furuhata[1]

Special Issue on Neurosonology and Cerebral Hemodynamics

## Abstract

**Background:** Transcranial ultrasound irradiation can enhance the effect of a thrombolytic-agent tissue plasminogen activator (tPA), depending on the intensity. Because of the ultrasound's interference, its intensity distribution near a transducer is not uniform, i.e., there are low-intensity cold spots and high-intensity hot spots. Furthermore, the distribution can be more inhomogeneous when the ultrasound passes through a human skull. At the cold spots, the enhancement of the tPA effect is less than in other areas, whereas at the hot spots, the risk of hemorrhages is higher. Therefore, the reduction of the difference in the intensity between the cold and hot spots, i.e., improving the uniformity of the ultrasound field, is important for effective and safer ultrasound irradiation. The purpose of this study is to show that the uniformity of the ultrasound field can be improved by random modulation of the activating signal used for the ultrasound emission.

**Methods:** A hydrophone measurement of the distribution of ultrasound passing through a human skull fragment in water was performed for each of the sinusoidal activations (500 kHz) and random modulation. To quantify the degree of uniformity of an intensity distribution, the term uniformity index is newly defined in this paper. This index is smaller for more homogeneous distribution.

**Results:** It was shown that ultrasound radiation was more homogeneous during random modulation. The uniformity index was smaller for sinusoidal activation than for random modulation in the near-field region.

**Conclusion:** This technique is expected to be useful for developing effective and safer therapeutic equipment.

**Keywords:** Sonothrombolysis, Uniformity, Random modulation, Transcranial ultrasonication.

[1]Medical Engineering Laboratory, Research Center for Medical Science, The Jikei University School of Medicine, Tokyo, Japan

Correspondence: Osamu Saito

Medical Engineering Laboratory, Research Center for Medical Science, The Jikei University School of Medicine

3-25-8, Nishi-shinbashi, 105-8461 Minato-ku, Tokyo, Japan

Email adress: osaito@jikei.ac.jp

Citation: Saito et al. Improving uniformity of intensity distribution of ultrasound passing through a human-skull fragment by random modulation. IJCNMH 2014; 1(Suppl. 1):S23

Received: 31 Aug 2013; Accepted: 20 Nov 2013; Published: 09 May 2014

Open Access Publication Available at http://ijcnmh.arc-publishing.org



ARC Publishing

## Introduction

It has recently been clinically demonstrated that transcranial ultrasound irradiation can enhance thrombolysis with the aid of a tissue plasminogen activator (tPA) [1]. The feasibility of transcranial sonothrombolysis has been studied for decades [2-4], such as in high-intensity focused ultrasound (HIFU) navigated by MRI [5, 6] and in sonothrombolysis with a defocused ultrasound beam [7, 8]. However, the safety of transcranial ultrasound irradiation has not been definitively proven. In particular, the TRUMBI trial [9] reported many cerebral hemorrhages despite using ultrasound at an intensity that seemed to be safe. One of the explanations for the hemorrhages is that the acoustic pressure was unexpectedly too high because of the generation of standing waves [10, 11], which were caused by multi-reflection of the ultrasound at the inner skull surface. It has been shown that the standing-wave problem can be solved by modulating the activating signal to the transducer [12-14].

In this work, we investigate the other problem that arises in the case of sonothrombolysis with a defocused ultrasound beam. Because of the interference properties of the ultrasound, its intensity distribution is not uniform near the transducer; there are lower-intensity (cold) spots and higher-intensity (hot) spots. At the cold spots, the tPA enhancement is less than that expected in other areas [15], whereas at the hot spots, the risk of cell damage, heating, and hemorrhages is higher [16]. To obtain an ultrasound field distribution that is suitable for thrombolysis, the distribution should be free of cold or hot spots. Therefore, reducing the difference in the intensity between the cold and hot spots or improving the uniformity of the ultrasound intensity distribution is important to increase the efficacy and safety of ultrasound irradiation.

The purpose of this study is to experimentally verify that random modulations of ultrasound can reduce the cold and hot spots or improve the uniformity of the ultrasound passing through a temporal bone. In our previous work [14], we showed that standing wave can be reduced by the random modulation method, which was based on the inversion of a sinusoidal wave phase at random time intervals. The method was termed random switching of both inverse carriers (RSBIC). In this paper, we investigated an effect of RSBIC method on ultrasound uniformity. Activating a transducer with a nominal peak of around 500 kHz using the RSBIC method, we measured the acoustic intensity distribution on the plane perpendicular to the direction of beam propagation using a hydrophone. To compare the uniformity between the sinusoidal case and the RSBIC case in a quantitative way, we introduce the uniformity index and denote it UI.

## Methods

### Random modulation method

We investigated a random modulation method called RSBIC, which was devised for reducing standing waves [14]. Here, we describe the method.

The RSBIC signal S as a function of time t is described by the equation $S(t)=A \sin[2\pi f_0 t+\varphi(t)]$, where A is the amplitude, $f_0$ is the carrier frequency (500 kHz in this study), and $\varphi(t)$ is the phase angle depending on t. The value of $\varphi(t)$ is set at either 0 or $\pi$. For the case in which $\varphi=0$, the signal S(t) belongs to the normal carrier; for the case in which $\varphi=\pi$, the signal belongs to the inverse carrier. The RSBIC signal is realized by switching between these two carriers at random time intervals. An example of the RSBIC signal waveform is shown in **Figure 1**. The random timing of switching is characteristic of the RSBIC. In our experiment, we constructed a special circuit in which the timing was electrically determined by the zero-cross timing of the thermal noise. The noise was generated by a Zener diode and was filtered by low-pass and high-pass filters. The lower and upper cut-off frequencies of the noise are the parameters of the RSBIC method. We set the lower cut-off frequency at 50 kHz and the upper cut-off frequency at 200 kHz as representative values. (If the noise has a component much higher than 500 kHz, one cycle of the sinusoidal wave at 500 kHz will be cut many times.)

### Measurement of the ultrasound field

The transducer we used has a nominal frequency of 500 kHz and a 6-dB bandwidth from 357 kHz to 665 kHz. This wide bandwidth is suitable for random modulation because many waves of different lengths can be superimposed. The plane-view shape of the transducer is a disk whose diameter is 24 mm. The wavelength is about 3 mm in water at a frequency of 500 kHz. We defined the boundary between the near field and the far field as the position of the farthest local maximal value of the ultrasound field from the surface of the transducer. The position is about 47 mm, calculated by $D^2/4\lambda-\lambda/4$, where D is the diameter of the transducer and $\lambda$ is the wavelength.

**Figure 2** shows a diagram of the experimental setup. The transducer was activated by a sinusoidal wave or RSBIC signal. The sinusoidal wave was generated by a signal generator (AFG3102; Tektronix, OR, USA) and increased by an amplifier (HSA4101; NF Corporation, Japan). In the case of RSBIC activation, an additional custom-made circuit was used for the conversion of the sinusoidal wave to a RSBIC signal. The applied signal was monitored with Oscilloscope1 (TDS3012; Tektronix, OR, USA).

A human skull fragment was placed about 5 mm from the transducer surface. The fragment was cut from the temporal bone part of a human skull. The size was about 3.5 cm × 8 cm. The thickness depends on the position, ranging from 0.6 mm to 2.3 mm.

The measurement of the ultrasound passing through the bone was performed by an acoustic intensity measurement system (AIMS) (Onda Corporation, CA, USA) with

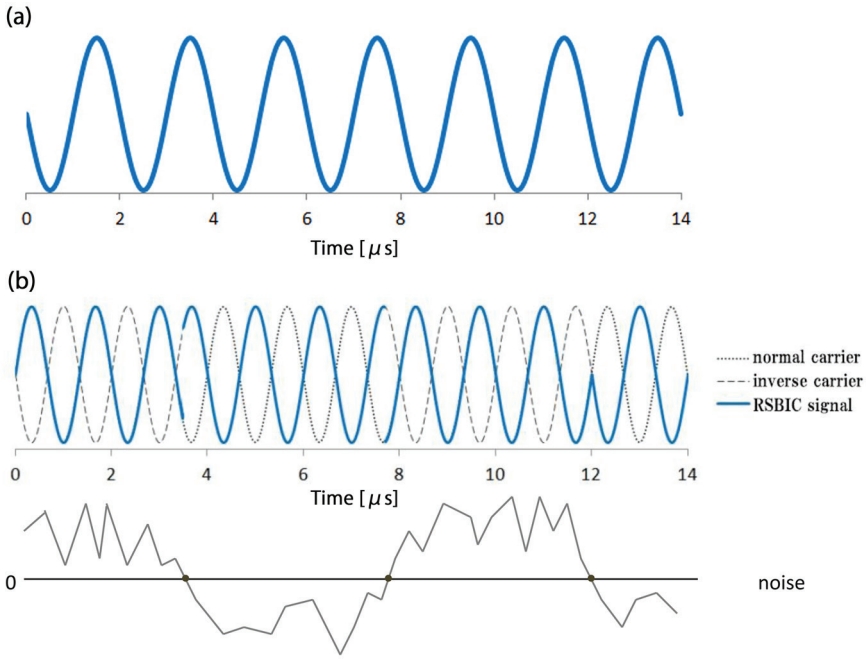


**Figure 1. (a)** A waveform of a sinusoidal wave. **(b)** The graph in the top panel is an example of a waveform of the RSBIC signal. The dotted line indicates the normal carrier, and the broken line indicates the inverse carriers. The RSBIC signal is generated by switching between the two carriers at random time intervals. The timing of the switching is determined by the zero-cross timing of the thermal noise, which is depicted in the bottom panel.

a needle hydrophone having an active tip, 0.4 mm in diameter (HNC-0400; Onda Corporation, CA, USA), and a wide bandwidth from 250 kHz to 10 MHz (-242.52±3.95 [dBV/μPa]). The precise position of the hydrophone could be controlled by a PC with automated measurement of the intensity distribution. The received signal by the hydrophone was monitored with Oscilloscope2 (DSO6012A; Agilent Technologies, MA, USA). Data were acquired in the range of [-20 mm, +20 mm] × [-20 mm, +20 mm], where the origin corresponded to the center of the transducer. Data were taken at intervals of points 1 mm in both directions. Changing the distance between the transducer surface and the measuring plane, we measured the intensity distribution.

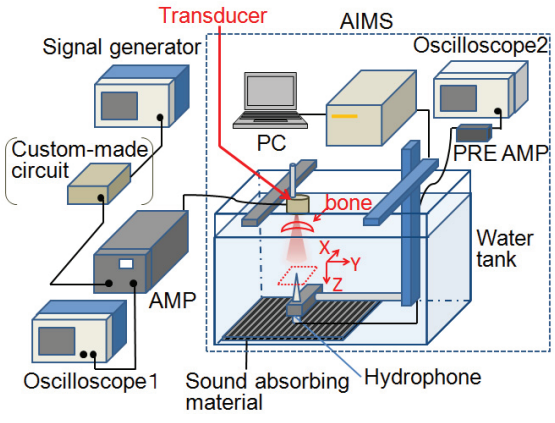


**Figure 2.** The experimental setup for scanning the ultrasound intensity.

### Definition of the uniformity index

To quantify the uniformity of the ultrasound intensity distribution, we propose a mathematical definition for UI. Here, we discuss the two-dimensional case. The one-dimensional case is discussed in the Appendix.

Let f(x,y) be the acoustic intensity (or pressure amplitude) of an ultrasound field on a two-dimensional (x, y) plane. The two-dimensional uniformity index (UI) is defined by the following formula:

$$UI = \frac{\int \sqrt{\left(\frac{\partial f}{\partial x}\right)^2 + \left(\frac{\partial f}{\partial y}\right)^2}\, dxdy}{\int f(x,y)\, dxdy} \quad [m^{-1}] \qquad (1)$$

It has the dimension of [Length$^{-1}$]. If the ultrasound intensity has many peaks and troughs, the value of f(x, y) will vary considerably depending on the position (x, y). In that case, the index becomes large because the contribution of the derivative terms in the numerator is larger than the integral term in the denominator. Conversely, the ultrasound is considered to be more homogeneous if the index decreases.

Equation (1) has the following properties: (i) intensity independence and (ii) rotational invariance. Intensity independence means that the index is invariant under the

transformation $f(x, y) \rightarrow \alpha f(x, y)$, where $\alpha$ is a constant value. Hence, the index can be determined irrespective of the transducer's voltage. Rotational invariance means that the index is unchanged under the following transformation:

$$\xi = \cos\theta\, x + \sin\theta\, y$$
$$\eta = -\sin\theta\, x + \cos\theta\, y \qquad \textbf{(2)}$$

where $\theta$ is an angle of rotation. Therefore, the index is independent of the direction of the x-coordinate.

## Results

The two-dimensional intensity distribution of an ultrasound propagating freely in water is shown in **Figure 3**. The diagrams to the left, (a) – (e), are the result of sinusoidal activation, and the diagrams to the right, (f) – (j), are from RSBIC activation. The uppermost diagrams, (a) and (f), show the intensity 5 mm from the transducer surface, while diagrams (b) and (g) show the intensity at 7 mm; (c) and (h) are at 20 mm; (d) and (i) are at 45 mm; and (e) and (j) show the intensity 80 mm from the surface. The activating voltage was 20 Vpp for each case. Because the shape of the transducer is disc-like, the intensity distribution has circular symmetry.

For the sinusoidal activation, the ring-shaped low-intensity and high-intensity regions are alternately distributed near the transducer [(a) and (b)]. In diagram (c), a cold spot can be seen at the origin. In diagram (d), the ultrasound is focused at the origin. As the distance from the transducer increases in the far-field region, the intensity becomes lower and the distribution becomes broader (e).

By comparing the RSBIC cases and the sinusoidal cases at the same distance, we can see that the intensity distributions of RSBIC cases in the near-field region [(f), (g), and (h)] are more homogeneous than that of the sinusoidal cases [(a), (b) and (c)]. In particular, the cold spot at the origin in diagram (c) disappears in diagram (h). As the distance increases [(d), (e), (i), and (j)], the distinctive differences in the distribution between the sinusoidal cases and RSBIC cases disappear.

The calculated UI are also shown for each diagram in **Figure 3**. When we compared the two methods at the same distance, the UI is smaller for the RSBIC than for the sinusoidal case in the near-field region, as expected, meaning the UI is suitable for quantifying the uniformity and is useful for practical applications.

By comparing the color scale of the RSBIC cases [(f) – (j)] with those of sinusoidal cases [(a) – (e)], we note that the maximum intensities of the RSBIC signals are lower than those of the sinusoidal cones: for example, at 5 mm, the maximum intensity is 3 [mW/cm$^2$] for the RSBIC (f), in contrast to 45 [mW/cm$^2$] for the sinusoidal case (a). This difference arises because energy is lost due to the transducer response.

In **Figure 4**, the two-dimensional distribution of an ultrasound passing through a temporal bone fragment is

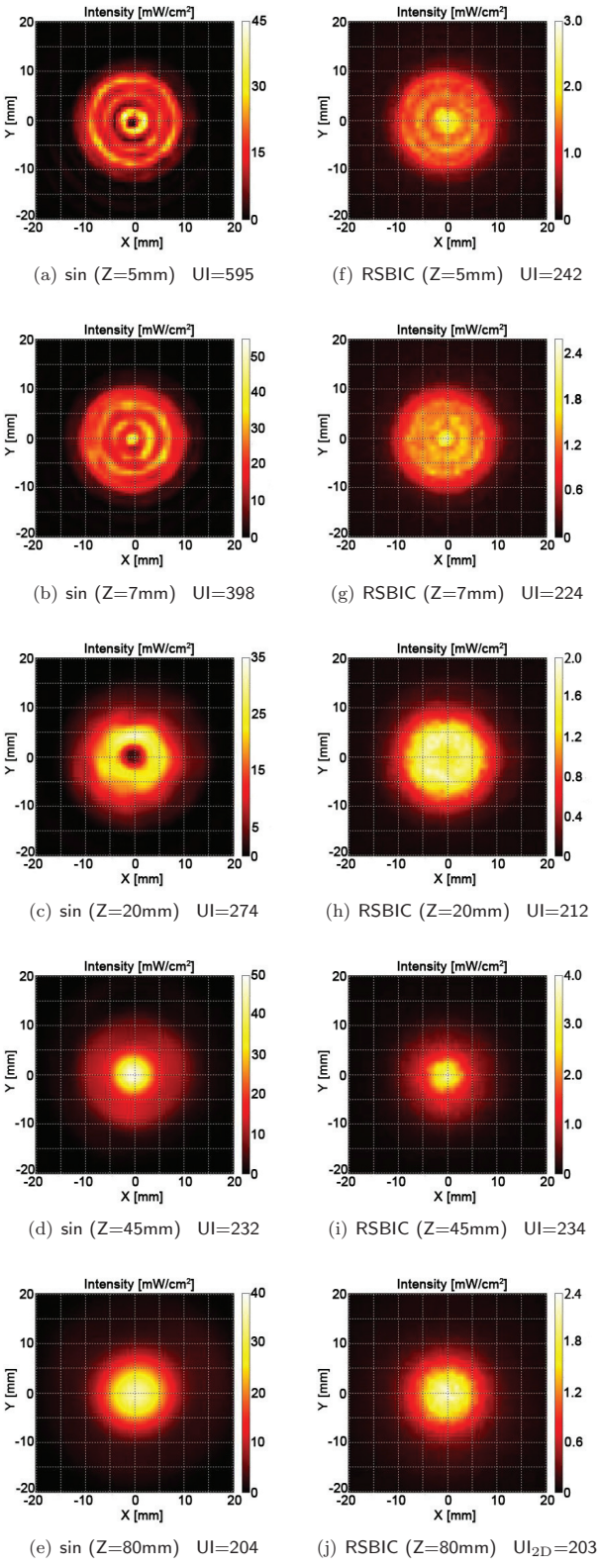


**Figure 3.** Two-dimensional distribution of the ultrasound propagating freely in water. The diagrams, **(a)–(e)**, are sinusoidal activation cases, and the diagrams, **(f) –(j)**, are RSBIC activation cases. Z is the distance from the transducer surface. The activating voltage was 20 Vpp, and the carrier frequency was 500 kHz. Data were collected at intervals of 1 mm for both the X and Y directions. In the case of RSBIC activation, the intensity was averaged for 500 μs. The lower cut-off frequency of the noise was 50 kHz, and the upper cut-off frequency of the noise was 200 kHz. The uniformity indices are shown for each diagram.

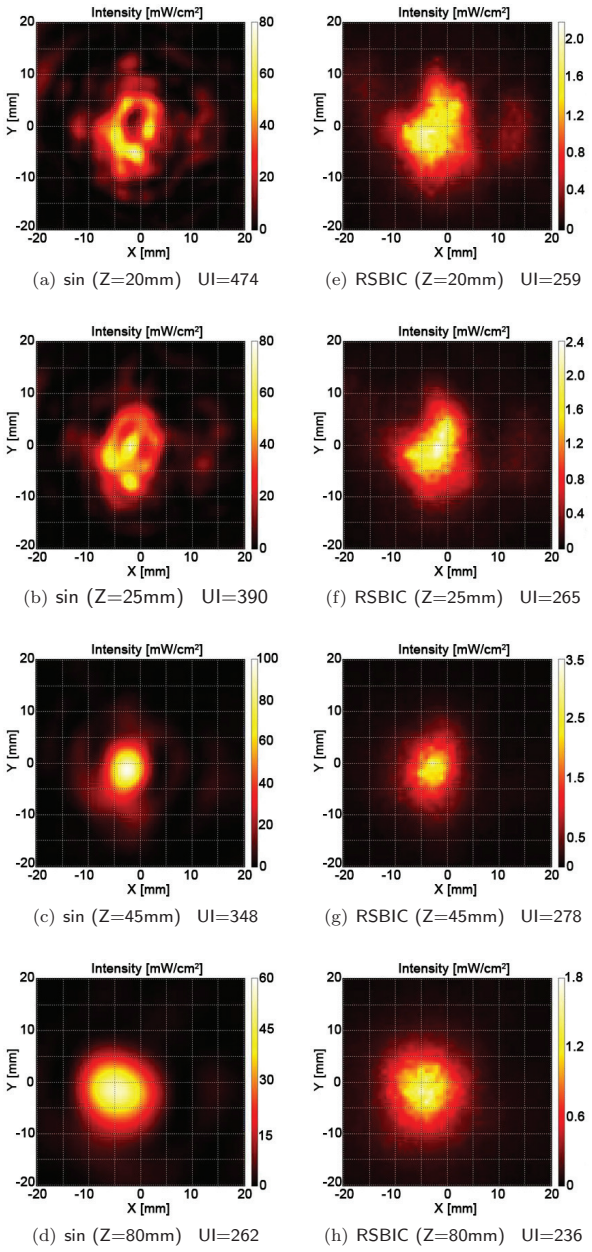


**Figure 4.** Two-dimensional distribution of the ultrasound passing through a temporal bone fragment. The diagrams **(a)–(d)** are sinusoidal activation cases, and the diagrams **(e)–(h)** are RSBIC activation cases. The activating voltage was 50 Vpp. The other parameters are the same as those in Figure 3.

shown. The diagrams to the left, (a) – (d), are sinusoidal cases, and the diagrams to the right, (e) – (h), are RSBIC cases. The uppermost diagrams, (a) and (e), show the intensity 20 mm from the transducer surface, while diagrams (b) and (f) show the intensity at 25 mm; (c) and (g) are at 45 mm; and (d) and (h) show the intensity 80 mm from the surface. The applied voltage was 50 Vpp for each case; hence, the ultrasound emitted by the transducer was 6.25 times as intense as the free-propagating cases.

Compared with the free-propagating cases (Figure 3), the intensity distribution does not have circular symmetry and is more inhomogeneous, most likely because of the non-uniform thickness, inhomogeneous texture, and curvature of the temporal bone fragment.

We can see that, in the case of bone transmission, the RSBIC method can improve the uniformity in the near-field region [(a), (b), (e) and (f)]. Particularly, the cold spot around (X = -2 mm, Y = +2 mm) in the sinusoidal case (a) disappeared in the RSBIC case (e).

The calculated UIs are also shown for each diagram in Figure 4. When we compared the two methods at the same distance, the UI are smaller for the RSBIC case than they are for the sinusoidal case. The difference is lager for the near-field region.

In diagram (d), the center of the ultrasound distribution is not at the origin, but instead is centered at (X = -5 mm, Y = -2 mm). This means that refraction has happened; the ultrasound beam direction was changed by transmission through the bone. This refraction also occurred for the RSBIC case (h).

## Discussion

We investigated the uniformity of an ultrasound passing through a human skull fragment in water. Compared to the free-propagating case, ultrasound passing through a bone was more inhomogeneous in the near-field region. It was shown that the RSBIC method can reduce the cold and hot spots, improving the uniformity of the ultrasound intensity distribution in the case of bone transmission as well as free propagation.

We discuss herein the reason for the improvement of the uniformity with the RSBIC signal. In our free-propagation case, every point on the surface of the transducer is considered to be a source. The ultrasound pressure at a given point is determined by the interference of pressure from all sources. If the signs of the pressure from the different sources are the same, interference is constructive and the pressure is enhanced. On the other hand, if the signs of the pressure are not the same, the interference is destructive. Cold spots arise from destructive interference, whereas hot spots arise from constructive interference. The location of the hot and cold spots changes with the frequency of the activating signal for the transducer because the interference, whether constructive or not, depends on the frequency of the activating signal. Because the RSBIC has a wide bandwidth (**Figure 4h** [14]), cold and hot spots corresponding to each component of the frequency arise at different locations; therefore, a cold spot of a frequency $f_1$ can be a hot spot of a different frequency component $f_2$. Hence, the cold and hot spots are obscured by the superposition of the waves of different frequencies in the RSBIC case. Furthermore, a randomized reversal of the phase, which is characteristic of the RSBIC, can change the constructive interference of pressure to a destructive one and vice versa. Thus, at a given point, whether the interference is constructive or deconstructive will change with time. Hence, when the

time-averaged intensity is measured, the cold and hot spots will be reduced.

In the case of bone transmission, the transmissivity differs according to the location on the bone because of differences in thickness and texture. Therefore, the uniformity of the ultrasound passing through the bone is more inhomogeneous than in the free-propagation case. In this case, the RSBIC signal can improve the uniformity, as in the free-propagation case.

For the purpose of quantitative evaluation of uniformity, we gave a two-dimensional definition of the uniformity index using equation (1). This definition is not unique, and there are other possible definitions. For example, we can obtain a dimensionless uniformity index using the product of eq. (1) and a term that has a dimension of [Length]. Because eq. (1) has the dimension of $[\text{Length}]^{-1}$, the product has no dimension. If the index is dimensionless, it has the property of scale invariance. In our case, a possible term of $[\text{Length}]^{-1}$ is the square-root of the measuring area

$$\sqrt{\int_{X_i}^{X_f}\int_{Y_i}^{Y_f} dxdy}$$

(where [Xi, Xf] × [Yi, Yf] is the range of the area). However, if we use this term, the uniformity index will depend on the measuring area.

The definition of uniformity index is not limited to two dimensions. A one-dimensional uniformity index is described in the **Appendix**. The extension to three dimensions may also be possible.

It is possible that a more suitable definition can be found using a completely different perspective.

In this study, results for a disc-shaped transducer were shown. For a square-shaped transducer, we can see that cold and hot spots will be arranged in a matrix in a plane near the transducer.

The size of the transducer was 24 mm in diameter in this study. For a larger transducer, the near-field region will be broader. Thus, the random modulation method will be effective for a broader range.

This experiment was performed in water, in which the attenuation of the ultrasound is negligible. However, the brain absorbs the ultrasound; the ultrasound attenuates along the pass. In the absorbent medium, the intensity at the far field is lower than it is in a non-absorbing medium. Hence, in the absorbent medium, the ratio of the intensity of the near field to that of the far field is higher than in a non-absorbent medium. Thus, the effect of the random modulation method will be higher for an absorbent medium.

Random modulation methods were first used to reduce standing waves in a human skull and have been shown to reduce standing waves [12-14]. Because random modulation methods can concurrently resolve both the standing-wave problem and the cold-hot-spots problem, they are attractive for the therapeutic use of ultrasound, such as in transcranial sonothrombolysis. We are planning to investigate an acceleration of thrombolysis using randomly modulated ultrasound. Our goal is to develop safer and more effective therapeutic equipment based on randomly modulated ultrasound emission.

## Appendix One-dimensional uniformity index

We define a uniformity index in the one-dimensional case using the following formula:

$$UI_{1D} = \frac{\int \left|\frac{df}{dx}\right| dx}{\int f(x)dx} \qquad (3)$$

where f(x) is the intensity (or pressure amplitude) of the ultrasound field on the one-dimensional spatial axis x. As in the case with two dimensions, the index has the dimension of $[\text{Length}^{-1}]$ and is invariant under the transformation f(x) → c f(x). Here, we attempt to clarify the meaning of the numerator. Let the starting point of the integral be α and the ending point be β, with f(α)=f(β)=0. We divide the interval [α, β] by the extremum of f(x):

$$\int_{\alpha}^{\beta} = \int_{\alpha}^{M_1} + \sum_{i=1}^{n-1}\left(\int_{M_i}^{m_i} + \int_{m_i}^{M_{i+1}}\right) + \int_{M_n}^{\beta} \qquad (4)$$

where Mi (i=1,…,n) are the local maximum values of f(x), and mi (i=1,…,n-1) are the local minimum values of f(x). Because the sign of df/dx is definitive for each interval, we can determine whether |df/dx|=df/dx or |df/dx|= -df/dx for each interval. Performing the integration for each interval, we obtain the expression:

$$\int_{\alpha}^{\beta}\left|\frac{df}{dx}\right| dx = 2\left(\sum_{i=1}^{n} f(M_i) - \sum_{i=1}^{n-1} f(m_i)\right) \qquad (5)$$

The first term in the parenthesis on the right side is the total sum of the local maximum values, and the second is the total sum of the local minimum values. Thus, the numerator of the index UI1D is determined by the extrema of f(x).

There is another candidate for UI1D. We can define UI1D by dividing equation (3) by Nα, where N is the number of extrema and α (0<α<1) is a parameter. The role of Nα is to suppress the uniformity index due to increments of the number of peaks (or hot spots) and troughs (or cold spots). As shown above, the numerator of the index is determined by the extremum. In particular, it depends on only the intensity at the extremum and not the intervals of the extremum on the axis.) Thus, if the numerator of the peaks and troughs are doubled (i.e., the number of extrema doubles), the numerator of the uniformity index is dou-

bled. Similarly, if the differences between the local maximum values and the local minimum values are doubled, the numerator of the uniformity index is doubled. Hence, doubling the number of the peaks and troughs is equivalent to doubling the difference between the local maximum and local minimum values. This might not seem to be a reasonable proposition. However, if we divide equation (3) by $N\alpha$, we can distinguish the doubling of the difference between local maxima and local minima from the doubling of the number of extrema.

## Abbreviations

AIMS: Acoustic intensity measurement system; HIFU: High-intensity focused ultrasound; RSBIC: Random switching of both inverse carriers; tPA: Tissue plasminogen activator; UI: Uniformity index

## Acknowledgments

The present study was supported by a Grant for Research on Advanced Technology (H21-008) from the Ministry of Health, Labour, and Welfare of Japan. The authors thank Dr. Jun Shimizu for cutting the human skull bone to be suitable for the present study.

## Competing interests

The authors declare no conflict of interest.

## References

1. Alexandrov AV, Molina CA, Grotta JC, Garami Z, Ford SR, Alvarez-Sabin J, Montaner J, Saqqur M, Demchuk AM, Moye LA, Hill MD, Wojner AW. Ultrasound-enhanced systemic thrombolysis for acute ischemic stroke. N Engl J Med 2004; 351:2170-2178.
2. Hynynen K, Clement G. Clinical applications of focused ultrasound – The brain. Int J Hyperthermia 2007; 23(2):193-202.
3. Culp WC, McCowan TC. Ultrasound augmented thrombolysis. Current Med Imaging Reviews 2005; 1(1):5-12.
4. Shimizu J, Fukuda T, Abe T, Ogihara M, Kubota J, Sasaki A, Azuma T, Sasaki K, Shimizu K, Oishi T, Umemura S, Furuhata H. Ultrasound safety with midfrequency transcranial sonothrombolysis: preliminary study on normal Macaca monkey brain. Ultrasound Med Biol 2012; 38(6):1040-1050.
5. Hynynen K, McDannold N, Clement G, Jolesz FA, Zadicario E, Killiany R, Moore T, Rosen D. Preclinical testing of a phased array ultrasound system for MRI-guided noninvasive surgery of the brain – A primate study. Eur J Radiology 2006; 59(2):149-156.
6. Song J, Pulkkinen A, Huang Y, Hynynen K. Investigation of standing-wave formation in a human skull for a clinical prototype of a large-aperture, transcranial MR-guided focused ultrasound (MRgFUS) phased array: an experimental and simulation study. IEEE Trans Biomed Eng 2012; 59(2):435-44.
7. Azuma T, Ogihara M, Kubota J, Sasaki A, Umemura S, Furuhata H. Dual-frequency ultrasound imaging and therapeutic bilaminar array using frequency selective isolation layer. IEEE Trans Ultrason Ferroelectr Freq Control 2010; 57(5):1211-24.
8. Shafer ME, Alleman J, Alexandrov A, Barlinn K. Development of an operator independent ultrasound therapeutic device for stroke treatment. 2012 IEEE International Ultrason Symposium Proceedings, 1948-1951.
9. Daffertshofer M, Gass A, Ringleb P, Sitzer M, Sliwka U, Els T, Sedlaczek O, Koroshetz WJ, Hennerici MG. Transcranial low-frequency ultrasound-mediated thrombolysis in brain ischemia: increased risk of hemorrhage with combined ultrasound and tissue plasminogen activator: results of a phase II clinical trial. Stroke 2005; 36(7):1441-1446.
10. Baron C, Aubry JF, Tanter M, Meairs S, Fink M. Simulation of intracranial acoustic fields in clinical trials of sonothrombolysis. Ultrasound Med Biol 2009; 35(7):1148-58.
11. Wang Z, Moehring MA, Voie AH, and Furuhata H. In vitro evaluation of dual mode ultrasonic thrombolysis method for transcranial application with an occlusive thrombosis model. Ultrasound Med Biol 2008; 34(1):96-102.
12. Tang SC, Clement GT. Standing wave suppression for transcranial ultrasound by random-modulation. IEEE Trans Biomed Eng 2010; 57(1):203-205.
13. Tang SC, Clement GT. Acoustic standing wave suppression using randomized phase-shift-keying excitations. J Acoust Soc Am 2009; 126(4):1667-1670.
14. Furuhata H, Saito O. Comparative study of standing wave reduction methods using random modulation for transcranial ultrasonication. Ultrasound Med Biol 2013; 39(8):1440-1450.
15. Zenitani T, Minamisawa S, Furuhata H. Experimental evaluation of the minimum effective acoustic intensity of sonothrombolysis with whole-blood clots of primates. Tokyo Jikeikai Medical Journal 2013; 128:35-40. [Japanese]
16. Schneider F, Gerriets T, Walberer M, Mueller C, Rolke R, Eicke BM, Bohl J, Kempski O, Kaps M, Bachmann G, Dieterich M, Nedelmann M. Brain edema and intracerebral necrosis caused by transcranial low-frequency 20-kHz ultrasound: a safety study in rats. Stroke 2006, 37(5):1301-1306.

INTERNATIONAL JOURNAL OF
CLINICAL NEUROSCIENCES
AND MENTAL HEALTH

ORIGINAL RESEARCH

# Collateral cerebral venous outflow by scalp veins in patients with parasagittal meningiomas

Vladimir Semenyutin[1], Dmitry Pechiborsch[1], Vugar Aliev[1], Andreas Patzak[2], Grigory Panuntsev[1], and Alexandr Kozlov[1]

Special Issue on Neurosonology and Cerebral Hemodynamics

## Abstract

**Background:** Invasion of the superior sagittal sinus (SSS) by parasagittal meningiomas (PSM) causes formation of collateral pathways of venous outflow (including scalp veins) from the cranial cavity. However their importance, considering this function, is still under question. The purpose of this study was to determine the importance of scalp veins in collateral cerebral venous outflow in patients with PSM.

**Methods:** Eight patients with PSM (52-73 year-old) with invasion of the SSS and 4 healthy volunteers were examined, in supine position, with bilateral transcranial Doppler monitoring (MultiDop X, DWL) of blood flow velocity (BFV) in both middle cerebral arteries (MCA), and with blood pressure (BP) monitoring using photoplethysmography (Ohmeda, Finapres 2300). In patients circular compression of scalp veins with pneumatic cuff around glabella and inion during 3 minutes was performed, while in volunteers a simultaneous transient complete compression of both internal jugular veins controlled by ultrasound in B-mode (Vivid E, GE) was performed.

**Results:** Significant changes of BFV, pulsatility index (PI) and BP were not detected during the whole period of compression of scalp veins. These data indicate a low importance of scalp veins in collateral venous outflow from the cranial cavity. Simultaneous compression of both internal jugular veins in all 4 volunteers caused BFV decrease by 9±4% ($p<0.05$) and PI increase by 18±12% ($p<0.05$) associated presumably with intracranial hypertension and impairment of venous outflow from the cranial cavity.

**Conclusions:** Temporary circular compression of scalp veins in patients with invasion of the SSS does not cause impairment of venous outflow from the cranial cavity, which presumably indicates their low importance.

**Keywords:** Scalp veins, Cerebral venous outflow, Parasagittal meningiomas, Collateral venous pathways.

[1]Russian Polenov Neurosurgical Institute, St. Petersburg, Russia
[2]Johannes-Mueller Institute of Physiology University Hospital Charité, Humboldt-University of Berlin, Berlin, Germany

Correspondence: Vladimir Semenyutin
Russian Polenov Neurosurgical Institute
191014 Mayakovsky str. 12, St.Petersburg, Russia
Email adress: lbcp@mail.ru

Citation: Semenyutin et al. Collateral cerebral venous outflow by scalp veins in patients with parasagittal meningiomas. IJCNMH 2014; 1(Suppl. 1):S24

Received: 09 Sep 2013; Accepted: 12 Dec 2013; Published: 09 May 2014

Open Access Publication Available at http://ijcnmh.arc-publishing.org



ARC Publishing

## Introduction

Parasagittal meningiomas (PSM) are intracranial tumors that arise from the superior sagittal sinus (SSS). 70% of PSM grow inside the lumen of the SSS. Partial and complete invasion of the SSS is present in 40% and 30% of patients with PSM respectively [1, 2]. Gradual occlusion of the SSS by PSM invasion causes formation of collateral pathways of venous outflow from the cranial cavity. Surgery is the main treatment option for PSM. However damage to these collateral venous pathways during surgical approach for PSM removal may lead to serious neurologic complications and even death due to cerebral edema and venous infarction. Their preoperative evaluation and intraoperative rational preservation is a standard in surgery of PSM. All neurosurgeons agree that scalp veins may take part in collateral venous outflow in patients with PSM [1–4]. This fact has been demonstrated angiographically nearly four decades ago [5]. However their importance considering this function is still under question. Possible importance of scalp veins concerning the whole cerebral venous system can influence surgical strategy and surgical outcome in patients with PSM.

The purpose of this study was to determine the importance of scalp veins in patients with PSM in collateral venous outflow from the cranial cavity.

## Methods

Eight patients with PSM (age range 52-73 years, mean age 62±8 years) with invasion of the SSS (complete invasion in four cases) and four healthy volunteers (30-40 years old) were studied by parallel bilateral transcranial Doppler monitoring (MultiDop X, DWL) of blood flow velocity (BFV) in both middle cerebral arteries (MCA) and blood pressure (BP) monitoring by photoplethysmography (Ohmeda Finapres 2300), in supine position. In patients circular compression of scalp veins with pneumatic cuff around glabella and inion (head-cuff) during 3 minutes was used. To be sure that scalp veins were actually compressed we detected BFV in proximal parts of superficial temporal artery and vein by an 8 MHz probe (**Figures 1–3**).

In volunteers we used simultaneous transient (during 30 s) complete compression of both internal jugular veins (with carotid arteries intact) controlled by ultrasound in B-mode (Vivid E, GE) in supine position (**Figure 4**). We used volunteers in order to detect hemodynamic changes when venous outflow from the cranial cavity is reliably compromised.

## Results

In our patients BFV, pulsatility index (PI) in MCA and BP did not change significantly ($p>0.5$) before and during all period of scalp compression. Group–averaged hemodynamic parameters before and during compression of scalp veins were 45±13 and 46±10 cm/s for BFV, 0.88±0.15 and 0.86±0.16 for PI, 101±31 and 100±25 mmHg for BP respectively. These data indicate a low importance of scalp veins in collateral venous outflow from the cranial cavity.

An example of the head-cuff test in one of our patients is presented on the **Figure 5**.

Simultaneous compression of both internal jugular veins in volunteers caused statistically significant ($p<0.05$) decrease of BFV and increase of PI and BP. These changes reversed to initial state after compression was finished. In all 4 volunteers in both left and right MCA PI increased by 7–36% (18±12%) while BFV decreased by 3–14% (9±4%). Group-averaged BFV, PI and BP before, during and after simultaneous compression of both internal jugular veins in our volunteers were the following: 76±18, 69±17 and 75±17 cm/s for BFV, 0.76±0.08, 0.89±0.06 and 0.77±0.11 for PI, 91±18, 99±20 and 90±19 mm Hg for BP respectively. We associate these changes with intracranial hyperten-

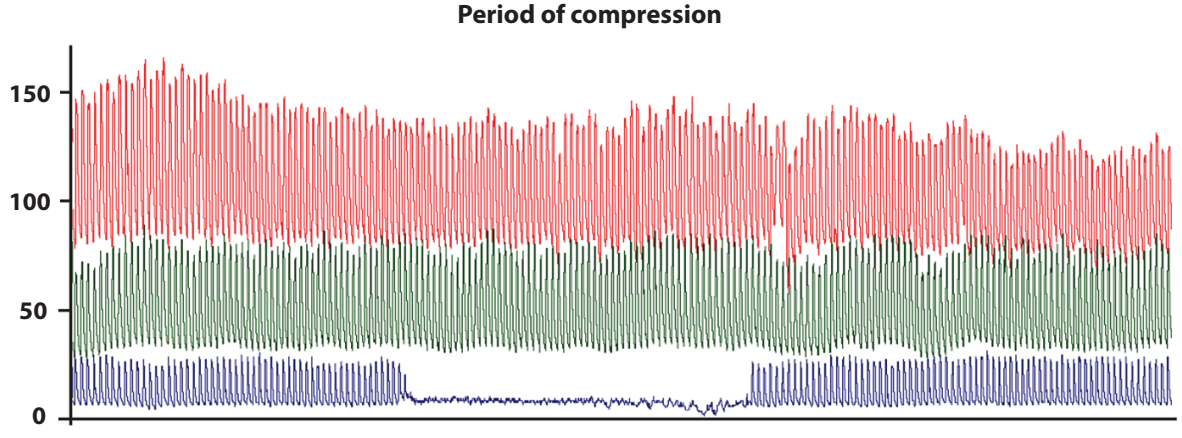


**Figure 1.** Control of scalp compression. Monitoring BP (red line), BFV in superficial temporal artery (blue) and MCA (green) before, during and after scalp compression.

BFV = Blood flow velocity; BP = Blood Pressure; MCA = Middle cerebral artery

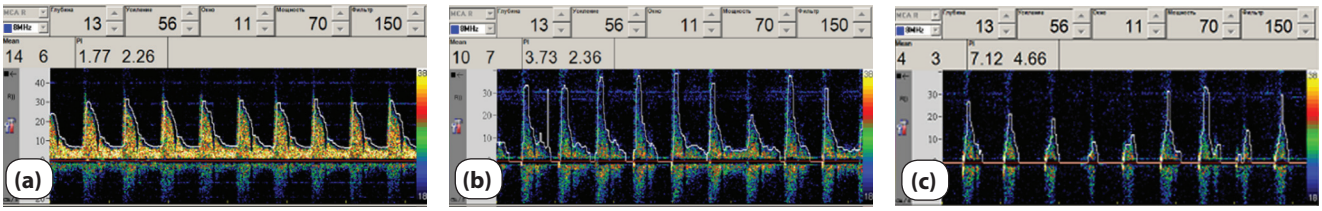


**Figure 2.** Changes of BFV spectra in superficial temporal artery before **(a)**, in the middle **(b)** and on the peak **(c)** of scalp compression.
BFV = Blood flow velocity

sion caused by impairment of venous outflow from the cranial cavity.

An example of a study on a volunteer is presented on the **Figure 6**.

## Discussion

PSM are the most common type of intracranial meningiomas. Rational preservation of direct and collateral venous pathways is a well-known key to good outcome in surgery of PSM. The collateral venous pathways include cortical anastomotic veins, cortical veins with end-to-end anastomoses, anastomoses of superficial with deep cerebral veins, meningeal veins, inferior sagittal sinus, diploic (including emissary) veins and scalp veins. It has been confirmed by S. Waga and H. Handa in 1976 on angiographic images in patients with PSM that scalp veins may take part in collateral venous outflow from the cranial cavity [5]. In their study scalp veins were detected as collateral venous pathways in 3 out of 13 patients with PSM with invaded SSS.

However some venous pathways, scalp veins included, are inevitably damaged, firstly during surgical approach to PSM, then during tumor removal trying to accomplish it more totally. Exclusion of several venous pathways during one-stage operation significantly increases the risk of severe complications.

Therefore some neurosurgeons believe that in some cases it is reasonable to divide operation into 2 (or even more stages) with a one–two week interval to gain time for cerebral venous system to find other ways of venous outflow [3, 4].

Scalp veins should be considered important in venous outflow from the cranial cavity if their compromise (dissection or compression) causes cerebral hemodynamic changes indicating worsening of cerebral venous outflow. Increase in intracranial pressure (ICP) is one example of these cerebral hemodynamic changes and we used it as criterion in our study. Transcranial Doppler monitoring is a well-known method of noninvasive evaluation of changes in ICP [6]. The ICP–PI relationship is dependent upon many factors, mostly $pCO_2$ and cerebral autoregulation, however quantitative evaluation of ICP by PI has been shown to be possible in some cases [7–9]. During our head-cuff test in patients with PSM we consider $pCO_2$ and cerebral autoregulation constant, therefore the ICP–PI relationship is expected to be strong. There are a lot of studies showing rise in PI after ICP increases as well as studies showing that ICP increases after blood flow in both internal jugular veins is abruptly compromised. Since we could not find a study in the literature that links rise in PI with blood flow compromise in both internal jugular veins we conducted our study with volunteers, which significantly ($p<0.05$) showed this relationship. The main idea to use volunteers in our study is to show that abrupt simultaneous compromise of venous outflow from the cranial cavity causes abrupt and statistically significant changes in cerebral hemodynamic parameters, namely decrease of BFV and increase of PI and BP. These changes reversed after compression was finished. It should be mentioned that since venous outflow from the cranial cavity is accomplished through vertebral venous plexus as well, changes of cerebral hemodynamic parameters in our volunteers could be absent.

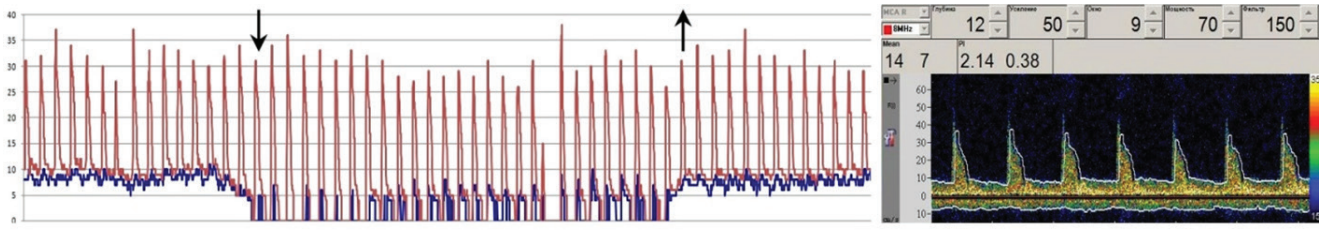


**Figure 3.** Simultaneous monitoring of BFV in superficial temporal artery (red line) and superficial temporal vein (blue line) before, during and after scalp compression. Arrows indicate start and finish of compression. Spectra of BFV in superficial temporal artery and vein before compression are presented on the right. BFV = Blood flow velocity

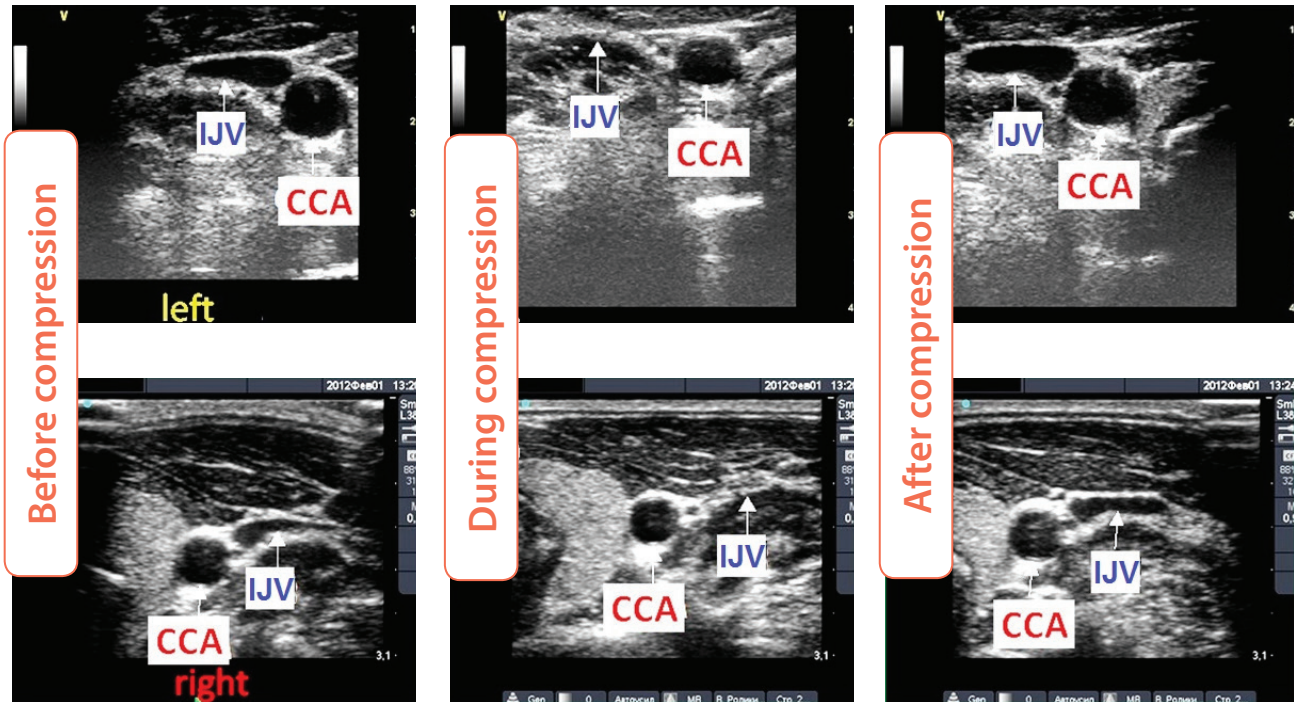


**Figure 4.** Ultrasound images in B-mode in axial plane before, during and after simultaneous compression of both internal jugular veins in a volunteer.
IJV = Internal jugular vein; CCA – Common carotid artery.

Tests of the importance of invaded SSS and bridging veins are performed in surgery of PSM, in order to evaluate the risk of venous sacrifice, when trying a more total resection (usually clipping tests) [10, 11]. For example, L. Sekhar, a prominent American neurosurgeon, uses as a standard a clipping test before PSM resection together with the fragment of the SSS (en bloc resection) [10]. The test comprises measurement of intrasinus pressure in the proximal part of the SSS before and after applying a clip on the invaded part of the SSS. Increase in intrasinus pressure after applying a clip means that the fragment of the SSS with partial or seemingly complete invasion is functionally important and should be preserved.

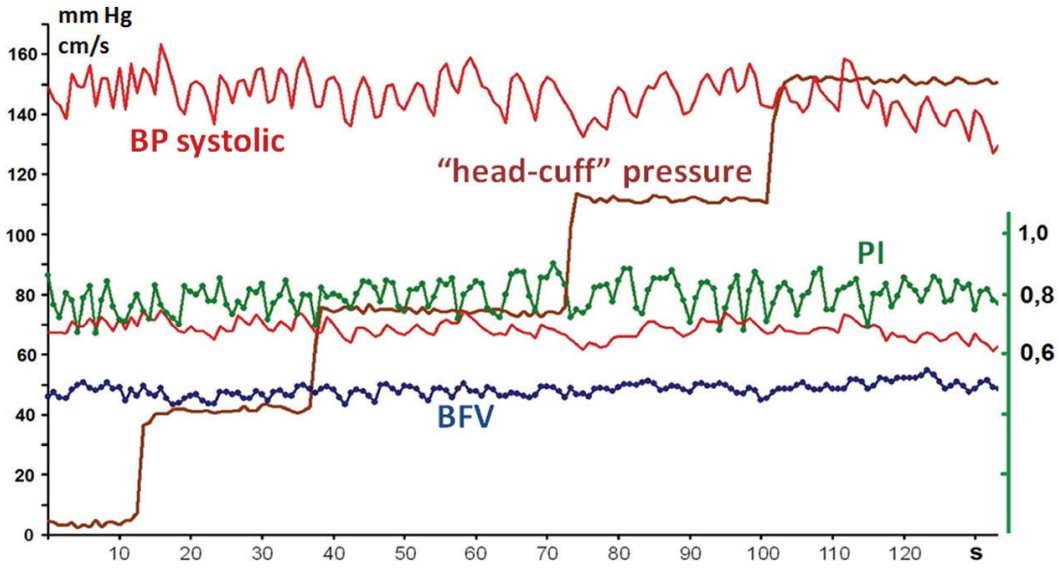


**Figure 3.** Dynamics of BP (red lines: upper – systolic, lower – diastolic), BFV (blue) and PI (green) in MCA during stepwise increase of head-cuff pressure (brown) in a patient with a giant (7 cm in diameter) bilateral PSM.
BFV = Blood flow velocity; BP = Blood pressure; MCA: Middle cerebral artery; PSM: Parasagittal meningiomas

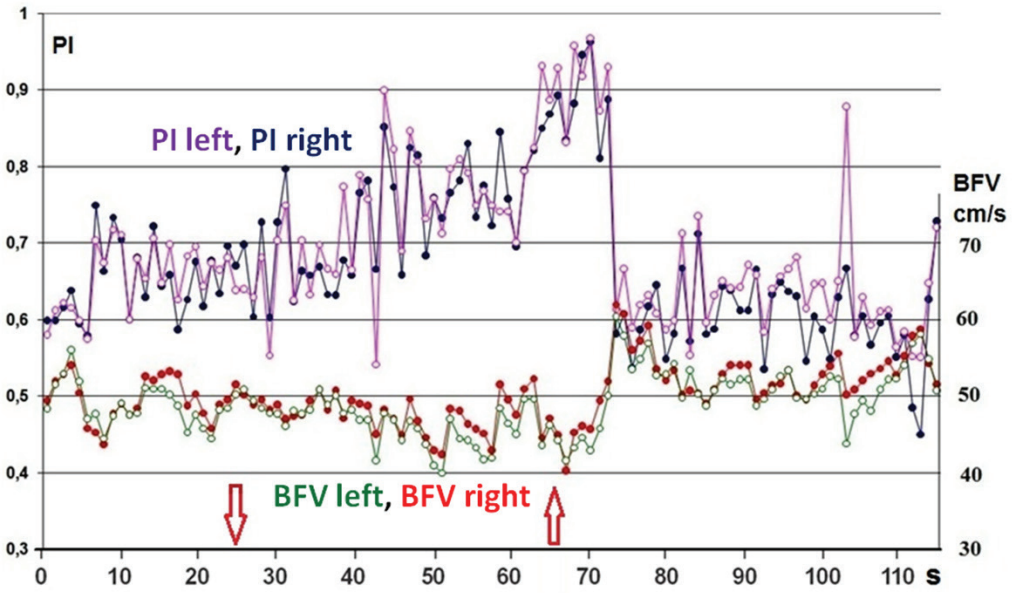


**Figure 6.** Dynamics of BFV and PI in both MCA in a volunteer during simultaneous compression of both internal jugular veins. Arrows indicate start and finish of compression. BFV = Blood flow velocity; BP = Blood pressure; MCA: Middle cerebral artery; PI: Pulsatility index.

A test for importance of scalp veins has actually been developed specifically at our Institute 20 years ago and is used presently. It is based on evaluation of electroencephalogram before and during head-cuff test with circular compression of scalp vessels [12]. Significant changes of bioelectrical activity during scalp compression indicate importance of scalp veins, which in turn indicates that the system of venous outflow from the cranial cavity is "saturated" or has low plasticity and the risk of one-stage operation is high. Of course, changes in bioelectrical activity are secondary to hemodynamic changes and reliability of using them is questionable. Actually all 8 patients in our study had positive result in head-cuff test using electroencephalogram.

## Conclusion

Circular compression of scalp veins in patients with PSM with invasion inside the SSS did not cause impairment of venous outflow from the cranial cavity in our study. This fact indicates low importance of scalp veins in collateral venous outflow from the cranial cavity in our patients, although they could act as collateral venous pathways.

However, in case of complete "saturation" of intracranial pathways of venous outflow it seems possible that scalp veins become important. In neither of our patients this was the case. Hence, further research is needed.

### Abbreviations

BFV: Blood flow velocity; BP: Blood pressure; ICP: Intracranial pressure; MCA: Middle cerebral artery; PI: Pulsatility index; PSM: Parasagittal meningiomas; SSS: Superior sagittal sinus

### Competing interests

The authors declare no conflict of interest.

### References

1. DiMeco F, Li KW, Casali C, et al. Meningiomas invading the superior sagittal sinus: surgical experience in 108 cases. Neurosurgery 2008; 62 (6 Suppl 3):1124-35.
2. Tomasello F, Conti A, Cardali S, et al. Venous preservation-guided resection: a changing paradigm in parasagittal meningioma surgery. J Neurosurg 2013; 119 (1):74-81.
3. Raza SM, Gallia GL, Brem H, et al. Perioperative and long–term outcomes from the management of parasagittal meningiomas invading the superior sagittal sinus. Neurosurgery 2010; 67(4):885-93.
4. Sindou MP, Alvernia JE. Results of attempted radical tumor removal and venous repair in 100 consecutive meningiomas involving the major dural sinuses. J Neurosurg 2006; 105(4):514-25.
5. Waga S, Handa H. Scalp veins as collateral pathway with parasagittal meningiomas occluding the superior sagittal sinus. Neuroradiology 1976; 11(4):199-204.
6. Rosenberg JB, Shiloh AL, Savel RH, et al. Non-invasive methods of estimating intracranial pressure. Neurocrit Care 2011; 15(3):599-608.
7. Behrens A, Lenfeldt N, Ambarki K, et al. Transcranial Doppler pulsatility index: not an accurate method to assess intracranial pressure. Neurosurgery 2010; 66(6):1050-7.
8. Belner J, Rommer B, Reinstrup P, et al. Transcranial Doppler sonography pulsatility index (PI) reflects intracranial pressure (ICP). Surg Neurol 2004; 62(1):45-5.
9. Moreno JA, Mesalles E, Gener J, et al. Evaluating the outcome of severe head injury with transcranial doppler ultrasonography. Neurosurg Focus 2000; 8(1): 8–16.
10. Sekhar LN, Chanda A, Morita A. The preservation and reconstruction of cerebral veins and sinuses. J Clin Neurosci 2002; 9(4):391-9.
11. Schmid–Elsaesser R, Steiger HJ, Yousry T, et al. Radical resection of meningiomas and arteriovenous fistulas involving critical dural

sinus segments: experience with intraoperative sinus pressure monitoring and elective sinus reconstruction in 10 patients. Neurosurgery 1997; 41(5):1005-16.

12. Tigliev GS, Gurchin AF, Kondrat'ev AN, et al. [Electroencephalographic assessment of the compensatory role of extracerebral veins in patients with brain tumors]. Fiziol Cheloveka 1993; 19(2):59-64.

# 05
# Case Reports

INTERNATIONAL JOURNAL OF
CLINICAL NEUROSCIENCES
AND MENTAL HEALTH

CASE REPORT

# Arteriovenous malformation in the carotid artery bifurcation as a rare cause of syncope: a case report

Dagmar Svackova[1], Jiri Neumann[1], Frantisek Charvat[2], Jiri Lacman[2], David Netuka[3], and Petra Bodnarova[1]

Special Issue on Neurosonology and Cerebral Hemodynamics

## Abstract

**Background:** Arteriovenous malformation (AVM) is defined as a convolute of abnormally connected arteries and veins, where capillary bed is missing. The most common localization of AVM is intracranial. Brain malformations are about 20 times more frequent than extracerebral ones. Clinical signs depend on the localization of the malformation; besides local pain or bleeding, steal phenomenon often can be seen.

**Case report:** We present a case of a 61-year-old woman, who was admitted to the hospital because of recurrent syncopes. During the neurosonologic examination we could see the acceleration of blood flow in the left common carotid artery (133 cm/s), a huge convolute of the vessels in the area of its bifurcation and accelerated, low resistant flow in the origin of external carotid artery with PSV 270 cm/s and low resistance index (0.3–0.4). The changes were seen also in the venous part, with sings of arterial flow there. Magnetic resonance angiography was performed, and confirmed a large malformation in the carotid artery bifurcation (about 8 cm). The patient was sent to endovascular diagnostics and treatment; on digital subtraction angiography, a high-flow malformation of left lingual artery on the left half of the tongue was diagnosed. The selective embolization of the lingual artery by the coils was performed with very good radiologic and clinical outcome.

**Conclusions:** A thorough neurosonologic examination is important and can raise the suspicion of an arteriovenous malformation, as in this very unusual case.

**Keywords:** Arteriovenous malformation, Carotid artery bifurcation, Neurosonology, Selective embolization.

[1]Department of Neurology, Hospital Chomutov, Chomutov, Czech Republic
[2]Department of Radiology, Military University Hospital, Prague, Czech Republic
[3]Neurosurgical Clinic, Military University Hospital, Prague, Czech Republic

Correspondence: Dagmar Svackova
Department of Neurology, Hospital Chomutov
Kochova 1185, 430 01 Chomutov, Czech Republic
Email adress: dagmarsvackova@gmail.com

Citation: Svackova et al. Arteriovenous malformation in the carotid artery bifurcation as a rare cause of syncope: a case report. IJCNMH 2014; 1(Suppl. 1):S25

Received: 30 Aug 2013; Accepted: 07 Nov 2013; Published: 09 May 2014

## Introduction

Arteriovenous malformation (AVM) is defined as a convolute of abnormally connected arteries and veins, where capillary bed is missing. The most common localization of AVM is intracranial. Brain malformations are about 20 times more frequent than extracerebral ones [1, 3].

Clinical signs depend on the localization of the malformation; besides of local pain or bleeding, steal phenomenon can also often can seen [2, 4].

## Case report

We present a 61-year-old woman, retired stock-clerk, who was in January 2011 admitted to the Department of Internal Medicine for recurrent syncopes. She complained of dizziness and general weakness several weeks prior to the admission. Her medical history included cholecystectomy and arthroscopy of the knee joint years ago, hypertension for which she had been taking an ACE inhibitor for 7 years, hyperlipidaemia for 5 years (taking Atorvastatine 10 mg per day). Her mother died at 72 years due to stroke. The patient had never smoked and drank minimal alcohol.

On examination: height 1.66 m, weight 75 kg, blood pressure 160/95 mmHg, pulse 76 bpm, otherwise normal physical and neurological findings. Basic laboratory assessment was normal, including thyroid stimulating hormone, full blood count, and coagulation parameters. She had slightly elevated level of cholesterol 5.6 mmol/l (2.9-5.0) and triglyceride 2.02 (0.45-1.7). Investigations performed: normal ECG, chest X-ray, 24-hour ECG monitoring, echocardiography, EEG. The patient was then presented to neurosonologic examination.

When we started the examination on the left common carotid artery (CCA), we could see slight velocity increase with peak-systolic velocity (PSV) 133 cm/s, end-diastolic velocity (EDV) 42 cm/s, and no signs of stenosis. Similar velocity increase was seen also in left the internal carotid artery (ICA) (121/29 cm/s). At the origin of the left external carotid artery (ECA) there was an increase of PSV 212 cm/s and EDV 104 cm/s. About 1 cm distal to the ECA origin there was a huge convolute of vessels mostly with low-resistant flow—resistance index (RI) 0.32 and pulsatility index (PI) 0.39 (**Figure 1a**, **Video 1 and 2**). Changes were also seen in the venous part, which had arterialized flow (**Figure 1b**). Other vessels examined were normal—right CCA, ICA, ECA, bilateral vertebral arteries, and, transcranially, vessels of the circle of Willis.

Magnetic resonance angiography was performed, and showed a large arteriovenous malformation in the left parapharyngeal area, about 8 cm large and fed by the left ECA (**Figure 1c and 1d**). Digital subtraction angiography demonstrated a high-flow AVM of the left half of the tongue, fed by the left lingual artery, and dilatation of the lingual artery to 6 mm (**Figure 1e**). Because it was in the tongue, AVM could not be solved by total embolization. Selective partial embolization with coils was performed with very good radiologic outcome (**Figure 1f**).

One month after (in March 2011), during neurosonologic examination, wwe could see on left ECA origin a certain flow velocity decrease, with PSV 193 cm/s and EDV 97 cm/s, RI raised from 0.32 to 0.51, flow velocity decrease was seen in left CCA and ICA, and there was a normal, mildly accelerated venous flow in draining vein (50 cm/s).

After 2 years of follow up the patient did not have any other problems, no syncopes, and the neurosonologic finding remains the same as in March 2011. On examination, we can only see dilated veins in the left half of her tongue, which sometimes makes her swallowing difficult and painful (**Figure 2**).

*Videos accessible at http://ijcnmh.arc-publishing.org*

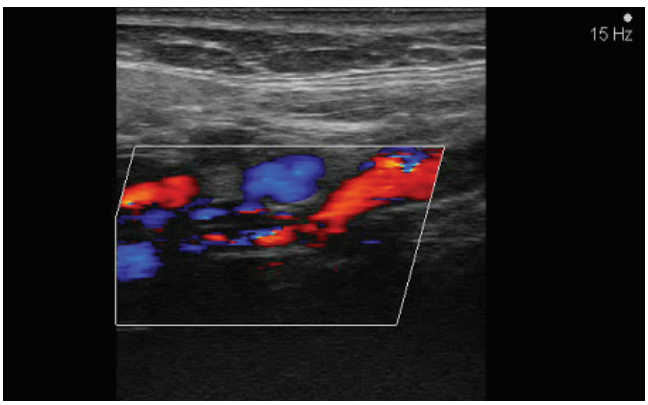


**Video 1.** Convolution of vessels in the origin of left external carotid artery—longitudinal plane.

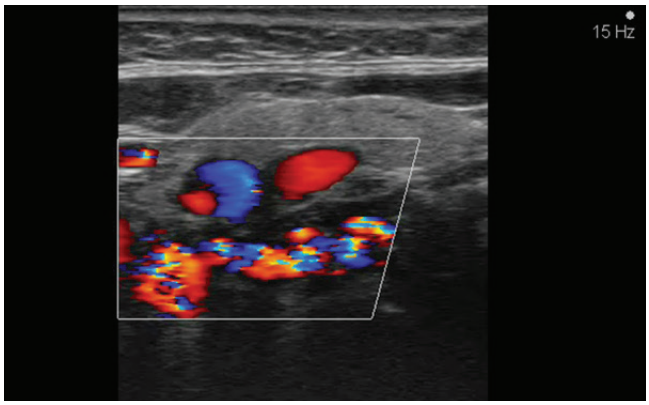


**Video 2.** Convolution of vessels in the origin of left external carotid artery—cross-sectional plane.

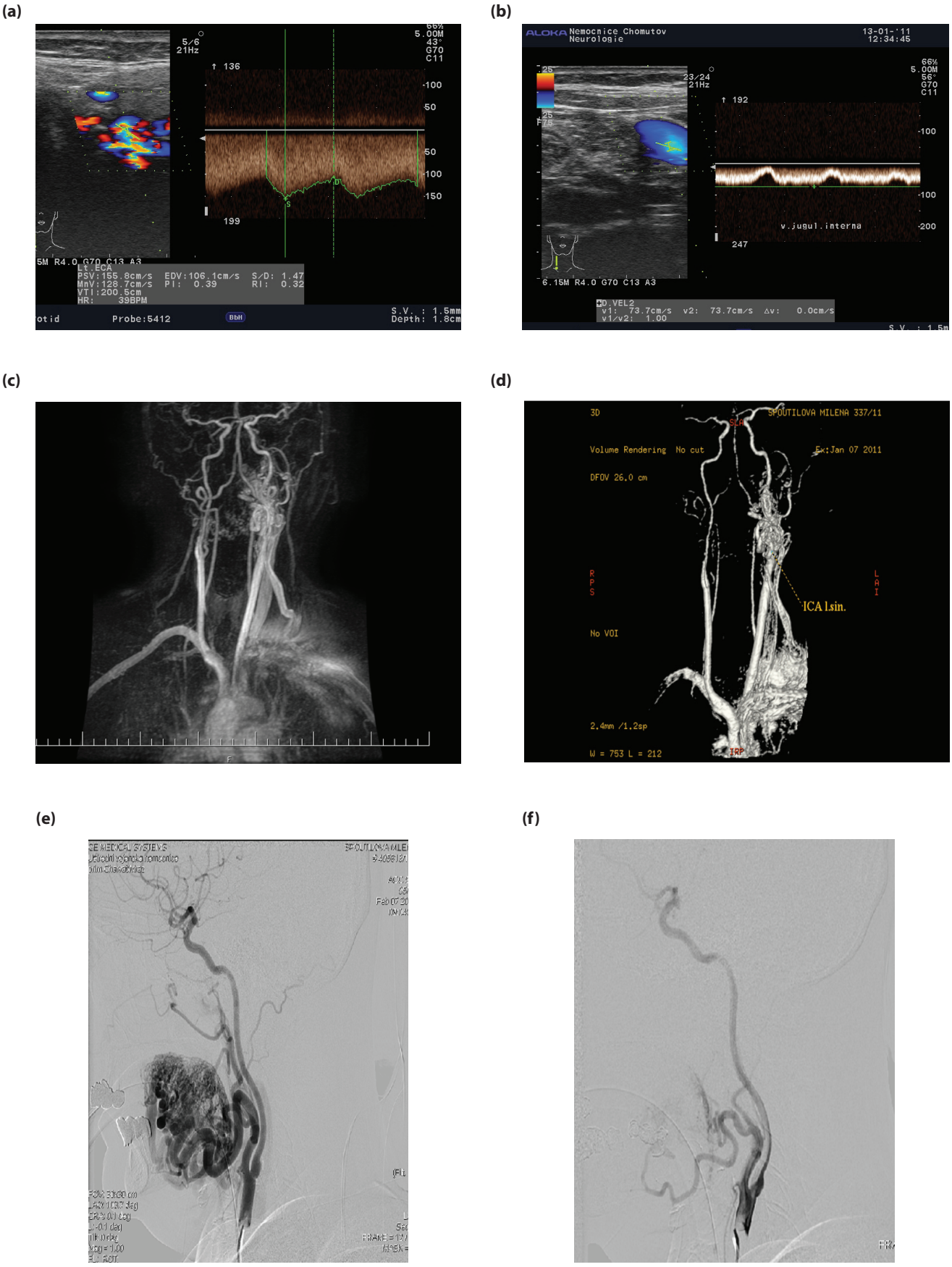


**Figure 1. (a)** Accelerated low-resistant flow distal to the origin of left external carotid artery; **(b)** Arterialized flow in draining vein; **(c)** magnetic resonance angiography—Large arteriovenous malformation in the left parapharyngeal area; **(d)** 3D magnetic resonance angiography—arteriovenous malformation in the left carotid artery bifurcation; **(e)** Digital subtraction angiography—filling of the left lingual artery; **(f)** Digital subtraction angiography after embolization—artery nearly eliminated, filling from collaterals.

**Figure 2**. Dilated veins in the left half of the tongue—area of arteriovenous malformation.

## Discussion

An AVM localized at the carotid artery bifurcation is extremely rare. In this case, the clinical state of the patient is good after endovascular treatment. Neurosonological findings improved, without any further progression in flow velocities. We conclude that the huge AVM in the carotid artery bifurcation could have caused recurrent syncopes by its steal phenomenon, with regard to the hemodynamic changes which were seen in the whole carotid area, although another possible cause of the syncope could be the local pressure and stimulation of the carotid sinus by the AVM [5, 6]. Further follow-up of the patient will be necessary.

### Abbreviations

ACE: Angiotensine-converting enzyme; AVM: Arteriovenous malformation; CCA: Common carotid artery; DSA: Digital subtraction angiography; ECA: External carotid artery; EDV; End-diastolic velocity; ICA; Internal carotid artery; PI: Pulsatility index; PSV: Peak-systolic velocity; RI: Resistance index

### Competing interests

The authors declare no conflict of interest.

### References

1. Školoudík D. Neurosonologie: Galén; 2003. p. 114-18.
2. Bohutova J, Mazanek J, Czech Radiol 2000; 54(4):207-12.
3. Valdueza JM, Schreiber SJ. Neurosonology and Neuroimaging of Stroke: Thieme; 2011. p. 146-48.
4. Zorzan G, Tullio A, Baj A, Sesenna E. [Arteriovenous malformations of the head and neck. Diagnosis and methods of treatment]. Minerva Stomatol 2001; 50(11-12):351-9.
5. Lee BB, Bergan JJ. Advanced management of congenital vascular malformations: a multidisciplinary approach. Cardiovasc Surg 2002; 10(6):523-33.
6. Ernemann U, Hoffmann J, Breuninger H, Reinert S, Skalej M. [Interdisciplinary concept for classification and treatment of vascular anomalies in the head and neck]. Mund Kiefer Gesichtschir 2002; 6(6):402-9.

INTERNATIONAL JOURNAL OF
CLINICAL NEUROSCIENCES
AND MENTAL HEALTH

CASE REPORT

# Bilateral steno-occlusive disease of the middle cerebral artery: a case report with clinical-hemodynamic mismatch

Helena Rocha[1], Pedro Castro[1], Rosa Santos[1], Elsa Azevedo[1], and Marta Carvalho[1]

Special Issue on Neurosonology and Cerebral Hemodynamics

## Abstract

**Background:** Bilateral steno-occlusive disease of middle cerebral artery (MCA) in young adults raises significant issues regarding etiology and treatment. The potential concomitance of hypoperfusion in the affected territories is of particular clinical relevance.

**Case report:** A 37-year-old man was admitted for a right MCA transient ischaemic attack. He was smoker, obese, dyslipidaemic, with previous history of heroin addiction and cured B and C hepatitis virus infections. Brain magnetic resonance and cardiac evaluation were normal. Transcranial color-coded sonography (TCCS) showed >50% proximal right MCA stenosis and distal left MCA occlusion. Treatment with aspirin and statin was started. Three months later, TCCS revealed >70% right MCA stenosis and left MCA occlusion. Selective angiography confirmed the steno-occlusive disease. Cerebrospinal fluid analysis revealed increased protein levels and a normal cell count. Corticotherapy was started, but the patient did not complied. Bilateral occlusion of MCA was noticed on TCCS, one month later, being the patient asymptomatic. Pulsed arterial spin labelling (PASL) revealed a severe decrease of cerebral blood flow in the distal part of both MCA territories.

**Conclusions:** The etiology of this progressive steno-occlusive disease remains unknown. Atherosclerosis may be a possible mechanism, however other potential etiologies must be considered giving the rapidly progressive character of the disorder. As it seems to be now stabilized, we wonder if it can be due to the vascular risk factors control and antithrombotic treatment or to a non-identified inflammatory monophasic cause. Serial TCCS played a major role in the assessment of disease progression.

**Keywords:** Progressive intracranial stenosis, Brain hypoperfusion, Transcranial color-coded sonography, Pulsed arterial spin labeling

[1]Department of Neurology, São João Hospital Centre, Faculty of Medicine of University of Porto, Porto, Portugal

Correspondence: Helena Rocha

Department of Neurology, São João Hospital Centre, Faculty of Medicine of University of Porto

Alameda Prof. Hernâni Monteiro, 4200 – 319, Porto, Portugal

Email adress: helen.roch@gmail.com

Citation: Rocha et al. Bilateral steno-occlusive disease of the middle cerebral artery: a case report with clinical-hemodynamic mismatch. IJCNMH 2014; 1(Suppl. 1):S26

Received: 07 Sep 2013; Accepted: 20 Nov 2013; Published: 09 May 2014

## Introduction

Progressive bilateral steno-occlusive arteriopathy in young adults is rare and raises significant issues concerning etiology, treatment, and prognosis [1, 2]. Atherosclerotic disease can be a major cause, but other causes such as vasculitis or non-inflammatory arteriopathies are not to be dismissed. [3, 4]. Imaging techniques are crucial for diagnosis and for follow-up, providing information about hemodynamic status and consequently about the risk of ischemia.

## Case report

A 37-year-old Caucasian man was admitted to the emergency room for two transitory episodes of dysarthria and sensory disturbance in the left face and arm. He worked as a cargo driver and had 6 years of formal education. He was smoker, obese, binge drinker, and previously addicted to heroin until fourteen years ago. His father had a stroke at the age of fifty, and additional family history was irrelevant. Physical examination, including neurological assessment was unremarkable. Brain CT, blood routines, ECG and electroencephalography were normal. Since the symptoms were suggestive of transient ischaemic attacks (TIA) he was started on aspirin and was admitted to the Neurology Department for further investigation.

An exhaustive analytical study was performed (**Box 1**) and revealed dyslipidemia and cured hepatitis B and C infections. Transcranial color-coded sonography (TCCS) revealed a pattern of thrombolysis in brain ischemia (TIBI) score of 4 in proximal right middle cerebral artery (MCA) and 3 in left MCA, suggesting respectively >50% stenosis and occlusion patterns (**Figure 1a and 1b**). Trans-esophageal echocardiogram was normal. Brain magnetic resonance imaging (MRI) with diffusion-weighted imaging (DWI) did not show parenchymal lesions suggestive of acute or previous ischemia (**Figure 2a**). Three-dimensional time-of-flight magnetic resonance angiography (MRA) showed an absent flow signal in the left MCA and a severe stenosis in the proximal right MCA (**Figure 2b**). The patient was discharged on aspirin and statin.

Three months later, a routine TCCS revealed worsening right MCA stenosis (TIBI 4 but with velocity ratio to pre-stenosis >3, suggesting stenosis >70%) and persistence of left MCA occlusion (**Figure 1c and 1d**). At that time the patient had quited smoking and lipid profile was already normal. Selective digital subtraction angiography (DSA) showed a focal stenosis of 50% of the supraclinoid portion of the right internal carotid artery (ICA); irregular vessel wall of proximal right MCA causing a severe stenosis (65-70%) at this location; and left MCA occlusion with collateralization by pial branches of anterior cerebral artery (ACA) and external carotid artery (**Figure 2d1 and 2d2**). Cerebrospinal fluid (CSF) analysis revealed increased protein (1,00g/L), with a normal cell count (5cells/uL). Despite lack of any particular evidence of cerebral vasculitis, but due to its possibility, a pulse of methilprednisonole 1g/day IV was administered for 5 days.

One month later bilateral MCA TIBI 3 occlusion pattern was noticed on TCCS, although the patient remained asymptomatic (**Figure 1e and 1f**). Cerebral vasoreactivity was tested with apnea test in the visible segment of what could be M1 segment of MCA, or a local collateral vessel, showing lack of reactivity (**Figure 3**). Oral prednisolone 60mg was started, but the patient did not comply for more than one week due to fear of potential side effects. The pattern of brain perfusion was evaluated with pulsed arterial spin labeling (PASL) MRI, which confirmed a severe decrease of cerebral blood flow in the distal part of both MCA territories (**Figure 2c**).

One year after the presenting symptoms, cerebral DSA confirmed persistence of bilateral proximal MCA occlusions, with extensive collateralization from pial vessels from ipsilateral ACA, and mild right supraclinoid ICA stenosis (**Figure 2d3 and 2d4**). Other cerebral and supra-aortic branches were unremarkable. Abdominal DSA showed no vessel abnormalities in other arterial territories.

The patient remains asymptomatic, without focal neurological deficits, although a more comprehensive neuropsychological assessment suggested a cognitive impairment (The Montreal Cognitive Assessment - MoCA 22/30) with memory dysfunction.

**Box 1.** Analytical study performed in the Neurology Department (only the abnormal results are discriminated).

**Complete blood count**

**Biochemical**
Glycaemia, protein, albumin
Serum electrolytes,
Inflammatory markers (C-Reactive protein, Sedimentation rate)
Thyroid, liver, renal function, ADA, ECA
Lipid profile (Total cholesterol 246mg/dl, LDL 169mg/dl, HDL 38mg/dl and triglycerides 193mg/dl)

**Viral Serology**
Serum titers for syphilis and HIV negative; previous hepatitis B and C virus infections (AcHBc positive, AgHBs negative; AcHCV positive, RNA HCV negative)

**Immunology**
ANA, anti-dsDNA, anti-ENAs, complement, ANCA, lupus anticoagulant, anticardiolipin, anti-B2 glycoprotein antibodies

**Coagulation / Prothrombotic study**
aPTT, PT, AT III, Protein C and S, MTHFR, Factor V Leiden, prothrombin G20210A mutation, homocystein (homozygous C677T MTHFR mutation)

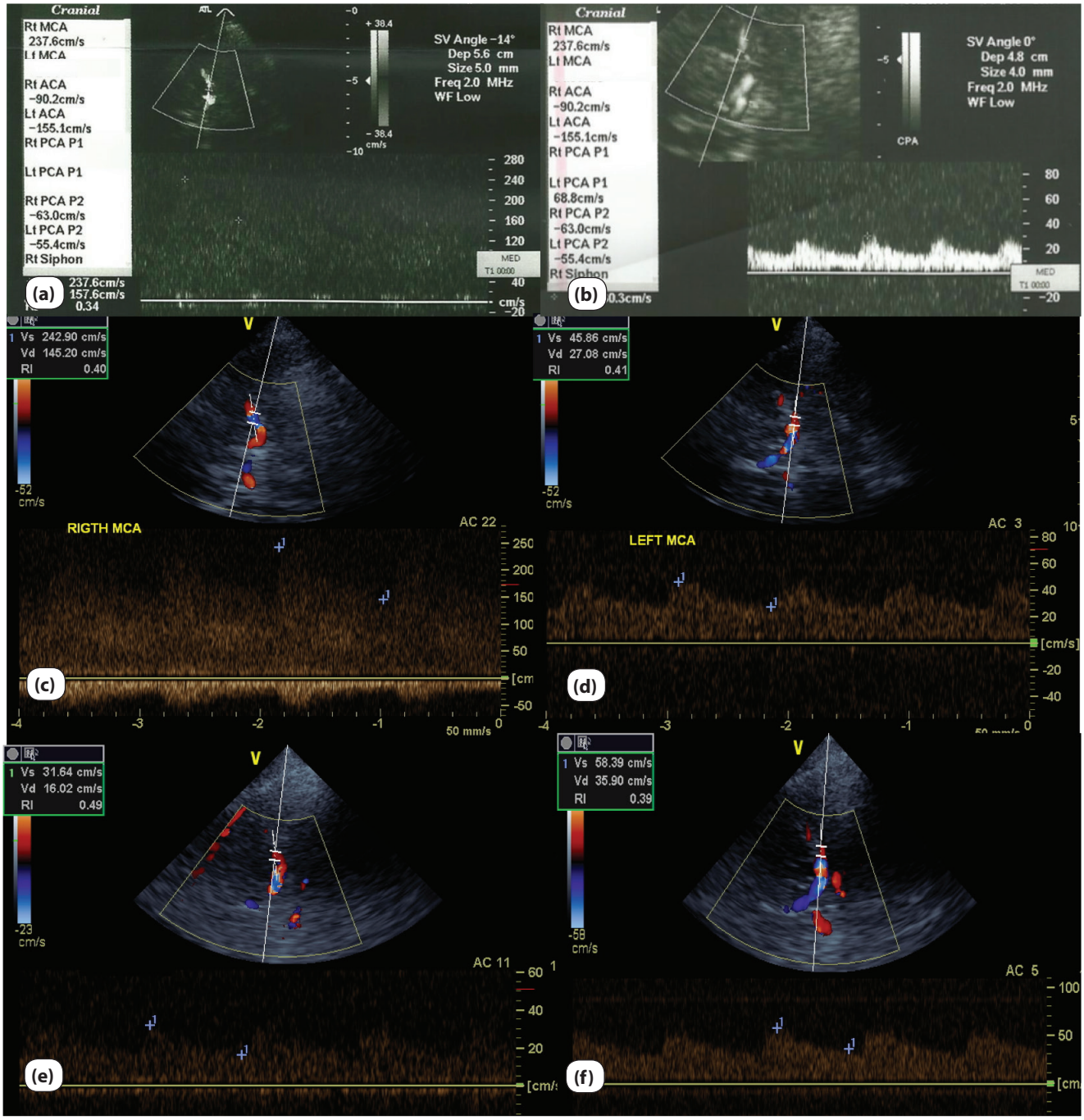


**Figure 1.** Transcranial color-coded sonography (TCCS) images. Admission: >50% proximal middle cerebral artery (MCA) stenosis **(a)** and MCA occlusion pattern **(b)**; 3 months later: 70% right MCA stenosis with a prestenotic index=4 **(c)** and left MCA occlusion pattern **(d);** 1 month later: right **(e)** and left **(f)** MCA occlusion pattern.

## Discussion

We report a case of bilateral progressive steno-occlusive disease of MCA in a 37-year-old man with multiple vascular risk factors, past history of illicit drugs consumption and markers of cured hepatitis B and C infections. The etiology remains unknown. Atherosclerosis may be a possible pathological mechanism in this case [3]. In fact, atherosclerotic stenosis of the major intracranial arteries may be the most common cause of stroke worldwide, although not in Caucasians. Patients with symptomatic severe intracranial stenosis (>70%) have a risk of recurrent stroke as high as 23% in 1 year [4-6]. In this particular case, the rapidly progressive character of the disease imposes the exclusion of other potential etiologies.

The prothrombotic study, performed as a routine in young adults, revealed normal homocystein level and homozygous C677T MTHFR mutation. The association between this genotype and cerebrovascular disease is still controversial although it has been previously reported as

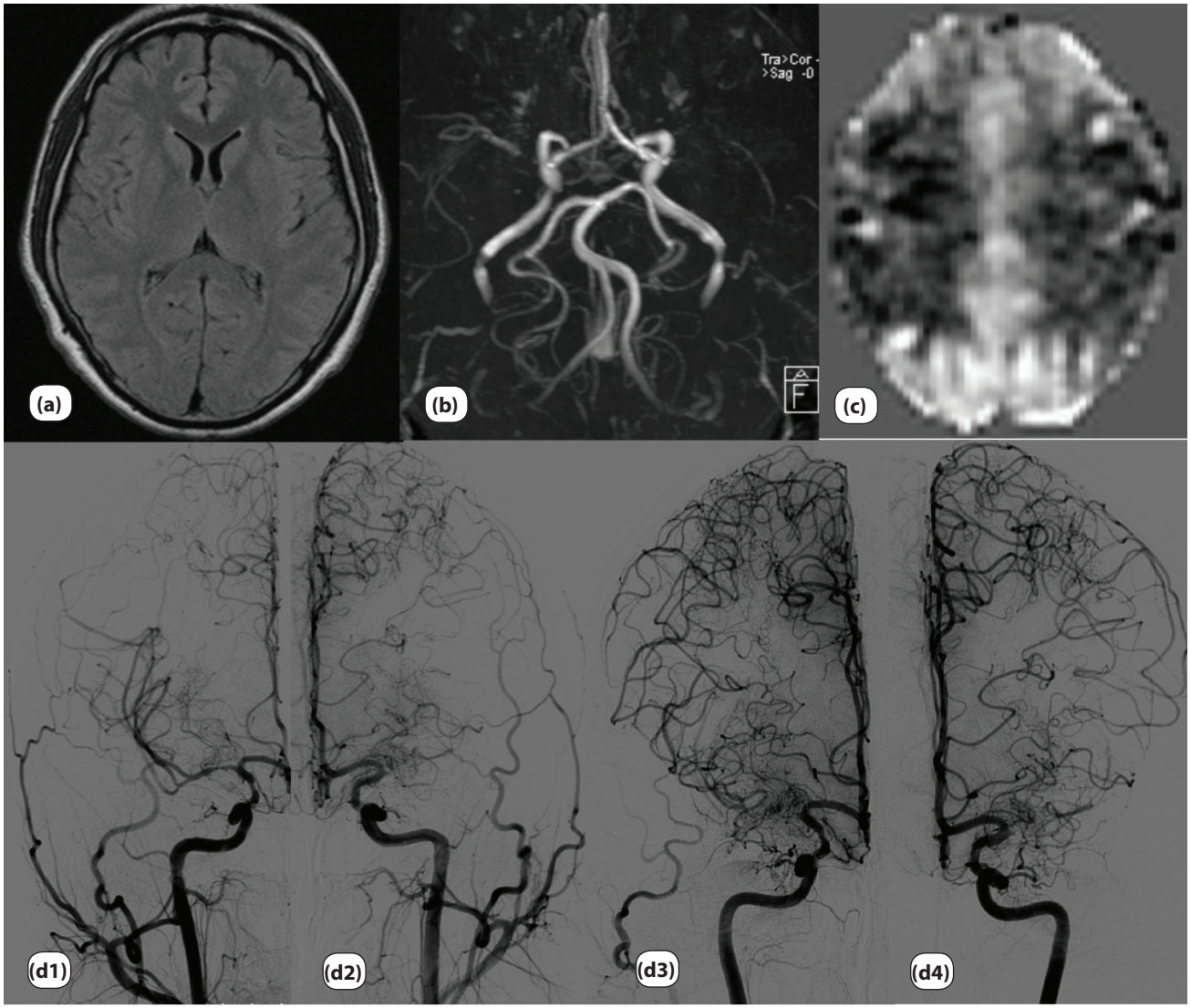


**Figure 2.** **(a)** Brain MRI with fluid attenuated inversion recovery (FLAIR) sequence: no parenchymal lesions; **(b)** Three-dimensional time-of-flight magnetic resonance angiography (MRA): absent flow signal in the left MCA and a severe stenosis in the proximal right MCA; **(c)** Pulsed arterial spin labeling (PASL): hypoperfusion in the distal part of both MCA territories; **(d)** Cerebral digital subtraction angiography (DSA): July 2012 – focal stenosis of 50% of the supraclinoid portion of the right ICA and irregular vessel wall with severe stenosis (65-70%) of proximal right MCA (**d1**), left MCA occlusion with collateralization due to pial branches of anterior cerebral artery (ACA) and external carotid artery branches (**d2**); One year later – proximal right (**d3**) and left MCA occlusions and left internal carotid artery (ICA) stenosis in the supraclinoid portion (**d4**) with exuberant collateralization.

a risk factor, specially for multiple-small artery disease, in cases of concomitant hyperhomocysteinemia, which is not the present case [7, 8].

Vasculitis of the central nervous system (CNS), primary or systemic, and connective tissue disorders, must be considered in young patients [9]. Even considering previous asymptomatic hepatitis C infection, it was spontaneously cured when the patient presented with neurologic symptoms. Systemic lupus erythematosus, antiphospholipid syndrome and Takayasu's disease are among the most common inflammatory disorders in which stroke can be a feature, but there is no clinical nor laboratory evidence of such disorders in this particular case [1]. Primary angiitis of the CNS is very rare and can manifest as a focal neurological deficit, stroke or cognitive impairment, especially when medium-sized vessels are involved [10-12]. Concerning our workup, the non-specific CSF findings, the normality of brain parenchymal MRI and the absence of irregularities such as beading or focal narrowing of brain vessels on DSA do not favor this diagnosis [10-13]. Even though, treatment with corticotherapy was tried, its effectiveness could not be evaluated because of patient's non-compliance. The angiographic collateralization pattern has some similarities with moyamoya vessels, which typically develop in cases of progressive stenosis of the terminal portion of the ICA and its main branches (ACA and MCA) [13-15]. Although the patient might have a moyamoya syndrome, the Moyamoya disease, which occurs typically in Asian people, is not a likely diagnosis [16, 17].

In what concerns heroin consumption, most strokes attributed to this drug occur acutely after its administration, mainly due to global brain hypoperfusion or cardio-

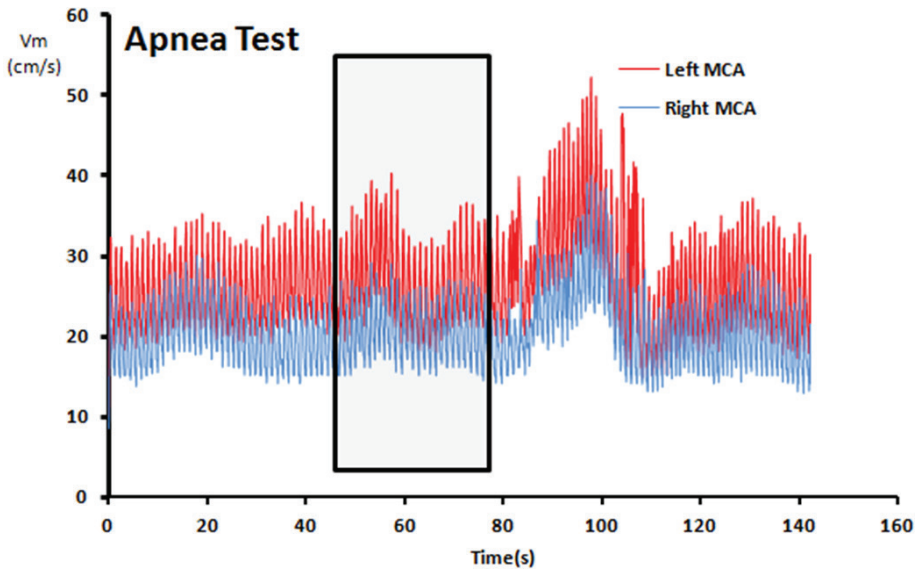


**Figure 3.** Apnea test: Cerebral blood flow velocity (cm/s) at middle cerebral artery (MCA) level was monitored with transcranial Doppler bilaterally (right, blue; left, red). Apnea was performed for 22 seconds (grey box). Note that cerebral blood flow waveforms remained unchanged during hypercapnia. Low Breath hold indexes (right -0.22; left 0.46) were calculated, confirming low cerebrovascular reactivity (normal values: 1.2 ± 0.6) [27].

embolism, because of infective endocarditis. A few reports also suggest an underlying vasculitic process but this is not widely accepted once there is no pathological proof [18, 19]. There is no evidence of recent consumptions in this patient.

We emphasize the usefulness of serial TCCS in the diagnosis and follow-up of intracranial stenosis. Being the patient asymptomatic and having a brain MRI without abnormalities, the routine evaluations with this non-invasive technique were crucial to assess disease progression [20-22]. Brain perfusion pattern was also evaluated using a non-invasive MRI method—PASL, that uses magnetically labeled water protons as an endogenous tracer [23-26], which revealed bilateral cerebral hypoperfusion. This was discrepant with the absence of focal signs, although it might explain the cognitive disturbance.

Apart from the rapid progression of the intracranial stenosis at first, the process seems to be now stabilized, as the patient remains asymptomatic and no other vessels abnormalities were detected. We wonder if this stability can be assigned to the vascular risk factors control and antithrombotic treatment effect or if there was a non-identified inflammatory monophasic cause. As mentioned, establishing an etiology remains a challenge.

## Abbreviations

ACA: Anterior cerebral artery; CSF: Cerebrospinal fluid; DSA: Digital subtraction angiography; DWI: Diffusion-weighted imaging; ICA: Internal carotid artery ; MCA: Middle cerebral artery; MRA: Magnetic resonance angiography; MRI: Magnetic resonance imaging; PASL: Pulsed arterial spin labeling; TCCS: Transcranial color-coded sonography; TIA: Transient ischaemic attacks

## Competing interests

The authors declare no conflict of interest.

## References

1. Ferro JM, Massaro AR, Mas JL. Aetiological diagnosis of ischaemic stroke in young adults. Lancet Neurol 2010; 9:1085-96.
2. Seneviratne BI. Ameratunga B. Strokes in Young Adults. BMJ 1972; 3:791-793.
3. Carvalho M, Oliveira A, Azevedo E, Bastos-Leite A. Intracranial Arterial Stenosis. J Stroke Cerebrovasc Dis 2013, pii: S1052-3057(13)00227-9.
4. Turan TN et al. Factors Associated with Severity and Location of Intracranial Arterial Stenosis. Stroke 2010; 41(8):1636–1640.
5. Chimowitz MI et al. Stenting versus Aggressive Medical Therapy for Intracranial Arterial Stenosis. N Engl J Med 2011; 365:993-1003.
6. Famakin BM, Chimowitz MI, Lynn MJ, Stern BJ, George MD. Causes and Severity of Ischemic Stroke in Patients with Symptomatic Intracranial Arterial Stenosis. Stroke 2009; 40(6):1999–2003.
7. Choia BO et al. Homozygous C677T mutation in the MTHFR gene as an independent risk factor for multiple small-artery occlusions. Thromb Res 2003; 111:39-44
8. Alluria RV et al. MTHFR C677T gene mutation as a risk factor for arterial stroke: a hospital based study. Eur J Neurol 2005; 12:40-44
9. Hajj-Ali RA. Primary angiitis of the central nervous system: differential diagnosis and treatment. Best Pract Res Clin Rheumatol 2010; 24:413–426
10. Alba MA et al. Central Nervous System Vasculitis: Still More Questions than Answers. Curr Neuropharmacol 2011; 9:437-448
11. Salvarani C, Brown Jr RD, Hunder GG. Adult primary central nervous system vasculitis. Lancet 2012; 380:767-77
12. Giannini C, Salvarani C, Hunder G, Brown RD. Primary central nervous system vasculitis: pathology and mechanisms. Acta Neuropathol 2012; 123:759–772

13. Kuroda S, Houkin K. Moyamoya disease: current concepts and future perspectives. Lancet Neurol 2008; 7:1056-66
14. Hirotsune N, Meguro T, Kawada S, Nakashima H, Ohmoto T. Long-term follow-up study of patients with unilateral Moyamoya disease. Clin Neurol Neurosurg 1997; 99(Suppl. 2):S178–S181
15. Yuxiang Gu et al. Efficacy of extracranial–intracranial revascularization for non-moyamoya steno-occlusive cerebrovascular disease in a series of 66 patients. J Clin Neurosci 2012: 19;1408–1415
16. Gowdie P, Twilt M, Benseler SM. Primary and Secondary Central Nervous System Vasculitis. J Child Neurol 2012; 27:1448-1459.
17. Burke GM. Burke AM. Sherma AK. Hurley MC. Batjer HH. Bendok BR. Moyamoya disease: a summary. Neurosurg Focus 2009; 26(4):E11
18. Fonseca AC, Ferro JM. Drug Abuse and Stroke. Curr Neurol Neurosci Rep 2013; 13(2):325
19. Esse K, Fossati-Bellani M, Traylor A, Martin-Schild S. Epidemic of illicit drug use, mechanisms of action/addiction and stroke as a health hazard. Brain Behav 2011; 1(1):44-54
20. Baumgartner et al. Contrast-Enhanced Transcranial Color-Coded Duplerx Sonography in ischemic Cerebrovascular Disease. Stroke 1997; 28:2473-2478
21. Zipper SG, Stolzb E. Clinical application of transcranial colour-coded duplex sonography - a review. Eur J of Neurol 2002; 9:1-8
22. Hokabergen AW. Majoie CB, Hulsmans FJ, Legemate DA. Assessment of the collareral function of the circle of Willis: three-dimensional time-of-fight MR angiography compared with transcranial coler-coded duplex sonography. Am J Neurorradiol 2003; 24(3):456-62
23. Wirestam R. Cerebral perfusion information obtained by dynamic contrast-enhanced phase-shift magnetic resonance imaging: comparison with model-free arterial spin labeling. Clin Physiol Funct Imaging 2010; 30:375–379
24. Martirosian P et al. Magnetic resonance perfusion imaging without contrast media. Eur J Nucl Med Mol Imaging 2010; 37(Suppl 1):S52–S64
25. Hartkamp NS et al. Mapping of cerebral perfusion territories using territorial arterial spin labeling: techniques and clinical application. NMR Biomed 2013; 26(8):901-12
26. Wang DJ. The Value of Arterial Spin-Labeled Perfusion Imaging in Acute Ischemic Stroke: Comparison With Dynamic Susceptibility Contrast-Enhanced MRI. Stroke 2012; 43:1018-1024
27. Markus HS, Harrison MJ. Estimation of cerebrovascular reactivity using transcranial Doppler, including the use of breath-holding as the vasodilatory stimulus. Stroke1992; 23:668-673

ARC Publishing

*Outstanding services in medical writing, statistics and publishing.*

Providing superior medical writing, statistics and training services, allowing you to comply with the highest clinical research quality standards and to get the most of your data.

Promoting the sharing of scientific knowledge through any form of publication.

# Publishing

ARC Publishing has an exclusive publishing service. It includes the preparation and publication of digital, web-based or printed periodicals, books, conference proceedings, etc.

### Journals

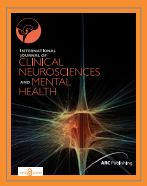


**IJCNMH**

The International Journal of Clinical Neurosciences and Mental Health is an open-access online journal published by ARC Publishing. It aims to publish high quality articles in the areas of Psychiatry, Mental Health, Medical Psychology, Neurosurgery and Neurology.

With an international editorial board of recognised experts in these medical areas, it publishes peer-reviewed articles in the following categories: original research, reviews, drug reviews, case reports, case snippets, viewpoints, letters to the editor, editorials and guest editorials.

The journal is available at ijcnmh.arc-publishing.org.

### Books

**Pharmaceutical Medicine Series**

The first number of the Pharmaceutical Medicine Series published by ARC Publishing is already available.

This number is entitled "Living Usability Lab" (Laboratório Vivo de Usabilidade in Portuguese) and it is edited by António Teixeira, Alexandra Queirós, and Nelson Pacheco da Rocha. This book intends to present the work mainly developed by the faculty and researchers of the University of Aveiro involved in the project Living Usability Lab for Next Generation Network.

The book is available online in an Open Access manner and it can be accessed at arc-publishing.org.

To know more details about our publishing services, please contact us: **info@arc-publishing.org**